Air Quality and Communicable Diseases Technical Report

A technical report prepared for the Australian Climate Service as part of the National Climate Risk Assessment

Justin Boyle, Ibrahim Diouf, Kathryn Emmerson, Maryam Golchin, Roslyn Hickson, Nehleh Kargarfard, Justine Sexton, Aminath Shausan, Laurence Wilson, Teresa Wozniak, Jin Yoon, Shane Seabrook, and Rajiv Jayasena

February 2025

Citation

Boyle J, Diouf I, Emmerson K, Golchin M, Hickson R, Kargarfard N, Sexton J, Shausan A, Wilson L, Wozniak T, Yoon J, Seabrook S, and Jayasena R (2025) Air Quality and Communicable Diseases Technical Report. A technical report prepared for the Australian Climate Service as part of the National Climate Risk Assessment. CSIRO, Australia. https://doi.org/10.25919%2F9nac-a029

Cover page image: Melbourne, Australia. Credit: Ming Han Low on Unsplash.

Contents

Figures

Tables

Acknowledgments

The Australian Climate Service is a partnership between the Bureau of Meteorology, CSIRO, the Australian Bureau of Statistics and Geoscience Australia. The CSIRO's Health and Biosecurity Research Unit has undertaken this project as an Australian Climate Service partner agency. The Australian Climate Service is developing the evidence base for Australia's National Climate Risk Assessment.

Executive summary

Australia's first National Climate Risk Assessment is being developed by The Australian Climate Service (ACS) with the Department of Climate Change, Energy, the Environment and Water (DCCEEW). This risk assessment identifies to what degree Australia's people, infrastructure, the economy, and landscapes are exposed and vulnerable to climate change this century. It informs national priorities for climate adaptation and resilience actions and has the potential to inform a range of Australia Government policy areas.

Drawing on capability across several Australian government agencies – including CSIRO, the Australian Bureau of Statistics (ABS) and the Bureau of Meteorology and Geoscience Australia – the National Climate Risk Assessment is developing a national evidence base which will be used to develop an Australia-wide picture of potential risks and adaptation options.

In 2024, ACS contracted CSIRO to provide targeted risk assessments under the NCRA Health and Social Support Systems (NCRA Second Pass Assessment), specifically 1) bushfire impacts on air quality and 2) the emergence and increased transmission of communicable diseases. This document reflects the technical report associated with these two workstreams. The document discusses topics including mortality from bushfires and may be triggering or stressful for some audiences.

Bushfire impacts on air quality and health

The objective of the bushfire impact workstream was to quantify the impacts that bushfires may create on the health system under different future climate scenarios. Using the 2019/20 summer bushfires as an example of an extreme event scenario, the study attempts to quantify the smoke-related health impacts if such an event were to occur in 2050. The air quality associated with this scenario would comprise changes between the present day and 2050 due to climate change, coupled with air quality levels estimated nationally for the 2019/20 bushfires.

Standard population-level modelling approaches were used to model the impact of bushfires on air quality and health. Health impact functions assessed four outcomes: all-cause mortality, cardiovascular-related hospital admissions, respiratory-related hospital admissions, and emergency department (ED) presentations related to asthma. It is acknowledged that there are broader outcomes associated with bushfires including mental health and financial impacts, and the investigation was based on a quantitative approach rather than qualitative review which may uncover alternative insights. Also broad assumptions are made in this modelling using impacts derived via statistical attribution rather than confirmed coroner reports or chart audits of hospital records.

Projections of climate to 2050 using 8 different global climate models indicate wide variation in estimates of air pollutants. To determine the health impacts of a severe bushfire in 2050, modelling comprised a bushfire component (based on the 2019/20 bushfire period) and a climate change component, with each having an expected impact on future air quality. Due to uncertainty between the climate change models, health impacts were quantified for all climate models and a

best and worst case identified. The results indicate that the health impacts due to climate change are between an eighth (12.5% - best base) and a quarter (25% - worst case) of the impacts estimated from the 2019/20 bushfires. It is noted that while the health impacts from the 2019/20 bushfires were substantial, they were less than 1% of broader mortality and inpatient admission impacts nationally for similar diagnoses, and approximately 4% of broader volume in the case of asthma-related ED presentations.

The assessment uses relative risks largely based on World Health Organization (WHO) recommendations for assessing impact from air quality. As sensitivity analyses, we assessed other relative risks published from systematic reviews and consider the health impacts from three different pollutants identified in bushfire smoke. Of all the different global climate models and relative risks assessed, they all generate approximately the same ratios in terms of future air quality and health impacts. Although the modelling of the bushfire component was based on the most extreme fire event in Australia to date, our analysis did not consider bushfire size, intensity and duration which are expected to change in a future warmer environment with more extreme fire weather.

To complement this assessment, the team generate new evidence assessing relative risks of health service use associated with bushfires, covering PBS, MBS as well as hospital datasets made available via the Australian Research Data Commons (ARDC) Bushfire Data Challenges program. It is understood that this is the first time this dataset has been used to generate Australian, nationally focused relative risks about health service use that compare well against published recommendations.

This assessment establishes that climate change is increasing the frequency and extremity of fire weather when most fires tend to occur and exposure to bushfire smoke contributes towards Australia's disease burden. The substantial evidence base suggests controlling fine particle pollution would result in fewer early deaths; however high particulate matter exposure occurs frequently for populations in central Australia. While concern about extreme events like bushfires is appropriate, there is not a way to remove dust as a risk factor from the country, and our future climate will contain all sources of particulate matter including those from non-anthropogenic emissions.

Emergence and increased transmission of communicable diseases

Routinely collected pathogens of concern

To enable an improved understanding of the climate driven risks for communicable diseases, we investigated the impact of climate change on influenza notifications nationwide and methicillin-resistant staphylococcus aureus (MRSA) in northern regional and remote Australia. We constructed prediction models to assess how variations in climate variables including, but not limited to, temperature, humidity, and precipitation might affect current and long-term future of influenza and MRSA prevalences.

By 2050, we projected that the rate of influenza would be 116 and 300 cases per 10,000 people under the low and very high greenhouse gas emission scenarios of SSP1-2.6 and SSP5-8.5 respectively, as a result of increasing maximum surface air temperature. This is an increase of

187% and 639% respectively compared to the average observed influenza rate in the 2010 – 2019 period.

By 2050, we projected that the rate of MRSA would be 87 and 102 cases per 10,000 people under the low and very high greenhouse gas emission scenario of SSP1-2.6 and SSP5-8.5 respectively, as a result of increasing maximum surface air temperature. This is an increase of 39% and 63% compared to the average observed MRSA rate in the 2014 – 2023 period.

Our analysis highlights the importance of ongoing support for surveillance and assessment of the impact of climate change on communicable diseases. We note, however, the following limitations in our study.

- We employed the output from one climate model
- We consolidated the entire Australian influenza cases as a single cohort. Similarly, the entire north Australian MRSA cases were considered as a single cohort.
- We analysed annual disease data.
- We modelled the effect of each climate variable separately.
- We considered only the effect of climate on health.

Potential spillover risk with climate change

To investigate how spillover risks across Australia might change with climate, we leveraged our existing estimate of spillover from 11 orders of animals in Australia under climate change. To perform a deeper assessment of how potentially high impact pathogens such as Japanese encephalitis virus (JEV) risks will change with climate change scenarios, ecological niche modelling for zoonotic climate sensitivity was undertaken. These projections should be interpreted cautiously. They are based on assumptions inherent in climate models and do not account for potential changes in human behaviour, land use, or wildlife movement.

The results show an estimate of the environmental suitability of the 11 orders of animals (8 mammals and 3 avian) and their corresponding viruses known to be able to cross to humans. It is important to note many of these would require introduction into Australia to actually be present. Although there is substantial variation between the models, some of the broader scale patterns in the changes remain largely consistent. The most consistent patterns were an increased potential zoonotic virus density in the west, reduced potential in the east, and substantial changes in Tasmania by 2050. This is a preliminary estimation based on simplified assumptions, intended to provide a rapid approximation. Further refinement and detailed analysis are required for more precise results. That is, there are many limitations to this study, with much caution needed in interpretation and use.

For JEV, the results show the differences in combined presence probabilities of 3 mosquito vectors and any of the 12 waterbird species or feral pigs. It is important to note that this is not directly spillover or transmission risk, but simply where the necessary species for transmission to occur are likely to be present in combination. An actual transmission layer, including key information like viral suitability and vector abundance, would be needed for transmission risk. Results based on several of the eight individual climate models had patterns of increased presence probability of species associated with the transmission of JEV in the north of the country, and decreases in the

south. A region around southern Western Australia showed a consistent decrease even in the extreme model projection. The changes observed from 2025 to 2090 are larger than 2025 to 2050 and appear to be driven largely by changes in the 3 mosquito populations.

Climate change induced mutations

To investigate how climate change induced mutations in a pathogen's genome that could have potential adverse impacts on survival, replication, and virulence, an analysis was undertaken to understand how pathogens could evolve in response to a changing climate. This could in turn have an impact on survivability, pathogenicity and infectivity of various diseases. We investigated this using historical genetic data to determine if the emergence of mutations could be correlated with changing climate with particular focus on pathogens relevant to Australia (salmonella, influenza virus and JEV).

Machine learning algorithms were used in the analysis to identify climate linked mutations where mutations associated with changes in minimum/maximum temperature and precipitation were identified. Analysis of the influenza identified a small subset of 4 mutations were common to all these climate conditions and mapping these mutations to high quality X-ray crystallography structures demonstrated that majority of mutations were outward facing, allowing them to interact with the environment. This work demonstrated the ability to identify mutations linked to changes in climate reinforcing the hypothesis that pathogens can adapt to changing conditions. This early evidence suggests that these mutations are linked to multiple climate changes (e.g. temperature and precipitation) and are in pathogenically important regions (e.g. the HA1 trimer in influenza virus).

The JEV analysis revealed several variant combinations that were linked to the El Nino cycle. The preferential association of these variants in samples originating from El Nino years could be indicative of co-evolution, two variants emerging in tandem in response to climate variability and change. Climate change has been hypothesised to influence the El Nino/La Nina cycle, potentially intensifying the climate events. If these variants are associated with El Nino, then an intensifying of this weather cycle would lead to an increase in the frequency these variant combinations are observed.

While this study highlights the importance of monitoring for these changes in the genomes of pathogens, there are limitations that need to be noted:

- Poor quality JEV and salmonella datasets: Limited genomic data and poor-quality metadata restricts the strength of analysis. Links between mutations and high-level climate events (e.g. El Nino/La Nina) have been identified and continued refinement of methods and cleaning of data will continue to provide insight.
- Correlation vs causation: Correlation of mutations with climate does not necessarily imply a direct functional link. Continued monitoring for emergence of these flagged mutations in the future will allow researchers to refine focus onto those mutations with significant evidence for a link to climate change.
- Functional implications of mutations: Structural modelling of mutations can provide insight, but function must be determined experimentally in the future.

1 Introduction

This work was undertaken for the National Climate Risk Assessment (NCRA, Second Pass Assessment) Health and Social Support System as risks to health and wellbeing from slow onset and extreme climate impacts from bushfires on air quality (Workstream 1) and from emergence and increased transmission of communicable diseases (Workstream 2).

1.1 Bushfire impacts on air quality and health (Workstream 1)

Activities undertaken in this workstream comprise quantification of the impacts that bushfires may create on health system demand and mortality under different future climate scenarios. Modelled air quality data is overlaid with existing health data from publications and public reports to describe the health system demand and mortality impacts under different scenarios.

The aim is to understand the impacts that major bushfire and air quality events have on the health system (e.g. hospital demand). This is assessed from available reports and intelligence that describe health system demand and modelled climate change scenarios for 2050.

Forecasts from CSIRO's Air Quality Forecasting System (AQFx) are used to model air quality associated with the 2019/20 summer bushfires as an example of an extreme event scenario. Future projections of changes in air quality were obtained from the National Environment Science Program (NESP) air quality modelling runs available for 2048-2052. The model runs highlight changes in Australia's air quality from climate change and includes dust storms, sea salt, summer urban smog events and emissions that increase with higher temperatures such as biogenic hydrocarbons. Air quality is mapped to affected populations to estimate exposure, and health system impacts quantified via health impact functions, which is aligned with the approach of global environmental agencies for informing air quality policy.

1.2 Emergence and increased transmission of communicable diseases (Workstream 2)

Activities undertaken in this workstream were focussed on assessing trends of a selected number of current diseases and their likely changes of overall spillover risk with climate variation. For potentially high impact pathogens such as Japanese encephalitis virus a deeper assessment was undertaken using future climate change to describe those climate scenarios which might develop concerning properties. This exploratory study was to enhance the understanding of potential impacts climate change could have on pathogens to evolve concerning properties beyond heat tolerant such as heat, humidity and rainfall influenced fitness, pathogenicity and transmissibility.

The exploratory analysis focussed on high impact pathogens to develop concerning properties (transmissibility) under extreme climate conditions. Three areas of explorations were undertaken to determine the impact from climate change:

a. Routinely collected pathogens of concern (influenza & MRSA).

b. Potential spillover risk with climate change (11 orders of animals, 8 mammals and 3 avian) including a deeper assessment of potentially high impact pathogen (Japanese encephalitis virus (JEV)).
c. Climate change induced mutations (influenza, salmonella and JEV).

These activities focused on how climate variation (e.g. temperature, humidity, rainfall, seasonality, El Nino and La Nina events) impacted disease prevalence of two pathogens using routinely collected surveillance data. We focussed on laboratory-confirmed influenza from the National Notifiable Diseases Surveillance System and methicillin-resistant staphylococcus aureus (MRSA) from a phenotypic passive CSIRO-based surveillance system called HOTspots. A prediction model was used to assess the future impact on disease prevalence of these two pathogens with changes in climate variables for 2050.

To investigate how spillover risks across Australia might change with climate, we leveraged our existing estimate of spillover from 11 orders of animals in Australia under climate change to investigate potential change in zoonotic virus density across Australia from 2020 to 2050, using projections from eight different Global Climate Models under two climate scenarios, RCP 4.5 and RCP 8.5. A deeper assessment was undertaken to explore how a potentially high impact pathogen such as JEV change with future climate scenarios. Ecological niche modelling for zoonotic climate sensitivity was undertaken with JEV to investigate geographic transmission risks based on climate model projections for the future period of 2050 and 2090.

To investigate how climate change induced mutations in a pathogen's genome could potentially impact the survival, replication, and virulence, an analysis was undertaken to predict pathogen sensitivity to climate variables to understand how pathogens could change under different climate scenarios. The approach explored pathogen climate sensitivity by a machine learning and statistical approaches using genome sequence alignments of pathogen species from different climates around the world, over time. Influenza, JEV and salmonella genomes were explored and correlations between mutations of Influenza virus and climate changes were established. These findings for influenza virus were extended to understanding the direction and degree to which they might impact pathogen survival, replication and virulence.

2 Bushfire impacts on air quality and health (Workstream 1)

Activities undertaken in this workstream are to quantify the impacts that bushfires may create on health system demand and mortality under different future climate scenarios. Analysis is prefaced with commentary on the pressure that climate change is exerting on fire globally and the evidence of health impacts from bushfire-related air quality. Modelling is then presented for estimating air quality associated with bushfires in 2050 and linking air quality with health impacts.

2.1 Bushfires and health

2.1.1 The planet is warming

Every year, an authoritative, international, peer-reviewed summary of the global climate is published which provides a detailed update on global climate indicators, notable weather events, and other data collected by environmental monitoring stations and instruments located on land, water, ice, and in space. According to the most recent release based on contributions from scientists from around the world (The 34th annual State of the Climate Report), greenhouse gas concentrations, the global temperature across land and the ocean, global sea level and ocean heat content all reached record highs in 2023 (Blunden and Boyer, 2024). While the COVID-19 pandemic led to a drop in global CO_2 emissions of 5% in 2020, CO_2 concentrations have risen again to record high levels and are now higher than at any time in the last two million years (UNEP, 2021).

The three dominant greenhouse gases in Earth's atmosphere — carbon dioxide, methane, and nitrous oxide — all reached new highs in 2023, where levels of these three gases in the atmosphere are now more than 50%, 166% and 25% respectively higher than pre-industrial levels (Blunden and Boyer, 2024). Human activities are estimated to have caused approximately 1°C of global warming above pre-industrial levels, and likely to reach 1.5°C between 2030 and 2052 (IPCC, 2018). Specific to our region, Australia's climate has warmed by an average of 1.51 ± 0.23 °C since national records began in 1910 (Bureau of Meteorology and CSIRO, 2024). 2024 was Earth's warmest year since global records began in 1850 (NOAA, 2025).

A 2021 report from the Intergovernmental Panel on Climate Change "Physical Science Basis" has been dubbed a "code red for humanity" by the United Nations Secretary-General, and documents in far greater detail and with higher certainty than previous assessments how climate change and extreme events can be attributed to the build-up of anthropogenic greenhouse gas emissions in the atmosphere (IPCC, 2021). It is unequivocal that human influence has warmed the atmosphere, ocean and land. It is virtually certain that hot extremes (including heatwaves) have become more frequent and more intense across most land regions since the 1950s, while cold extremes have become less frequent and less severe, with high confidence that human-induced climate change is the main driver of these changes. Global surface temperature will continue to increase until at

least mid-century under all emissions scenarios considered by the Intergovernmental Panel on Climate Change (IPCC, 2021).

2.1.2 Heatwaves and droughts contribute to bushfire occurrences

Severe drought, heat and low humidity are becoming more extreme as the climate warms. Bushfires have been a natural and geologically ancient feature of the Earth system (Johnston et al., 2024). However, as climate change makes hot and dry conditions – often termed "fire weather" – more common and severe, vegetation dries out and landscapes become more flammable, pushing up the odds of bushfire occurrences (van Oldenborgh et al., 2021).

In Australia, fire weather is largely monitored using the forest fire danger index which indicates the fire danger on a given day based on observations of temperature, rainfall, humidity and wind speed (Bureau of Meteorology and CSIRO, 2024). A recent study found that in many regions of the world, the pace at which fire weather conditions are increasing is accelerating faster than climate models predicted (Jones et al., 2022). The length of the fire weather season (when most fires tend to occur) has already expanded significantly in many regions since the 1980s. Increases in the frequency and extremity of fire weather have been globally pervasive due to climate change, meaning that landscapes are primed to burn more frequently (Bowman et al., 2017). Overall, climate change is exerting a pervasive upwards pressure on fire globally by increasing the frequency and intensity of fire weather, and this upwards pressure will escalate with each increment of global warming (Jones et al., 2022). Climate change projections suggest an increase in days conducive to extreme bushfire events by 20 to 50% in disaster-prone landscapes, with sharper increases in the subtropical Southern Hemisphere and European Mediterranean Basin (Bowman et al., 2017).

However, climate change is not the only factor driving changes in bushfire activity. Weather conditions affecting vegetation growth and the build-up of fuels, the presence of human ignitions in regions that are not naturally fire-prone, and the fragmentation of fire-prone landscapes by agriculture are examples of factors that can locally or regionally outweigh fire weather as controls on fire activity (Jones et al., 2022).

2.1.3 Bushfire smoke

Bushfire smoke is considered a significant emission source of gaseous pollutants and particulate matter (PM). Active trace gases (e.g. sulphur dioxide (SO_2), nitrogen oxides (NO_x), ammonia (NH_3)) released from biomass burning are major precursors of secondary aerosols and tropospheric ozone in the atmosphere (Karanasiou et al., 2021). The combustion of biomass generates greenhouse gases emissions, such as methane (CH_4) and carbon dioxide (CO_2) roughly equivalent to the combustion of fossil fuels (IPCC, 2014: 877). The Australian bushfires from the summer of 2019–20 emitted more CO_2 than Australian annual fossil carbon emissions (van der Velde et al., 2021). Particles emitted from and formed in bushfire smoke plumes are typically a mixture of black carbon, brown carbon and organic carbon and can also contain inorganic material (ash) and heavy metals from contaminated biomass fuel. Most of the particle emissions arising from biomass burning fall in the $PM_{2.5}$ fraction (particulate matter with an aerodynamic diameter of less than or equal to 2.5µm) (Reid et al., 2005).

Although biomass burning is a relatively small source category with a global contribution to mortality by ambient fine particles ($PM_{2.5}$) and ozone (O_3) of about 5%, its areal range is large (e.g. in South America and Africa) and is the main source of air pollution in large parts of Canada, Siberia, Africa, South America and Australia (Karanasiou et al., 2021). Australian cities are frequently affected by bushfire smoke given their proximity to highly flammable native vegetation and hot dry weather conditions that favour combustion (Johnston et al., 2011).

Methods for reducing the hazard of bushfires include prescribed burning of potential bushfire fuel by fire management agencies. As these burns use the same fuels as bushfires, smoke from such fires can also be considered bushfire smoke (Jegasothy et al., 2023).

2.1.4 Health impacts

Bushfires can have substantial impacts on human health directly and indirectly through exposure to heat (e.g. burns and destructive impacts), emissions (smoke-related health impacts), and altered ecosystem functioning (e.g. biodiversity, amenity, water quality, and climate impacts) (Johnston et al., 2024). This investigation focuses on smoke-related health impacts. Bushfire events can cause large emissions of gaseous and particulate matter (PM) air pollutants, with PM thought to be the main health risk from bushfire smoke – particularly $PM_{2.5}$ which makes up around 90% of PM emitted from bushfires (Jegasothy et al., 2023).

Ambient air quality in Australia is regulated by the National Environment Protection Measure (NEPM), which sets for example, a maximum 24-hour mean concentration of 50 $\mu g/m^3$ for particulate matter less than 10µm in diameter (PM_{10}) and 25 $\mu g/m^3$ for PM2.5 (Department of Climate Change, 2021). Each state and territory are required by the NEPM to annually report all breaches of this standard, including the sources of pollution.

The effects of bushfire smoke on population and occupational health and the gaps in research are highlighted below.

Respiratory system impacts

The major impact of bushfire smoke on the healthcare system comes from patients seeking care for respiratory symptoms (Black et al., 2017). Emergency visits for respiratory symptoms increase in smoke-affected areas, and more specifically, patients are more likely to visit hospital emergency departments for asthma, bronchitis, dyspnea, and chronic obstructive pulmonary disease (COPD) symptom (pooled effects have been estimated as 4.1% and 4.8% increased risk of respiratory emergency visits, per 10 $\mu g/m^3$ increases in $PM_{2.5}$ and PM_{10} respectively (Karanasiou et al., 2021). Hospital admissions and outpatient visits for respiratory symptoms also increase with bushfire smoke exposure. Bushfire smoke exposure is associated with increases in specific symptom scores and surrogate markers (e.g. significant increase in COPD symptom scores on days when ambient particulate counts spike due to bushfires). In asthma patients, bushfire smoke exposure is associated with increases in asthma symptoms, asthma hospitalisations, emergency department visits, and increased corticosteroid and rescue inhaler use (Borchers Arriagada et al., 2019; Elliot et al., 2013; Johnston et al., 2006).

Studies performed on firefighters report a decline in forced expiratory capacity in 1 s (FEV1) following a full season of firefighting compared to preseason values but an eventual return to

baseline FEV1 in the post season, although the recovery period appears to be on the order of months following exposure (Black et al., 2017). Studies comparing pre-shift and post-shift values instead of preseason and postseason values, report no change in FEV1, suggesting that lung function decline is not an acute event but is rather associated with longer smoke exposures.

Cardiovascular system impacts

In contrast to respiratory health risks, the data on cardiovascular risks from bushfire smoke are mixed. Multiple studies report no increase in hospital admissions or ED visits for cardiovascular events during bushfire events, while other studies have shown increases in cardiac events during bushfires. Australian examples include a reported association between bushfire $PM_{2.5}$ and risk of out of hospital cardiac arrest from the 2006–2007 bushfires in Victoria (Dennekamp et al., 2015; Haikerwal et al., 2015) and increased outpatient cardiovascular visits among Indigenous Australians following bushfires (Johnston et al., 2007). These studies raise the question whether bushfire smoke may be associated with cardiovascular health effects in specific populations or exposure conditions. In the future, discrepancies between studies may be explained by better characterising the exposure in question.

Numerous epidemiological, biomedical and clinical studies indicate that ambient particulate matter in air pollution is strongly associated with increased cardiovascular disease such as myocardial infarction, cardiac arrhythmias, ischemic stroke, vascular dysfunction, hypertension and atherosclerosis (Du et al., 2016). The molecular mechanisms for PM-caused cardiovascular disease include direct toxicity to the cardiovascular system or indirect injury by inducing systemic inflammation and oxidative stress in peripheral circulation.

Theoretically, PM_{10} particles preferentially deposit in the upper airways, meanwhile $PM_{2.5}$ and ultrafine particles more easily reach the smallest airways and alveoli, and ultrafine particles may further penetrate the alveolar-capillary membrane and spread into systemic circulation (Du et al., 2016). It has been reported that ultrafine particles can be found in remote organs which may indicate that they could induce specific organ toxic effects (Du et al., 2016). In addition, ambient aerosols appear when ambient particles interact with atmospheric gases (ozone, sulphur and nitric oxides and carbon monoxide). Each of those aerosols can have independent and potentially synergistic or antagonistic effects with each other and with PM.

Several pathways have recognised that can explain the link between PM particles and cardiovascular diseases: a direct pathway, where $PM_{2.5}$ and ultrafine particles directly translocate into the bloodstream and target remote organs; or indirect pathways including pulmonary oxidative stress and inflammatory response, which is less acute and occurs after several hours or days of inhalation, and interaction on the autonomic nervous system via specific lung receptors (Du et al., 2016).

A recently published umbrella review covering 56 articles published between 2010 and 2020 including 20 meta-analyses demonstrated a robust correlation between short-term exposure to PM_{10} and $PM_{2.5}$ and an elevated risk of hospital admissions related to stroke (de Bont et al., 2022). The strongest evidence was found between higher short- and long-term ambient air pollution exposure and all-cause CVD mortality and morbidity, stroke, and ischemic heart diseases. Short-term exposures to $PM_{2.5}$, PM_{10}, and nitrogen oxides (NO_x) were consistently associated with increased risks of hypertension and triggering of myocardial infarction, and stroke. Long-term

exposures of $PM_{2.5}$ were largely associated with increased risk of atherosclerosis, incident myocardial infarction, hypertension, and incident stroke and stroke mortality (de Bont et al., 2022). Few studies evaluated other CVD outcomes including arrhythmias, atrial fibrillation, or heart failure but they generally reported positive statistical associations. Stronger associations were found in Asian countries and vulnerable subpopulations, especially among the elderly, cardiac patients, and people with higher weight status.

From their systematic review and meta-analysis of 68 studies covering 23 million participants, Niu et al. (2021) also report that exposure to air pollution was positively associated with an increased risk of stroke hospital admission (from $PM_{2.5}$, PM_{10}, SO_2, NO_2, CO, and O_3), incidence ($PM_{2.5}$, SO_2, and NO_2), and mortality ($PM_{2.5}$, PM_{10}, SO_2, and NO_2).

Mortality

Data on overall mortality risk during a bushfire event are mixed. Too little data is available on the specific risks of bushfire smoke to make a conclusive comparison between bushfire smoke mortality and mortality from other air pollution sources. Many studies have found small associations between increased particulate matter due to bushfires and overall mortality. For example, when studying extreme air pollution events and mortality in Sydney from 1994-2007, Johnston et al. (2011) found a 5% increase in odds of non-accidental mortality in the day following a bushfire smoke event, and also that dust events were associated with a 15% increase in non-accidental mortality at a lag of 3 days. However, at least one study suggests that the mortality rate observed during bushfire events is consistent with the increase in mortality from elevated $PM_{2.5}$, regardless of source (Hänninen et al., 2009). Thus, it is difficult to determine whether any portion of the increased mortality risk observed during bushfire events is uniquely attributable to bushfire smoke. Also, as confounders to this problem, bushfires and dust storms tend to coincide with high ambient temperatures and higher maximum ozone concentrations, both of which have been independently associated with increased risk of mortality (Johnston et al., 2011). Researchers in this field have also at times made a distinction between all-cause mortality and cardiovascular mortality and respiratory mortality.

Jegasothy et al. (2023) examined the risk of mortality from bushfire-related $PM_{2.5}$ in Sydney from 2010-2020 and found a 10 $\mu g/m^3$ increase in bushfire $PM_{2.5}$ was associated with a 3.2% increase in risk of all-cause mortality in the 3 days following exposure. These effects were present in those aged 65 years and over, while no effect was observed in people under 65 years. Other studies report smaller and non-significant outcomes. Morgan et al. (2010) found a 0.8% increase in all-cause mortality per 10 $\mu g/m^3$ rise in PM_{10} during 32 bushfire days in Sydney but reported no association with cardiovascular mortality or respiratory mortality. Hänninen et al. (2009) found increases in mortality in the order of 1% per 10 $\mu g/ m^3$ rise in PM_{10} associated with forest fires in Finland.

Karanasiou et al. (2021) undertook a systematic review on the health effects of bushfire emissions in the framework of the WHO activities on air pollution. A total of 81 papers were considered as relevant for mortality and morbidity effects and WHO experts and external advisors were solicited for their critical analysis and consolidated expertise in the field. They report that PM_{10} and $PM_{2.5}$ concentrations originating from bushfires were associated with all-cause mortality, with pooled effects estimated at 1.3% and 1.9% increased all-cause mortality per 10 $\mu g/m^3$ rise in PM_{10} and $PM_{2.5}$ respectively. They also found the risk of cardiovascular mortality was increased by 3.3% for a

10 μg/m^3 rise in PM2.5 concentration. A more recent examination of 21.6 million cardiovascular and 7.7 million respiratory deaths in 380 cities across 24 countries report lower effects: 0.9% for cardiovascular mortality and 1.3% for respiratory mortality per 10μg/m^3 increase in $PM_{2.5}$ (Schwarz et al., 2024).

Studies in sub-population groups

Multiple studies have assessed whether specific populations are more susceptible to bushfire smoke exposure than the general population. Health effects from bushfires are related to age, pre-existing health conditions, gender, ethnicity and socio-economic status (Karanasiou et al., 2021). Larger positive associations between bushfire smoke and cardiorespiratory morbidities are observed for the elderly, middle-aged and older adults compared to other age groups.

There is inconclusive evidence of increased vulnerability to adverse health effects from bushfire smoke exposure among children. Some studies report a higher risk of increased respiratory-symptoms, asthma, and hospital contacts associated with bushfire smoke for children compared with other age groups (Karanasiou et al., 2021). For example, in a study assessing childhood asthma and air pollutants in Melbourne, Erbas et al. (2005) report consistent associations between childhood ED asthma presentations and PM_{10} concentrations, with a strongest association of RR = 1.17 (95% CI 1.05 to 1.31) and associations also observed for asthma ED presentations following NO_2 and ozone exposure. However, others (Johnston et al., 2006; Johnston et al. 2014; Jalaludin et al., 2000) report no associations present in children (<15 years) for any respiratory and cardiovascular outcome.

Indigenous Australians have been reported to experience higher rates of hospitalisation for respiratory infections and ischaemic heart disease associated with exposure to bushfire smoke than non-indigenous people (Hanigan et al., 2008, Johnston et al., 2007). This effect may be explained by underlying health status, access to medical services, or other social characteristics of this group. Socioeconomic status is another factor that may influence health effects from bushfire exposure. Jones et al. (2020) reported that lower socioeconomic status may have increased the risk of out-of-hospital cardiac arrest due to smoke exposure during bushfires whereas others have reported no differences in health outcomes between different socioeconomic groups (Henderson et al., 2011). Some studies have also demonstrated links between bushfire smoke exposure and pre-term birth and decreased birth weights (Karanasiou et al., 2021).

Hospital impacts

Many of the studies referenced in the above commentary describe impacts on hospitals in terms of higher rates of ED presentations and hospital admissions.

Haikerwal et al. (2016) analysed the 2006/2007 bushfire period in Victoria which, until that time, was the longest running collection of fires recorded in Victoria. The air quality during this period was substantially diminished with elevated surface concentrations of $PM_{2.5}$ found for most of the bushfire season. The maximum daily $PM_{2.5}$ concentration recorded across large parts of Victoria was greater than 200 μg/m^3 which substantially exceeded the allowable air quality standards for $PM_{2.5}$ as set by regulatory bodies (in Australia the advisory standard is 25 μg/m^3 for a 24-h period). There were around 15–20 days when $PM_{2.5}$ level was greater than 50 μg/m^3 (twice the advisory standard). The study found that an interquartile range increase in $PM_{2.5}$ levels of 8.6 μg/m^3 was

associated with an increase in emergency department attendances for asthma by 2% on the day of exposure, with a stronger association for women >20 yrs. No associations were found for COPD.

Johnston et al. (2014) investigated the association between forest fire smoke events and hospital emergency department visits in Sydney from 1996–2007. Fire smoke event days were associated with increases in emergency visits for all non-trauma conditions (3%), respiratory conditions (7%), asthma (23%), and COPD (12%).

Morgan et al. (2010) also investigated bushfires in Sydney and noted associations between daily particle levels from bushfires and hospital admissions for respiratory problems. They found that a 10 $\mu g/m^3$ increase in bushfire PM_{10} was associated with a 1% increase in all respiratory hospital admissions, a 4% increase in in COPD admissions (at a 2-day lag), and a 5% increase in adult asthma admissions.

For a study over the 7-month period of the dry season in Darwin, Johnston et al. (2002) found increased asthma emergency visits associated with PM_{10} (adjusted rate ratio of 1.2 per 10 $\mu g/m^3$ rise in PM_{10}), especially when PM_{10} exceeded 40 $\mu g/m^3$ (adjusted rate ratio, 2.4) compared with days when PM_{10} levels were less than 10 $\mu g/ m^3$. A later study undertaken in the same city found associations for asthma symptoms (IRR 1.24) and oral steroid medication use (IRR 1.035) with a 10 $\mu g/m^3$ increase in PM_{10} concentrations over a 7-month period (Johnston et al., 2006). Still in Darwin, Johnson et al. (2007) found a positive, but not statistically significant, relationship between PM_{10} and all respiratory admissions (OR 1.08) for each 10 $\mu g/m^3$ rise in PM_{10}, with a larger effect in the indigenous sub-population (OR 1.17). When examining smaller subgroups of respiratory conditions, a significant association was found for COPD hospital admissions (OR 1.21), which was greater for Indigenous residents admitted for COPD (OR 1.98), and for asthma and COPD combined (OR 1.19) but not for asthma (OR 1.14) (Johnston et al., 2007). For the same city, Hanigan et al. (2008) found that an increase of 10 $\mu g/m^3$ PM_{10} was associated with a 5% increase in all-cause respiratory hospital admissions during bushfires. A stronger association was found for Indigenous people than non-Indigenous (RR 1.15 vs. 1.007).

Martin et al. (2013) examined the association between bushfire smoke events and hospital admissions in Sydney, Newcastle and Wollongong from 1994 to 2007. They found that in Sydney, bushfire smoke events were associated with a 5% increase in all-cause respiratory-hospital admissions, COPD-hospital admissions increased 13%, and asthma 12%. Bushfire smoke events were also associated with increased admissions for respiratory conditions in Newcastle and Wollongong. Smith et al. (1996) also in Sydney, found no increase in asthma visits with PM_{10} increase during episode of exposure to bushfire emissions.

Hasnain et al. (2024) reviewed hospital admissions related to cerebrovascular disease (comprising ICD-10 diagnoses codes I60-I69) for an area comprising 7 local government areas around Newcastle NSW for the 2019–20 bushfire season in Australia. They found no significant increase in daily admissions for cerebrovascular disease over the entire bushfire period but found an association between particulate matter and high smoke days with increased hospital admissions for one specific cerebrovascular disease (ischaemic stroke).

Tham et al. (2009) in 3 Victoria cities in Australia affected by PM from bushfires found the strongest associations between PM_{10} and daily respiratory emergency visits (RR 1.018) but no significant associations were identified for hospital admissions. Chen et al. (2006) in Brisbane, Australia, found an increase of PM_{10} from low (<15 $\mu g/m^3$) to high level (>20 $\mu g/m^3$) was

accompanied by an increase of 19% in respiratory hospital admissions for bushfire days (RR 1.19) versus 13% for background days (RR 1.13).

Mental health

An increased rate of mental health disorders post-bushfire has been found in both the adult and paediatric population. Mental health impacts include increased rate of PTSD, depression, and generalised anxiety, from the time a bushfire occurs to years after (To et al., 2021). Behavioural changes in children following a bushfire event can include increased irritability and changes in concentration, sleep, and academic performance (To et al., 2021).

Researchers studying the mental health impact of bushfires have typically used surveys administered to study participants to gain an appreciation of mental health outcomes. When assessing the health impacts of prolonged exposure to bushfire smoke in the ACT and surrounding area during the 2019-20 bushfire season, Rodney et al. (2021) report that while almost all participants in their survey experienced at least one physical health symptom that they attributed to smoke (most commonly eye or throat irritation and cough), over half of responders self-reported symptoms of anxiety and/or feeling depressed and approximately half reported poorer sleep. Approximately 17% of people sought advice from a medical health practitioner, most commonly a general practitioner, to manage their symptoms. This observation is relevant to the modelling of air quality and PBS and MBS items related to mental health which is presented later in this report (see Section 2.3.9). Other researchers assessing this same event in the ACT grouped interview responses into the themes of disruption to daily life, physical and psychological effects, and shifting social connectedness (Williamson et al., 2022).

Other researchers report that while exposure to bushfire smoke may have mental health impacts, particularly in episodes of chronic and persistent smoke events, the evidence is inconsistent and limited (Eisenman and Galway, 2022). Qualitative studies disclose a wider range of impacts across multiple mental health and well-being domains and priorities for future research should include differentiating between mental illness and emotional well-being and identifying the causal processes that link bushfire smoke to mental health and well-being effects. This recommendation is also relevant to the statistical modelling presented in Section 2.3.9.

Novel terms have appeared in the literature to describe emotional and mental health responses to natural disasters such as solastalgia, eco-anxiety, and ecological grief, which may become more prominent as a result of predicted changes to bushfire patterns (To et al., 2021).

Medications

Exposure to bushfire smoke has also been associated with increases in medication use but again the evidence is inconsistent. Borchers Arriagada et al. (2019) describe three studies which demonstrated a positive and statistically significant association between $PM_{2.5}$ and salbutamol dispensations. Caamano-Isorna et al. (2011) reported a higher consumption of drugs for obstructive airway diseases among pensioners during the months following bushfires in regions affected by bushfires versus those unaffected by fire. Künzli et al. (2006) found increases in medication use and medical consultations with an increase in the duration of smoke exposure and in PM_{10} levels over 5 days in asthmatic individuals, however no associations were found for asthma attacks and use of medical services. Johnston et al. (2006) found no associations between $PM_{2.5}$ and the use of reliever medication or the mean number of times reliever medication was

used each day, but a positive association was reported for commencing the use of reliever medication and oral steroids. When assessing the association between sugar cane burning and acute respiratory illness on the island of Maui, Mnatzanaganian et al. (2015) found no significant associations between pharmacy prescriptions filled for medications used to treat respiratory conditions or conjunctivitis and days when cane was burned.

Gaps are assessing the long-term health impact of bushfire smoke

Most of the evidence on smoke-related health impacts is collected for $PM_{2.5}$ while other pollutants are less well understood and would benefit from more research since toxicity might differ. More research on multipollutant models, although methodologically challenging due to collinearity, might disentangle individual pollutant effects as well as explore the potential interaction between pollutants (de Bont et al., 2022).

A better mechanistic understanding of the body's response to bushfire smoke would lead toward health-relevant biomarkers of exposure, which are needed to track long-term effects of bushfire smoke exposure in the human population (Black et al., 2017). Studies in firefighters showing lung function decrements after a bushfire season suggest that lung function can return to baseline over a long follow-up period. However, the cumulative effect of repeated bushfire smoke injury and repair cycles on the lung is completely unknown. Similarly, it is unknown whether individuals with long-term sequelae and possible lung injury from COVID-19 have heightened risks from air pollution exposure (de Bont et al., 2022).

Likewise, little is known about the long-term effects on children. Exposure to air pollution during susceptible periods in childhood is associated with an altered growth trajectory in the lung. A mechanism explaining the health effects of bushfire smoke would help to predict how bushfire smoke interacts with the developing lung and other long-term health considerations in specific populations (Black et al., 2017).

2.1.5 References (bushfires and health)

Arriagada, N. B., Horsley, J. A., Palmer, A. J., Morgan, G. G., Tham, R., & Johnston, F. H. (2019). Association between fire smoke fine particulate matter and asthma-related outcomes: Systematic review and meta-analysis. Environmental Research, 179, 108777. https://doi.org/10.1016/j.envres.2019.108777 .

Blunden, J., & Boyer, T. (2024). State of the Climate in 2023. Bulletin of the American Meteorological Society, 105(8), S1-S484. https://doi.org/10.1175/2024BAMSStateoftheClimate.1

Bowman, D. M., Williamson, G. J., Abatzoglou, J. T., Kolden, C. A., Cochrane, M. A., & Smith, A. M. (2017). Human exposure and sensitivity to globally extreme wildfire events. Nature Ecology & Evolution, 1(3), 58. https://doi.org/10.1038/s41559-016-0058.

Bureau of Meteorology & Commonwealth Scientific and Industrial Research Organisation. (2024). State of the Climate 2024. http://www.bom.gov.au/state-of-the-climate/.

Caamano-Isorna, F., Figueiras, A., Sastre, I., Montes-Martínez, A., Taracido, M., & Piñeiro-Lamas, M. (2011). Respiratory and mental health effects of wildfires: an ecological study in Galician

municipalities (north-west Spain). Environmental Health: A Global Access Science Source, 10, 48. https://doi.org/10.1186/1476-069X-10-48.

Chen, L., Verrall, K., & Tong, S. (2006). Air particulate pollution due to bushfires and respiratory hospital admissions in Brisbane, Australia. International Journal of Environmental Health Research, 16(03), 181-191. https://doi.org/10.1080/09603120600641334.

de Bont, J., Jaganathan, S., Dahlquist, M., Persson, Å., Stafoggia, M., & Ljungman, P. (2022). Ambient air pollution and cardiovascular diseases: An umbrella review of systematic reviews and meta-analyses. Journal of Internal Medicine, 291(6), 779-800. https://doi.org/10.1111/joim.13467.

Dennekamp, M., Straney, L. D., Erbas, B., Abramson, M. J., Keywood, M., Smith, K., Sim, M. R., Glass, D. C., Del Monaco, A., Haikerwal, A., & Tonkin, A. M. (2015). Forest fire smoke exposures and out-of-hospital cardiac arrests in Melbourne, Australia: a case-crossover study. Environmental Health Perspectives, 123(10), 959-964. https://doi.org/10.1289/ehp.1408436.

Du, Y., Xu, X., Chu, M., Guo, Y., & Wang, J. (2016). Air particulate matter and cardiovascular disease: the epidemiological, biomedical and clinical evidence. Journal of Thoracic Disease, 8(1), E8–E19. https://doi.org/10.3978/j.issn.2072-1439.2015.11.37.

Eisenman, D. P., & Galway, L. P. (2022). The mental health and well-being effects of wildfire smoke: a scoping review. BMC Public Health, 22(1), 2274. https://doi.org/10.1186/s12889-022-14662-z.

Elliott, C. T., Henderson, S. B., & Wan, V. (2013). Time series analysis of fine particulate matter and asthma reliever dispensations in populations affected by forest fires. Environmental Health, 12, 1-9. https://doi.org/10.1186/1476-069X-12-11.

Erbas, B., Kelly, A. M., Physick, B., Code, C., & Edwards, M. (2005). Air pollution and childhood asthma emergency hospital admissions: estimating intra-city regional variations. International Journal of Environmental Health Research, 15(1), 11-20. https://doi.org/10.1080/09603120400018717.

Haikerwal, A., Akram, M., Del Monaco, A., Smith, K., Sim, M. R., Meyer, M., Tonkin, A. M., Abramson, M. J., & Dennekamp, M. (2015). Impact of Fine Particulate Matter (PM2.5) Exposure During Wildfires on Cardiovascular Health Outcomes. Journal of the American Heart Association, 4(7), e001653. https://doi.org/10.1161/JAHA.114.001653.

Haikerwal, A., Akram, M., Sim, M. R., Meyer, M., Abramson, M. J., & Dennekamp, M. (2016). Fine particulate matter (PM2.5) exposure during a prolonged wildfire period and emergency department visits for asthma. Respirology, 21(1), 88–94. https://doi.org/10.1111/resp.12613.

Hanigan, I.C., Johnston, F.H. & Morgan, G.G. (2008). Vegetation fire smoke, indigenous status and cardio-respiratory hospital admissions in Darwin, Australia, 1996–2005: a time-series study. Environmental Health, 7(42). https://doi.org/10.1186/1476-069X-7-42.

Hänninen, O. O., Salonen, R. O., Koistinen, K., Lanki, T., Barregard, L., & Jantunen, M. (2009). Population exposure to fine particles and estimated excess mortality in Finland from an East

European wildfire episode. Journal of Exposure Science & Environmental Epidemiology, 19(4), 414-422. https://doi.org/10.1038/jes.2008.31.

Hasnain, M. G., Garcia-Esperon, C., Tomari, Y. K., Walker, R., Saluja, T., Rahman, M. M., Boyle, A., Levi, C. R., Naidu, R., Filippelli, G., & Spratt, N. J. (2024). Bushfire-smoke trigger hospital admissions with cerebrovascular diseases: Evidence from 2019–20 bushfire in Australia. European Stroke Journal, 9(2), 468-476. https://doi.org/10.1177/23969873231223307.

Henderson, S. B., Brauer, M., MacNab, Y. C., & Kennedy, S. M. (2011). Three measures of forest fire smoke exposure and their associations with respiratory and cardiovascular health outcomes in a population-based cohort. Environmental Health Perspectives, 119(9), 1266-1271. https://doi.org/10.1289/ehp.1002288.

Intergovernmental Panel on Climate Change. (2014). Climate change 2014: Mitigation of climate change (Contribution of Working Group III to the Fifth Assessment Report of the Intergovernmental Panel on Climate Change). Cambridge University Press. https://www.ipcc.ch/report/ar5/wg3/.

Intergovernmental Panel on Climate Change. (2018). Summary for policymakers. In V. Masson-Delmotte, P. Zhai, H. Pörtner, et al. (Eds.), Global warming of 1.5°C. An IPCC special report on the impacts of global warming of 1.5°C above pre-industrial levels and related global greenhouse gas emission pathways, in the context of strengthening the global response to the threat of climate change, sustainable development, and efforts to eradicate poverty (pp. 3-24). Cambridge University Press. https://doi.org/10.1017/9781009157940.001.

Intergovernmental Panel on Climate Change. (2021). Climate change 2021: The physical science basis. Contribution of Working Group I to the Sixth Assessment Report of the Intergovernmental Panel on Climate Change (V. Masson-Delmotte, P. Zhai, A. Pirani, et al., Eds.). Cambridge University Press. https://doi.org/10.1017/9781009157896.

Jalaludin, B., Smith, M., O'Toole, B., & Leeder, S. (2000). Acute effects of bushfires on peak expiratory flow rates in children with wheeze: a time series analysis. Australian and New Zealand Journal of Public Health, 24(2), 174-177. https://doi.org/10.1111/j.1467-842X.2000.tb00138.x.

Jegasothy, E., Hanigan, I. C., Van Buskirk, J., Morgan, G. G., Jalaludin, B., Johnston, F. H., Guo, Y., & Broome, R. A. (2023). Acute health effects of bushfire smoke on mortality in Sydney, Australia. Environment International, 171, 107684. https://doi.org/10.1016/j.envint.2022.107684.

Johnston, F. H., Kavanagh, A. M., Bowman, D. M., & Scott, R. K. (2002). Exposure to bushfire smoke and asthma: an ecological study. Medical Journal of Australia, 176(11), 535-538. https://doi.org/10.5694/j.1326-5377.2002.tb04551.x.

Johnston, F. H., Webby, R. J., Pilotto, L. S., Bailie, R. S., Parry, D. L., & Halpin, S. J. (2006). Vegetation fires, particulate air pollution and asthma: a panel study in the Australian monsoon tropics. International Journal of Environmental Health Research, 16(6), 391-404. https://doi.org/10.1080/09603120601093642.

Johnston, F. H., Bailie, R. S., Pilotto, L. S., & Hanigan, I. C. (2007). Ambient biomass smoke and cardio-respiratory hospital admissions in Darwin, Australia. BMC Public Health, 7, 1-8. https://doi.org/10.1186/1471-2458-7-240.

Johnston, F., Hanigan, I., Henderson, S., Morgan, G., & Bowman, D. (2011). Extreme air pollution events from bushfires and dust storms and their association with mortality in Sydney, Australia 1994–2007. Environmental Research, 111(6), 811-816. https://doi.org/10.1016/j.envres.2011.05.007.

Johnston, F. H., Purdie, S., Jalaludin, B., Martin, K. L., Henderson, S. B., & Morgan, G. G. (2014). Air pollution events from forest fires and emergency department attendances in Sydney, Australia 1996–2007: a case-crossover analysis. Environmental Health, 13, 1-9. https://doi.org/10.1186/1476-069X-13-105.

Johnston, F. H., Williamson, G., Borchers-Arriagada, N., Henderson, S. B., & Bowman, D. M. (2024). Climate change, landscape fires, and human health: a global perspective. Annual Review of Public Health, 45. https://doi.org/10.1146/annurev-publhealth-060222-034131.

Jones, C. G., Rappold, A. G., Vargo, J., Cascio, W. E., Kharrazi, M., McNally, B., & Hoshiko, S. & the CARES Surveillance Group. (2020). Out-of-hospital cardiac arrests and wildfire-related particulate matter during 2015–2017 California wildfires. Journal of the American Heart Association, 9(8), e014125. https://doi.org/10.1161/JAHA.119.014125.

Jones, M. W., Abatzoglou, J. T., Veraverbeke, S., Andela, N., Lasslop, G., Forkel, M., Smith, A. J. P., Burton, C., Betts, R. A., van der Werf, G. R., Sitch, S., Canadell, J. G., Santín, C., Kolden, C., Doerr, S. H., & Le Quéré, C. (2022). Global and regional trends and drivers of fire under climate change. Reviews of Geophysics, 60(3), e2020RG000726. https://doi.org/10.1029/2020RG000726.

Karanasiou, A., Alastuey, A., Amato, F., Renzi, M., Stafoggia, M., Tobias, A., Reche, C., Forastiere, F., Gumy, S., Mudu, P., & Querol, X. (2021). Short-term health effects from outdoor exposure to biomass burning emissions: A review. Science of The Total Environment, 781, 146739. https://doi.org/10.1016/j.scitotenv.2021.146739.

Künzli, N., Avol, E., Wu, J., Gauderman, W. J., Rappaport, E., Millstein, J., Bennion, J., McConnell, R., Gilliland, F. D., Berhane, K., Lurmann, F., Winer, A., & Peters, J. M. (2006). Health effects of the 2003 Southern California wildfires on children. American Journal of Respiratory and Critical Care Medicine, 174(11), 1221-1228. https://doi.org/10.1164/rccm.200604-519OC.

Martin, K. L., Hanigan, I. C., Morgan, G. G., Henderson, S. B., & Johnston, F. H. (2013). Air pollution from bushfires and their association with hospital admissions in Sydney, Newcastle and Wollongong, Australia 1994–2007. Australian and New Zealand Journal of Public Health, 37(3), 238-243. https://doi.org/10.1111/1753-6405.12065.

Mnatzaganian, C. L., Pellegrin, K. L., Miyamura, J., Valencia, D., & Pang, L. (2015). Association between sugar cane burning and acute respiratory illness on the island of Maui. Environmental Health, 14, 1-8. https://doi.org/10.1186/s12940-015-0067-y.

Morgan, G., Sheppeard, V., Khalaj, B., Ayyar, A., Lincoln, D., Jalaludin, B., Beard, J., Corbett, S., Lumley, T. (2010). Effects of bushfire smoke on daily mortality and hospital admissions in

Sydney, Australia. Epidemiology, 21(1), 47-55. https://doi.org/10.1097/EDE.0b013e3181c15d5a.

National Environment Protection (Ambient Air Quality) Measure 2021 (Australia). https://www.legislation.gov.au/F2007B01142.

NOAA National Centers for Environmental Information, Monthly Global Climate Report for Annual 2024, published online January 2025, https://www.ncei.noaa.gov/access/monitoring/monthly-report/global/202413

Niu, Z., Liu, F., Yu, H., Wu, S., & Xiang, H. (2021). Association between exposure to ambient air pollution and hospital admission, incidence, and mortality of stroke: an updated systematic review and meta-analysis of more than 23 million participants. Environmental Health and Preventive Medicine, 26, 1-14. https://doi.org/10.1186/s12199-021-00937-1.

Reid, J. S., Koppmann, R., Eck, T. F., & Eleuterio, D. P. (2005). A review of biomass burning emissions part II: intensive physical properties of biomass burning particles. Atmospheric Chemistry and Physics, 5(3), 799-825. https://doi.org/10.5194/acp-5-799-2005.

Rodney, R. M., Swaminathan, A., Calear, A. L., Christensen, B. K., Lal, A., Lane, J., Leviston, Z., Reynolds, J., Trevenar, S., Vardoulakis, S., & Walker, I. (2021). Physical and mental health effects of bushfire and smoke in the Australian Capital Territory 2019–20. Frontiers in Public Health, 9, 682402. https://doi.org/10.3389/fpubh.2021.682402.

Schwarz, M., Peters, A., Stafoggia, M., de'Donato, F., Sera, F., Bell, M. L., Guo, Y., Honda, Y., Huber, V., Jaakkola, J. J. K., Urban, A., Vicedo-Cabrera, A. M., Masselot, P., Lavigne, E., Achilleos, S., Kyselý, J., Samoli, E., Hashizume, M., Ng, C. F. S., Pereira da Silva, S. N.Zanobetti, A. (2024). Temporal variations in the short-term effects of ambient air pollution on cardiovascular and respiratory mortality: a pooled analysis of 380 urban areas over a 22-year period. The Lancet Planetary Health, 8(9), e657-e665. https://doi.org/10.1016/S2542-5196(24)00168-2.

Smith, M. A., Jalaludin, B. I. N., Byles, J. E., Lim, L., & Leeder, S. R. (1996). Asthma presentations to emergency departments in western Sydney during the January 1994 bushfires. International Journal of Epidemiology, 25(6), 1227-1236. https://doi.org/10.1093/ije/25.6.1227.

Tham, R., Erbas, B., Akram, M., Dennekamp, M., & Abramson, M. J. (2009). The impact of smoke on respiratory hospital outcomes during the 2002–2003 bushfire season, Victoria, Australia. Respirology, 14(1), 69-75. https://doi.org/10.1111/j.1440-1843.2008.01416.x.

To, P., Eboreime, E., & Agyapong, V. I. (2021). The impact of wildfires on mental health: a scoping review. Behavioral Sciences, 11(9), 126. https://doi.org/10.3390/bs11090126.

United Nations Environment Programme. (2021). Emissions Gap Report 2021: The Heat Is On. https://www.unep.org/resources/emissions-gap-report-2021.

van der Velde, I. R., van der Werf, G. R., Houweling, S., Maasakkers, J.D., Borsdorff, T., Landgraf, J., Tol, P., van Kempen, T.A., van Hees, R., Hoogeveen, R., Veefkind, J.P., Aben, I. (2021). Vast CO_2 release from Australian fires in 2019-2020 constrained by satellite. Nature, Sep;597(7876):366-369. https://doi.org/10.1038/s41586-021-03712-y

Van Oldenborgh, G. J., Krikken, F., Lewis, S., Leach, N. J., Lehner, F., Saunders, K. R., van Weele, M., Haustein, K., Li, S., Wallom, D., Sparrow, S., Arrighi, J., Singh, R. K., van Aalst, M. K., Philip, S.

Y., Vautard, R., & Otto, F. E. L. (2020). Attribution of the Australian bushfire risk to anthropogenic climate change. Natural Hazards and Earth System Sciences, 21(3), 1-46. https://doi.org/10.5194/nhess-21-941-2021.

Williamson, R., Banwell, C., Calear, A. L., LaBond, C., Leach, L. S., Olsen, A., Walsh, E. I., Zulfiqar, T., Sutherland, S., & Phillips, C. (2022). Bushfire smoke in our eyes: community perceptions and responses to an intense smoke event in Canberra, Australia. Frontiers in Public Health, 10, 793312. https://doi.org/10.3389/fpubh.2022.793312.

2.2 Air quality modelling

Unfortunately, modelled air quality simulations that include bushfire smoke in the 2050 period do not exist. A work-around for this problem is proposed: to add the air quality forecast model (AQFx) data from the extreme bushfire period in 2019/2020 to the changes in air quality expected by 2050. These expected changes come from the National Environment Science Program (NESP) air quality runs available for 2048-2052. The NESP model runs highlight changes in Australia's air quality from climate change and includes dust storms, sea salt, summer urban smog events and emissions that increase with higher temperatures such as biogenic hydrocarbons. The air quality model runs use input meteorology from 4 Global Climate Models (GCMs) under 2 different socioeconomic pathways (SSPs) for 2048-2052. The changes by 2050 are ascertained by comparison to current day runs (2013-2017) for each of the GCMs.

Baseline air quality is expected to change under a warming climate due to increased drought and higher temperatures impacting chemical reaction rates and emissions generation.

Importantly, the approach does not consider that similar bushfires in a future warmer climate may be bigger and more intense than the 2019/20 fire. The Future Climate and Hazard Insights report (pending publication in review) shows an example where the coverage of dangerous fire weather related to the 2009 Victoria Black Saturday fire was expected to be about 3 times larger under 2°C of global warming.

2.2.1 Climate change assessment method

The CSIRO chemical transport model

The chemical transport model (CTM) is a modelling framework designed to predict the concentrations of gases and aerosols due to emissions, transport, chemical reaction and deposition (Cope et al., 2009). To represent air quality in the future, emissions here are represented via a 'bottom-up' method where processes are related to input meteorology rather than based on ground and satellite-based observations like AQFx.

Meteorological conditions are provided to the CTM by the Conformal Cubic Atmospheric Model (CCAM) (McGregor and Dix, 2008). CCAM can downscale meteorological data from any source to the CTM, be it from observations, or in the case of this project, using output from Global Climate Models (GCMs). It is the CTM that produces the pollutant concentrations for the NESP2 "air quality in a changing climate" project.

The model chemistry scheme is MOZART-T1 (Emmons et al., 2019) incorporating the latest research on isoprene oxidation pathways via additional radical production under low NO_x conditions. Background chemistry conditions at the boundaries of the CTM come from measurements from the Kennaook-Cape Grim Baseline Atmospheric Research Station on the northwest coast of Tasmania. Other boundary conditions are provided from a global chemistry version of the Australian Community Climate and Earth System simulator (Woodhouse et al., 2015).

The aerosol framework is a two-bin sectional scheme, processing organic species by the Volatility Basis Set (Shrivastava et al., 2008) and processing inorganic species via ISORROPIA_II (Fountoukis

and Nenes, 2007). The high and low NO_x aerosol mass yields for the organic species, including isoprene, are provided by Tsimpidi et al. (2010).

NESP2 "Air quality in a changing climate" model runs

Four Global Climate Models (GCMs) were chosen from a group of CMIP6 models (Climate Model Intercomparison Project 6) being used in the Australian Climate Services project, based on the Grose et al. (2023) assessment of what the resulting impacts on Australia were going to be by 2100 (Table 1). The four models chosen represent a wide geographical spread in where they are produced/developed.

Table 1 Outcomes for Australia by 2100 from chosen Global Climate Models (GCM) for Australia. Taken from Grose et al. (2023).

Table 1 Outcomes for Australia by 2100 from chosen Global Climate Models (GCM) for Australia

MODEL	GCM NAME	DESCRIPTION
ACC	ACCESS-ESM1.5	A hotter and much drier future
CNRM	CNRM-ESM2-1	A much hotter future, much drier especially in the east, but wetter in the northwest
NCAR	NCAR CESM2	A hotter future, wetter in parts of the east and north
NOR	NorESM2-MM	Lower warming, mid-range changes in rainfall

Taken from Grose et al. (2023)

CCAM downscaled meteorology has been produced at a horizontal resolution of 20 km and a 1 hourly time resolution for the years 2048-2052. Five years are chosen centred on 2050, as use of a single year may not be representative of the entire decade. Each of the four GCMs have been run for two socio economic pathways (SSPs): SSP1-2.6 and SSP3-7.0 (Figure 1).

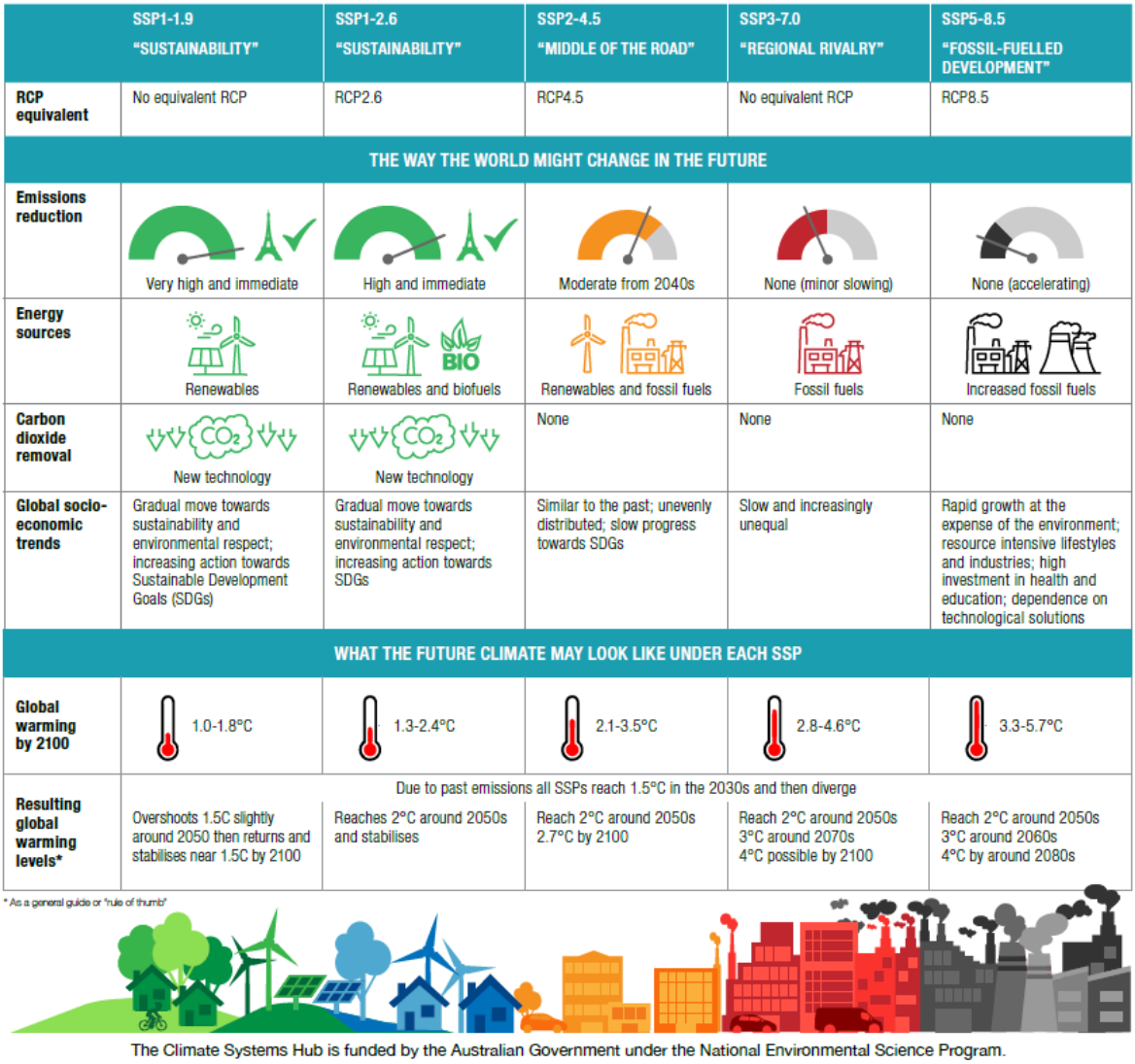

Figure 1 Understanding SSPs. Taken from the NESP Climate Systems Hub's SSP explainer factsheet (CSH, 2024).

SSP1-2.6 is relevant to trying to keep under the 2°C target by 2100. The climate outcomes assume a high level of emissions reduction has been undertaken globally, e.g. no diesel.

SSP3-7.0 is described as 'regional rivalry' where the climate outcomes assume some continued use of fossil fuels. It is a more moderate scenario than the worst case SSP585 scenario that results in an 8.5 W m-2 outcome in 2100.

To be clear, the CTM only uses the meteorological outputs from the GCMs, not the emission pathways described by the SSPs.

For the purposes of this report, NESP2 model runs will be referred to as the model and SSP number, e.g. ACC126 for the ACCESS-ESM1.5 model at SSP1-2.6.

Comparison to the current years

The data from the GCMs are considered to be 'raw' output, and thus contain a model bias. Thus, resulting concentrations of pollutants from one model cannot be directly compared to another unless biases are removed. Removal of biases was beyond the scope of the project. In consultation with the Climate Systems Hub, an acceptable work-around was to compare each future period (2048 to 2052) with a run from the current period (2013 to 2017) from the same GCM. This

removes the model bias. Thus, the differences between the future and current model runs can be compared directly.

$$Difference = \frac{\sum_{2048}^{2052} future - \sum_{2013}^{2017} current}{5}$$

A positive difference indicates the future period is higher, whilst a negative difference implies the future period is lower than current conditions.

2.2.2 Climate change assessment results

Changes in meteorological variables by the 2050 period

Data for the summer period is used (December to February). Each of the GCMs predict different outcomes by the 2048-2052 period (Figure 2), and these data are a good example why output from a single model cannot be used to study what might occur in future. It is much better to examine a range in outcomes.

Of note is that each model is providing quite similar patterns of results at SSP1-2.6 and SSP3-7.0 by the 2050 period. This is because the majority of model divergence is expected to occur between 2050 and 2100. However, there are differences which can be teased out here.

The NCAR and NOR models predict increased temperatures of up to 8 K, particularly in southwest WA. Higher temperatures increase emissions of natural volatile organic compounds from vegetation and increase the likelihood of urban smog forming. There are some regions of ocean around Australia that are predicted to have lower temperatures in 2048-2052 than the current time period (coloured blue, down to -1 K). Only ACC126 and ACC370 predict lower temperatures of -0.2 K over the land – west WA for ACC126 and northern WA in ACC370.

Western Australia is also subject to higher windspeeds (7-12 m/s) and reduced cloud cover (by 0.44 units) in the NCAR and NOR models. Both ACC126 and ACC370 models predict lower wind speeds in the Southern Ocean (-20 m/2), whereas the CNRM models predict the opposite (12-18 m/2). Higher oceanic wind speeds will increase the emission of sea salt to the air, whilst higher wind speeds over land could increase dust emissions. Dust emissions are also a function of soil moisture and vegetation coverage.

Lower cloud cover is predicted in most of the models across all the model grid, which could increase photosynthesis and photolysis rates in the future. Both ACC models predict increased cloud cover (0.13-0.16 units) across the central and southern parts of Australia.

Higher rainfall in the north of Australia is predicted by both ACC and NCAR models (4-9 mm/h), otherwise a decrease is predicted for the rest of Australia by most models (up to -10 mm/h). Lower rainfall is a factor in dust production, but also impacts the rainout rate of airborne particles.

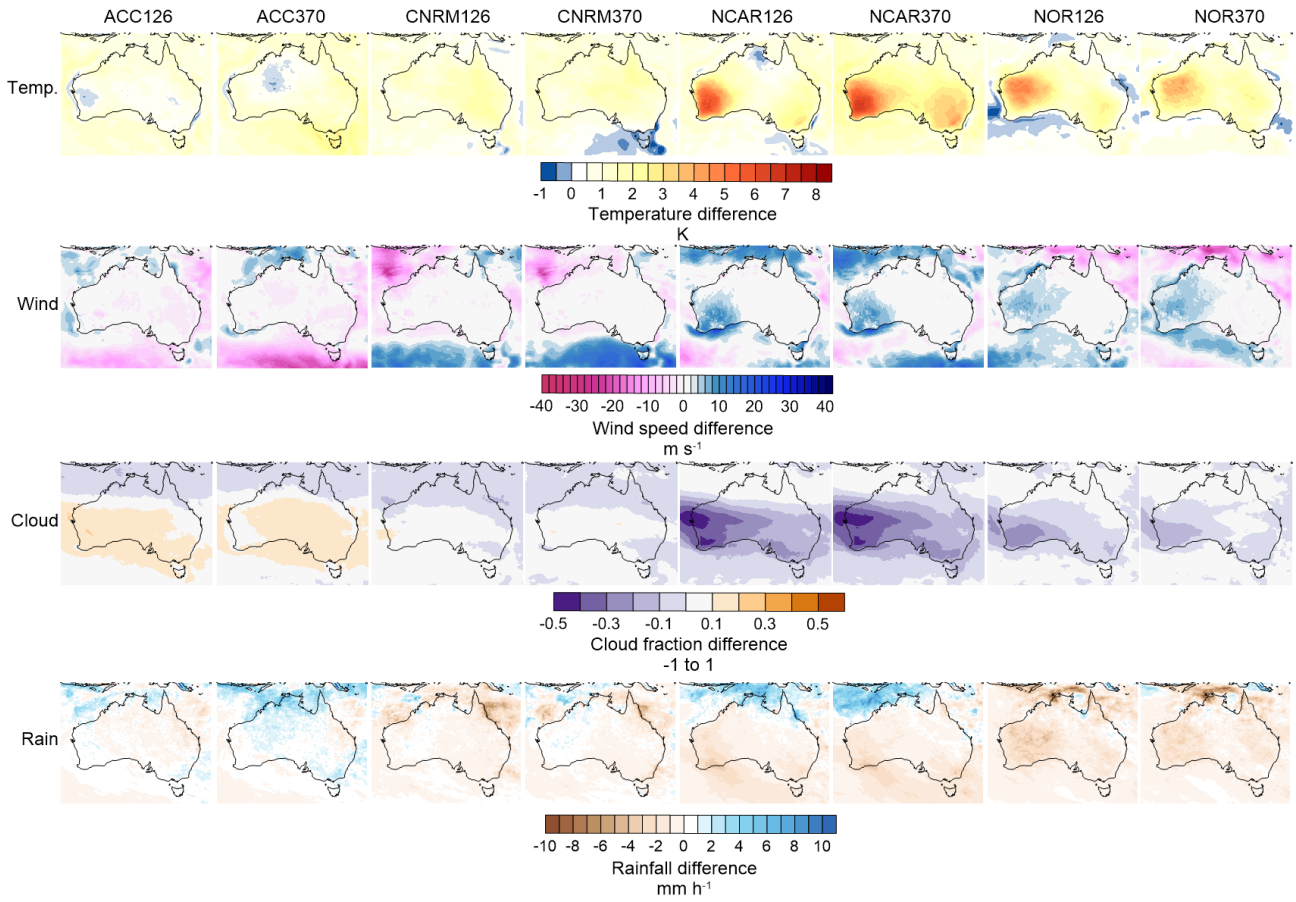

Figure 2 Five-yearly average summer (DJF) differences in meteorological variables between future (2048-2052) and present (2013-2017) runs for the 8 GCMs across Australia. From top, temperature, wind speed, cloud cover and rainfall.

Changes in airborne pollutants by the 2050 period (excluding bushfires)

The impacts of climate change on airborne pollutants from the NESP2 runs are now discussed. The five yearly monthly differences for each pollutant are presented, noting that day to day variations could be higher.

Differences in PM_{10} for December and January in all 8 models are shown in Figure 3. The legend shows differences in PM_{10} between -50 and +60 $\mu g/m^3$. Starting with models that predict mostly a decrease to PM_{10} in future are ACC and CNRM. ACC370 in particular has high rainfall predicted in northern Australia than other models, which would help to wash particles from the atmosphere. The reduction in PM_{10} over the land is of the order of 1 or 2 $\mu g/m^3$. The largest reductions are restricted to small locations in the dust driving regions, e.g. NOR370 in in central Australia, and ACC370 in WA in January. These are attributed to slightly lower windspeeds at these locations in the future.

All models show some degree of increase in dust emissions in central and southern Australia. NCAR126 and NCAR370 are predominantly predicting increases to PM_{10} across all of Australia with peaks in southeastern WA and west WA. NOR126 and Nor370 are the only models to predict different patterns for December (increase) and January (decrease) in the mostly dust producing regions.

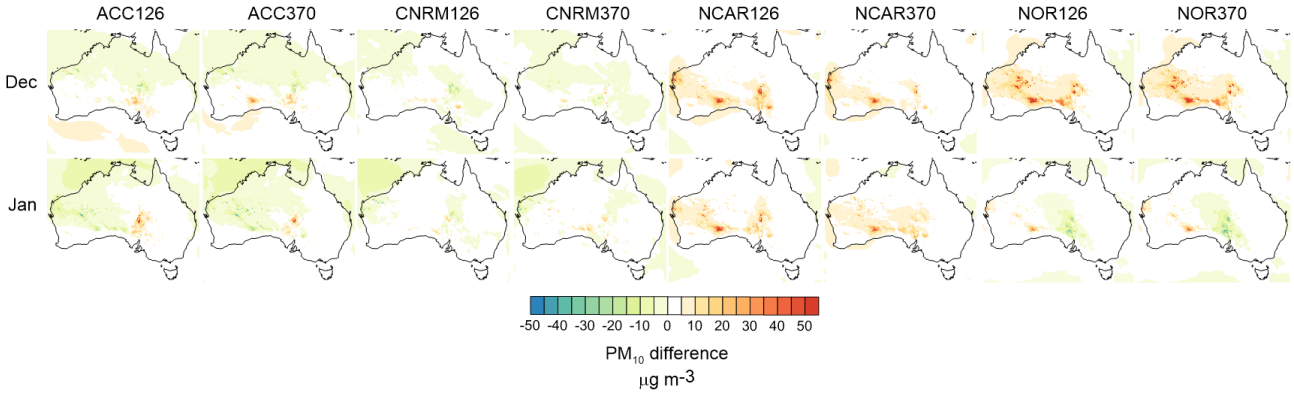

Figure 3 Five-yearly average differences in PM_{10} between future (2048-2052) and present (2013-2017) runs for the 8 GCMs across Australia. Top row is December, bottom row is January.

There are similarities in the patterns of $PM_{2.5}$ difference predictions (Figure 4) as there were for PM_{10}. This is because PM_{10} contains all particles smaller than 10 □m, and thus by definition incorporates $PM_{2.5}$ within it. The legend for the $PM_{2.5}$ difference is between -10 and +10 □g/m^3. Larger decreases are observed in January for the ACC and CNRM models in the northeast oceanic regions, whilst increases occur in the Southern Ocean regions of these models. NCAR predicts the largest increase of all the models, with western WA prominent. The decrease in $PM_{2.5}$ in NOR370 during January in central Australia follows the same pattern as for PM_{10}.

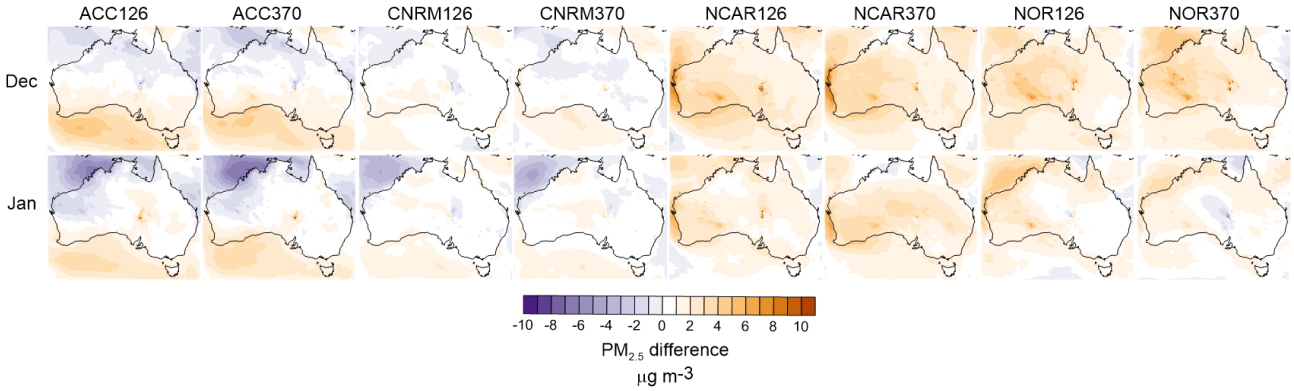

Figure 4 Five-yearly average differences in $PM_{2.5}$ between future (2048-2052) and present (2013-2017) runs for the 8 GCMs across Australia. Top row is December, bottom row is January.

Figure 5 shows the 5-yearly monthly differences in ozone for the 8 models. The legend shows changes between -4 and +6 ppb. Ozone is a secondary pollutant, produced via chemical reactions of primary pollutants such as biogenic volatile organic compounds and oxidants. Ozone is therefore sensitive to temperature induced changes in natural emissions from vegetation, which are set to increase under a warming climate. A 2 ppb increase in the dominant natural volatile organic compound isoprene caused up to a 20 ppb increase in peak hourly ozone in Sydney (Emmerson et al., 2020). Ozone is also very sensitive to photolysis rates, which themselves are dependent on levels of cloud cover. More ozone is expected in regions of higher temperatures and lower cloud cover. As tropospheric ozone has a lifetime of up to several weeks in non-polluted areas (Stevenson et al., 2006), it can be found in remote regional and oceanic locations. In polluted areas, ozone reacts much faster with a lifetime of a few hours, contributing to smog formation. All models but CNRM370 predict an increase of 2-4 ppb (as a monthly average) ozone in cities on the southeast coast.

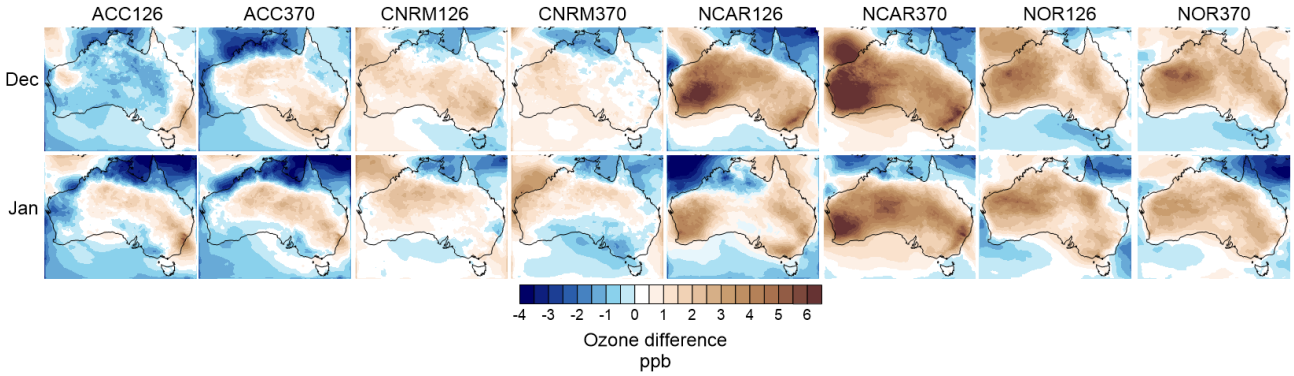

Figure 5 Five-yearly average differences in ozone between future (2048-2052) and present (2013-2017) runs for the 8 GCMs across Australia. Top row is December, bottom row is January.

And finally, Figure 6 shows how concentrations of NO_2 might vary in future according to the GCMs. The differences are +/- 2 ppb and the largest increases and decreases are highly localised near to Australia's major coastal cities. This effect is solely caused by changes in the speed of chemical reactions due to changes in meteorology, as the anthropogenic emissions have not changed in any of our 2048 to 2052 runs. ACC126 and ACC370 are the only models predicting increased NO_2 close to Sydney, Brisbane, Adelaide and Perth whilst all the other models predict decreases in NO_2. NCAR370 predicts the greatest spread of increased NO_2 concentrations across Australia than any of the GCMs, whilst the largest spread of decreased NO_2 over the land occurs in ACC126 in December and NCAR126 in January.

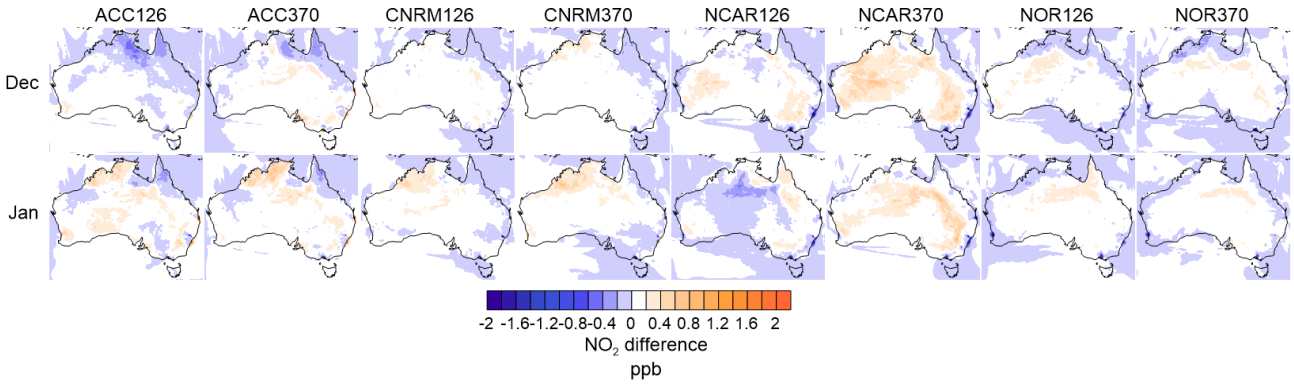

Figure 6 Five-yearly average differences in NO_2 between future (2048-2052) and present (2013-2017) runs for the 8 GCMs across Australia. Top row is December, bottom row is January

2.2.3 Bushfire smoke assessment method

As model data for 2050 that includes bushfire smoke does not exist, the 2019/2020 summer bushfires was used as an extreme event example. Forecasts from CSIRO's Air Quality Forecasting System (AQFx - https://www.csiro.au/en/research/disasters/bushfires/Smoke-forecasting) are used to model air quality associated with these bushfires.

AQFx was developed by CSIRO and used operationally at the Bureau of Meteorology to forecast smoke from prescribed burns and bushfires (Reisen, 2022). AQFx incorporates weather forecasts at 9km spatial resolution across Australia for up to 2-3 days ahead. Currently AQFx uses a layered approach to describe how the fire burns and spreads:

1. A top-down approach which calculates the daily fuel burnt from satellite observations of fire radiative power (FRP), assuming persistence for the following day;

2. A bottom-up approach where daily area burnt is determined from the near real-time bushfire boundaries in the digital atlas (https://digital.atlas.gov.au/apps/641aa0a80e254082bcf0d8cfeed3b56d/explore) or calculated from satellite hotspot density. Daily fuel burnt is calculated from fuel load (fine and coarse) and burning efficiency;
3. A prognostic approach where the area burnt is derived from a fire spread model (e.g., PHOENIX or SPARK) to estimate the likely areas burned for the following day.

AQFx then uses smoke emission rates (combustion vs smouldering) and applies a dynamic plume rise algorithm (based on fire energy output) to transport the smoke. The energy output is derived from the SPARK fire spread model. The AQFx system also incorporates the Chemical Transport Model (CTM, described earlier) and uses other natural and anthropogenic emissions using inventories, aiming to produce as realistic a picture of air quality concentrations for Australia as possible, on an hourly basis.

2.2.4 Bushfire smoke assessment results

For this project, AQFx data was obtained from 1 December 2019 to 31 January 2020. This period incorporates the period known as the 'black summer' bushfires, acknowledged as the most extreme fire event in Australia to date (Binskin, 2020). During the final quarter of 2019 and the first of 2020, bushfires burned in many forested regions of Australia, and smoke affected large numbers of people in New South Wales, Queensland, the Australian Capital Territory and Victoria. The scale and duration of these bushfires was unprecedented in Australia (Borchers Arriagada et al., 2020) and smoke was so severe it affected cities in Argentina, 11,000 km away (Hasnain et al., 2024). It also produced a wide-spread phytoplankton bloom in the Southern Ocean (Tang et al., 2021). The likelihood of the extreme drought and fire weather associated with the Black Summer was estimated to be a 1 in 200-year event in the current climate from a large ensemble of climate simulations (Squire et al., 2021).

Severe air pollution events from bushfires and dust are usually short-lived, but the resulting particulate matter (PM) can reach extreme concentrations, travel vast distances, and affect densely populated areas far from their source (Johnston et al., 2011).

One of the worst days for smoke exposure in southeast Australia in this period was 1 January 2020. Residents of Canberra were subject to $PM_{2.5}$ levels more than 38 times the limit on this day, but extreme levels of smoke persisted for more than a week (Emmerson and Keywood, 2021). AQFx output for $PM_{2.5}$ as a 24-hour average for 1st January 2020 is shown in Figure 7.

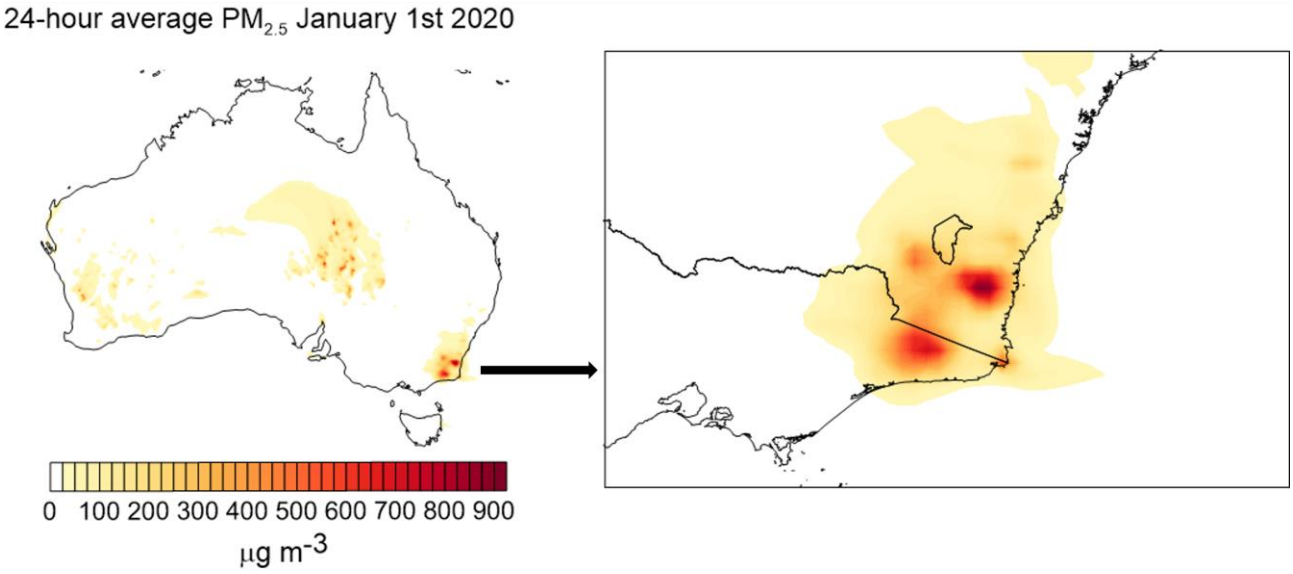

Figure 7 24-hourly $PM_{2.5}$ on 1st January 2020 from AQFx

Note that high levels of $PM_{2.5}$ exist elsewhere in Australia due to components such as dust. Emissions of dust are a wind-blown process, and peak in summer when conditions are hot and dry.

For similarity with the NESP2 climate change model runs, AQFx data was re-gridded to be the same 20km spatial resolution across Australia.

2.2.5 Discussion

Each of the GCMs have produced different outcomes for the 2050 period and confirms that it was necessary to spend the time running the CTM with the 8 different GCMs and SSPs. This work has examined changes by 2050 to meteorological inputs for the chemical transport model in terms of temperatures, wind speed, rainfall and cloud cover predictions. Meteorology is the main driver of natural emissions such as dust, sea salt and biogenic volatile organic compounds. In running the models for 2050 without changes to anthropogenic emissions, we estimate what the 'climate penalty' is for Australia – changes that will occur due to climate change alone. Changes to temperature and cloud cover will also impact the speed of chemical reactions causing differences in the concentrations of secondary pollutants such as ozone and NO_2. Additional ozone is also produced from reactions of biogenic volatile organic compounds, which themselves are increased under higher temperature and photosynthetic conditions.

2.2.6 Recommendations for air quality modelling

We need to devise a strategy for how smoke emissions from bushfires can be modelled under future climate scenarios.

An indication of when a fire might start is given by the forest fire danger index that considers vegetation dryness, air temperature, wind speed and humidity. These metrics are assessed every 2 years by the State of the Climate report for Australia, who observed up to 25 additional dangerous fire weather days since the 1950s (Bureau of Meteorology and CSIRO, 2022). The trends suggest further increases to dangerous fire weather days by 2050 and beyond. An increase in fire intensity is also expected which will impact on plume rise and smoke dispersion/impacts.

Whilst the FFDI only considers one fuel type, the National Bushfire Intelligence Capability (NBIC) are working towards delivering an 8-fuel model ensemble for the Australian Fire Danger Rating System (AFDRS). The AFDRS will combine weather parameters with vegetation parameters to estimate fire spread and severity. We can incorporate the AFDRS projections into the prognostic approach within AQFx to derive smoke emissions in future.

2.2.7 Data provision (air quality modelling)

These model data (AQFx and NESP2 runs) were generated on a 24-hour average basis, at a spatial resolution of 20 km. The AQFx data was from 1st December 2019 to 31st January 2020. The NESP2 data were presented as 5-yearly 24-hour averaged difference between the future (2048 to 2052) and current (2013 to 2017) time periods.

2.2.8 Acknowledgments (air quality modelling)

The AQFx team (Julie Noonan, Fabienne Reisen and Martin Cope) for the modelled data from the bushfire period.

John Clarke from the Climate Systems Hub for conversations on the use of raw GCM data.

Marcus Thatcher and Stacey Osbrough for provision of the meteorological data used in the NESP2 model runs.

2.2.9 References (air quality modelling)

Binskin, M. (2020). Royal Commission into National Natural Disaster Arrangements. https://www.royalcommission.gov.au/natural-disasters/report.

Borchers Arriagada, N., Palmer, A. J., Bowman, D. M., et al. (2020). Unprecedented smoke-related health burden associated with the 2019-20 bushfires in eastern Australia. Medical Journal of Australia, 213(6), 282-283. https://doi.org/10.5694/mja2.50545.

Bureau of Meteorology & Commonwealth Scientific and Industrial Research Organisation. (2022). State of the Climate 2022. http://www.bom.gov.au/state-of-the-climate/.

Climate Systems Hub. (2024). What are SSPs? National Environmental Science Program. https://nesp2climate.com.au/wp-content/uploads/2024/01/Understanding-SSPs-1.pdf.

Cope, M., Lee, S., Noonan, J., Lilley, B., Hess, D., & Azzi, M. (2009). Chemical Transport Model - Technical Description. Commonwealth Scientific and Industrial Research Organisation. https://www.cawcr.gov.au/technical-reports/CTR_015.pdf.

Emmerson, K. M., & Keywood, M. D. (2021). Australia state of the environment 2021: Air quality. Australian Government Department of Climate Change, Energy, the Environment and Water. https://doi.org/10.26194/k7x7-0j76.

Emmerson, K. M., Possell, M., Aspinwall, M. J., Pfautsch, S., & Tjoelker, M. G. (2020). Temperature response measurements from eucalypts give insight into the impact of Australian isoprene emissions on air quality in 2050. Atmospheric Chemistry and Physics, 20, 6193–6206. https://doi.org/10.5194/acp-20-6193-2020.

Emmons, L. K., Schwantes, R. H., Orlando, J. J., Tyndall, G., Kinnison, D., Lamarque, J.-F., Marsh, D., Mills, M. J., Tilmes, S., Bardeen, C., Buchholz, R. R., Conley, A., Gettelman, A., Garcia, R., Simpson, I., Blake, D. R., Meinardi, S., & Pétron, G. (2019). The Chemistry Mechanism in the Community Earth System Model Version 2 (CESM2). Journal of Advances in Modeling Earth Systems, 12, e2019MS001882. https://doi.org/10.1029/2019MS001882.

Fountoukis, C., & Nenes, A. (2007). ISORROPIA II: A computationally efficient thermodynamic equilibrium model for K^+–Ca^{2+}–Mg^{2+}–NH_4^+–Na^+–SO_4^{2-}–NO_3^-–Cl^-–H_2O aerosols. Atmospheric Chemistry and Physics, 21. https://doi.org/10.5194/acp-7-4639-2007.

Grose, M., Narsey, S., Trancoso, R., Mackallah, C., Delage, F., Dowdy, A., Di Virgilio, G., Watterson, I., Dobrohotoff, P., Rashid, H. A., Rauniyar, S., Henley, B., Thatcher, M., Syktus, J., Abramowitz, G., Evans, J. P., Su, C.-H., & Takbash, A. (2023). A CMIP6-based multi-model downscaling ensemble to underpin climate change services in Australia. Climate Services, 30, 100368. https://doi.org/10.1016/j.cliser.2023.100368.

Hasnain, M. G., Garcia-Esperon, C., Tomari, Y. K., Walker, R., Saluja, T., Rahman, M. M., Boyle, A., Levi, C. R., Naidu, R., Filippelli, G., & Spratt, N. J. (2024). Bushfire-smoke trigger hospital admissions with cerebrovascular diseases: Evidence from 2019–20 bushfire in Australia. European Stroke Journal, 9(2), 468-476. https://doi.org/10.1177/23969873231223307.

Johnston, F., Hanigan, I., Henderson, S., Morgan, G., & Bowman, D. (2011). Extreme air pollution events from bushfires and dust storms and their association with mortality in Sydney, Australia 1994–2007. Environmental Research, 111(6), 811-816. https://doi.org/10.1016/j.envres.2011.05.007.

McGregor, J. L., & Dix, M. R. (2008). An updated description of the Conformal-Cubic Atmospheric Model. In K. Hamilton & W. Ohfuchi (Eds.), High Resolution Simulation of the Atmosphere and Ocean (pp. 51–76). Springer. https://doi.org/10.1007/978-0-387-49791-4_4.

Reisen, F. (2022). Smoke forecasting using AQFx for the 2019-2020 summer bushfires. National Council for Fire and Emergency Services (AFAC) conference 2022, Adelaide, Australia. https://www.afac.com.au/insight/technology/article/current/331.-smoke-forecasting-using-aqfx-for-the-2019-2020-summer-bushfires.

Squire, S. D. T., Richardson, D., Risbey, J. S., Black, A. S., Kitsios, V., Matear, R. J., Monselesan, D., Moore, T. S., & Tozer, C. R. (2021). Likelihood of unprecedented drought and fire weather during Australia's 2019 megafires. NPJ Climate and Atmospheric Science, 4, 1–12. https://doi.org/10.1038/s41612-021-00220-8.

Stevenson, D. S., Dentener, F. J., Schultz, M. G., Ellingsen, K., van Noije, T. P. C., Wild, O., Zeng, G., Amann, M., Atherton, C. S., Bell, N., Bergmann, D. J., Bey, I., Butler, T., Cofala, J., Collins, W. J., Derwent, R. G., Doherty, R. M., Drevet, J., Eskes, H. J., Fiore, A. M., Gauss, M., Hauglustaine, D. A., Horowitz, L. W., Isaksen, I. S. A., Krol, M. C., Lamarque, J.-F., Lawrence, M. G., Montanaro, V., Müller, J.-F., Pitari, G., Prather, M. J., Pyle, J. A., Rast, S., Rodriguez, J. M., Sanderson, M. G., Savage, N. H., Shindell, D. T., Strahan, S. E., Sudo, K., & Szopa, S. (2006). Multimodel ensemble simulations of present-day and near-future tropospheric ozone. Journal of Geophysical Research: Atmospheres, 111. https://doi.org/10.1029/2005JD006338.

Tang, W., Llort, J., Weis, J., Perron, M. M. G., Basart, S., Li, Z., Sathyendranath, S., Jackson, T., Sanz Rodriguez, E., Proemse, B. C., Bowie, A. R., Schallenberg, C., Strutton, P. G., Matear, R., & Cassar, N. (2021). Widespread phytoplankton blooms triggered by 2019–2020 Australian wildfires. Nature, 597, 370–375. https://doi.org/10.1038/s41586-021-03805-8.

Tsimpidi, A. P., Karydis, V. A., Zavala, M., Lei, W., Molina, L., Ulbrich, I. M., Jimenez, J. L., & Pandis, S. N. (2010). Evaluation of the volatility basis-set approach for the simulation of organic aerosol formation in the Mexico City metropolitan area. Atmospheric Chemistry and Physics, 10, 525–546. https://doi.org/10.5194/acp-10-525-2010.

Woodhouse, M. T., Luhar, A. K., Stevens, L., Galbally, I. E., Thatcher, M., Uhe, P., Wolff, H., Noonan, J., & Molloy, S. (2015). Australian reactive gas emissions in a global chemistry-climate model and initial results. Air Quality and Climate Change, 49, 31–38. https://search.informit.org/doi/10.3316/informit.690374348503299.

2.3 Health system demand and mortality impact

2.3.1 Methods of impact assessment

Quantitative estimates of air pollution health impacts have become an increasingly critical input to policy decisions. Methods of air pollution health risk assessment are well established and have been adopted in many global projects including the first global burden of disease (GBD) study (Cohen et al., 2005; Lopez 2013) and its later revisions which is the largest and most comprehensive effort to quantify health impacts from major risk factors. Health impacts associated with air pollution vary by duration (chronic or transient), degree (severe or minor) and temporality (caused shortly after exposures or lagged by several years) (Martenies et al., 2015).

Estimation of health impacts associated with air pollution at a population level is based on statistical attribution. The primary measure of interest is the attributable fraction (AF), representing the fraction of cases or deaths that would not have occurred in the absence of exposure to a specific risk factor either in the exposed population or the population as a whole (Steenland and Armstrong, 2006).

When exposure is dichotomous (exposed/nonexposed), the AF among the exposed (AFexp) may be calculated using relative risks:

$$AF_{exp} = \frac{(R_1 - R_{0)}}{R_1} = \frac{(RR - 1)}{RR}$$

where R1 is the risk of disease among the exposed, R0 is the risk among the nonexposed, and RR = R1/R0 is the risk ratio. This can be extended to define a population attributable fraction:

$$PAF = \frac{p_e(RR - 1)}{p_e(RR - 1) + 1}$$

where p_e= is the percentage of the total population exposed. Note this formula is valid only when there is no confounding and weighting individual AFs generated for each confounding variable is recommended (Steenland and Armstrong, 2006). Multiplying the PAF by the baseline rate in the population (y0, cases per person per year) and the number of people in the population (P) gives the number of attributable cases in the population.

A simplified version of this is often modelled where the entire population of a region is considered exposed (i.e. p_e=1 in the formula above). This is referred to as a health impact function and has been the standard approach for most cost-benefit analyses of regulations affecting environmental quality. Health impact functions have been used to estimate the burden of disease associated with air pollution in many studies including within the US Environmental Protection Agency's Environmental Benefits Mapping and Analysis Program (Davidson et al., 2007; Hubbell et al., 2005) and numerous studies in Australian settings (Broome et al., 2015; Borchers Arriagada et al. 2020a; Borchers Arriagada et al. 2020b; Johnston et al., 2021).

The population attributable fraction and health impact functions require information including the size of the exposed population, incidence rates for the health outcomes of interest, baseline and exposure concentrations, and relative risks for each pollutant-outcome pair. Prospective applications also require projections of population size and incidence rates (Martenies et al., 2015).

Effect estimates/relative risks are drawn from the epidemiological literature, including large observational studies, as well as smaller studies of targeted populations and can be chosen from a single study or pooled across multiple studies. Effect estimates are based on concentration-response functions which statistically estimate the relationship between exposure to pollutants and health outcomes, with concentrations of pollutants acting as a surrogate for outdoor exposure (Ru et al., 2023). Concentration-response functions require regular evaluation and update to incorporate new developments in science, and the CRFs between exposure to ambient air pollution and mortality and some morbidity outcomes have been extensively studied, systematically documented and regularly updated.

Most existing concentration-response functions for exposure to air pollution assume a fixed risk estimate as a log-linear function over an extrapolated exposure range. The log-linear concentration-response model can be expressed as:

$$RR = e^{\beta \cdot \Delta x}$$

where β is the coefficient of the concentration–response effect and Δx is the change in pollutant above the counterfactual level, usually defined as the 5th percentile or the minimum of each study. However nonlinear functions exist which include additional parameters to allow for the curvature and shape of the CRF to change across the range of exposures. A recent systematic review of several health outcomes including cardiovascular and respiratory hospital admissions, and asthma emergency department visits relating to air quality identified that nonlinear CRFs produced more than doubled global estimates on average, depending on the outcome (Ru et al., 2023). The review found that impact assessments are sensitive locally to which functional form is applied, and generally non-linear CRFs produce higher estimates in most regions of the world. Differences are also apparent when considering an 'annual average' exposure approach versus using a 'daily' exposure approach. The log-linear CRFs can closely approximate linear functions, especially over narrow ranges of pollutant levels. The nonlinear CRFs, however, can deviate more from a linear function form, and the extent of deviation depends on the distribution of daily exposures over the year, and on the shape of the specific CRFs.

The intention of this investigation is to align with other Australian studies of health impact assessment from exposure to bushfire smoke and the approach adopted by European and US environmental agencies. Hence the form of the health impact function aligns also with that adopted by these studies (Borchers Arriagada et al. 2020a; Borchers Arriagada et al. 2020b; Johnston et al., 2021; Hubbell et al., 2005; Berman et al., 2012):

$$\Delta y = Pop.y_0.(e^{\beta \cdot \Delta x} - 1)$$

where Δy is the change in the number of cases or deaths, Pop is the potentially affected population, y_0 is the baseline incidence rate; β is the effect estimate; and Δx is the estimated change in the pollutant of interest. Using this approach, the delta changes of pollution exposure together with the population and effect estimates for selected health outcomes such as mortality, cardiovascular or respiratory related hospital admissions, can provide estimates of the health impacts associated with pollutant exposure.

Note that this equation has been expressed in the literature in slightly different forms. For example, Martenies et al. (2015) and Sacks et al. (2018) describe the relationship as $\Delta y =$

$= Pop.y_0.\left(1 - e^{-\beta \cdot \Delta x}\right)$ which is derived from $RR = e^{\beta \cdot \Delta x}$ where $\Delta x = (x_0 - x_1), x_0 > x_1$, whereas the form applied in this investigation is derived from $RR = e^{-\beta \cdot \Delta x}, -\Delta x = (x_0 - x_1), x_0 < x_1$.

2.3.2 Pollutants of interest

Section 2.1.3 of this report described how bushfire smoke is a source of particulate matter (PM), but also other gases such as sulphur dioxide, nitrogen oxides, ammonia, ozone, methane and carbon dioxide. Given that a) $PM_{2.5}$ makes up around 90% of PM emitted from bushfires (Jegasothy et al., 2023); b) most of the particle emissions arising from biomass burning fall in the $PM_{2.5}$ fraction (Reid et al., 2005); c) $PM_{2.5}$ particles are able to penetrate deeply within the alveoli and are thought to have the greatest role in affecting human health in particular respiratory and cardiovascular morbidity (Pope and Dockery, 2006); and d) the Global Burden of Disease study - the largest and most comprehensive effort to quantify health impacts from major risk factors – uses $PM_{2.5}$ as the basis for air pollution risk assessment (GBD, 2021), $PM_{2.5}$ was the main focus of interest of this investigation.

Numerous other studies also focus on $PM_{2.5}$ as the main pollutant of intertest as there is growing understanding that fine particles are the most harmful for human health among the entire size distribution (U.S. Environmental Protection Agency, 2022; Carey et al., 2013) and there is a relatively high correlation between $PM_{2.5}$ and PM_{10} (i.e., mostly above 70% (Zhou et al., 2016; Brook et al., 1997)).

However, given the existence of other pollutants within bushfire smoke, additional analysis is presented on the health impacts from ozone (O_3) and nitrogen dioxide (NO_2). The relative contributions of health impacts from these other pollutants in the presence of $PM_{2.5}$ are challenging to determine, and it is impractical to consider the impacts of ozone and NO_2 exposure independently. A systematic review of mortality risks from NO_2 and O_3 exposure (Huangfu and Atkinson, 2020) found that in some studies, associations between NO_2 and mortality was attenuated upon adjustment for co-pollutants (Beelen et al., 2014; Carey et al., 2013; Fischer et al., 2015; Turner et al., 2016) but not in others.

2.3.3 Counterfactual concentrations

Health impact functions can estimate the incidence attributable to pollution relative to 'pristine' or 'background' levels (Fann et al., 2012) but are generally used to evaluate incremental impacts associated with a change in concentration, e.g., effects of a new standard relative to existing concentrations (Berman et al., 2012; U.S. Environmental Protection Agency, 2022).

The quantitative characterisation of the risk of health effects attributed to specific air pollution concentrations is often challenging because the counterfactual concentration levels of pollutants (the background expected concentration if exceptional events did not occur) depend on the study question.

For example, the large WHO project ‘‘Health risks of air pollution in Europe - HRAPIE’’ was implemented to provide evidence-based concentration-response functions for quantifying air pollution health impacts to support air quality policy for the European Union (WHO, 2013). The project’s team of experts identified concentration-response functions linking mortality and morbidity with exposure to particulate matter, ozone and nitrogen dioxide to provide the scientific

basis for formulating policy actions to improve air quality and thereby reduce the burden of disease associated with air pollution in Europe. In terms of the health effects from exposure to $PM_{2.5}$, the HRAPIE report recommended that quantification of the effects of $PM_{2.5}$ on mortality be undertaken at all concentrations (Héroux et al., 2015). Similarly, Ru et al. (2023) in their systematic review of 93 studies of morbidity impacts associated with short term $PM_{2.5}$ exposure, found that either the 5th percentiles or the minimum of each study turned out to be below 1μg/m^3 for all outcomes and therefore did not consider the existence of meaningful counterfactual levels. Others have adopted non-zero counterfactual concentrations (e.g. between 5.8 and 8.8 μg/m^3 of $PM_{2.5}$ as comparison or baseline conditions to represent non-anthropogenic 'background' levels (Murray et al., 2003; Burnett et al., 2014; Krewski et al., 2009), or looked at the long term historical averages of $PM_{2.5}$ for specific regions (Borchers Arriagada et al. 2020b) or the expected "Non-bushfire" concentrations (Jegasothy et al., 2023) when attempting to quantify the specific health impacts from bushfire smoke.

For risk factors considered in the latest Global Burden of Disease study (GBD 2021) and the Australian version of this (AIHW, 2024a), the theoretical minimum risk exposure distribution (TMRED) used for PM2.5 is 2.4–5.9 μg/m^3. This is in the context that for many risk factors, no exposure is not appropriate, either because it is physiologically impossible (for example, blood pressure or body mass index), or because there are lower limits beyond which exposure cannot feasibly be reduced (i.e. 2.4–5.9 μg/m^3 in the case of $PM_{2.5}$).

The objective of this investigation is to quantify the impacts that bushfires may create on health system demand and mortality under different future climate scenarios. Using the 2019/20 summer bushfires as an example of an extreme event scenario, the study attempts to quantify the health impacts if such an event were to happen again in 2050. The output from the 8 Global Climate Models described in Section 2.2 captured the change from present air quality levels to those estimated for 2050 using relative differences averaged across a 5-year period centred on 2015 (present day) and 2050 (future). The health impacts from other pollutant sources (not just bushfire smoke) are ever present; dust and other sources of particulate matter cannot be eradicated as a risk factor from the country and it would likely be present in future scenarios. Further, there is evidence in the literature that the mortality rate observed during bushfire events is consistent with the increase in mortality from elevated pollutant levels, regardless of source (Hänninen et al., 2009) and also that any level of $PM_{2.5}$ increases hazards of hospital admissions and mortality and that there is no lower threshold (Schwartz et al., 2002, Ru et al., 2023). For these reasons, we do not remove any baseline (e.g. non-anthropogenic) contributions as we are interested in outcomes associated with exposure to estimated air quality associated with a similar bushfire event in 2050 (i.e. the counterfactual concentrations are 0 μg/m^3).

2.3.4 Health outcomes and their relative risks

The relative severity of health impacts following population-level exposure to air pollution have been described in a conceptual framework of an air pollution pyramid (Melody and Johnston, 2015). Death is the ultimate health outcome, followed by hospital admissions, emergency department attendances and ambulance call outs, primary health care attendances, medication use, etc. with the base of the pyramid representing the proportion of people that are overall affected. In this framework, the largest proportion of people who experience impacts from

bushfire smoke and airborne particulate matter may not have significant symptoms or may not visit a health professional.

Due to their importance and use in prior studies within the Australian setting, this investigation focuses on four health outcomes:

1. all-cause mortality;

2. cardiovascular-related hospital admissions;

3. respiratory-related hospital admissions; and

4. ED presentations related to asthma.

While the estimated mortality burden is unquestionably important, it is also important to estimate morbidity, such as hospital admissions and emergency department visits, which allow for an accounting of non-fatal health impacts.

A distinction exists between relative risks for short-term exposure versus long-term exposure. In longitudinal cohort studies, long-term average pollution exposures of individual cohort participants are estimated, and the contribution of the geographical variation among these exposures to the risk of adverse events over the entire follow-up period is determined by survival analysis, adjusting for characteristics that may affect disease risk (Beverland et al., 2012). In contrast, many studies of short-term exposure effects have examined relationships between daily counts of deaths in a given population and daily pollutant and meteorological variables recorded at central monitoring sites using regression modelling. This type of time-series study has limited capacity to take account of spatial variation in individual exposures or to investigate the possible modification of pollution effects by individual risk factors such as age, smoking history, and previous disease, although analysis using case-crossover methods (Carracedo-Martinez et al., 2010) may reduce some of these difficulties. The estimates of air pollution effects from long-term exposure studies involving cohorts have generally been considerably larger than those from short-term time-series studies even after adjusting for other individual risk factors (Pope 2007). It is plausible that larger magnitudes of association between long-term exposure and mortality may be attributable to cumulative effects that increase the sensitivity of highly exposed population subgroups.

It is important to note that as bushfire smoke increases the yearly burden of air pollution, the long-term impacts will get more and more important. Short term (daily) effect estimates may underestimate prolonged impacts (e.g. the Hazelwood study). This investigation assesses short term impacts for a future bushfire scenario. For our main analysis, we apply short-term relative risks recommended by HRAPIE (Héroux et al., 2015) for mortality and hospital admissions and from a systematic review for asthma ED presentations (Borchers Arriagada et al., 2019) which have also been used in other Australian bushfire studies (Johnston et al., 2021; Borchers Arriagada et al., 2020a; Borchers Arriagada et al., 2020b). However other sources of relative risks for $PM_{2.5}$ exposure and for other pollutants are considered as a sensitivity analysis (Table 2). All sources are syntheses of multiple studies and therefore the range of uncertainty associated with any one model is reduced.

Table 2 Relative risks applied to selected health outcomes based on short-term exposure to selected pollutants

	RELATIVE RISK PER 10 MG/M^3 (95% CI); REFERENCE			
Estimated population level outcome	$PM_{2.5}$ Main analysis	$PM_{2.5}$ Sensitivity analysis	O_3	NO_2
Mortality	1.0123 (1.0045–1.0201); Héroux et al., 2015	1.0065 (1.0044- 1.0086); Orellano et al., 2020	1.0043 (1.0034–1.0052); Orellano et al., 2020	1.0072 (1.0059–1.0085); Orellano et al., 2020
Respiratory-related hospital admissions	1.019 (0.9982-1.0402); Héroux et al., 2015	1.0135 (1.0104-1.0166); Ru et al., 2023	1.0044 (1.0007–1.0083); Héroux et al., 2015	1.0180 (1.0115–1.0245); Héroux et al., 2015
Cardiovascular-related hospital admissions	1.0091 (1.0017-1.0166); Héroux et al., 2015	1.010 (1.006-1.014); Ru et al., 2023	1.0089 (1.0050–1.0127); Héroux et al., 2015	1.0066 (1.0032-1.0101); Mills et al., 2015
Asthma ED presentations	1.066 (1.038-1.094); Borchers Arriagada et al., 2019	1.043 (1.026-1.062); Ru et al., 2023	1.005 (0.999–1.011) Agache et al., 2024	1.010 (1.000–1.020); Agache et al., 2024

An alternative relative risk for mortality from $PM_{2.5}$ exposure (RR: 1.0065; 95% CI: 1.0044-1.0086) assessed in the sensitivity analysis is based on a systematic review and meta-analysis of 196 articles relating to short-term exposure to $PM_{2.5}$ and mortality (Orellano et al., 2020). WHO commissioned this systematic review to build on the HRAPIE exposure-response function from 2013, and it uses a random effects model from 27 studies, including one in Australia. HRAPIE, on the other hand, relies on meta-analysis of 12 single-city studies and one multicity study, all in Europe. This alternative relative risk was adopted in a recent assessment of the mortality burden attributable to exceptional $PM_{2.5}$ air pollution events in Australian cities (Hertzog et al., 2024). This same systematic review is also the source of the relative risks for mortality associated with exposure to O_3 and NO_2.

The alternative relative risks for the hospital admission and ED presentation outcomes from $PM_{2.5}$ exposure are based on the systematic review undertaken by Ru et al. (2023). Their analysis considered both log-linear and non-linear concentration response functions, and here we adopt a fixed risk estimate as a log-linear function similar to other Australian studies and ease of interpretation given that the confidence intervals of nonlinear CRFs depend on the concentration and are thus only an approximation when considering a unit increase in pollutant concentration.

The short-term relative risks recommended by HRAPIE (Héroux et al., 2015) are also adopted for other pollutant-outcome pairs where available. For NO_2-associated CVD admissions, Mills et al. (2015) report percentage increases (0.66 (0.32-1.01)) associated with a 10 µg/m^3 increase in NO_2 as opposed to relative risks. The relative risk presented in Table 2 (1.0066 (1.0032-1.0101)) is derived from this percentage increase, where beta is taken as log(1.0066)/10.

Relative risks for asthma ED visits associated with NO_2 and O_3 exposure have been adopted from a recent systematic review specifically focused on asthma outcomes, where risks for pollutant exposure on ED visits were assessed over a 0-4 lag day period following exposure. The highest relative risks over the 5-day period were adopted for this investigation (lag3 for NO_2 and lag4 for O_3). Note the highest relative risk for asthma ED visits following exposure to $PM_{2.5}$ from this meta-analysis is 1.023 (1.007–1.039) for lag3 (3 days between exposure and ED visit). Adopting this

relative risk would result in fewer asthma ED visits than using the reference sources for $PM_{2.5}$ exposure adopted in this investigation.

Epidemiological short-term studies used to assess health impacts have mostly assumed a constant health risk over time. Shifts in the underlying population distribution (e.g. longer life expectancy, ageing populations, and increased prevalence of chronic diseases) could further contribute to changes in effect estimates by different exposure-response functions for subpopulations. A recent study of over 21.6 million cardiovascular and 7.7 million respiratory deaths across 24 countries found there were no temporal changes in associations between ambient particulate matter and mortality over the 22-year study period (Schwarz et al., 2024). The study authors found that although air pollution concentrations decreased over the study period, the effect sizes per unit increase in air pollution concentration had not changed and there was no reduction in the slope of the exposure-response function. This supports an assumption in this investigation that there are no temporal changes in the risks from exposure to the individual pollutants (e.g. $PM_{2.5}$) between now and 2050.

2.3.5 Pollutant exposure

Exposure to PM2.5, O_3 and NO_2 was obtained as described in Section 2.2.4. Daily PM2.5, O_3 and NO_2 estimates from 1 Dec 2019 to 31 January 2020 representing the 2019/20 bushfire period were obtained from the AQFx model as an example of an extreme event scenario. Climate change daily differences between the present day (based on a 5-year average centred on 2015) and a future time period (based on a 5-year average centred on 2050) were obtained from 8 different Global Climate Models ('ACC-126', 'ACC-370', 'CNRM-126', 'CNRM-370', 'NCAR-126', 'NCAR-370', 'NOR-126', and 'NOR-370').

i.e. the difference for every day =

$$\text{future}\left(\frac{2048+2049+2050+2051+2052}{5}\right) - \text{base}\left(\frac{2013+2014+2015+2016+2017}{5}\right)$$

Air quality data was provided on the basis of a gridded 'surfaces' model comprising 178 x 210 cells, each covering an area 20 x 20km, some of which are ocean, unburnable areas, and many cells comprising no population. A surfaces model approach avoids the constraints of approaches based on air quality monitoring stations which are limited to population centres, industrial hotpots and a few rural air quality hotspots e.g. northern Tasmania. For example, the locations of air quality monitoring stations in 2019/2020 taken from the 2021 State of the Environment report (Emmerson and Keywood, 2021) are shown in Figure 8.

Source: Christy Geromboux, Centre for Air pollution, energy and health Research

Figure 8 Air quality monitoring stations in Australia

A surfaces model approach is aligned with methods used in the Australian Burden of Disease Study (AIHW, 2024a) and also avoids some of the following assumptions made by researchers assessing the health impacts of Australian bushfires of studies (e.g. Borchers Arriagada et al., 2020b; Johnston et al., 2021):

- The population of a geographic area is exposed to the same quality of air at a monitoring station that is within a given radius (e.g. 100km). For every air quality monitoring station, the method involves assessing which region centroids are within the threshold radius. An assumption is made that the entire population of the region is exposed to the pollutant measured at the air quality station. With this condition, Johnston et al. (2021) when examining the impact of the 2019/2020 Australian megafires, estimated that 74% of the state of Qld (5 million people), 95% of NSW (8 million people), 100% of ACT (420 thousand people), 93% of Victoria (6 million people) were exposed.
- The 100km radius between region centroid and air quality station is arbitrary and maybe 50km, or even 10km might be more appropriate.
- A region centroid can be within the threshold radius (e.g. 100km) of more than one air quality station. The method of determining exposure rates for each region is by the inverse distance rule, where monitoring stations closest to the region centroid are given highest weighting.

Geographic correspondence files were used to convert the gridded air quality data (netCDF format) to SA2 geography. This was done using the raster package in R. Modelled air quality data is limited in that it estimates ambient air pollution levels rather than actual exposure to air pollution but has the advantage over previous methods using monitoring stations only in that estimates are based on measurements from larger areas of Australia and based on bottom-up emission inventories and vegetation maps. However, there are the same issues in that there can be variation in estimated levels of air pollution and actual levels experienced by the population. There is also likely to be a substantial amount of variation between regions in the amount of time that people generally spend outside, being exposed to air pollution. For simplicity, we assumed all persons were equally exposed to the same level of ambient air pollution at a given location.

Similar to the approach described by Johnston et al. (2021), the maximum daily concentrations of $PM_{2.5}$ were constrained to 150 $\mu g/m^3$ in recognition that bushfires can produce daily concentrations of PM2.5 well above usual background concentrations, and that concentration response relationships for extreme daily $PM_{2.5}$ concentrations above this level have not been well characterised.

2.3.6 Baseline incidence rates

Baseline mortality rates were obtained from the Australian Bureau of Statistics (ABS) which provide counts of deaths in each SA2 region in 2019 and 2020 (ABS, 2023a). We used the annual number of deaths in each of these two years (divided by 365) to calculate the daily number of deaths. It is acknowledged that mortality rates in winter are likely to differ to summer periods and using seasonally adjusted rates would provide a more accurate representation of the underlying mortality patterns.

Baseline hospital admission and ED outcome crude rates were sourced from the Australian Institute of Health and Welfare (AIHW) and reflected rates over a 6-month summer period (AIHW, 2021a). Incidence rates could only be obtained for SA4 regions (so 'child' SA2 regions were all assigned the same crude rate as their 'parent' SA4). The source data contains crude rates for asthma ED presentations (Table S4 in the source dataset), respiratory admissions (Table S2 in the source dataset) and cardiovascular admissions represented by the sum of 'Selected heart conditions' and 'Cerebrovascular conditions' (Table S2 in the source dataset; note: as the population of each SA4 used as the denominator in deriving crude rates is the same, we can directly add crude rates together). We used rates based on weekly observations over a 6-month summer period (1 Sept-1 Mar), where weekly averages were divided by 7 to get daily figures. For respiratory and cardiovascular-related admissions, we used a 5-year average (2014–15 to 2019–20) of weekly observations over the same 6-month period (1 September - 1 March), and for asthma ED presentations, 6 months of weekly observations over 1 September 2018 – 1 March 2019.

When considering cardiovascular admissions related to $PM_{2.5}$ and NO_2 exposure, baseline incidence rates were derived from the sum of 'Selected heart conditions' and 'Cerebrovascular conditions' (Table S2 in the source dataset). However, when assessing cardiovascular admissions associated with O_3 exposure, the source of the relative risks for CVD admissions (Héroux et al., 2015) specified that the risk was for CVD admissions excluding stroke. Thus, for O_3 exposure, because the relative risk excluded stroke, the baseline incidence rate was based on 'Selected heart conditions' only, and 'Cerebrovascular conditions' weren't added, unlike for $PM_{2.5}$ and O_3 exposure.

An assumption made in this investigation was in the absence of reliable estimates, baseline incidence rates were also applied when considering health impacts for the future time period of 2050. Speculation about future health status and incidence rates requires knowledge about societal change elements that are challenging to estimate. For example, changes in population age structure, demographic characteristics, health workforce issues, healthcare funding, availability of new treatments, emergence of new respiratory diseases etc. Future incidence rates of the outcomes assessed may differ from the baseline conditions applied here.

2.3.7 Population

Baseline population by SA2 region was sourced from the Australian Bureau of Statistics (ABS, 2024).

As health impacts needed to be estimated at a future time point (2050), by necessity it was required to estimate the population for each SA2 region at that time point. Population projections by SA2 level have been generated out to 2032 by the Australian Bureau of Statistics for Geoscience Australia as part of the Digital Atlas of Australia (Geoscience Australia, 2024) and at national and state levels for 2071 (ABS 2023b). Population projections for 2050 were estimated by extrapolation of SA2 population projections from 2023 to 2032 outwards to 2050, and checking that when extrapolated further to 2071, estimates were within the range of 2071 projections by ABS (between 34.3 and 45.9 million people by 2071). In accordance with ABS methodology, some SA2 regions are unlikely to have any urban development (cemeteries, airports, heavily forested areas) so were held constant for the projection period.

2.3.8 Results of statistical attribution via health impact functions

Modelling framework

To determine the health impacts of a severe bushfire in 2050, modelling comprised two components:

1. Bushfire component: daily $PM_{2.5}$, O_3 and NO_2 estimates were obtained for 1 December 2019 to 31 January 2020 representing the 2019/20 bushfire period were obtained from the AQFx model as an example of an extreme event scenario.
2. Climate change component: Daily $PM_{2.5}$, O_3 and NO_2 estimates for 1 December to 31 January representing the climate change differences between 2050 and present day were obtained from the Global Climate Models.

Gridded air quality data was converted to SA2 geography to match against population (2019 for the bushfire component and projections to 2050 for the climate change component) and baseline incidence rates. The modelling framework is presented in Figure 9 – which shows the bushfire component of the modelling (the climate change component was modelled similarly).

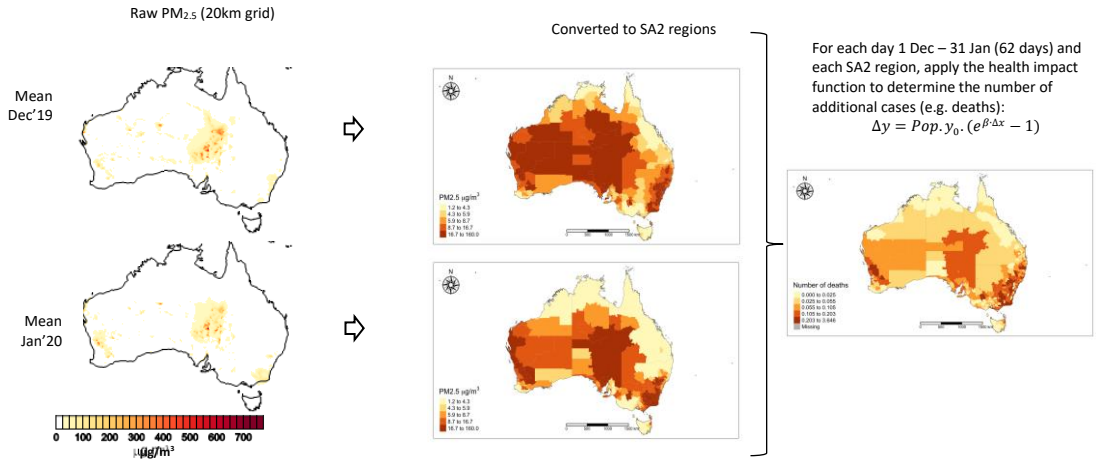

Figure 9 Modelling framework for determining health impacts from bushfire smoke exposure

Since the baseline incidence rates applied in the health impact function are derived for each health outcome on a daily basis (e.g. deaths per day, hospital admissions per day etc.), the estimated number of additional cases are calculated for each day over the period 1 December 2019 – 31 January 2020 for the bushfire scenario analysis, and 1 December – 31 January for the climate change scenario analysis that assesses differences between 2050 and present day. The total number of cases is the sum of daily estimates over the two months.

It should be acknowledged that a limitation of this modelling is lagged effects of exposure. This means that for any given day, we use pollutant levels estimated for that day to derive health impacts associated with that exposure, but then for the next day, we use that next day's pollutant levels to estimate health impacts from that exposure and so on across the analysis period. In reality, there are potentially additional impacts on days following exposure on the first day that persist (i.e. the day of exposure is considered to have health risks as presented in Table 2, but the following days conceivably have non-zero relative risks that add to the main effect from pollutant levels observed on those days). For example, Borchers Arriagada et al. (2019) report $PM_{2.5}$ associations with asthma-related hospital admissions for up to at least 3 days after exposure and with asthma-related ED visits on the same day of exposure.

The plots of $PM_{2.5}$ shown in Figure 9 show mean levels over December 2019 and January 2020. Whilst this is the bushfire period, $PM_{2.5}$ levels have other sources including dust and the modelled values are not just due to bushfire smoke. Similarly while bushfire smoke is a source of ozone and nitrous oxides, nitrous oxides are also generated by car and truck exhausts and industry, and ozone forms when volatile organic compounds and nitrous oxides react together in the atmosphere during warm, sunny weather. Thus, these pollutants are also not just due to bushfire smoke.

Mean $PM_{2.5}$, O_3, and NO_2 levels per day by state/territory are shown in Figure 10 and Figure 11, and it can be seen there were high rates on particular days in December and January, especially for ACT and NSW.

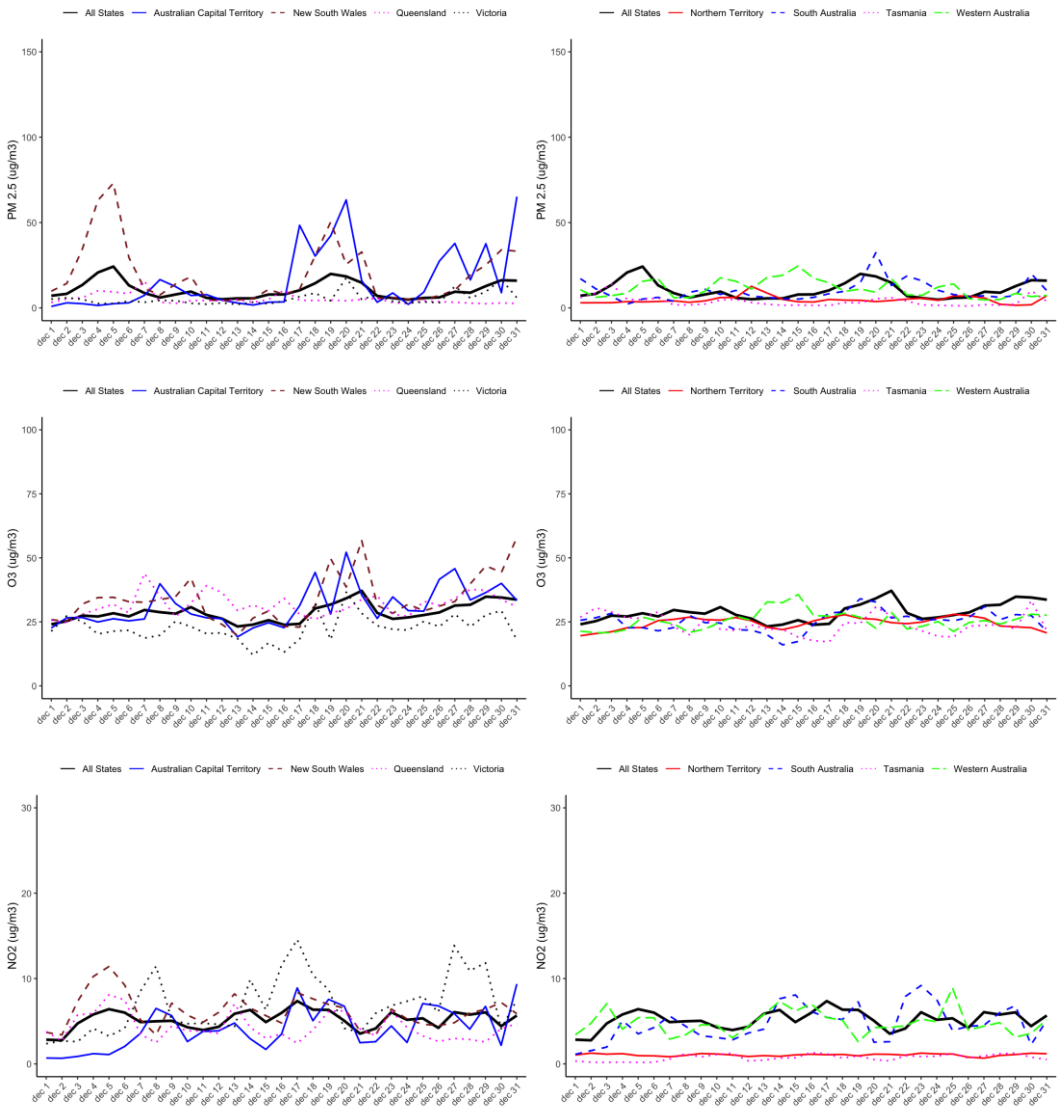

Figure 10 Mean levels of assessed pollutants per day by state/territory for Dec 2019

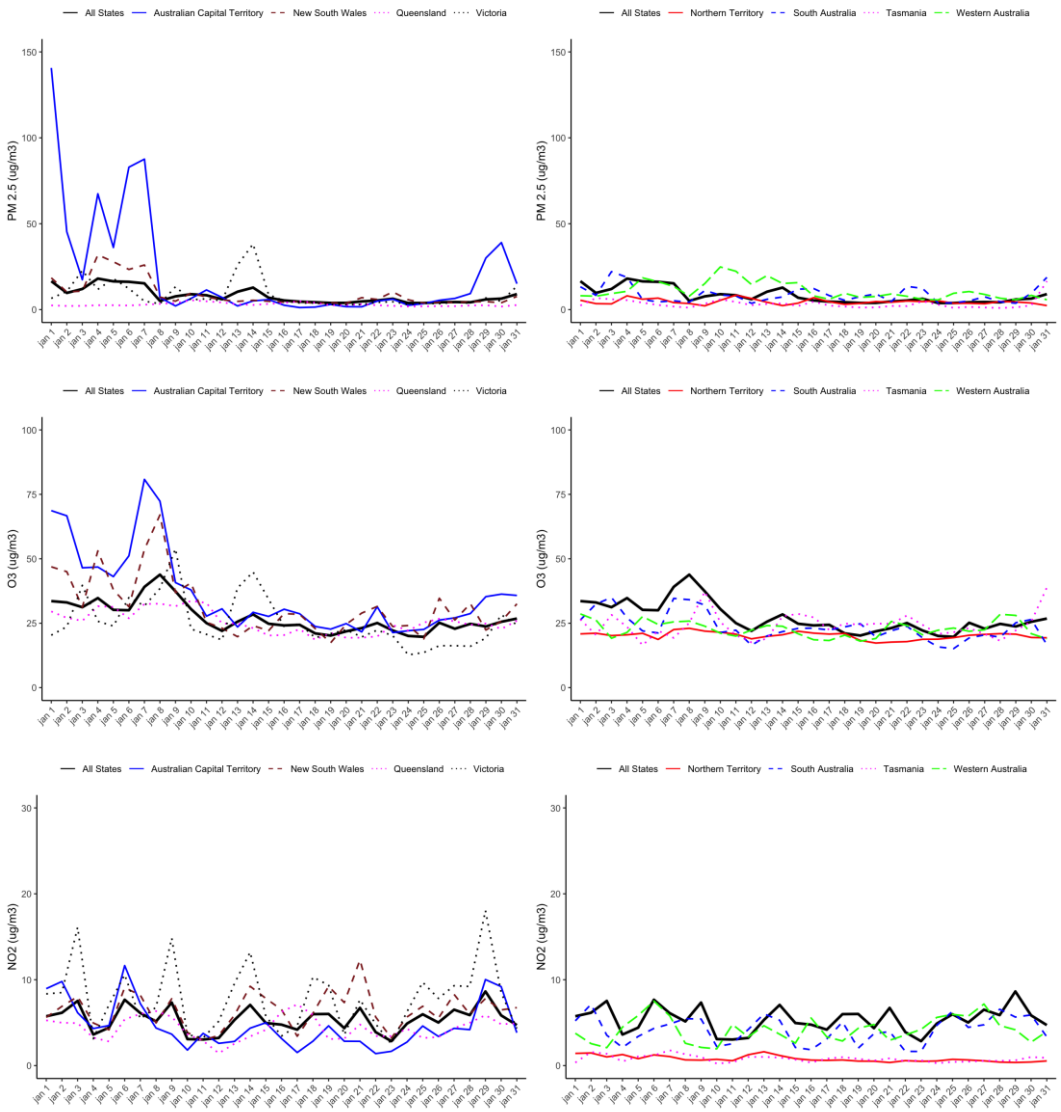

Figure 11 Mean levels of assessed pollutants per day by state/territory for Jan 2020

Health impact estimates

Results of the impact assessments for the selected health outcomes following $PM_{2.5}$ exposure are presented in Table 3 and Table 4. These estimates all have a measure of uncertainty which is essential to include in this discussion, indicated by the 95% confidence intervals shown in brackets. It should be noted that the magnitude of the outcomes for the bushfire component do not exactly match other published estimates of the health impacts of the 2019/20 fire season which are presented later in Table 8. This is due to underlying differences in the model used (air quality monitoring station approach versus a surfaces model derived from the satellite-based AQFx model) and a different duration of analysis (December 19-January 20 versus October 19-March 20). Nevertheless, the tabled estimates generated from the AQFx model output are within the confidence interval range of other published estimates.

Table 3 Results of health impact estimates for a severe bushfire in 2050 - Main analysis for $PM_{2.5}$

ESTIMATED POPULATION LEVEL OUTCOMES (ADDITIONAL CASES)	RELATIVE RISK	BUSHFIRE COMPONENT	WORST CASE FUTURE (MODEL 'NCAR370' OUT OF 8 GCMS)		BEST CASE FUTURE (MODEL 'CNRM370' OUT OF 8 GCMS)	
			CLIMATE CHANGE COMPONENT	RATIO BUSHFIRE: CLIMATE CHANGE	CLIMATE CHANGE COMPONENT	RATIO BUSHFIRE: CLIMATE CHANGE
Deaths	1.0123 (1.0045–1.0201)	313 (113-517)	73 (27-119)	4 : 1	39 (14-63)	8 : 1
Respiratory-related hospital admissions	1.019 (0.9982-1.0402)	1368 (0-2982)	316 (2-664)	4 : 1	167 (7-350)	8 : 1
Cardiovascular-related hospital admissions	1.0091 (1.0017-1.0166)	634 (117-1168)	149 (28-270)	4 : 1	79 (15-143)	8 : 1
Asthma ED presentations	1.066 (1.038-1.094)	935 (512-1410)	185 (108-261)	5 : 1	97 (56-136)	10 : 1

Table 4 Results of health impact estimates for a severe bushfire in 2050 – Sensitivity analysis for $PM_{2.5}$

ESTIMATED POPULATION LEVEL OUTCOMES (ADDITIONAL CASES)	RELATIVE RISK (95% CI)	BUSHFIRE COMPONENT	WORST CASE FUTURE (MODEL 'NCAR370' OUT OF 8 GCMS)		BEST CASE FUTURE (MODEL 'CNRM370' OUT OF 8 GCMS)	
			CLIMATE CHANGE COMPONENT	RATIO BUSHFIRE: CLIMATE CHANGE	CLIMATE CHANGE COMPONENT	RATIO BUSHFIRE: CLIMATE CHANGE
Deaths	1.0065 (1.0044- 1.0086)	164 (111-218)	39 (26-51)	4 : 1	21 (14-27)	8 : 1
Respiratory-related hospital admissions	1.0135 (1.0104-1.0166)	965 (740-1191)	225 (174-276)	4 : 1	119 (92-146)	8 : 1
Cardiovascular-related hospital admissions	1.010 (1.006-1.014)	698 (417-982)	163 (98-228)	4 : 1	87 (52-121)	8 : 1
Asthma ED presentations	1.043 (1.026-1.062)	584 (343-872)	122 (74-174)	5 : 1	63 (39-91)	9 : 1

The relative risks defined earlier in Table 2 are included in the tables for reference. These risks represent the probability of the event occurring in exposed persons versus the probability of the event occurring in the non-exposed persons. It can be observed that although, small, there are heightened risks for persons exposed to poor air quality. For all cases, the relative contribution from the bushfire component exceeds that due to climate change, with ratios essentially the same regardless of the choice of relative risks assessed via the sensitivity analysis. This means that both the best and worst case scenarios indicate minor health impacts are associated with air quality in 2050 compared to present day conditions, and then adding the bushfire component contributes to additional adverse outcomes.

As the relative risks each have associated uncertainty, so too do the estimated health outcomes and the expected range of each is also presented, derived from the lower and upper limits of the 95% confidence interval of the relative risks.

The results of health impacts associated with O_3 and NO_2 exposure are presented in Table 5 and Table 6. It can be observed that the health impacts from NO_2 exposure are generally lower than from $PM_{2.5}$ or O_3 exposure, and cardiovascular-related hospital admissions is highest for O_3 exposure compared with $PM_{2.5}$ and NO_2.

In this assessment, health impacts from O_3 and NO_2 are generated as a sensitivity analysis for comparison only and are not added to impacts attributed to $PM_{2.5}$ exposure. This is due to the potential issue of overcounting effects as the pollutants do not exist in isolation from each other, although other studies have added health impacts from different pollutants together (e.g. Fann et al., 2012). As noted in Section 2.3.2, some studies report attenuation of the main effect upon adjustment for co-pollutants while others do not (Huangfu and Atkinson, 2020). When assessing mortality and air pollution exposure in Sydney, Hanigan and colleagues (2019) report that $PM_{2.5}$ and NO_2 were highly correlated (0.73, $P < 0.001$) and hence were modelled separately. While the health impacts from each pollutant are tabled separately below, it can be seen that as with $PM_{2.5}$, the relative contribution from the bushfire component exceeds that due to climate change for O_3 and NO_2, with ratios between each component slightly higher than for $PM_{2.5}$.

Table 5 Results of health impact estimates for a severe bushfire in 2050 – O_3 analysis

			Worst case Future (Model 'NCAR370' out of 8 GCMs)		Best case Future (Model 'CNRM370' out of 8 GCMs)	
Estimated population level outcomes (additional cases)	**Relative Risk**	**Bushfire component**	**Climate change component**	**Ratio Bushfire: Climate Change**	**Climate change component**	**Ratio Bushfire: Climate Change**
Deaths	1.0043 (1.0034–1.0052)	339 (268-410)	61 (48-73)	6 : 1	24 (19-29)	14 : 1
Respiratory-related hospital admissions	1.0044 (1.0007–1.0083)	997 (158-1890)	169 (27-319)	6 : 1	68 (11-128)	15 : 1
Cardiovascular-related hospital admissions	1.0089 (1.0050–1.0127)	1697 (949-2431)	285 (160-406)	6 : 1	112 (63-160)	15 : 1
Asthma ED presentations	1.020 (0.998–1.042)	779 (0-1676)	137 (2-286)	6 : 1	51 (3-107)	15 : 1

Table 6 Results of health impact estimates for a severe bushfire in 2050 – NO_2 analysis

			Worst case Future (Model 'ACC370' out of 8 GCMs)		Best case Future (Model 'NCAR126' out of 8 GCMs)	
Estimated population level outcomes (additional cases)	**Relative Risk**	**Bushfire component**	**Climate change component**	**Ratio Bushfire: Climate Change**	**Climate change component**	**Ratio Bushfire: Climate Change**
Deaths	1.0072 (1.0059–1.0085)	114 (93-134)	23 (19-27)	5 : 1	9 (8-11)	13 : 1
Respiratory-related hospital admissions	1.0180 (1.0115–1.0245)	814 (520-1109)	154 (99-209)	5 : 1	62 (40-85)	13 : 1
Cardiovascular-related hospital admissions	1.0066 (1.0032-1.0101)	289 (140-442)	55 (27-84)	5 : 1	22 (11-33)	13 : 1
Asthma ED presentations	1.010 (1.000–1.020)	72 (0-144)	13 (0-26)	6 : 1	5 (0-11)	14 : 1

Climate model findings

For climate change impacts associated with $PM_{2.5}$ and ozone exposure, model 'CNRM-370' consistently provided the best case scenario of cleaner air quality, whereas model 'NCAR-370' consistently provided the most pessimistic estimates.

For NO_2, model 'NCAR-126' consistently provided the best case, and model 'ACC-370' the worst case. NO_2 titrates with ozone in the atmosphere, therefore it is expected that the order of models would change in the best/worst case scenario.

A description of these climate models is provided in Section 2.2.1. It is also interesting to note that both the best and worst case climate scenarios for $PM_{2.5}$ and O_3 come from the same socio-economic pathway SSP3-7.0 "Regional Rivalry" for which the climate outcomes are based on no emissions reduction and fossil fuels as the sole energy source. However, it is noted that the air quality models are only using the meteorological outcomes from each GCM and are not using the emissions prescribed by the SSPs.

By 2050, the NCAR and NOR models are the hottest, particularly in the west, whilst ACC is the coolest overall. The temperatures and rainfall levels in the CNRM models by 2050 are the most similar to current conditions of all the models. The air quality response to the predicted climate outcomes is non-linear and is a product not only of emission but the level of dilution and atmospheric transport conditions those emissions go into.

The major observation from these results is that each 'family' of models is more similar than when comparing results from inter-families. i.e. 'ACC-126' and 'ACC-370' tend to generate similar results but 'ACC-126' and 'NOR-126' are different. The analysis demonstrates the importance of picking a range of global climate models and not just socio-economic pathways.

2.3.9 Complementary statistical modelling of air quality and health service use

To complement the assessment of health impacts using population-level health impact functions, additional modelling was undertaken on historic bushfire-related air quality and health service use data.

This was to complement the statistical attribution approach to improve an Australian-centric understanding of the risks of bushfire smoke on service use. Statistical modelling was undertaken of the relationships between historical bushfire-related $PM_{2.5}$, health outcomes and temperature as a confounder.

Data sources

Air quality

Data on historical bushfire-related air quality was obtained from The Centre for Safe Air's Clean Air and health Research Data and Analysis Technology (CARDAT) platform. This dataset was recently used by Hertzog et al. (2024) in their health impact assessment of the mortality burden attributable to exceptional $PM_{2.5}$ air pollution events in Australian cities, which uses the same risk factor for mortality that was explored in the sensitivity analysis for this investigation (1.0065 per 10 $\mu g/m^3$, 95% CI: 1.0044- 1.0086, based on Orellano et al., 2020).

This dataset consists of daily $PM_{2.5}$ predictions from a random forest model of the 'Bushfire Smoke project V1.3' and spans January 2001 – June 2020 (Hanigan et al., 2023). The data was produced on a 5km Australia-wide grid and contains daily $PM_{2.5}$ predictions from a random forest model developed by Ivan Hanigan and Nicolas Borchers Arriagada along with a daily decomposition of the predictions into trend, seasonal and remainder components. Values range from -12 to 720 $\mu g/m^3$ globally, and these extreme values occur in the early months of 2020. Monthly medians and means generally lie within 5 to 10 $\mu g/m^3$.

For interest, comparisons of mean $PM_{2.5}$ levels for December 2019 and January 2020 between this CARDAT $PM_{2.5}$ dataset and the AQFx model output for the same period are shown below. Model output is shown converted to SA2 regions (left hand plots), and estimated mortality (right hand plots), generated from the health impact function and relative risk (1.0123, 95% CI: 1.0045–1.0201) used in the main analysis.

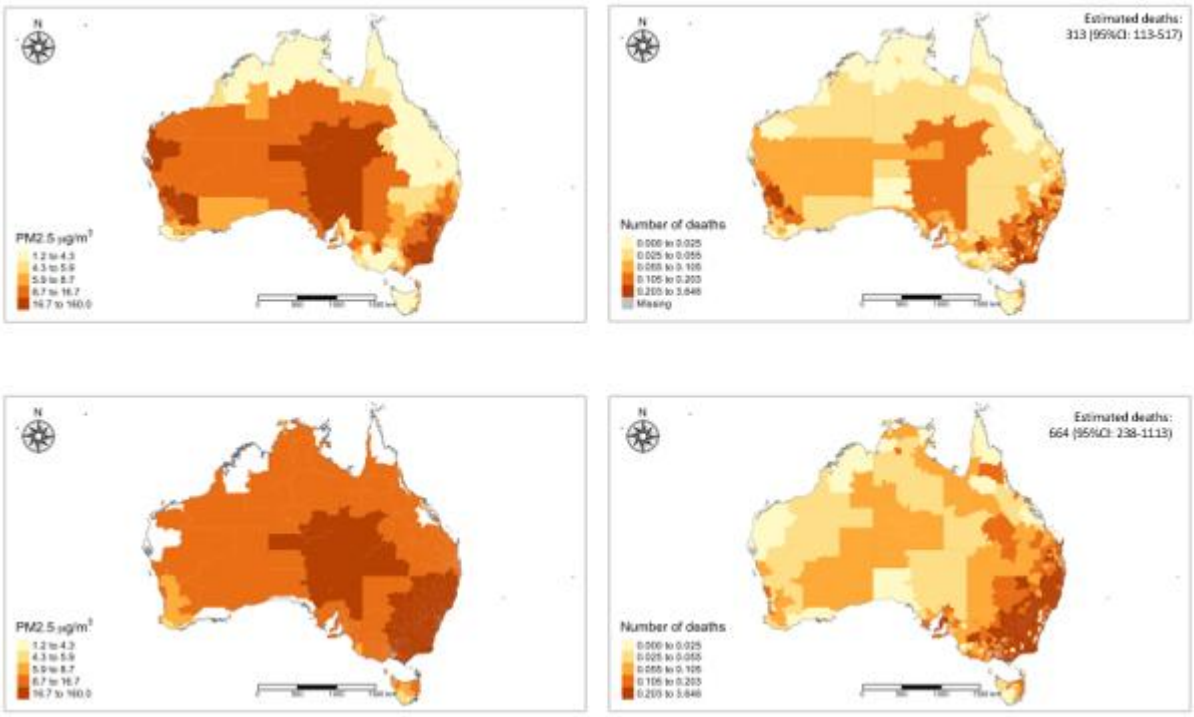

Figure 12 Comparison of modelled output of mean $PM_{2.5}$ over Dec'19 and Jan'20 by SA2 region – top: AQFx model output (main analysis); Bottom: CARDAT model output (complementary investigation)

Health service use

Health service use data was obtained from AIHW's publicly available dataset 'Geography and time-specific health data for environmental analysis' (AIHW, 2024b) which is part of an Australian Research Data Commons (ARDC) Bushfire Data Challenges program. The dataset contains health service use data for health conditions that are potentially associated with or exacerbated by bushfire and bushfire smoke impact though no causal attribution is implied with its provision.

The data only provide a partial picture of health. As described in Section 2.3.4, the largest proportion of people who experience impacts from bushfire smoke and airborne particulate matter may not have significant symptoms or may not visit a health professional. In addition, the data are reflective of health services provided and not the unmet need which may exist. Bushfires and other environmental events can be disruptive to health service facilities and staffing and may require people to move from their usual address.

The health service use data was provided with caveats from Australian Institute of Health and Welfare (AIHW) that it may not be appropriate or suitable for understanding patterns in health service requirements or prevalence over time and by geography, as a range of factors can lead to increases or decreases in service use. It's important to note these caveats again here:

- The data provide a partial snapshot of service provision for any particular condition and only show need that has been met. For example, natural disasters may affect people's ability to reach services or the ability for services to operate normally, and in general, due to capacity constraints, the health system may not immediately be able to satisfy a surge in need. People may stay home to avoid exposure to environmental hazards (i.e. bushfire smoke).
- The data is administrative and therefore can be subject to a range of factors such as variation in administrative processes, or changes in policy, diagnosis codes or diagnosis coding practices.
- Data custodians apply a range of rules and principles to protect privacy and confidentiality and some elements are denoted as 'not presented'.

This release contains up to 20 years of weekly data of health service use relating to specific health conditions by SA4 region. Data are presented for respiratory, cardiovascular, and mental health conditions, including:

- Hospitalisations (2002–03 to 2021–22)
- Hospital emergency department presentations (2014–15 to 2021–22)
- Medicare Benefits Schedule service claims (2002–03 to 2021–22)
- Pharmaceutical Benefits Scheme (PBS) and Repatriation Pharmaceutical Benefits Scheme (RPBS) prescriptions dispensed (2002–03 to 2021–22).

AIHW have grouped count data into health conditions (e.g. for hospitalisations these groupings are based on ICD10 diagnoses codes), and some of the groupings are subsets of broader conditions within the collection (as depicted in Figure 13).

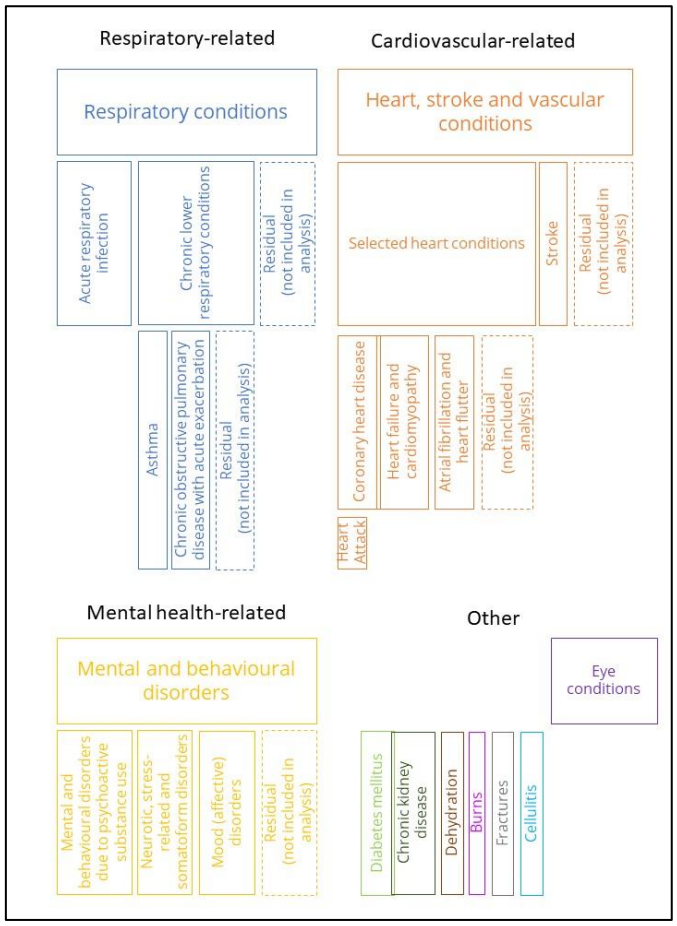

Figure 13 Hierarchical groupings of health conditions represented in the AIHW 'Geography and time-specific health data for environmental analysis' (source: AIHW, 2024b)

Of the data elements included in this collection, the following were identified as priorities for this analysis.

ED presentations and Hospitalisations (inpatient admissions) datasets

- 'Respiratory conditions' (RC);
- 'Heart, stroke and vascular conditions' (HSVC);
- 'Burns' (BC);
- 'Mental and behavioural disorders' but excluding the smaller subset of 'Mental and behavioural disorders due to psychoactive substance use' (i.e. the difference in counts between these two health conditions) (MBD).

MBS Dataset

Respiratory test items, Asthma cycle of care items, Cardiovascular diagnostic procedures and investigations, Cardiovascular diagnostic imaging services, and Mental health services items.

PBS Dataset

- 'Respiratory prescriptions';
- 'Cardiovascular prescriptions';
- 'Mental health prescriptions'.

Temperature

As a confounder to the problem of exposure to ambient particulate matter, bushfires and dust storms tend to coincide with high ambient temperatures which has been independently associated with increased risk of mortality (Johnston et al., 2011). Therefore, historic estimates of maximum daily temperature were obtained for the period 2001-2020 from the Australian Gridded Climate Data collection via National Computational Infrastructure (NCI), a high-performance computing and data services facility, located at the Australian National University in Canberra and supported by the Australian Government's National Collaborative Research Infrastructure Strategy (NCRIS). The Australian Gridded Climate Data collection is the Bureau of Meteorology's official dataset for climate analyses covering the variables of rainfall, temperature as well as vapour pressure at daily and monthly timescales. The dataset provides consistent temporal and spatial analyses across Australia for each observed data variable. This accounts for spatial and temporal gaps in observations, and the gridded analysis techniques provide useful estimates in data-sparse regions such as central Australia.

Statistical analysis

Geographic correspondence files were used to convert the gridded daily air quality and temperature data (both provided as 5km x 5km grids in netCDF format) to SA4 regions to spatially match against the AIHW data relating to service use. Also, as the AIHW data is provided on a weekly time interval, daily values of $PM_{2.5}$ and maximum temperature were aggregated to weekly values by averaging the seven days up to and including the start of the week of interest. For example, if the AIHW week start is 7 July, values of $PM_{2.5}$ and maximum temperature would be averaged for 1 July, 2 July, 3 July, 4 July, 5 July, 6 July, and 7 July. This is referred to as Lag 0. Lagging the 7-day rolling mean by up to 3 days before the start of the week was considered to allow for insights concerning temporal differences between exposure and service use.

AIHW health service use data has been provided as raw counts and crude rates (count per 100,000 population). For the response variable, raw counts are used with an offset (modelled with a Poisson or negative binomial GLM) rather than crude rates (which would normally be fitted using a standard linear model). One limitation of using a linear model with crude rates is that the predictions can sometimes be negative, which is unrealistic in this context.

All analyses were performed using R statistical software (version 4.4.0). A Generalised Additive Model (GAM) based on a Poisson distribution was used to examine the association between ambient $PM_{2.5}$ and maximum temperature of a priori interest and counts of the response variable. Where data was overdispersed (higher variance than expected), Negative Binomial (NB) with a log link was used. Risk ratios (RR) and 95% confidence intervals were calculated.

A single-pollutant model was considered as follows:

$$E(Y) = g\text{-}1\ (\text{offset}(\log(\text{Population})) + \text{intercept} + \sum I\ PM25\_lagM(i) + \sum I\ \ Temperature\_lagM(i) +$$

$$s(year, k=6) + s(month, k=6) + s(State, k=3, RE)),\ i = 1, \ldots, 4,$$

where Y indicates the count for a given week for the outcome of interest (e.g. visits to ED for a respiratory condition) and g indicates the link function (log). Based on the weekly $PM_{2.5}$ concentrations and maximum temperatures, three 7-day moving average of $PM_{2.5}$ concentrations

and maximum temperatures (average of 0-,1-,2-, and 3-day lags relative to the visits to 7-day prior windows) were modelled. Long-term temporal trends ('year' and 'month') were accounted for by using smoothing splines with 6 degrees of freedom and spatial effects were accounted for using the random effect ('State').

Relationships were assessed between health service use, air quality and temperature for the six financial years July 2014 – June 2020.

Results of statistical modelling of air quality and health service use

The results of the statistical modelling are presented in Appendix A for brevity with select results presented here. Relationships were assessed using Poisson and Negative Binomial Generalised Additive Models, and since all models showed overdispersion, NB GAM was used.

Scatterplots show a weak relationship between the number of ED presentations and air quality, and the number of ED presentations was noted to be more dependent on the season rather than a direct effect from the pollutant level. The plot presented in Figure 14 indicates counts of ED presentations for two health condition groupings – Respiratory and Heart/stroke/vascular conditions - as a function of month and mean $PM_{2.5}$ concentration (indicated by the size of the dot). The greater seasonality and winter peaks associated with respiratory ED presentations can be appreciated, and it can be seen that respiratory-related counts in winter are higher than months with larger $PM_{2.5}$ concentrations at other times of the year (including December 2019 and January 2020). Unusually high counts for ACT heart conditions in 2015 and 2016 can also be observed which may be an artefact associated with the previously mentioned caveat that the health data is administrative and therefore can be subject to variation in administrative processes, or changes in policy.

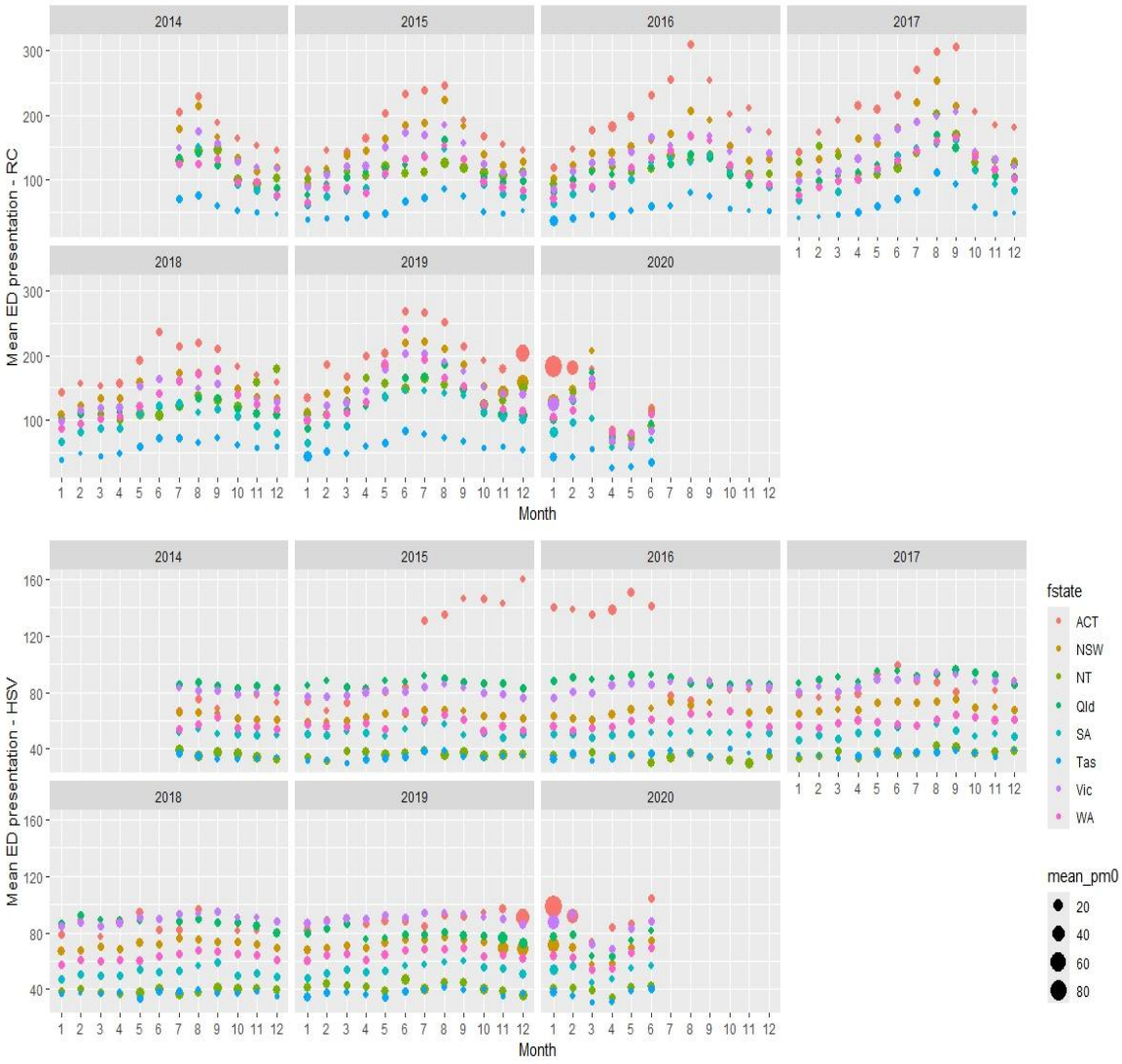

Figure 14 Historic ED presentations relating to respiratory conditions (top) and heart, stroke and vascular conditions (bottom)

The modelling of inpatient admissions due to burn conditions was excluded because of the small sample size (4624 cases over a 20-year period). Weekly admission counts for burn cases varied between 5 to 45, and the proportions of burn cases across the SA4 regions were too small to allow for a reliable model fit. Model diagnostic plots have been included in Appendix A. Weekly counts of national inpatient admissions for burns are presented over in Table 7 and Figure 15. The record associated with 23 burn admissions for week commencing 02 Feb 2009 in Melbourne was referred to as “Black Saturday” when 173 people perished. The high counts of 45 in June 2015 was recorded for the Cairns SA4 region.

Table 7 Frequency of weekly counts of national inpatient admissions for burns

NUMBER OF CASES	FREQUENCY (NUMBER OF WEEKS)
5	2113
6	1326
7	611
8	311
9	134
10	65
11	31
12	16
13	8
14	4
15*	3
23**	1
45^	1

* 13 Jan 2003 ACT, 10 Apr 2006 Qld, 02 Feb 2009 VIC-Gippsland, ** 02 Feb 2009 VIC-Melbourne, ^ 08 Jun 2015 Qld-Cairns

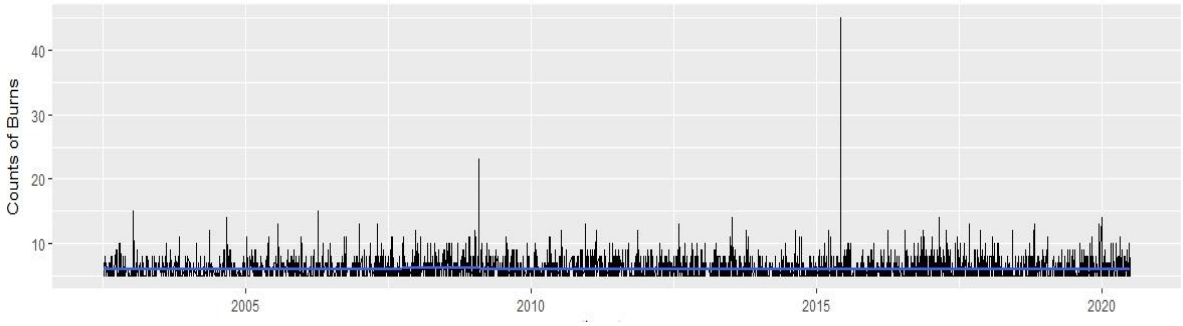

Figure 15 Weekly counts of national inpatient admissions for burns

Another observation is that unlike ED presentation and inpatient admission data, long-term trends of PBS and MBS data reflect annual end of year patterns which for the case of MBS items may be related to a decrease in service activity over the Christmas/New Year period and for the case of PBS data, it may be an artefact associated with how that data gets captured and reported. A notable increase in mental health MBS items in 2007 and mental health prescriptions from around 2012 can be observed which differs to other conditions that were assessed which generally have less abrupt year to year changes which may be administrative artefacts.

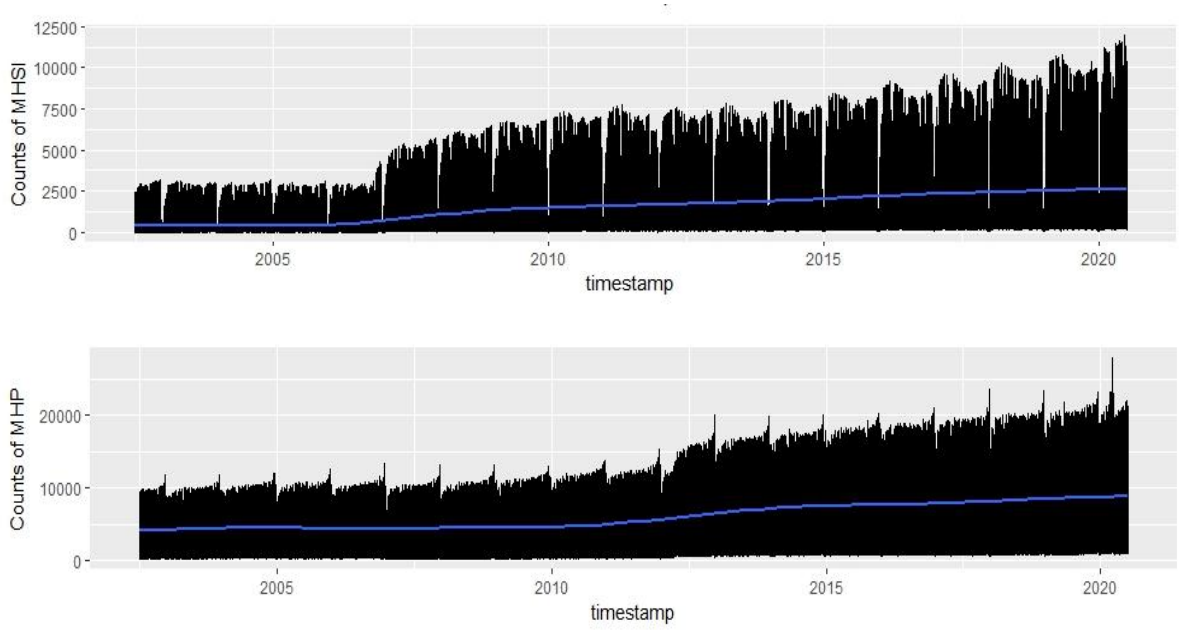

Figure 16 Long term trends in MBS items relating to mental health (top) and PBS mental health prescriptions (bottom)

However, one of the most valuable contributions of this complementary investigation is the statistical model output in terms of the generation of Australian-centric relative risks for the selected indicators of health service use relating to bush-fire specific exposure to particulate matter.

Figure 17 shows plots of derived relative risks of the modelled variables for four select outcomes: respiratory ED presentations, respiratory inpatient admissions, heart/stroke/vascular inpatient admissions and mental health prescriptions.

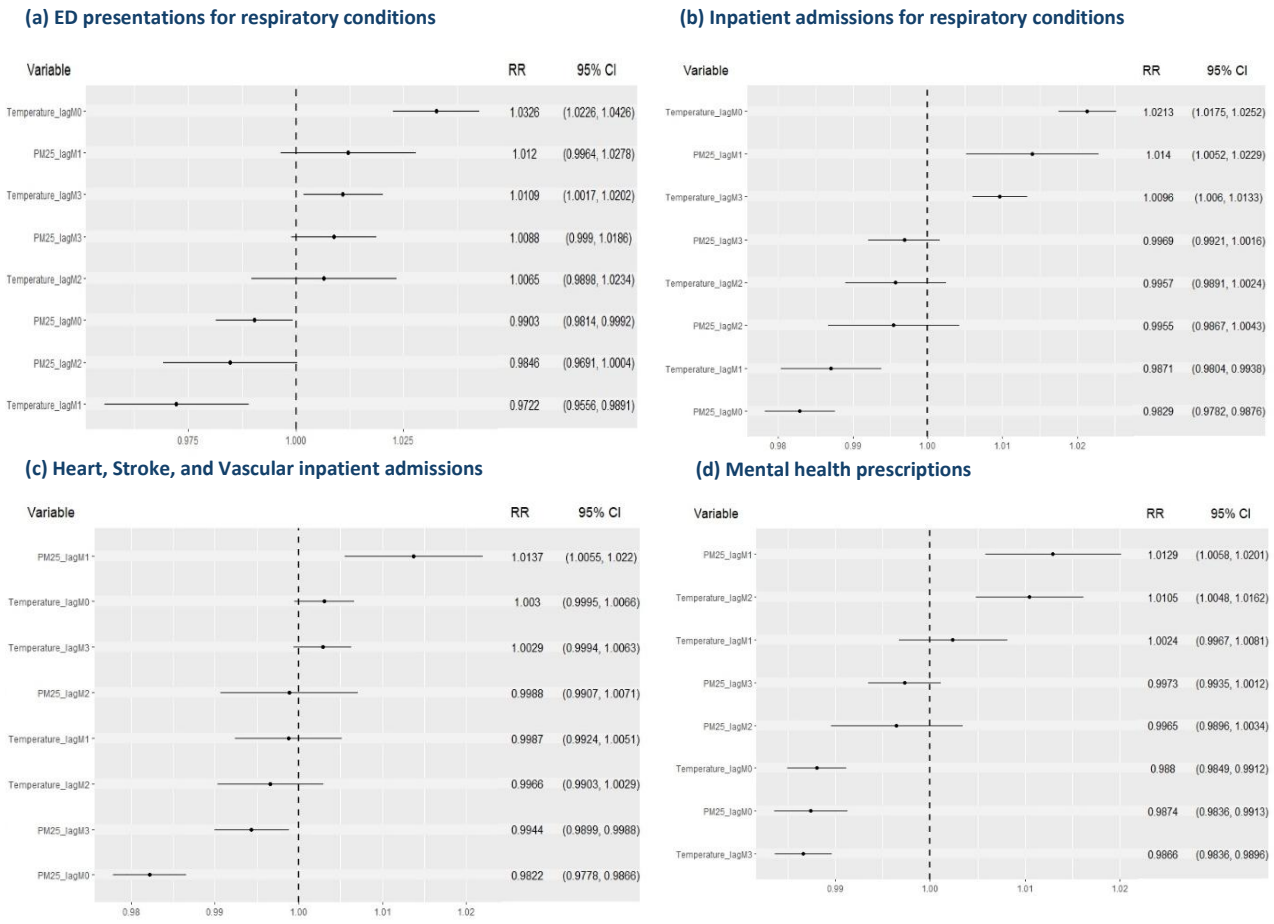

Figure 17 Derived relative risks for (a) Respiratory ED presentations, (b) Respiratory inpatient admissions, (c) Heart, Stroke, and Vascular inpatient admissions, and (d) Mental health prescriptions

It can be observed that the effect of PM is stronger for lagged values (denoted as M1 for a 1-day lag, M2 for a 2-day lag, M3 for a 3-day lag) than on the same day (M0). The stronger impact of temperature on respiratory-related hospitalisations compared to air quality is apparent (higher relative risks). It can also be seen that after accounting for temperature, the relative risks associated with $PM_{2.5}$_lagM1 are above 1, supporting an association between air quality and these outcomes.

Also of note, the derived relative risk exposure to $PM_{2.5}$ for respiratory admissions was 1.014 per 10 µg/m^3 (95%CI: 1.0052-1.0229). This compares well with the relative risk adopted in the health impact function (as recommended by WHO for short term exposure of $PM_{2.5}$ -refer Section 2.3.4) to quantify impacts for this cohort which was 1.019 per 10 µg/m^3 (95% CI: 0.9982-1.0402).

The derived relative risk for $PM_{2.5}$ exposure for Heart, Stroke, and Vascular inpatient admissions was 1.0137 per 10 µg/m^3 (95%CI: 1.0055-1.022). This is slightly higher than the WHO relative risk used for the main analysis (1.0091, 95% CI: 1.0017-1.0166) and sensitivity analysis (1.010, 95% CI: 1.006-1.014) but within the 95% confidence interval of each.

2.3.10 Healthcare risks in context

It is important to frame the health impacts from bushfires relative to exposure to other risk factors.

The disease burden due to risk factors is known as attributable burden. It is the amount by which disease burden would be reduced if exposure to the risk factor had been avoided or reduced to the lowest possible exposure. Deaths can also be attributed to risk factors using the same methods.

The Australian Burden of Disease Study 2018, published in 2021, estimated the disease burden and deaths due to 40 risk factor components or exposures that combine into 20 individual risk factors (AIHW, 2021b). Figure 18 shows these risk factors sorted in order of disease burden. In 2018, 1.3% of the total disease burden in Australia and 2% of deaths was due to air pollution. These estimates reflect the amount of burden and deaths that could have been avoided if all people in Australia were not exposed to particulate matter 2.5µg/m^3 ($PM_{2.5}$). For generating these estimates, exposure was causally linked to six diseases - coronary heart disease, COPD, stroke, type 2 diabetes mellitus, lung cancer and lower respiratory infections. Air pollution was responsible for 8.6% of coronary heart disease total burden, 8.3% of stroke burden, 6.7% of both COPD and type 2 diabetes burden, 5.7% of lower respiratory infections burden and 3.4% of lung cancer burden. Total disease burden attributable to air pollution was 2.2 times greater in the lowest (most disadvantaged) socioeconomic group compared with the highest (least disadvantaged) group.

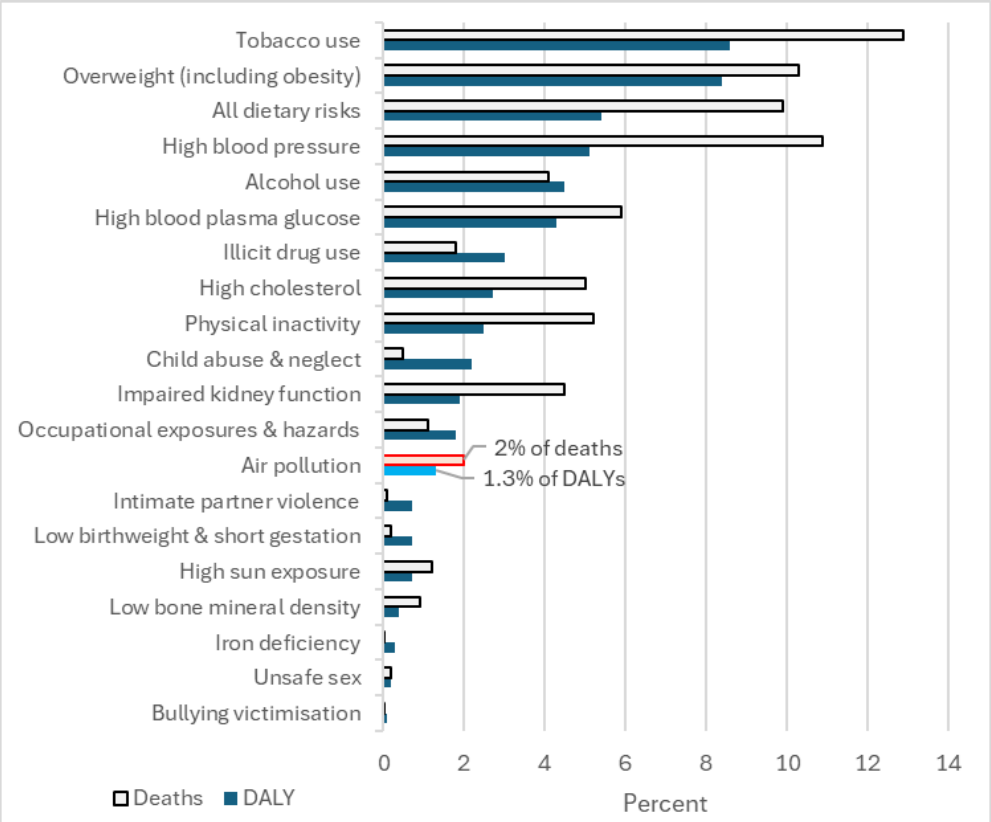

Figure 18 Percentage of disease burden (measured as Disability-Adjusted Life Years) and deaths attributable to air pollution in Australia in 2018; Data source: AIHW, 2021b

Globally over the period 2010 to 2019, exposure to ambient particulate matter pollution was among the largest increases in risk to human health, although the risk of household air pollution has declined (GBD, 2019). The latest version of the GDB study (GBD, 2021) states that among the specific risk factors analysed, particulate matter air pollution was the leading contributor to the global disease burden in 2021, contributing 8.0% of total Disability Adjusted Life Years, followed by

high systolic blood pressure (7.8%), smoking (5.7%), low birthweight and short gestation (5.6%) and high fasting plasma glucose (5.4%).

The changing trends in outdoor concentrations of $PM_{2.5}$ air pollution from 1850 to 2021 have been visualised as air quality stripes (https://airqualitystripes.info/) with indicative air quality ratings provided such as "Very Good", "Fair", "Moderate" etc. While not yet developed for Australia apart from Canberra, they aim to raise awareness of the health effects of $PM_{2.5}$ and have also inspired the creation of the biodiversity stripes which show biodiversity loss and ocean acidification stripes.

The substantial evidence base briefly described in this investigation suggests that controlling fine particle pollution would result in thousands of fewer early deaths per year. In view that ambient fine particulate matter is the world's leading environmental health risk factor, reducing the disease burden of $PM_{2.5}$ requires specific strategies that target dominant sources. The Global Burden of Disease from Major Air Pollution Sources (GBD MAPS) project provided a comprehensive evaluation of contributions to the ambient $PM_{2.5}$ disease burden from source sectors and fuels across 204 countries (McDuffie et al., 2021). The study estimated that approximately a million deaths worldwide (27% of the total mortality attributable to $PM_{2.5}$) would be avoidable by eliminating fossil fuel combustion, with coal contributing over half of that burden. Residential (19%), industrial (12%, and energy (10%) sector emissions were among the dominant global sources of $PM_{2.5}$. Regions with the largest anthropogenic contributions were generally found to have the highest numbers of attributable deaths, which clearly demonstrates the importance of reducing these emissions to realise reductions in global air pollution and its disease burden.

In terms of local risk exposure, while concern about extreme events like bushfires is appropriate, there is high particulate exposure occurring all the time for populations in central Australia. There isn't a way to remove dust from the country, and our present and future environment will contain non-anthropogenic emissions too.

The relative risks for mortality from short term $PM_{2.5}$ exposure recommended by WHO and adopted for the main analysis of this study was 1.0123 per 10 $\mu g/m^3$. This means that for an increase in $PM_{2.5}$ of 10$\mu g/m^3$, the mortality risks of those exposed compared to those unexposed is 1.2%. The study also assumes a log-linear concentration-response model (RR=e^(β·Δx)), and so a relative mortality risk of 10% between exposed and unexposed would arise for an increase concentration level of $PM_{2.5}$ of 78$\mu g/m^3$. It should also be noted that this investigation and most current risk assessments assume that the excess relative risk does not vary with age, but the GBD 2010 estimates incorporated age dependency of the air pollution relative risks. It is also noted that these risks are for short-term exposure, based on estimated average daily levels of $PM_{2.5}$. It is intuitive that risks associated with longer term exposure representing sustained poor air quality are higher (e.g. 1.062 per 10 $\mu g/m^3$, 95%CI 1.040–1.083, Heroux et al., 2015) based on average annual levels of $PM_{2.5}$.

Specific to bushfire-related impacts, Section 2.1.4 of this report described some of the many studies assessing the impact on emergency department presentations and hospital admissions. For example, Johnston et al. (2021) estimated that there were an additional 1138 hospital admissions for cardiovascular diseases, 2092 admissions for respiratory diseases and 1523 ED visits for asthma associated with the 2019 – 2020 wildfire season in Australia. These were estimated using the WHO relative risks from 24h exposure to $PM_{2.5}$ (Héroux et al., 2015) which the

present investigation also adopts. Fire season was defined as the 6 months 1 October – 31 March each year.

An attempt is made here to frame these impacts in terms of overall volume of these outcomes for a similar period (Table 8). Notes on the data sources are listed below the table.

Table 8 Published estimates of the health impacts of the 2019/20 fire season relative to national figures for that time period

	NUMBER ATTRIBUTABLE TO 2019/20 BUSHFIRES (95%CI)	TOTAL VOLUME OF SIMILAR DIAGNOSES AND TIME PERIOD	PROPORTION (PROPORTION RANGE)
Deaths – derived	429 (154–712)	78,940	0.5% (0.2%-0.9%)
Deaths – confirmed	33 including 9 firefighters	78,940	0.04%
Respiratory admissions derived from AIHW source A - or - derived from AIHW source B	2092 (0–4638)	241,100 - or - 226,626	0.9% (0-1.9%) - or - 0.9%
Cardiovascular/Cerebrovascular admissions derived from AIHW source A derived from AIHW source B	1138 (210–2113)	242,026 - or - 288,951	0.5% (0.09%-0.9%) - or - 0.4%
Asthma ED presentations – derived from AIHW source A	1523 (750–2466)	35,022	4.3% (2.1%-7.0%)

The number of cases attributable to the 2019 - 2020 bushfires was sourced from Johnston et al. (2021). Confirmed deaths are from Parliament of Australia (2020). It is to be noted that individual deaths are never coded as directly caused by air pollution and statistical attribution (derived deaths) is adopted for population impact assessments.

Regarding AIHW Source A: AIHW have made available hospital count data for the period 1 September 2019 – 1 March 2020 to accompany their report on the short-term health impacts of the 2019–20 Australian bushfires (AIHW, 2021a). This report includes analysis of relative changes in the 2019/20 season compared to the previous 5-year average. The source data contains counts of asthma ED presentations (Table S4 within the source data), respiratory admissions (Table S2 of the source data) and cardiovascular admissions represented by the sum of 'Selected heart conditions' and 'Cerebrovascular conditions' (Table S2 of the source data). There are a few distinctions between the diagnoses codes and time period used by Johnston et al. (2021) and AIHW analysis:

a. The 6-month analysis period is offset by one month (1 September – 1 March) compared to the fire season considered by Johnston et al. (1 October – 31 March);
b. While respiratory admissions are defined similarly (diagnosis codes J00-J99), Johnston et al. have additionally included counts for rheumatic heart diseases (diagnosis codes I00-I09), and diseases of arteries, arterioles, capillaries, veins, lymphatic vessels and lymph nodes (diagnosis codes I70-I89) in their analysis;

c. Johnston et al. excluded acute severe asthma (diagnosis code J46) when considering asthma-related ED presentations.

Notes on AIHW Source B: Using the same definitions used to define respiratory (ICD10 diagnosis codes J00-J99) and cardiovascular (ICD10 codes I00-I90 admissions), AIHW report there were 453,252 respiratory admissions and 577,902 cardiovascular admissions in public and private Australian hospitals over the 2019-20 financial year (AIHW, 2021c). An alternative estimate of the admissions over the 6-month fire season considered by Johnston et al. (1 October - 31 March) is 50% of these values (226,626 respiratory and 288,951 cardiovascular admissions) although it is possible that there are higher counts of these diagnoses over winter rather than the summer fire season. AIHW's publicly accessible dataset capturing ED presentations in public hospitals for the 2019-20 financial year (AIHW, 2020) report only counts for the full range of diseases of the respiratory system (diagnosis codes J00–J99, n= 618,619) and counts for the specific diagnosis of asthma are not discernible.

While not an exact match in terms of diagnosis codes and time period, it is still a reasonable source from which to estimate proportional contributions of the impacts form bushfires.

The table indicates that in the context of national figures for the same period, while indeed the health impacts from the 2019-20 bushfires are substantial, they are less than 1% of broader mortality and inpatient admission impacts for similar diagnoses, and approximately 4% of broader volume in the case of asthma-related ED presentations. It is acknowledged that the modelled outcomes (hospitalisations and deaths) represent the most severe but rarer outcomes from population exposure to smoke, so don't capture the entirety of the public health burden.

It is challenging to speculate about proportional contributions at a future time period such as 2050. One view is that these proportional impacts on the health system may decrease, as hospitalisation rates in Australia are growing faster than the population. Over the last 10 years to 2022–23, inpatient admissions have increased from 395 to 415 per 1000 population (AIHW, 2024c), and ED presentations have increased from 296 to 334 per 1000 population (AIHW, 2023: 8,800,919 ED visits in 2022-23, or 334 per 1000 pop; AIHW, 2013: 6,712,224 ED visits in 2012-13, or 296 per 1000 pop). However, the number of estimated cases due to air quality in the future is a function of both the population and also the incidence rate at the future time period (as well as potentially updated relative risks). As well as the population increasing, the incidence rate will possibly be higher too due to the population getting older and sicker, and thus those proportions won't necessarily decrease.

2.3.11 Summary and next steps

This investigation provides a rigorous assessment of the evidence of mortality and health system impacts associated with an extreme bushfire event in 2050. The evidence is clear: climate change is increasing the frequency and extremity of fire weather when most fires tend to occur and exposure to bushfire smoke contributes towards Australia's disease burden. The substantial evidence base suggests that controlling fine particle pollution would result in fewer early deaths, particularly in other global hotspots given that ambient fine particulate matter is the world's leading environmental health risk factor. This ranking has many governments focused on reducing anthropogenic particulate matter as priorities for action.

This investigation also highlights there is high particulate matter exposure occurring all the time for populations in central Australia. While concern about extreme events like bushfires is appropriate, there isn't a way to remove dust as a risk factor from the country, and our future climate will contain all sources of $PM_{2.5}$ and PM_{10} including those from non-anthropogenic emissions.

The narrative on bushfire risk also needs to evolve with allowance for adjustments as the evidence-base grows. Risks change as the underlying population changes and globally, exposure to ambient particulate matter pollution is among the largest increases in risk to health, even given that air pollution concentrations have decreased in many regions. There are numerous assumptions made in population-level modelling and the academic and research sector are important voices in regard to being abreast of the evolving evidence to ensure that policy in this contentious area is informed by best practice.

Future pathways to explore related to this investigation are as follows.

This investigation has benefited from the prior efforts of personnel behind the creation of national data repositories made available by Australian Government initiatives, which ultimately assists in improving the lives of Australians through evidence-based climate-change policy. This aligns with Recommendation 15.4 of the 2020 Royal Commission into National Natural Disaster Arrangements (Binskin, 2020) around developing consistent and compatible methods and metrics to measure health impacts related to natural disasters and taking steps to ensure the appropriate sharing of health and mental health datasets.

We recommend continued investment in open data lakes comprising deidentified health data and environmental data at a spatial resolution where local differences in demographics are key to providing targeted service delivery. Such information is valuable across sectors into both state and federal-responsibility areas of primary care, Aboriginal community controlled health organisations, residential aged care and disability support services. The dimension of these data collections should be driven by outcomes of interest which are likely to be the key health usage performance indicators of the government of the day.

In the provision of these data collections, there needs to be security protocols agreed as standards to protect the privacy of individuals. This absolute requirement is essential given the sophistication of matching performance of linking between supposedly disparate datasets. The benefits of targeted service delivery described above are outweighed by a single adverse outcome following linkage.

Cross agency collaboration in efforts to improve resilience against this risk is warranted, for example developing and deploying surveillance systems tracking critical signals of interest at a national level. Such a platform could bring statistical process control and anomaly detection methodology together on indexed and curated githubs where codebase can grow to support related broader applications.

This investigation focused on $PM_{2.5}$ in accordance with global agreement of it being the main contributor of air quality health risks. Estimates were also generated for ozone and NO_2 exposure which also have known health impacts. However, the relative contributions of health impacts from simultaneous exposure to multiple pollutants need to be determined from statistical models incorporating these pollutants (it is impractical to add the impacts of exposure from each pollutant

as if these were independent risks, as there are overlapping exposure effects). The complementary statistical modelling described in Section 2.3.9 used temperature as a confounder, and future studies could add historical observations of other pollutants to account for simultaneous presence, similar to Johnston et al. (2011). Also, some of the AIHW data elements that were considered as response variables in the statistical modelling exercise could instead be considered as explanatory variables. For example, PBS 'Mental health prescriptions' could be considered as an explanatory variable in a model assessing ED presentations or inpatient admission related to 'Mental and behavioural disorders'.

More broadly, extending the analysis of health impacts to thermal comfort impacts is also a logical next step. It is understood related work by the Australian Climate Service for the National Climate Risk Assessment has started assessing thermal comfort.

2.3.12 Acknowledgements (health impact assessment)

We make a special thanks to three subject matter experts in particular who provided input to this modelling. We are appreciative firstly to Nicolas (Nico) Borchers Arriagada from the Menzies Institute for Medical Research at the University of Tasmania, whose nationally focused examinations of this subject demonstrate his insight for health impact modelling and applying novel AI approaches to improve the quality of smoke models. We thank Nico for the advice and steering us towards a 'surfaces' model approach and the contributions towards datasets hosted on the CARDAT platform for the research community to inform national analysis such as undertaken in this investigation.

We would like to thank Ivan Hanigan from Curtin University for provisioning access to the CARDAT bushfire smoke dataset, especially the responsiveness of the CARDAT Data Management Team including Cassandra Yuen and Prof Geoff Morgan from the University of Sydney. The research community is indebted to those efforts and acknowledge this facilitation is provided in-kind in the context of high demand for the services provided. We appreciate the advice on the merits of the relative risks for mortality, the importance of framing the counterfactual clearly, and caution around speculating about the level and condition of health services in future scenarios driven by an ageing and sicker population and changing health workforce.

We acknowledge input provided from Fay Johnston from the Menzies Institute for Medical Research at the University of Tasmania who has contributed much to the evidence base for this growing global focus area. We thank Fay for providing sage advice about this type of modelling, especially on the peppery topic of estimating incidence rate changes from demographic and climate changes, i.e. considering climate but also the ageing population.

We acknowledge Geoscience Australia for the access to population projections of SA2 regions to 2032 prepared by the Australian Bureau of Statistics. We thank Melanie Harris from Climate Data Services within the Bureau of Meteorology, and Research Data Management Specialists at NCI Australia who facilitated access to BoM's official dataset for climate analyses "Australian Gridded Climate Data (AGCD) / Australian Water Availability Project (AWAP)" via NCI's zv2 project (https://my.nci.org.au/mancini/project/zv2). We also acknowledge the funding sources and personnel behind the development and validation of the AQFx model (Air Quality Forecasting System) designed by CSIRO and managed and delivered by the Bureau of Meteorology.

2.3.13 References (Health Impact Assessment)

Agache, I., Canelo-Aybar, C., Annesi-Maesano, I., Cecchi, L., Rigau, D., Rodríguez-Tanta, L. Y., Nieto-Gutierrez, W., Song, Y., Cantero-Fortiz, Y., Roqué, M., Vasquez, J. C., Sola, I., Biagioni, B., Chung, F., D'Amato, G., Damialis, A., Del Giacco, S., Vecillas, L. L., Dominguez-Ortega, J., Galàn, C., … Akdis, C. A. (2024). The impact of outdoor pollution and extreme temperatures on asthma-related outcomes: A systematic review for the EAACI guidelines on environmental science for allergic diseases and asthma. Allergy, 79(7), 1725–1760. https://doi.org/10.1111/all.16041.

Australian Bureau of Statistics. (2023a). Deaths, Australia. Data Cubes: Table 4: Deaths, Summary, Statistical Area Level 2, 2012 to 2022, September 2023. Available from https://www.abs.gov.au/statistics/people/population/deaths-australia/latest-release (accessed September 2024).

Australian Bureau of Statistics. (2023b). Population Projections, Australia. Released Nov 2023. Available from https://www.abs.gov.au/statistics/people/population/population-projections-australia/latest-release (accessed September 2024).

Australian Bureau of Statistics. (2024). Regional population. Data Cubes: Population estimates by SA2 and above, 2001 to 2023, Released March 2024. Available from https://www.abs.gov.au/statistics/people/population/regional-population/latest-release#data-downloads (accessed September 2024).

Australian Institute of Health and Welfare. (2013). Australian hospital statistics 2012-13: emergency department care. Canberra: AIHW.

Australian Institute of Health and Welfare. (2020). Emergency department care 2019–20 data tables. Table 4.8: Emergency department presentations(a) by age group and principal diagnosis in ICD-10-AM(b) chapters, public hospitals, 2019–20. Available from https://www.aihw.gov.au/reports-data/myhospitals/content/data-downloads (accessed September 2024).

Australian Institute of Health and Welfare. (2021a). Data update: Short-term health impacts of the 2019–20 Australian bushfires, last updated Aug 2024. Available from https://www.aihw.gov.au/reports/environment-and-health/data-update-health-impacts-2019-20-bushfires/contents/about (accessed Sept 2024).

Australian Institute of Health and Welfare (2021b). Australian Burden of Disease Study 2018: Interactive data on risk factor burden, last updated Aug 2023. Available from https://www.aihw.gov.au/reports/burden-of-disease/abds-2018-interactive-data-risk-factors/contents/summary (accessed Sept 2024).

Australian Institute of Health and Welfare. (2021c). Admitted patient care 2019–20; 4: Why did people receive care? Table 4.6: Separations, by principal diagnosis in ICD-10-AM chapters, public and private hospitals, 2019–20. Available from https://www.aihw.gov.au/reports-data/myhospitals/content/data-downloads (accessed Sept 2024).

Australian Institute of Health and Welfare (2023). Hospitals info & downloads: Data downloads: Emergency department care 2022–23 data tables, Dec2023. Available from

https://www.aihw.gov.au/reports-data/myhospitals/content/data-downloads (accessed Sept 2024).

Australian Institute of Health and Welfare. (2024a). Australian Burden of Disease Study: Methods and supplementary material 2018 Web report. Last updated: 24 Nov 2021, Cat. no: BOD 26 DOI: 10.25816/te11-2a60, Available from https://www.aihw.gov.au/reports/burden-of-disease/abds-methods-supplementary-material-2018/contents/about (accessed Sept 2024).

Australian Institute of Health and Welfare. (2024b). Geography and time-specific health data for environmental analysis, last updated Mar 2024. Available from https://www.aihw.gov.au/reports/environment-and-health/geography-time-specific-data-environment/data (accessed Sept 2024).

Australian Institute of Health and Welfare. (2024c). Admitted patients. Available from https://www.aihw.gov.au/reports-data/myhospitals/sectors/admitted-patients (accessed Sept 2024).

Beelen, R., Raaschou-Nielsen, O., Stafoggia, M., Andersen, Z. J., Weinmayr, G., Hoffmann, B., Wolf, K., Samoli, E., Fischer, P., Nieuwenhuijsen, M., Vineis, P., Xun, W. W., Katsouyanni, K., Dimakopoulou, K., Oudin, A., Forsberg, B., Modig, L., Havulinna, A. S., Lanki, T., Turunen, A., … Hoek, G. (2014). Effects of long-term exposure to air pollution on natural-cause mortality: An analysis of 22 European cohorts within the multicentre ESCAPE project. Lancet, 383(9919), 785–795. https://doi.org/10.1016/S0140-6736(13)62158-3.

Berman, J. D., Fann, N., Hollingsworth, J. W., Pinkerton, K. E., Rom, W. N., Szema, A. M., Breysse, P. N., White, R. H., & Curriero, F. C. (2012). Health benefits from large-scale ozone reduction in the United States. Environmental Health Perspectives, 120(10), 1404–1410. https://doi.org/10.1289/ehp.1104851.

Beverland, I. J., Cohen, G. R., Heal, M. R., Carder, M., Yap, C., Robertson, C., Hart, C. L., & Agius, R. M. (2012). A comparison of short-term and long-term air pollution exposure associations with mortality in two cohorts in Scotland. Environmental Health Perspectives, 120(9), 1280–1285. https://doi.org/10.1289/ehp.1104509.

Binskin, M. (2020). Royal Commission into National Natural Disaster Arrangements. https://www.royalcommission.gov.au/natural-disasters/report.

Borchers Arriagada, N., Horsley, J. A., Palmer, A. J., Morgan, G. G., Tham, R., & Johnston, F. H. (2019). Association between fire smoke fine particulate matter and asthma-related outcomes: Systematic review and meta-analysis. Environmental Research, 179(Pt A), 108777. https://doi.org/10.1016/j.envres.2019.108777.

Borchers Arriagada, N., Palmer, A. J., Bowman, D. M., & Johnston, F. H. (2020). Exceedances of national air quality standards for particulate matter in Western Australia: sources and health-related impacts. The Medical Journal of Australia, 213(6), 280–281. https://doi.org/10.5694/mja2.50547.

Borchers Arriagada, N., Palmer, A. J., Bowman, D. M., Morgan, G. G., Jalaludin, B. B., & Johnston, F. H. (2020). Unprecedented smoke-related health burden associated with the 2019-20 bushfires in eastern Australia. The Medical Journal of Australia, 213(6), 282–283. https://doi.org/10.5694/mja2.50545.

Brook, J. R., Dann, T. F., & Burnett, R. T. (1997). The relationship among TSP, PM_{10}, $PM_{2.5}$, and inorganic constituents of atmospheric participate matter at multiple Canadian locations. Journal of the Air & Waste Management Association, 47(1), 2-19.

Broome, R. A., Fann, N., Cristina, T. J., Fulcher, C., Duc, H., & Morgan, G. G. (2015). The health benefits of reducing air pollution in Sydney, Australia. Environmental Research, 143(Pt A), 19–25. https://doi.org/10.1016/j.envres.2015.09.007.

Burnett, R. T., Pope, C. A., 3rd, Ezzati, M., Olives, C., Lim, S. S., Mehta, S., Shin, H. H., Singh, G., Hubbell, B., Brauer, M., Anderson, H. R., Smith, K. R., Balmes, J. R., Bruce, N. G., Kan, H., Laden, F., Prüss-Ustün, A., Turner, M. C., Gapstur, S. M., Diver, W. R., … Cohen, A. (2014). An integrated risk function for estimating the global burden of disease attributable to ambient fine particulate matter exposure. Environmental Health Perspectives, 122(4), 397–403. https://doi.org/10.1289/ehp.1307049.

Carey, I. M., Atkinson, R. W., Kent, A. J., van Staa, T., Cook, D. G., & Anderson, H. R. (2013). Mortality associations with long-term exposure to outdoor air pollution in a national English cohort. American Journal of Respiratory and Critical Care Medicine, 187(11), 1226–1233. https://doi.org/10.1164/rccm.201210-1758OC.

Carracedo-Martínez, E., Taracido, M., Tobias, A., Saez, M., & Figueiras, A. (2010). Case-crossover analysis of air pollution health effects: A systematic review of methodology and application. Environmental Health Perspectives, 118(8), 1173–1182. https://doi.org/10.1289/ehp.0901485.

Cohen, A. J., Ross Anderson, H., Ostro, B., Pandey, K. D., Krzyzanowski, M., Künzli, N., Gutschmidt, K., Pope, A., Romieu, I., Samet, J. M., & Smith, K. (2005). The global burden of disease due to outdoor air pollution. Journal of Toxicology and Environmental Health. Part A, 68(13-14), 1301–1307. https://doi.org/10.1080/15287390590936166.

Davidson, K., Hallberg, A., McCubbin, D., & Hubbell, B. (2007). Analysis of $PM_{2.5}$ using the Environmental Benefits Mapping and Analysis Program (BenMAP). Journal of toxicology and environmental health. Part A, 70(3-4), 332–346. https://doi.org/10.1080/15287390600884982.

Emmerson, K. M., & Keywood, M. D. (2021). Australia state of the environment 2021: Air quality. Australian Government Department of Climate Change, Energy, the Environment and Water. https://doi.org/10.26194/k7x7-0j76.

Fann, N., Lamson, A. D., Anenberg, S. C., Wesson, K., Risley, D., & Hubbell, B. J. (2012). Estimating the national public health burden associated with exposure to ambient $PM_{2.5}$ and ozone. Risk analysis: An Official Publication of the Society for Risk Analysis, 32(1), 81–95. https://doi.org/10.1111/j.1539-6924.2011.01630.x.

Beelen, R., de Hoogh, K., Breugelmans, O., Kruize, H., Janssen, N. A., & Houthuijs, D. (2015). Air Pollution and Mortality in Seven Million Adults: The Dutch Environmental Longitudinal Study (DUELS). Environmental Health Perspectives, 123(7), 697–704. https://doi.org/10.1289/ehp.1408254.

GBD 2019 Risk Factors Collaborators (2020). Global burden of 87 risk factors in 204 countries and territories, 1990-2019: a systematic analysis for the Global Burden of Disease Study 2019.

Lancet (London, England), 396(10258), 1223–1249. https://doi.org/10.1016/S0140-6736(20)30752-2.

GBD 2021 Risk Factors Collaborators (2024). Global burden and strength of evidence for 88 risk factors in 204 countries and 811 subnational locations, 1990-2021: a systematic analysis for the Global Burden of Disease Study 2021. Lancet (London, England), 403(10440), 2162–2203. https://doi.org/10.1016/S0140-6736(24)00933-4.

Geoscience Australia. (2024). SA2 population projections 2022 to 2032. ABS Digital Atlas Australia. Dataset published June 2024. Available from https://digital.atlas.gov.au/datasets/digitalatlas::sa2-population-projections-2022-to-2032/about (accessed September 2024).

Hanigan, I. C., Rolfe, M. I., Knibbs, L. D., Salimi, F., Cowie, C. T., Heyworth, J., Marks, G. B., Guo, Y., Cope, M., Bauman, A., Jalaludin, B., & Morgan, G. G. (2019). All-cause mortality and long-term exposure to low level air pollution in the '45 and up study' cohort, Sydney, Australia, 2006-2015. Environment International, 126, 762–770. https://doi.org/10.1016/j.envint.2019.02.044.

Hanigan, I., Yuen, C., Gopi, K., Borchers-Arriagada, N., van Buskirk, J., & Morgan, G. (2023). Bushfire-specific $PM_{2.5}$ Australia 2001-2020 v1.3. Centre for Air Pollution, Energy and Health Research. https://doi.org/10.17605/OSF.IO/WQK4T.

Hänninen, O. O., Salonen, R. O., Koistinen, K., Lanki, T., Barregard, L., & Jantunen, M. (2009). Population exposure to fine particles and estimated excess mortality in Finland from an East European wildfire episode. Journal of Exposure Science & Environmental Epidemiology, 19(4), 414-422. https://doi.org/10.1038/jes.2008.31.

Henschel, S., Chan, G., & World Health Organization. (2013). Health risks of air pollution in Europe–HRAPIE project: new emerging risks to health from air pollution–results from the survey of experts (No. WHO/EURO: 2013-6696-46462-67326). Available from https://apps.who.int/iris/handle/10665/153692 (accessed September 2024).

Héroux, M. E., Anderson, H. R., Atkinson, R., Brunekreef, B., Cohen, A., Forastiere, F., Hurley, F., Katsouyanni, K., Krewski, D., Krzyzanowski, M., Künzli, N., Mills, I., Querol, X., Ostro, B., & Walton, H. (2015). Quantifying the health impacts of ambient air pollutants: recommendations of a WHO/Europe project. International Journal of Public Health, 60(5), 619–627. https://doi.org/10.1007/s00038-015-0690-y.

Hertzog, L., Morgan, G. G., Yuen, C., Gopi, K., Pereira, G. F., Johnston, F. H., Cope, M., Chaston, T. B., Vyas, A., Vardoulakis, S., & Hanigan, I. C. (2024). Mortality burden attributable to exceptional $PM_{2.5}$ air pollution events in Australian cities: A health impact assessment. Heliyon, 10(2), e24532. https://doi.org/10.1016/j.heliyon.2024.e24532.

Huangfu, P., & Atkinson, R. (2020). Long-term exposure to NO_2 and O_3 and all-cause and respiratory mortality: A systematic review and meta-analysis. Environmental International, 144, 105998. https://doi.org/10.1016/j.envint.2020.105998.

Hubbell, B. J., Hallberg, A., McCubbin, D. R., & Post, E. (2005). Health-related benefits of attaining the 8-hr ozone standard. Environmental Health Perspectives, 113(1), 73–82. https://doi.org/10.1289/ehp.7186.

Jegasothy, E., Hanigan, I. C., Van Buskirk, J., Morgan, G. G., Jalaludin, B., Johnston, F. H., Guo, Y., & Broome, R. A. (2023). Acute health effects of bushfire smoke on mortality in Sydney, Australia. Environment International, 171, 107684. https://doi.org/10.1016/j.envint.2022.107684.

Johnston, F., Hanigan, I., Henderson, S., Morgan, G., & Bowman, D. (2011). Extreme air pollution events from bushfires and dust storms and their association with mortality in Sydney, Australia 1994–2007. Environmental Research, 111(6), 811-816. https://doi.org/10.1016/j.envres.2011.05.007.

Johnston, F. H., Borchers-Arriagada, N., Morgan, G. G., Jalaludin, B., Palmer, A. J., Williamson, G. J., & Bowman, D. M. (2021). Unprecedented health costs of smoke-related PM2. 5 from the 2019–20 Australian megafires. Nature Sustainability, 4(1), 42-47. https://doi.org/10.1038/s41893-020-00610-5.

Krewski, D., Jerrett, M., Burnett, R. T., Ma, R., Hughes, E., Shi, Y., Turner, M. C., Pope, C. A., 3rd, Thurston, G., Calle, E. E., Thun, M. J., Beckerman, B., DeLuca, P., Finkelstein, N., Ito, K., Moore, D. K., Newbold, K. B., Ramsay, T., Ross, Z., Shin, H., … Tempalski, B. (2009). Extended follow-up and spatial analysis of the American Cancer Society study linking particulate air pollution and mortality. Research Report (Health Effects Institute), (140), 5–136.

Lopez A. D. (2013). Reducing risks to health: what can we learn from the Global Burden of Disease 2010 Study? International Journal of Public Health, 58(5), 645–646. https://doi.org/10.1007/s00038-013-0503-0.

Martenies, S. E., Wilkins, D., & Batterman, S. A. (2015). Health impact metrics for air pollution management strategies. Environment International, 85, 84–95. https://doi.org/10.1016/j.envint.2015.08.013.

Melody SM and Johnston FH. (2015). Coal mine fires and human health: What do we know? International Journal of Coal Geology, Dec;152(B):1–14.

McDuffie, E., Martin, R., Yin, H., & Brauer, M. (2021). Global Burden of Disease from Major Air Pollution Sources (GBD MAPS): A Global Approach. Research Report (Health Effects Institute), 2021(210), 1–45.

Mills, I. C., Atkinson, R. W., Kang, S., Walton, H., & Anderson, H. R. (2015). Quantitative systematic review of the associations between short-term exposure to nitrogen dioxide and mortality and hospital admissions. BMJ open, 5(5), e006946. https://doi.org/10.1136/bmjopen-2014-006946.

Murray, C. J., Ezzati, M., Lopez, A. D., Rodgers, A., & Vander Hoorn, S. (2003). Comparative quantification of health risks conceptual framework and methodological issues. Population Health Metrics, 1(1), 1. https://doi.org/10.1186/1478-7954-1-1.

Orellano, P., Reynoso, J., Quaranta, N., Bardach, A., & Ciapponi, A. (2020). Short-term exposure to particulate matter (PM_{10} and $PM_{2.5}$), nitrogen dioxide (NO_2), and ozone (O_3) and all-cause and cause-specific mortality: Systematic review and meta-analysis. Environment International, 142, 105876. https://doi.org/10.1016/j.envint.2020.105876.

Parliament of Australia. (2020). 2019–20 bushfires—frequently asked questions: a quick guide. Available from https://parlinfo.aph.gov.au/ (accessed Sept 2024).

Pope, C. A., 3rd, & Dockery, D. W. (2006). Health effects of fine particulate air pollution: lines that connect. Journal of the Air & Waste Management Association (1995), 56(6), 709–742. https://doi.org/10.1080/10473289.2006.10464485.

Pope C. A., 3rd (2007). Mortality effects of longer term exposures to fine particulate air pollution: review of recent epidemiological evidence. Inhalation Toxicology, 19 Suppl 1, 33–38. https://doi.org/10.1080/08958370701492961.

Reid, J. S., Koppmann, R., Eck, T. F., & Eleuterio, D. P. (2005). A review of biomass burning emissions part II: intensive physical properties of biomass burning particles. Atmospheric Chemistry and Physics, 5(3), 799-825. https://doi.org/10.5194/acp-5-799-2005.

Ru, M., Shindell, D., Spadaro, J. V., Lamarque, J. F., Challapalli, A., Wagner, F., & Kiesewetter, G. (2023). New concentration-response functions for seven morbidity endpoints associated with short-term $PM_{2.5}$ exposure and their implications for health impact assessment. Environment International, 179, 108122. https://doi.org/10.1016/j.envint.2023.108122.

Sacks, J. D., Lloyd, J. M., Zhu, Y., Anderton, J., Jang, C. J., Hubbell, B., & Fann, N. (2018). The Environmental Benefits Mapping and Analysis Program - Community Edition (BenMAP-CE): A tool to estimate the health and economic benefits of reducing air pollution. Environmental Modelling & Software: With Environment Data News, 104, 118–129.

Schwartz, J., Laden, F., & Zanobetti, A. (2002). The concentration-response relation between PM (2.5) and daily deaths. Environmental Health Perspectives, 110(10), 1025–1029. https://doi.org/10.1289/ehp.021101025.

Schwarz, M., Peters, A., Stafoggia, M., de'Donato, F., Sera, F., Bell, M. L., Guo, Y., Honda, Y., Huber, V., Jaakkola, J. J. K., Urban, A., Vicedo-Cabrera, A. M., Masselot, P., Lavigne, E., Achilleos, S., Kyselý, J., Samoli, E., Hashizume, M., Ng, C. F. S., Pereira da Silva, S. N.... Zanobetti, A.. (2024). Temporal variations in the short-term effects of ambient air pollution on cardiovascular and respiratory mortality: a pooled analysis of 380 urban areas over a 22-year period. The Lancet Planetary Health, 8(9), e657-e665. https://doi.org/10.1016/S2542-5196(24)00168-2.

Steenland, K., & Armstrong, B. (2006). An overview of methods for calculating the burden of disease due to specific risk factors. Epidemiology (Cambridge, Mass.), 17(5), 512–519. https://doi.org/10.1097/01.ede.0000229155.05644.43.

Turner, M. C., Jerrett, M., Pope, C. A., 3rd, Krewski, D., Gapstur, S. M., Diver, W. R., Beckerman, B. S., Marshall, J. D., Su, J., Crouse, D. L., & Burnett, R. T. (2016). Long-term ozone exposure and mortality in a large prospective study. American Journal of Respiratory and Critical Care Medicine, 193(10), 1134–1142. https://doi.org/10.1164/rccm.201508-1633OC.

U.S. Environmental Protection Agency, 2022. Supplement to the 2019 Integrated Science Assessment for Particulate Matter (Final Report, 2022). Available from https://cfpub.epa.gov/ncea/isa/recordisplay.cfm?deid=354490 (accessed September 2024).

Zhou, X., Cao, Z., Ma, Y., Wang, L., Wu, R., & Wang, W. (2016). Concentrations, correlations and chemical species of $PM_{2.5}$/PM_{10} based on published data in China: Potential implications for the revised particulate standard. Chemosphere, 144, 518–526. https://doi.org/10.1016/j.chemosphere.2015.09.003.

3 Emergence and increased transmission of communicable diseases (Workstream 2)

Activities undertaken in this workstream will build on the soon to be published Climate and Communicable Disease Discussion Paper (CSIRO, 2024), focussing on assessing trends of a select number of current diseases, and the likely changes of overall spillover risk with climate variation. This workstream will perform a deeper assessment for potentially high impact pathogens using climate change scenarios and describe those scenarios under which these pathogens might develop concerning properties.

The soon to be published Climate and Communicable Disease Discussion Paper identified three key areas of interest that were further explored in this workstream. The first area emphasised the importance of prioritising national investment in building resilience against communicable diseases, which includes ongoing support for surveillance and assessing the impact on vulnerable populations across Australia. To investigate this, we analysed national and subnational surveillance data to assess how climate change is affecting methicillin-resistant Staphylococcus aureus (MRSA) in northern regional and remote Australia, as well as influenza notifications nationwide. The second area focused on mosquito-borne diseases as the most climate-sensitive in Australia. We assessed the potential future impact of climate change and disease spillover on Japanese encephalitis. The third area demonstrated the value of new technologies, such as genome-wide evolutionary dynamics, to better understand the climate sensitivity of diseases and assess its impact on seasonal influenza.

3.1 Investigating the impact of climate on high prevalence bacterial and viral pathogens of concern using routinely collected surveillance data

Climate change is influencing the epidemiology of infectious diseases, including antimicrobial resistant (AMR) infections (e.g; methicillin-resistant staphylococcus aureus (MRSA)) and viral infections (e.g; influenza) (Patz et al., 1996; Dave and Lee, 2019; Fisman, 2017). Variations in climate factors including temperature, humidity, and precipitation can impact the prevalence and transmission dynamics of pathogens (Martinez, et al., 2019). The global warming-related changes in disease epidemiology are associated with changes in ecosystems, population susceptibility, and increased exposure to causative agents (Marani et al., 2021; McMichael et al., 2007; Altizer et al., 2007).

In particular, climate change may alter the incidence and severity of respiratory infections by affecting vectors and host immune responses. Young children and older adults appear to be particularly vulnerable to rapid fluctuations in temperature changes. For example, a small study showed an increase in the incidence in childhood upper respiratory infections in Australia has been associated with sharp temperature changes from one day to the next (Xu et al., 2014). Extreme weather events, such as heat waves, floods, major storms, drought, and wildfires, are also believed to change the incidence of respiratory infections (Lane et al., 2022).

Changes in AMR rates due to climate may be a result of multiple factors. For example, changes in environmental conditions may affect bacterial survival rate or the interaction between host and the environment (Magnano San Lio et al, 2023) and worsen the impact of existing antibiotic selective pressure. Evidence suggests that that climate, particularly, seasonal changes can influence AMR by affecting patterns of antibiotic use (Martinez, et al., 2019; Rahul et al., 2023).

Analysing these interactions is essential for understanding how climate fluctuations contribute to infectious disease patterns and for informing public health actions. Surveillance, modelling and analysis are two approaches to assess the impact of climate change on infectious disease. Changes in the epidemiology of disease may reflect climate related factors, such as temperature changes. Modelling studies offer another approach to estimating the effects of climate change on infectious disease and are useful for future prediction.

This work examines the impact of climate variations including temperature, humidity, and precipitation on infectious disease prevalence focusing on viral species (influenza) and high prevalence bacterial species (MRSA), employing routinely collected surveillance data. The two routinely collected pathogens include (i) laboratory-confirmed influenza from the National Notifiable Diseases Surveillance System (NNDSS) (DoHAC, 2023) and (ii) methicillin-resistant Staphylococcus aureus (MRSA) from a passive CSIRO-owned disease surveillance system (HOTspots) (hereafter referred to as HOTspots) (Australian e-Health Research Centre, 2023). The health impacts of climate variation on 2050, were built on projections of future exposures generated by global climate models.

3.1.1 Methods

Datasets

Disease datasets

We used two surveillance datasets: (i) influenza notifications from 01 January 2008 to 31 December 2019 for all Australia, except the Australian Capital Territory (ACT) region, and (ii) MRSA counts for northern Australia from 01 January 2007 to 2023.

NNDSS influenza dataset provides state and territory level notifications, on weekly basis, for four types of influenza (A, B, C, and untyped). We considered all four types in our analysis. Our analysis is based on the publicly available NNDSS database, which does not include the ACT region, hence it was excluded from our analysis. Although NNDSS database provides data beyond 2019, we only considered the pre-Covid-19 period, to most clearly illustrate the relationship between climate and human health factors.

HOTSpots dataset contains laboratory confirmed phenotypic data for key pathogens (WHO, 2024) across 24 Statistical Area Level 3 (SA3) regions (Australian Bureau of Statistics, 2023) corresponding to three jurisdictions in northern Australia (far north Western Australia, Northern Territory and far north Queensland). HOTspots collate antimicrobial susceptibility test data from four main pathology providers for bloodstream infections, urinary tract infections, respiratory infections, and skin and soft tissue infections from patients attending primary healthcare clinics and hospitals. We considered both hospital and community acquired MRSA infection and all specimen types. The methodology of the HOTspots has been previously described in (Wozniak et al., 2022; Wozniak et al., 2020).

Population datasets

Three population datasets were used, of which two were from the ABS and the remaining was from the National Aeronautics and Space Administration Socioeconomic Data and Applications Center (SEDAC, https://sedac.ciesin.columbia.edu).

The two ABS population datasets were (i) the national state and territory population (ABS, 2023) and (ii) the region population at SA3 level (ABS 2022-2023). The first one provides quarterly growth of the Australian population between June 1981 to December 2023. We applied this dataset to compute the per-capita influenza rates. The second one offers annual region population between 2001 to 2023. We applied this second dataset to compute per-capita MRSA rates.

From SEDAC, we obtained the Gridded Population of the World (GPW, v4) dataset, which led us to calculate the population density-weighted averages of the climate variables over a 1° ×1° grid spacing across Australia.

Climate datasets

We employed two climate datasets which include (i) the Bureau of Meteorology Atmospheric high-resolution Regional Reanalysis for Australia – Version 2 (BARRA2) (Su et al., 2022) for the period 01 January 2007 to 31 December 2023 (ii) the ACCESS-CM2 Global Climate Model (GCM) from a group of the sixth Coupled Model Inter- comparison Project (CMIP6) (Grose et al., 2023) for the period 01 January 2035 to 01 January 2064.

BARRA2 comprises the retrospective regional atmospheric reanalysis over Australia and surrounding regions, spanning from 01 January 1979 to present day. It utilises existing historical atmospheric data to adjust a high-resolution computational model of the atmosphere, facilitating the retrieval of historically indicative gridded charts of the necessary variables for our analysis. We extracted six climate variables from BARRA2 including average surface air temperature, maximum surface air temperature, minimum surface air temperature, relative humidity, and precipitation.

CMIP6 dataset contains bias-corrected and statistically downscaled future climate projections over Australia and surrounding regions, covering the period 01 January 2035 to 01 January 2064. We considered three specific Shared Socioeconomic Pathways (SSP) from the ACCESS-CM2 model. Each SSP characterises a possible future socioeconomic development and its impact on the climate. These pathways, which have been collectively approved by the international climate community, are labelled in order of escalating levels of greenhouse gas emission as SSP1-2.6 (low), SSP2-4.5 (intermediate), and SSP5-8.5 (very high). These pathways provide a means to understand the potential impacts of different climate actions or inactions. From the CMIP6 dataset, we obtained future projections for the same climate variables as the ones we derived from BARRA2 dataset, except average surface air temperature which was not available in the ACS CMIP6 dataset.

Modelling

We implemented modelling in three stages. Initially, we performed correlation analysis between individual historic climate variables and each disease dataset. We then constructed independent linear regression models for predicting each disease rate from the historic climate variables in BARRA2 dataset which depicted significant correlation with the respective disease rate by employing a non-parametric bootstrapped sampling technique. Subsequently, we derived future

projected disease rate utilising CMIP6 dataset and the model which showed the strongest relationship between historic climate variable and the disease rate. This approach was previously applied for projecting the impact of climate on demand for respiratory-related ICU average length of stay in Australia (Poon et al., 2023). We detail these three stages in the following sections.

Outcome variables

We considered two independent outcome measures - annual influenza rate for the period 2008 to 2019 and annual MRSA rate for the period 2007 to 2023. Each measure was computed by first summing the respective disease counts per year and then dividing by the respective population of Australia in that year to produce per capita rates. For influenza, the annual Australian population, except ACT, from the state and territory population dataset of ABS was used. For MRSA, the annual population corresponding to the north Australia from the region population dataset of ABS was applied.

Predictor variables

We studied seven historic climate variables relative to BARRA2 dataset: (i) average surface air temperature (ii) maximum surface air temperature (iii) minimum surface air temperature (iv) diurnal temperature range (v) wet-bulb-globe temperature (vi) relative humidity and (vii) precipitation. Diurnal temperature range was computed by subtracting the minimum surface air temperature from the maximum surface air temperature. Similarly, we calculated wet-bulb-globe temperature from the average surface air temperature and relative humidity as described in Poon et al. (2023).

Each predictor variable was averaged over Australia, where the average was weighted by the local Australian population density corresponding to the geographic location of the health data. This population density weighting is required because changes in the climate to regions with no population is irrelevant to the geographic regions of Australia considered in this analysis. As outlined in Poon et al. (2023), we performed the following steps to derive population weighted climate variables.

a. Extracted each climate variable from the monthly averaged BARRA2 dataset. As an example, Figure 19a illustrates the average annual maximum surface air temperature from BARRA2 for the period 2007 to 2023. Majority of Australian regions show maximum surface air temperature of above 25°C with the northern and central regions increasing to greater degrees.
b. Interpolated the SEDAC population density grid (Figure 19b) onto the climate variable.
c. Calculated the weighted average climate variable based on the SEDAC population density map.

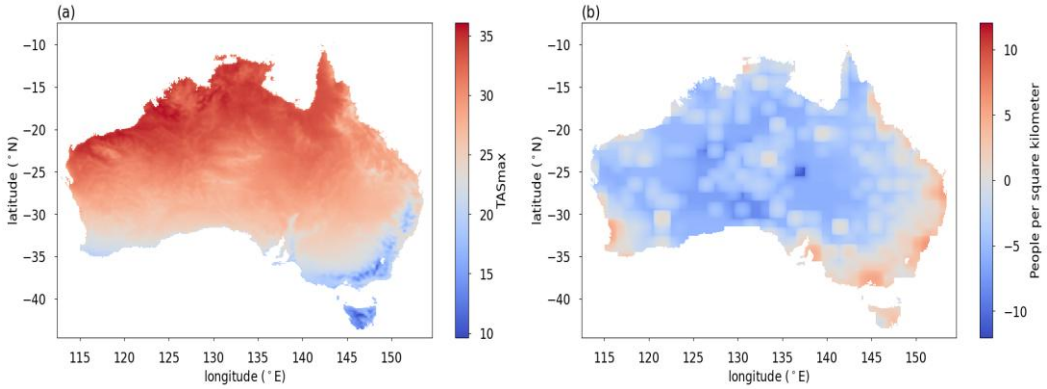

Figure 19 Maps showing: (a) Average annual maximum surface air temperature (TASmax) from BARRA2 dataset for the period 2007 to 2023 and (b) logarithm of the population of Australia on 01 January 2020. Both maps illustrate the respective measure for all Australia, except the ACT region

All predictor variables were annually averaged prior to analysis.

Disease rate prediction model

As a first step, we analysed the Pearson correlation between each outcome (O) variable and the annual population density-weighted climate predictor variables (CV). Only those predictors which showed significant correlation (positive or negative) were considered further. For each outcome variable, we then developed independent linear regression models for predicting it based on each significantly correlated climate variables. We further performed a non-parametric bootstrapping for each model to estimate the errors in the model as outlined in Poon et al. (2023):

a. Estimated the parameters (slope (m) and intercept (β)) of the regression model (O=β+ m CV) with n = 12 samples for influenza rates (and n = 17 samples for MRSA rates), using ordinary least square method.
b. Derived the predicted disease rates ($\hat{O}$) based on the model in i)
c. Computed the prediction errors (ϵ=O-$\hat{O}$)
d. Sampled with replacement from the prediction errors n = 12 times for influenza rates (or n = 17 times for MRSA rates) to produce the pseudo error set ($\tilde{\epsilon}$)
e. Obtained a pseudo set of outcome samples ($\tilde{O}$= O+$\tilde{\epsilon}$)
f. Computed the new slope, offset and correlation coefficients from the pseudo samples.

Above steps were repeated 10,000 times to produce the probability density functions of the slope, intercept, and correlation coefficient for each CV.

Future disease rate projections

To derive future disease rate projections, we used monthly climate projections for three distinct standardised climate scenarios (SSP1-2.6, SSP2-4.5, SSP5-8.5) based on the ACCESS-CM2 climate model from CMIP6 dataset for the period 01 January 2035 to 01 January 2064. For each scenario, we computed annual population density-weighted climate variables where the weighting was done based on the local Australian population density corresponding to the geographic location of the health data. These annual population density-weighted climate projections were then used to derive potential future disease rate projections based on the established prediction models.

To estimate the projected disease rates by 2050, we averaged the decadal predictions for the period with mid-point being 2050. We then computed the percentage change in disease rate between 2050 estimate and the average disease rate observed in the last decade for which the disease data was modelled.

% change in 2050=

(average future period (2045 to 2055)-average(last decade))/(average(last decade)) ×100

In the above formular, the last decade for influenza and MRSA corresponds to 2010 to 2019 and 2014 to 2023, respectively.

3.1.2 Results

In this report, we only provide results from the prediction models which showed the strongest predictive relationship between the outcome and predictor variables.

Prediction model for influenza rates

Between 01 January 2008 and 31 December 2019, there were 1,049,294 influenza cases reported in the NNDSS dataset, with average annual rate of 36 cases per 10,000 population. The climate variable which showed the strongest correlation with influenza rate was the average surface air temperature. However, CMIP6 dataset from ACS does not include this variable, hence we chose the second strongest correlated variable, the maximum surface air temperature, to construct a predictive model for influenza rate (Figure 20).

Figure 20a depicts the significant relationship between the logarithm of the annual influenza rate and the annual population density-weighted maximum surface air temperature for all Australia, excluding ACT (r=0.785; p¡0.002). Corresponding probability density functions of the slope, intercept, and correlation coefficient for this relationship from 10,000 bootstrapped samples are illustrated in Figure 20b-d. We estimated that for a 1°C increase in annual maximum surface air temperature, the annual influenza rate will increase by 40,877 cases per 10,000 population in Australia, excluding ACT.

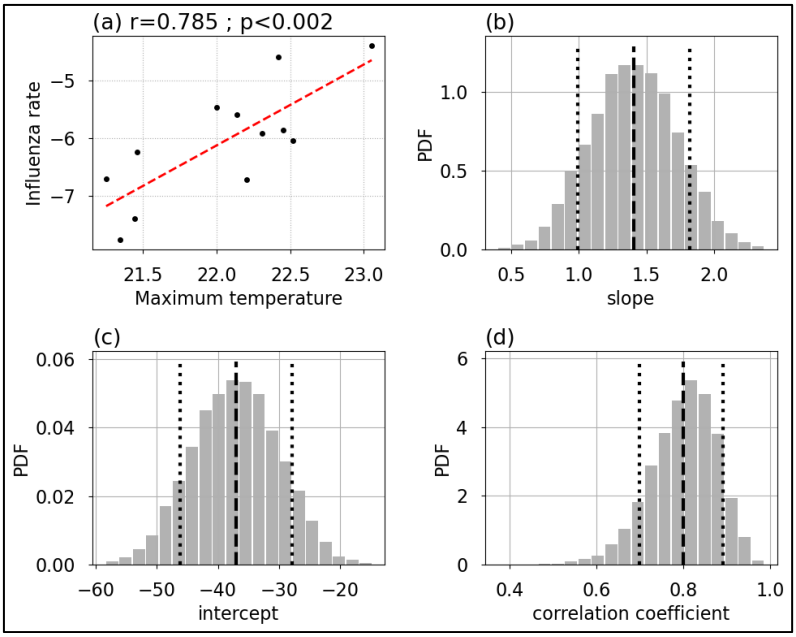

Figure 20 Model for predicting influenza rate based on maximum surface air temperature. (a) logarithm of raw influenza rate versus annual population density-weighted maximum surface air temperature along with the regression line (red); and results from non-parametric bootstrapping producing the probability density functions of (b) slope; (c) intercept; and (d) the corresponding correlation coefficient.

Projected influenza rate by 2050

On average, the projected annual maximum surface air temperature for the 2050 period (2045 to 2055), from CMIP6 scenarios is above 25°C in most Australian regions (Figure 21, left panels), with the northern and central regions increasing to greater degrees. While the southern parts, including the coastal regions of Victoria, South Australia, south Western Australia, and Tasmania are projected to have maximum surface air temperature below 25°C. Compared to the baseline period of 2010 to 2019 (the last decade for the modelled influenza rates), the average annual maximum surface air temperature is projected to increase between 2°C to 4°C in in the northern and central parts of Australia, with increasing differences exhibiting in the order of increasing level of greenhouse gas emission scenarios (low, intermediate, and very high).

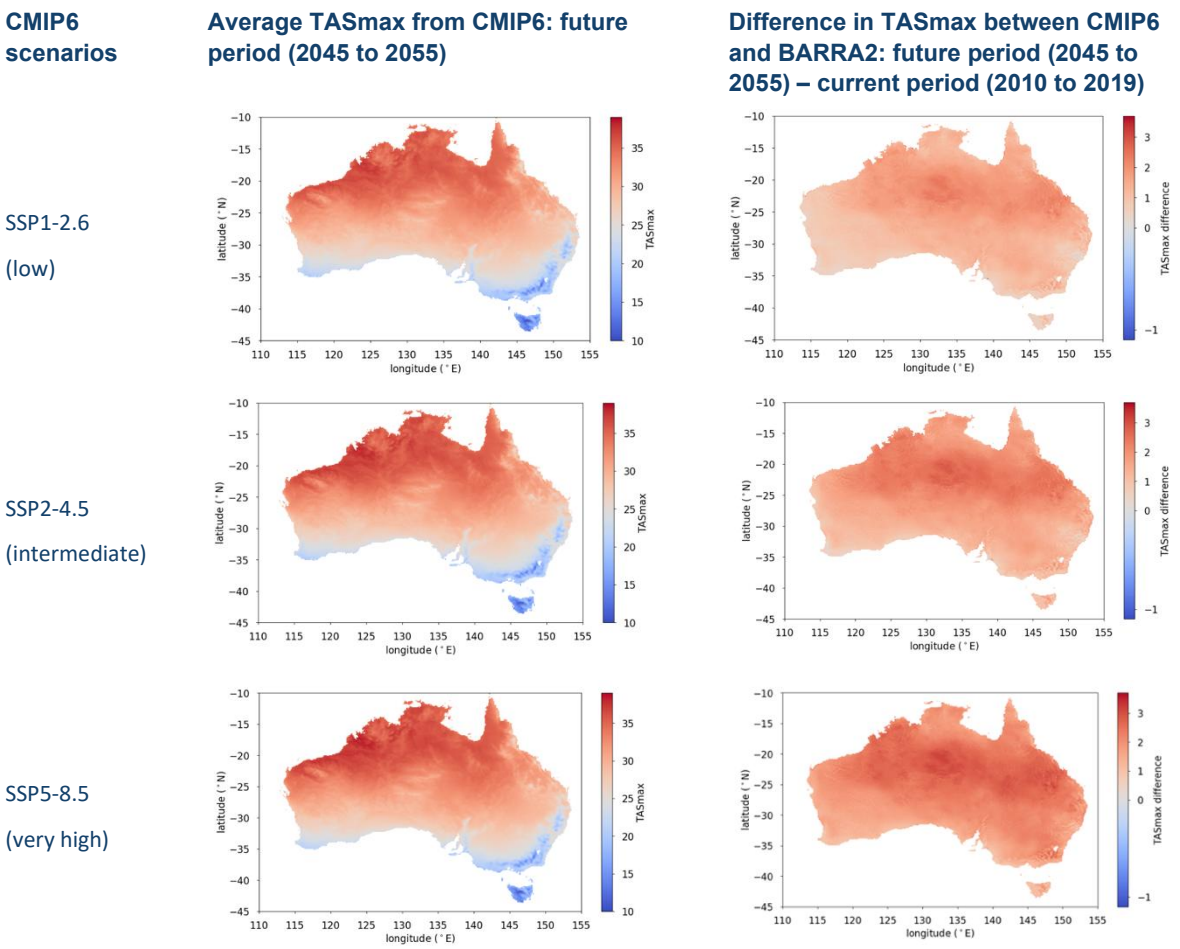

Figure 21 Maps showing average decadal maximum surface air temperature (TASmax) from CMIP6 scenarios for the period 2045 to 2055 (left-hand column) and the difference in average decadal maximum surface air temperature between CMIP6 scenarios and BARRA2 dataset, where the decade for the BARRA2 dataset corresponds the period 2010 to 2019 (right-hand column). Rows correspond to the projected scenarios for low (SSP1-2.6, row 1), intermediate (SSP2-4.5) and very high (SSP5-8.5) greenhouse gas emissions. Each map shows the computed measure for all Australia excluding the ACT region.

We applied the established model in Figure 20 to predict future projections for the period 2035 to 2064, employing the population density-weighted maximum surface air temperature from CMIP6 dataset. By 2050, we projected that the rate of influenza will be 116 cases per 10,000 population, 165 cases per 10,000 population, and 300 cases per 10,000 population under SSP1-2.6, SSP2-4.5, and SSP5-8.5, respectively. In comparison to the average observed influenza rate for the decade 2010 to 2019, these projected rates correspond to an increase of more than 100% under each SSP scenario (187%, 306%, 639% for SSP1-2.6, SSP2-4.5, and SSP5-8.5, respectively). Our projections indicate a widening difference in influenza rate between SSP1-2.6 and SSP5-8.5 (SSP5-8.5/SSP1-2.6 = 2.6) compared to the difference between SSP1-2.6 and SSP2-4.5 (SSP2-4.5/SSP1-2.6 = 1.4).

Prediction model for MRSA rate

Between 01 January 2007 and 31 December 2023, there were 87,167 MRSA cases reported in HOTspots, with average annual rate of 48 cases per 10,000 population. Average surface air temperature showed the strongest correlation with MRSA rate. As previously noted, this variable is not available in the ACS CMIP6 dataset, and we used the second strongly correlated variable, the maximum surface air temperature, to build a predictive model for MRSA rate (Figure 22).

Figure 22a illustrates the significant relationship between MRSA rate and the annual population density-weighted maximum surface air temperature over north Australia (r=0.638; p¡0.005). Corresponding probability density functions of the slope, intercept, and correlation coefficient of the model are illustrated in Figure 22b-d. We estimated that a 1°C increase in the annual maximum surface air temperature will increase the annual MRSA rate by 26 cases per 10,000 population in north Australia.

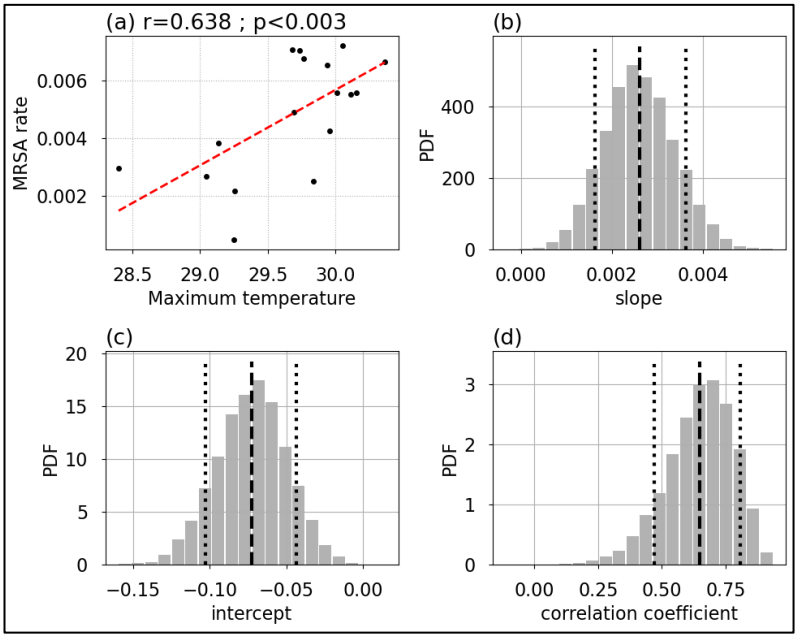

Figure 22 Model for predicting MRSA rate based on maximum surface air temperature. (a) raw MRSA rate versus annual population density-weighted maximum surface air temperature together with the regression line (red); and results from non-parametric bootstrapping producing the probability density functions of (b) slope; (c) intercept; and (d) the corresponding correlation coefficient.

Projected MRSA rate by 2050

Overall, the annual maximum surface air temperature from each SSP scenario is projected to be above 32°C in most parts of north Australia (Figure 23, left panels), except the coastal regions in Queensland, Northern Territory, and southwest of Western Australia. In comparison to the baseline period of 2014 to 2023, which corresponds to the final decade in which MRSA rate was modelled, the average annual maximum surface air temperature is projected to increase between 0.5°C to 3.5°C in across all north Australia. Between the three greenhouse gas emission scenarios, the SSP5-8.5 (very high) showed the most increase in the difference in maximum surface air temperature, followed by SSP2-4.5 (intermediate), and lowest for SSP1-2.6 (low).

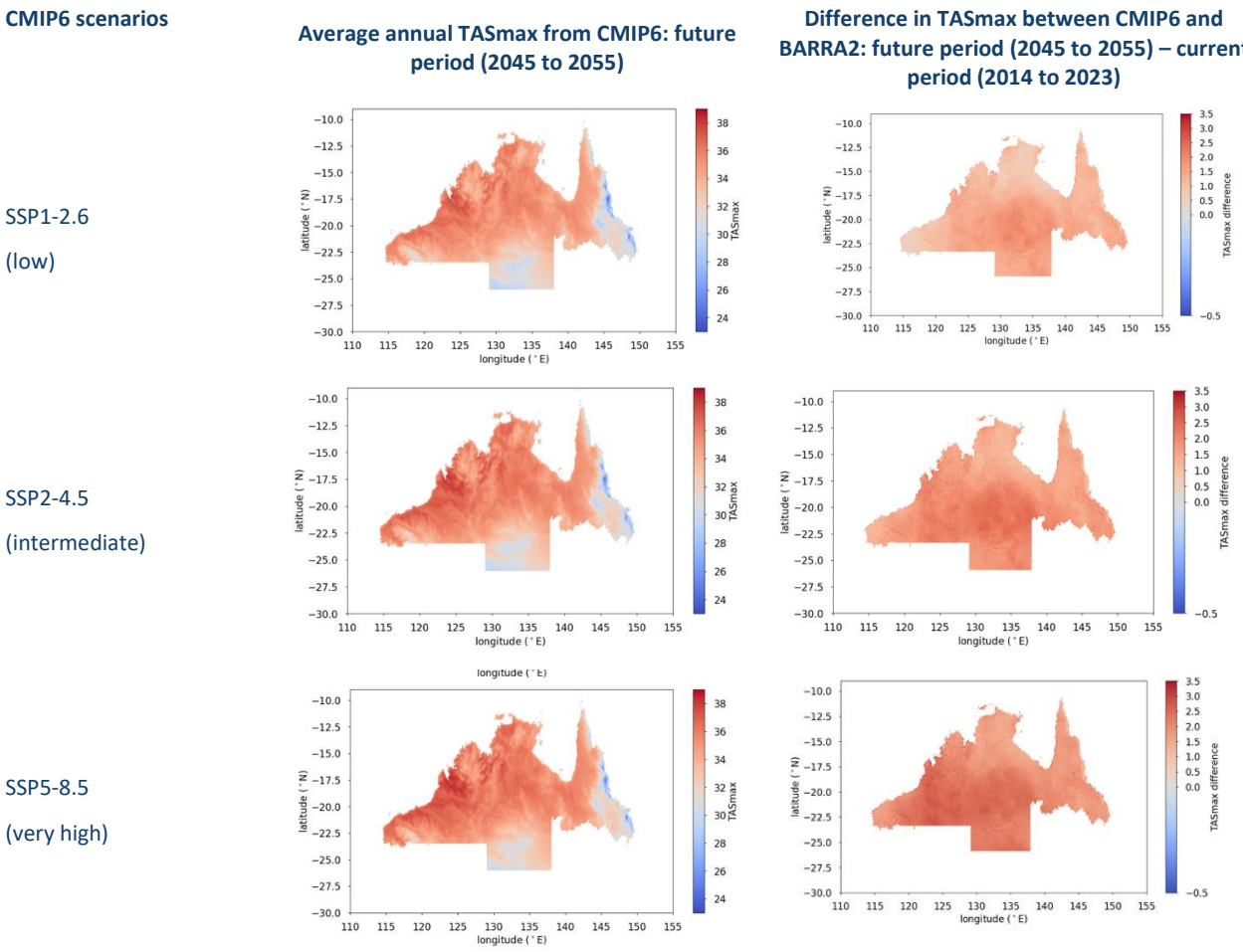

Figure 23 Maps showing the average decadal maximum surface air temperature (TASmax) in northern Australia. The left-hand column displays TASmax from CMIP6 dataset for the future period of 2045 to 2055. The right-hand column displays the difference of TASmax between future period (from CMIP6 dataset) and current period (from BARRA2 dataset). Rows correspond to the projected scenarios for low (SSP1-2.6, row 1), intermediate (SSP2-4.5) and very high (SSP5-8.5) greenhouse gas emissions.

We used the established model in Figure 22 to predict future projections for MRSA rate for the period 2035 to 2064, employing the population density-weighted maximum surface air temperature from CMIP6 dataset. We projected that the rate of MRSA will be 87 cases per 10,000 population (under SSP1-2.6); 97 cases per 10,000 population (under SSP2-4.5), and 102 cases per 10,000 population (under SSP5-8) in 2050. Compared to the baseline period of 2014 to 2023, these rates correspond to an increase of more than 30% under each SSP scenario (39%, 54%, 63% for SSP1-2.6, SSP2-4.5, and SSP5-8.5, respectively). Our projections indicate similar differences in MRSA rate between SSP2-4.5 (SSP2-4.5/SSP1-2.6 = 1.1) and SSP5-8.5 (SSP5-8.5/SSP1-2.6 = 1.2) with respect to that for SSP1-2.6.

3.1.3 Discussion

This work examined the projected changes due to variations in climate variables - average surface air temperature, maximum surface air temperature, minimum surface air temperature, diurnal temperature range, wet-bulb-globe temperature, relative humidity, and precipitation for influenza and MRSA by 2050. Influenza was modelled for Australia (excluding the ACT region) and MRSA was modelled for northern Australia. Using historic BARRA2 reanalysis data, we found that the average

surface air temperature was the strongest predictor for both disease rates. However, due to this variable not incorporated in the CMIP6 dataset generated by ACS, we used the maximum surface air temperature to construct predictive models, separately, for each disease rate. These models were applied to three potential future climate scenarios based on variations in greenhouse gas emission levels (SSP1- 2.6 (low), SSP2-4.5 (intermediate), SSP5-8.5(very high)), to estimate the impact of climate change on influenza and MRSA prevalence by 2050.

By 2050, we projected that influenza will be 300 cases per 10,000 people under the extreme scenario of SSP5-8.5 (very high greenhouse gas emissions). This signifies an increase of 639% of influenza rate compared to the average influenza rate observed for the period 2010 to 2019 (40 cases per 10,000 people). Similarly, under the same scenario (SSP5-8.5), we projected that rate of MRSA will be 102 cases per 10,000 people. This suggests an increase of 63% in comparison to the average observed MRSA rate for the period 2014 to 2023 (62 cases per 10,000 people).

All these estimates are based on the output from one climate model. To do proper uncertainty analysis, we need to consider more climate models from CMIP6 dataset. We previously performed a similar analysis based on multi-model CMIP5 dataset, which provided future projections for influenza and MRSA accounting for uncertainty in the predictions (see Appendix C, Figure C1). However, the CMIP5 data was not bias-corrected nor statistically downscaled. There are other sources of uncertainty which we propose to address as detailed in the following section.

3.1.4 Next steps

This work has some limitations.

Firstly, due to time constraint, we only considered a single climate model from the CMIP6 dataset. In the future, an uncertainty analysis should be conducted using the regional climate downscaling simulations of selected CMIP6 models produced by ACS (NCRA overview paper)

Second, we considered both influenza and MRSA surveillance datasets as a single cohort (one for influenza and one for MRSA) and we did not explore specific geographical region, or certain demographics which may exhibit heightened vulnerability to specific climate variations. Future analysis should investigate if a particular geographic location, or specific demographic populations are more susceptible to certain climate variables by undertaking region-specific analysis.

Third, we considered the annual time scale to model both influenza and MRSA. Future work should explore a range of time scales (e.g; weeks, months, seasons) to examine the influence of temporal variations in climate on disease prevalence.

Fourth, due to ambiguities associated with influenza infection and related complications from Covid-19, such as the social distancing measures, changes to health seeking behaviour of the community, and focused testing response activities, we did not include data post-COVID-19 period.

Fifth, we constructed a separate predictive model for each climate variable. Future modelling should investigate a range of linear and nonlinear models linking multiple climate variables for predicting disease prevalence. This would allow us to account for interaction between predictor variables as well as explore potential multicollinearity.

Lastly, we focused only on the effect of climate on health. Future work should need to investigate the impact of non-climate factors such as aging population, access to healthcare, overcrowded housing on health.

3.1.5 Acknowledgements (Investigating the impact of climate on high prevalence bacterial and viral pathogens of concern using routinely collected surveillance data)

We acknowledge Dr Vassili Kitsios (CSIRO Environment) for providing helpful feedback to this analysis and providing CMIP5 and JRA55 datasets. We also thank Malcolm King (CSIRO Environment) and Chloe Mackallah (CSIRO Environment) for delivering the CMIP6 and BARRA2 datasets.

3.1.6 References (Investigating the impact of climate on high prevalence bacterial and viral pathogens of concern using routinely collected surveillance data)

Altizer, S., Bartel, R., & Han, B. A. (2011). Animal migration and infectious disease risk. Science, 331(6015), 296–302. https://doi.org/10.1126/science.1194694.

Australian eHealth Research Centre. (2023). HOTspots. Commonwealth Scientific and Industrial research Organisation. Available from https://amr-hotspots.net (accessed 2023, May 8).

Australian Bureau of Statistics. (2021). Australian Statistical Geography Standard (ASGS) Edition 3. Released July 2021. Available from: https://www.abs.gov.au/statistics/standards/australian-statistical-geography-standard-asgs-edition-3/latest-release (accessed May 2023).

Australian Bureau of Statistics. (2023). National, state and territory population. Available from https://www.abs.gov.au/statistics/people/population/national-state-and-territory-population/latest-release (accessed July 2024).

Australian Bureau of Statistics (ABS). (2024). Regional population; 2022-23. Available from: https://www.abs.gov.au/statistics/people/population/regional-population/latest-release (accessed July 2024).

Dave, K., & Lee, P. C. (2019). Global geographical and temporal patterns of seasonal influenza and associated climatic factors. Epidemiologic Reviews, 41(1), 51–68. https://doi.org/10.1093/epirev/mxz008.

Department of Health and Aged Care. (2023). National Notifiable Diseases Surveillance System (NNDSS) public dataset – influenza (laboratory confirmed), Australian Government. Available from https://www.health.gov.au/resources/publications/national-notifiable-diseases-surveillance-system-nndss-public-dataset-influenza-laboratory-confirmed (accessed May 2024).

Fisman D. N. (2007). Seasonality of infectious diseases. Annual Review of Public Health, 28, 127–143. https://doi.org/10.1146/annurev.publhealth.28.021406.144128.

Grose. M.R, Narsey. S., Trancoso. R., Mackallah. C., Delage. F., Dowdy. A., Di Virgilio. G., Watterson. I., Dobrohotoff. P., Rashid. H.A., Rauniyar, S., Henley, B., Thatcher, M., Syktus, J., Abramowitz, G., Evans, J. P., Su, C., & Takbash, A. (2023). A CMIP6- based multi-model

downscaling ensemble to underpin climate change services in Australia. Climate Services, 30. https://doi.org/10.1016/j.cliser.2023.100368.

Kobayashi. S., Ota. Y., Harada. Y., Ebita. A, Moriya. M., Onoda. H., Onogi. K., Kamahori. H., Kobayashi. C., Endo. H., Miyaoka, K., & Takahashi, K. (2015). The JRA-55 reanalysis: General specifications and basic characteristics. Journal of the Meteorological Society of Japan. Ser. II, 93(1). https://doi.org/10.3390/ijerph20031681.

Lane, M. A., Walawender, M., Carter, J., Brownsword, E. A., Landay, T., Gillespie, T. R., & Kraft, C. S. (2022). Climate change and influenza: a scoping review. The Journal Of Climate Change and Health, 5, 100084. https://doi.org/10.1016/j.joclim.2021.100084.

Magnano San Lio, R., Favara, G., Maugeri, A., Barchitta, M., & Agodi, A. (2023). How Antimicrobial Resistance Is Linked to Climate Change: An Overview of Two Intertwined Global Challenges. International Journal of Environmental Research and Public Health, 20(3), 1681. https://doi.org/10.3390/ijerph20031681.

Marani, M., Katul, G. G., Pan, W. K., & Parolari, A. J. (2021). Intensity and frequency of extreme novel epidemics. Proceedings of the National Academy of Sciences of the United States of America, 118(35), e2105482118. https://doi.org/10.1073/pnas.2105482118.

Martinez, E. P., Cepeda, M., Jovanoska, M., Bramer, W. M., Schoufour, J., Glisic, M., Verbon, A., & Franco, O. H. (2019). Seasonality of antimicrobial resistance rates in respiratory bacteria: A systematic review and meta-analysis. PloS one, 14(8), e0221133. https://doi.org/10.1371/journal.pone.0221133.

McMichael, T., Blashki, G., & Karoly, D. J. (2007). Climate change and primary health care. Australian Family Physician, 36(12). https://search.informit.org/doi/10.3316/informit.355393328611803.

Patz, J. A., Epstein, P. R., Burke, T. A., & Balbus, J. M. (1996). Global climate change and emerging infectious diseases. JAMA, 275(3), 217–223. https://doi.org/10.1001/jama.1996.03530270057032.

Poon, E. K. W., Kitsios, V., Pilcher, D., Bellomo, R., & Raman, J. (2023). Projecting future climate impact on national Australian respiratory-related intensive care unit demand. Heart, Lung & Circulation, 32(1), 95–104. https://doi.org/10.1016/j.hlc.2022.12.001.

Rahul, R., Maheswary, D., Damodharan, N., & Leela, K. V. (2023). Unveiling global public interest and seasonal patterns of antibiotics and antibiotic resistance: An infodemiology study with implications for public health awareness and intervention strategies. International Journal of Medical Informatics, 179, 105231. https://doi.org/10.1016/j.ijmedinf.2023.105231.

Su, C. H., Dharssi, I., Le Marshall, J., Le, T., Rennie, S., Smith, A., ... & Warren, R. A. (2022). BARRA2: Development of the next-generation Australian regional atmospheric reanalysis. Bureau of Meteorology.

Taylor, K. E., Stouffer, R. J., & Meehl, G. A. (2012). An Overview of CMIP5 and the Experiment Design. Bulletin of the American Meteorological Society, 93(4), 485-498. https://doi.org/10.1175/BAMS-D-11-00094.1.

World Health Organization. (2024). WHO Bacterial Priority Pathogens List, 2024: bacterial pathogens of public health importance to guide research, development and strategies to prevent and control antimicrobial resistance. https://www.who.int/publications/i/item/9789240093461.

Wozniak, T. M., Cuningham, W., Ledingham, K., & McCulloch, K. (2022). Contribution of socio-economic factors in the spread of antimicrobial resistant infections in Australian primary healthcare clinics. Journal of Global Antimicrobial Resistance, 30, 294–301. https://doi.org/10.1016/j.jgar.2022.06.005.

Wozniak. T.M., Cuningham. W, Buchanan. S., Coulter. S, Baird. R.W., Nimmo. G.R., Blyth. C.C, Tong. S.Y.C., Currie B. J., and Ralph. A.P. (2020). Geospatial epidemiology of Staphylococcus aureus in a tropical setting: an enabling digital surveillance platform. Scientific Reports, 10(1), 13169. https://doi.org/10.1038/s41598-020-69312-4.

Xu, Z., Hu, W., & Tong, S. (2014). Temperature variability and childhood pneumonia: an ecological study. Environmental Health, 13, 1-8. https://doi.org/10.1186/1476-069X-13-51.

3.2 Investigate spillover risk changes with climate variations

Spillover occurs when a pathogen moves from one species to another, which may or may not result in a subsequent outbreak. In the case of zoonotic spillover, this refers to transmission of a pathogen from wildlife to humans. These represent future possible threats of lower probability but potentially higher impact than the previous section, which focused primarily on trends in current high priority communicable diseases. Since over 70% of emerging infectious diseases are zoonotic in origin, and all pandemics in the last 50 years have been, we start by considering a proxy for how spillover risk might change. In particular, we build on our existing estimate of the potential spatial density of viruses known to have crossed from animals to humans, and how this might change under eight different climate change models centred around 2050, for two different emissions scenarios. We refer to this as “spillover risk”, though we note this is the potential number of viruses that could be supported if the hosts are actually present and the virus is introduced, and we are also not explicitly incorporating any information about the human population. This is a correlative approach with climate variables, so should be taken with caution that there is substantial room for improvement in making the predictions more biologically sensible and reliable.

We also use a case study to illustrate a more biologically robust approach, and how much more intensive they are to compute in terms of data requirements and computational power. Given we know mosquitoes are particularly climate sensitive, and that JEV was identified as a priority pathogen in the communicable disease discussion paper (CSIRO, 2024), we build spatial species distribution models for Australia, with a focus on climate features to describe each species' ecological niche. Since transmission requires the presence of hosts and vectors, we use this as a proxy for JEV risk. We then use the same eight climate models for two different scenarios to project how these species spatial distributions might change centred around 2050 and 2090.

3.2.1 Method

For both parts of this work, we use climate data from the Australian Government's Climate Change in Australia (CCiA) portal, which provides application-ready gridded datasets at a 5 km resolution. Both the spillover and JEV risk proxy estimates use 0.05 × 0.05 decimal degrees (approximately 5km × 5km). This dataset includes various climate variables such as precipitation, evaporation, relative humidity, surface solar radiation, and near-surface air temperatures. The projection of these climate variables is provided under two Representative Concentration Pathway (RCP) scenarios, RCP 4.5 and RCP 8.5, and for eight climate models:

- MIROC5 (Watanabe et al. 2010): Model for Interdisciplinary Research on Climate, version 5.
- HadGEM2-CC (Martin et al. 2011): Hadley Centre Global Environment Model, version 2, Carbon Cycle.
- GFDL-ESM2M (Dunne et al. 2013): Geophysical Fluid Dynamics Laboratory Earth System Model 2M.
- CanESM2 (Chylek et al. 2011): Canadian Earth System Model, version 2.
- CNRM-CM5 (Voldoire et al. 2013): Centre National de Recherches Météorologiques Climate Model, version 5.

- CESM1-CAM5 (Neale et al. 2012): Community Earth System Model 1, with the Community Atmosphere Model, version 5.
- NorESM1-M (Bentsen et al. 2013): Norwegian Earth System Model, version 1, medium resolution.
- ACCESS1-0 (Bi et al. 2013): Australian Community Climate and Earth-System Simulator, version 1.0.

These models provide diverse projections of future climate conditions, helping to capture the range of possible changes in climate variables that could influence zoonotic virus density. By comparing outputs from multiple models, we can better understand the uncertainties and variations in future climate scenarios.

Table 9 provides a summary of the data used and methods for both approaches, with more detail provided in the following sections.

Table 9 Summary of data and analytical approaches for the two proxies studied for future spillover risks.

SCENARIO	DATA SOURCES	ANALYTICAL MODEL APPROACH	FEATURES (COVARIATES)
Spillover risk proxy	Climate change in Australia (CSIRO and Bureau of Meteorology 2011) Zoonotic virus counts per animal order (Mollentze and Streicker 2020) IUCN species distributions ('IUCN' 2022)	Extra Tree Regressor with baseline year 2020. Animals: 11 orders of avian and mammalian species.	Temperature (min, max, mean) Relative humidity Evaporation Solar radiation Precipitation
JEV risk proxy	Climate Change in Australia(CSIRO and Bureau of Meteorology 2011) Atlas of Living Australia (Belbin et al. 2021) AGCD/AWAP(Australian Bureau of Meteorology 2019; Jones, D., Wang, W., and Fawcett, R. J. W. 2009) /CSIRO(Donohue, R. et al. 2017) VectorMap (http://www.vectormap.si.edu)	Species distribution (ecological niche) modelling using Maximum Entropy. Baseline year 2025. Animals: 12 waterbird species 3 mosquito vectors Feral pigs	Temperature indices Precipitation indices Aridity indices (precipitation/ evaporation) Water deficit indices (precipitation/ evaporation) Evaporation indices (Morton's areal pan evaporation)

Spillover risk proxy: Potential zoonotic virus pathogen density estimate

To investigate how spillover risks across Australia might change with climate, we leveraged our existing estimate (Golchin et al., 2024) of potential spatial virus density based on viruses known to cross to humans from 11 orders of animals in Australia (Mollentze and Streicker 2020). These 11 orders are: Rodentia, Primates, Perissodactyla, Lagomorpha, Diprotodontia, Chiroptera, Cetartiodactyla, Carnivora, Passeriformes, Galliformes, Anseriformes. We used this estimate as the target variable to train Extra Trees Regressor (ETR) models for each of the eight models for the two climate scenarios (RCPs 4.5 and 8.5). ETR is an ensemble learning method, combining multiple decision trees to enhance predictive accuracy and stability. To generate training data, we used the climatic variables:

- solar radiation,
- relative humidity,

- rainfall,
- minimum temperature,
- mean temperature,
- maximum temperature, and
- evaporation.

Pixels containing missing values in any of the climate variables and estimated zoonotic virus density were removed. We then developed 16 different models for each RCP and climate model combination by applying StandardScaler on the feature set and using Extra Trees Regressor. This comprehensive approach allowed us to assess the impact of different climate scenarios on estimated zoonotic virus density. Five other tree-based regression approaches were explored for the ACCESS1-0 climate model under RCP 4.5 scenario, but ETR was chosen for its combination of R-squared value (approx. 0.9), root mean square error value (approx. 0.8) and the computational ime (<45 seconds).

To ensure a fair comparison between the 2020 and 2050 predictions, we used the trained models to predict results for both years and excluded the data obtained from Golchin et al. (2024). To compare the prediction results from 2050 and 2020, we calculated a difference map by subtracting the prediction values for the year 2020 from the prediction values for the year 2050 (Table 10, column “Difference map 2050-2020”). Visualising the difference maps highlighted the spatial distribution of differences between the predictions of 2050 and 2020, providing insights into areas of significant change or stability. Positive (red) values on the maps show the increase in potential zoonotic virus density, whereas negative (blue) values on the difference maps show that the potential zoonotic virus density is decreased by 2050 in those areas.

We also calculated the uncertainty of the outputs of eight different climate models under the RCP 4.5 and RCP 8.5 scenarios. To do so, the median, 10th percentiles (the lower end), and 90th percentiles (the upper end) of the predictions were calculated to understand the distribution and variability of the potential zoonotic virus density.

Japanese encephalitis risk proxy: Combined host and vector species presence probabilities based on ecological niches

For the deeper and more biologically-based assessment of Japanese encephalitis virus (JEV), we use ecological niche modelling building on previous research identifying the distribution of JEV vectors (Furlong et al., 2022) and enzootic risk of JEV in Australia (Furlong et al., 2023), to investigate how spatial distributions of vectors and hosts shift under different climate change scenarios. Maximum Entropy (MaxEnt) modelling (Phillips, Anderson, and Schapire 2006; Phillips et al. 2017; Anderson 2023) was used to develop species distribution models across Australia for three mosquito species (*Culex annulirostris, Culex sitiens, and Culex quinquefasciatus*); 12 species of Australian waterbirds (*Ardea intermedia, Ardea, Ardea pacifica, Bubulcus ibis, Butorides striata, Botaurus poiciloptilus, Egretta novaehollandiae, Egretta garzetta, Egretta sacra, Ephippiorhynchus asiaticus, Ixobrychus flavicollis, and Nycticorax caledonicus*) and feral pigs (*Sus Scrofa*). Models were built using presence-absence observation records from 1950 to 2024 and 14 climatic variables based on the historic period 1986 – 2010. Details of the climatic indices are:

- Temperature:

  - Monthly minimum, minimum temperature
  - Monthly maximum, maximum temperature
  - Annual temperature range
  - Monthly maximum temperature range
  - monthly minimum temperature range
- Precipitation:
  - Monthly maximum total precipitation
- Aridity (precipitation/evaporation):
  - Mean annual aridity
  - Minimum monthly aridity
  - Maximum monthly aridity
- Water deficit (precipitation – evaporation):
  - Annual water deficit
  - Maximum monthly water deficit
- Morton's areal pan evaporation:
  - Annual total evaporation
  - Minimum monthly evaporation
  - Maximum monthly evaporation

Each model produced predictions of presence probability for the species across Australia and model performance was recorded based on spatial k-folds cross-validation.

For mosquitos and water birds, presence probabilities were merged to produce an overall presence probability for any species as:

$$P_s = 1 - \left[\prod_{i=1}^{N} 1 - p_{i,s}\right]$$

where 〖 p〗 _(i,s) are the estimated presence probabilities for species i, for the mosquito vectors (N=3) or water birds (N =12). We then combined the presence probabilities of species in an epidemiologically appropriate way for the potential transmission of JEV (referred to throughout as "combined JEV species probability"). Specifically, the combined JEV species probability is calculated as the presence probability of mosquitos AND water birds OR feral pigs:

$$P_{JEV} = P_{mosquito} \times \left(\left(P_{water\ birds} + P_{feral\ pigs}\right) - \left(P_{water\ birds} \times P_{feral\ pigs}\right)\right).$$

To understand the potential changes in combined JEV species presence probabilities, the MaxEnt models were projected using CMIP5 climate change projections under the two scenarios (RCPs 4.5 and 8.5) to 2050 and 2090. Specifically, we used climate data generated from the eight climate models, allowing us to assess the impact of different climate models and scenarios on the species presence probabilities of JEV in Australia.

3.2.2 Results

We show the differences between our target year and 2050 for the eight different climate models under the two different scenarios (RCPs 4.5 and 8.5) for both the spillover and JEV risk proxies. For the JEV risk proxy, we also show the difference between 2025 and 2090 and show how the mosquito population presence predictions change at the Local Government Area (LGA) levels.

To demonstrate the variance between the proxies, we also show the median and ranges spatially for each of the projections. To summarise the spatial information, we include tables summarising the number of LGA regions with median values in key bands (numbers of potential viruses for the spillover proxy, presence probability >0.5 for the JEV proxy).

Spillover risk proxy (potential zoonotic virus density)

We show the differences between the estimated spillover risk proxy, potential zoonotic virus density, for 2020 and the 2050 projection for the eight climate models and two scenarios in Figure 24. The colour scale on the maps, ranging from -50 to +50, represents the change in zoonotic virus density. Blue areas indicate regions where potential zoonotic virus density is expected to decrease, while red areas highlight regions with a potential increase by 2050. Although there is substantial variation between the models, there is an increased potential for zoonotic virus density in the western portion of Australia and a reduction in the eastern portion.

Table 10 provides an overview of the projected distribution of zoonotic virus density across 519 LGAs in Australia for the years 2020 and 2050, under two climate scenarios (RCPs 4.5 and 8.5). The table categorises LGAs into five density brackets, ranging from 0 to 100, with the numbers in parentheses indicating the range across the eight climate models. In both 2020 and 2050, the majority of LGAs fall within the (40-60) and (60-80) projected value ranges. The projected number of LGAs in the higher range brackets (60-80) increases significantly from 2020 to 2050 under both scenarios, particularly RCP 4.5. In addition, by 2050, the number of LGAs with values in the lowest bracket (0-20) decreases to zero in both RCP scenarios, suggesting fewer LGAs will have very low values in the future.

In Appendix B we show the results for all eight models and both RCP scenarios in full in Figure B1 and the associated uncertainties between the climate models in Figure B2.

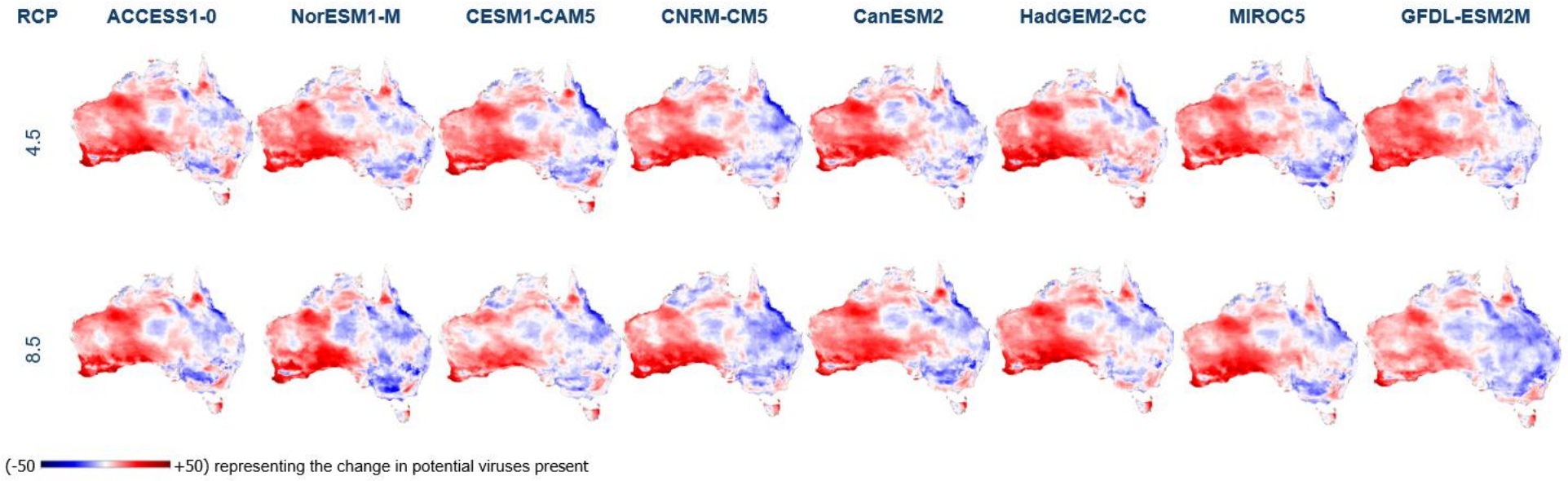

Figure 24 Change in potential density of zoonotic viruses under different climate model projections, with the colour bar

Table 10 Number of LGA's, out of 519 total, with projected values in each bracket range. Values represent the median while, parentheses indicate range (min, max) across the eight climate models

YEAR	RCP	(0-20)	(20-40)	(40-60)	(60-80)	(80-100)
2020	4.5	1 (5, 0)	154 (195, 103)	205 (191, 214)	151 (127, 167)	8 (1, 35)
	8.5	1 (5, 0)	154 (195, 104)	206 (192, 214)	150 (126, 166)	8 (1, 35)
2050	4.5	0 (0, 0)	36 (120, 12)	274 (259, 215)	209 (140, 290)	0 (0, 2)
	8.5	0 (0, 0)	45 (123, 13)	276 (275, 230)	198 (121, 272)	0 (0, 4)

Japanese encephalitis risk proxy (combined JEV species presence probabilities)

To investigate the combined JEV species presence probabilities, we considered the spatial trends in projected probabilities as the median change across the eight climate models. Large scale spatial patterns were consistent across climate change scenarios and periods (see Figure B3). Primarily, combined JEV presence probability was higher around the coastline of Australia (Figure 25), except the coastlines of most of Western and Southern Australia.

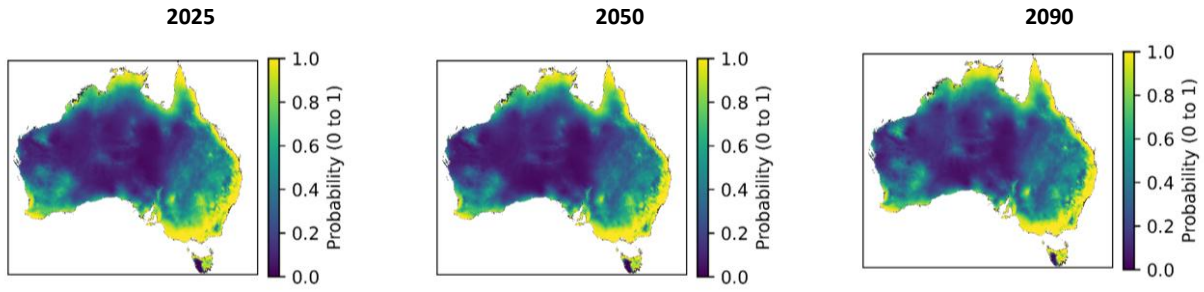

Figure 25 Combined JEV species presence probability for RCP 8.5. Probabilities (0 to 1) represent the median across the eight climate models for the 2025, 2050 and 2090 periods

We then consider the projected change in presence probabilities from 2025 to 2050 and from 2025 to 2090 for each climate model and climate change scenario. Spatial patterns and magnitudes of change were different for each climate model (Figure 26). Changes under the RCP 4.5 scenario were low and inconsistent between 2050 and 2090 periods based on the median model projections. However, model medians highlighted stronger decreases in the southern half of Australia and increases in the northern half with little to no change along coastlines and in central Australia. This north-south divide was most evident in the median change of models under RCP 8.5, which had larger changes both in decreases and increases (Figure 26). While the variability in model projections could range from decreases to increase across Australia, there was a region in southern Western Australia that had projected decreases even in the higher range of model estimates (see Figure B4 of Appendix B). The variability of these differences for RCP 8.5 (see Figure 27) shows a consistent decrease in combined JEV species probabilities in the south-western corner of Australia.

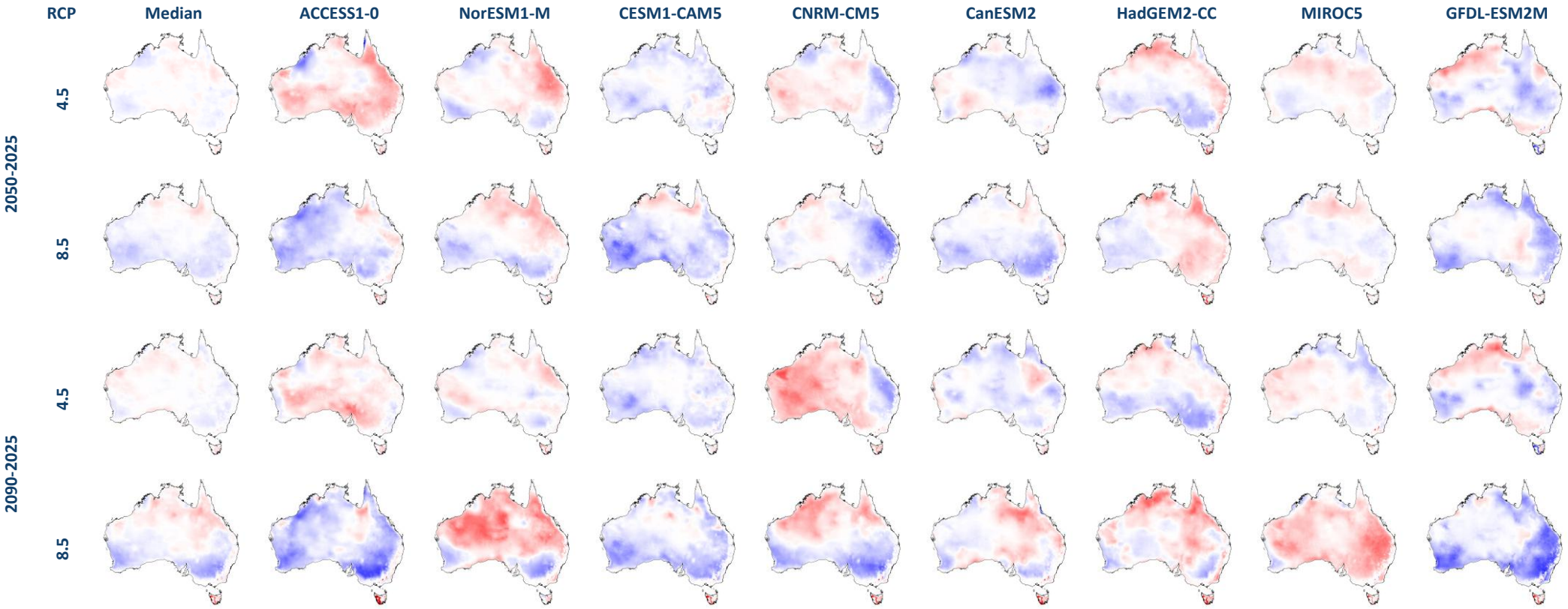

Changes range decreases (dark blue) to increases (dark red), with a maximum change in probability of 1. White areas represent no change in probability (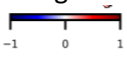

).

Figure 26 Combined JEV species presence probability changes for individual models from 2025 to 2050 and 2025 to 2090

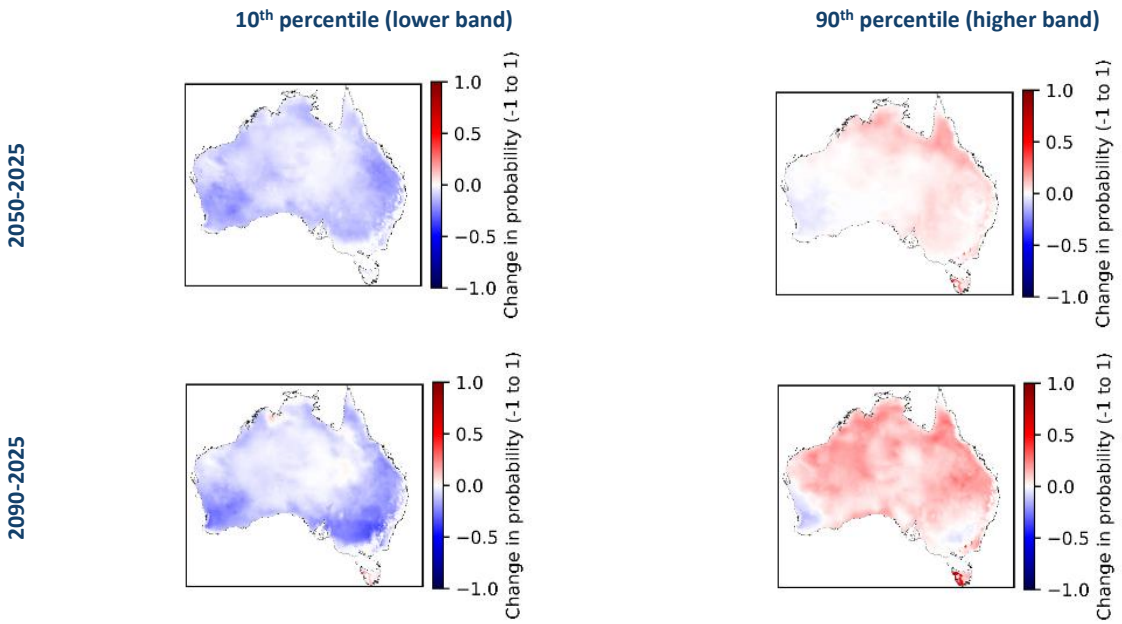

Figure 27 Variability across the eight climate models in the changes in combined JEV species presence probabilities for RCP 8.5

Finally, we further processed the high-resolution projections of our most extreme scenario to the LGA level by taking the spatial average (Figure 28) and summarising the number of LGAs with combined JEV species presence probabilities greater than 0.5 for each period (Table 11). Spatial patterns in the change in presence probabilities at the LGA level were consistent with the higher resolution data. Mosquito spatial distribution and changes dominated the overall species presence maps, likely due to the spatially ubiquitous distribution of waterbirds across Australia (Figure 28). Changes in the number of LGAs with presence probabilities greater than 0.5 were larger for RCP 8.5 than for RCP 4.5, with RCP 4.5 changes being minimal across projection periods.

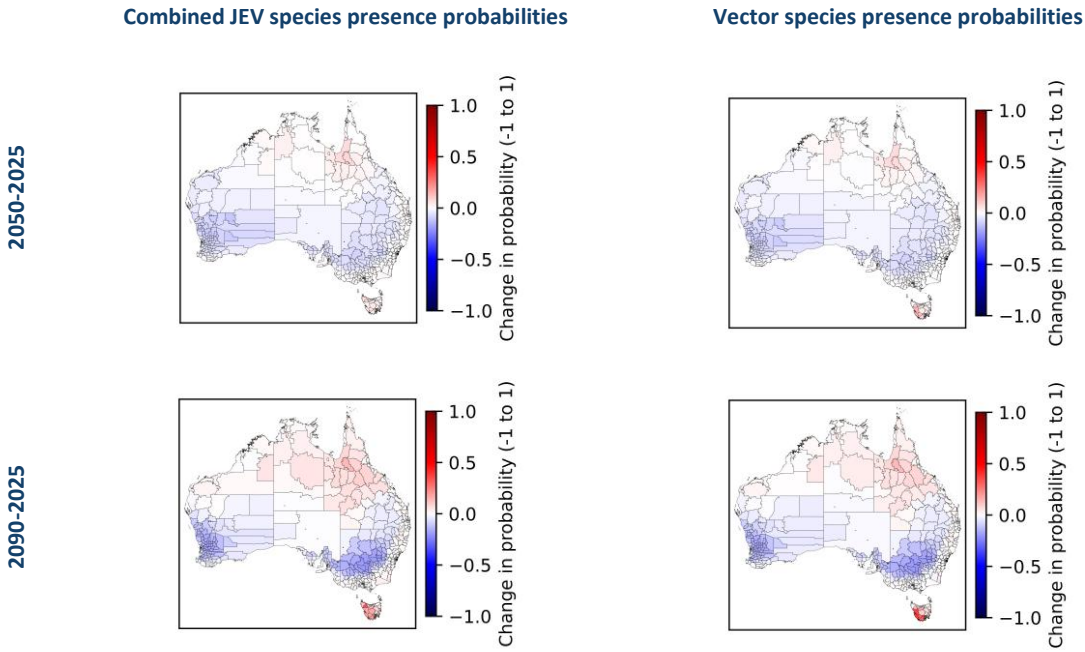

Figure 28 Combined JEV species presence probability changes and vector-only changes for RCP 8.5 across years at the LGA level

Table 11 Number of LGAs, out of 516 total, with greater than 0.5 combined JEV species presence probabilities for each climatic period. Values represent the median while, parentheses indicate range (min, max) across the eight climate models

	RCP	2025	2050	2090
Combined JEV species presence probability	4.5	432.5 (394, 457)	426.5 (375, 458)	424.0 (377, 464)
	8.5	440.5 (400, 462)	417.5 (369, 442)	399.5 (323, 461)
Mosquito presence probability	4.5	435.0 (399, 459)	430.0 (378, 461)	427.0 (378, 466)
	8.5	443.5 (404, 464)	420.0 (373, 446)	401.0 (329, 463)

3.2.3 Discussion

These projections should be interpreted cautiously. They are based on assumptions inherent in climate models and do not account for potential changes in human behaviour, land use, or wildlife movement.

Spillover risk proxy (potential zoonotic virus density)

The 2020 virus density estimate is built on estimates by IUCN of host species presence, and their ability to potentially be infected and transmit pathogens known to cross to humans, per the Mollentze and Streicker (2020) results. It is important to note that these viruses are *not necessarily currently present* and may require introduction to become an actual transmission let alone spillover risk. Further, the projections under climate change require both the host species distributions to change accordingly, and subsequently any of the viruses to continue to be viable in the different climate and/or possibly to be introduced. The adaptation of the viruses is further

explored in Section 3.3. There has also been some criticism of the viruses identified by Mollentze and Streicker (2020), with their findings considered to be underestimates, meaning this is likely an underestimate of the virus density likely to be found in each spatial region.

Another major caution about interpretation of these results is that a higher potential number of zoonotic viruses is only one axis of risk: the consequences of those viruses can vary drastically. As such, a higher number of (potentially) present viruses may not warrant more mitigation efforts than a lower number with potentially more severe outcomes. The method we have used does not allow for identification of the virus species, which needs to be explored to fully understand the actual risks.

One of the major insights from these projections is that a homogenisation effect increases with the more extreme RCP 8.5 scenario compared with RCP 4.5. That is, there is less variation as the minimums increase and maximums decrease (Figure B1). The second major insight is how consistent the large scale spatial patterns are for the projected changes, with consistently increased potential virus density in the western portion of Australia, decreases in the east, and substantial changes in Tasmania (Figure 24). Under both RCP scenarios, we see a noticeable shift in the geographic distribution of zoonotic virus density, especially under the higher emission scenario RCP 8.5. Future research may also consider alternative methods for downscaling climate data rather than the scaling approaches used by CCiA, which may affect differences in the projected spatial variability.

While these findings offer valuable insights, further research is needed to refine these models and incorporate more dynamic ecological and epidemiological data, such as distributions and density of zoonotic viruses and their host species, their potential adaptations to changing environmental factors, and models for the transmission process.

JEV risk proxy (combined JEV species presence probabilities)

Combined JEV species presence probabilities were built from models of species probabilities for three mosquito vectors, 12 water birds and feral pigs, based on the climatic conditions of where these species have been seen before. Median projections suggest that the coastlines of Australia have the highest (close to 1) combined JEV species presence probabilities under all scenarios and time periods. This is reflected as a band of no change, even under the most extreme projected increases seen for the MIROC 5 model under RCP 8.5 for 2090 (Figure 25). This model suggested widespread moderate to high increases in JEV combined presence probability, however, on balance the median changes suggested moderate increase to northern Australia and decreases to southern Australia, with a region around southern Western Australia showing a more consistent decrease even in the extreme model projection.

Regions of high change (either decreases or increases) tended to be in more inland regions of low to moderate probability, while coastal regions of high probability and central regions of very low to no probability, tended not to change. This is reflected in the number of LGAs with a probability of greater than 0.5 (Table 11). The majority of LGAs were greater than 0.5 for each period, with some decrease between 2025 and 2090. The majority of LGAs are also located in coastal regions, while areas such as central and Western Australia have fewer, larger LGAs. A key takeaway from these results is that regions of high presence probability are likely to remain high under climate

change projections and represent the majority of LGAs, while regions that are most likely to experience increases or decreases have lower probabilities.

The spatial distribution of JEV combined presence probability appears to be largely driven by mosquito presence probability. This may be due to the ubiquitous distribution of Australian water bird species and highlights the importance of exploring the relative contribution of key epidemiologically relevant species to understand why we see the projected change patterns.

The combined JEV species presence probability reflects where conditions are suitable but does not consider whether the species would need to be introduced or could feasibly drift into these locations. It also does not account for the presence of JEV itself. Converting presence probability into a more rigorous risk projection would require incorporating human populations and domestic piggery locations, estimates of vector abundance, and modelling the transmission process.

3.2.4 Next steps

The spillover risk proxy is actually potential zoonotic virus density, and we use a correlative approach to estimate climate effects. An updated estimate using more comprehensive sources of potential viruses could be used, and the approach could be extended to other forms of pathogens (bacteria, etc). For more ecologically and biologically realistic projections, ecological niche models should be developed for each of the viruses and species involved, as done for the JEV case study. This would enable a picture of both how many and which viruses, allowing for an estimate of the consequences of (potential) presence for a full risk estimation. Such models could subsequently be coupled with the adaptation estimates conducted in Section 3.3.

Once a more nuanced picture of potential viruses present is built, transmission models should be used to understand the natural epidemic cycles, and transmission risks could be estimated through the likelihood of transmission to humans based on spatial proximity and human populations. This would be a step towards estimating human incidence risks. This would require knowledge on the natural transmission cycle of each virus, vector competence, cross species transmission probabilities, and some understanding of prevalence or incidence in each of the host types. Where human health outcomes are known, this could be used to more fully estimate risks.

We have not considered what happens with human populations under climate change projections. This would need to be included in any transmission layers. Human population changes are likely to have substantial impact on how much these potential risks are realised, as it will change contact rates (and so exposure risks).

We used the older climate models as they had the various indices we needed for biological reasons. This should be adapted to the more recent climate models, which will require the computation of these indices.

3.2.5 Acknowledgments

We would like to acknowledge Dr Andrew Hoskins for his insight into species distribution modelling of feral pigs. Data availability (Spillover)

Data are available online on request for the spillover risk results presented in Figure 24, B1, and B2 (Golchin et al. 2025) and the JEV presence probability results presented in Figures 25, 26 and 27, are available online, on request (Sexton et al. 2025).

3.2.6 References (Spillover)

Anderson, C. B., (2023). elapid: Species distribution modeling tools for Python. Journal of Open Source Software, 8(84), 4930. https://doi.org/10.21105/joss.04930.

Australian Bureau of Meteorology. (2019). Australian Gridded Climate Data (AGCD) / AWAP; v1.0.0 Snapshot (1900-01-01 to 2018-12-31). https://doi.org/10.4227/166/5a8647d1c23e0.

Belbin, L., Wallis, E., Hobern, D., & Zerger, A. (2021). The Atlas of Living Australia: History, current state and future directions. Biodiversity Data Journal, 9, e65023. https://doi.org/10.3897/BDJ.9.e65023.

Bentsen, M., Bethke, I., Debernard, J. B., Iversen, T., Kirkevåg, A., Seland, Ø., Drange, H., Roelandt, C., Seierstad, I. A., Hoose, C., & Kristjánsson, J. E. (2013). The Norwegian Earth System Model, NorESM1-M – Part 1: description and basic evaluation of the physical climate. Geoscientific Model Development, 6(3), 687–720. https://doi.org/10.5194/gmd-6-687-2013.

Bi, D., Dix, M., Marsland, S., O'Farrell, S., Rashid, H., Uotila, P., Hirst, A., Kowalczyk, E., Golebiewski, M., Sullivan, A., Yan, H., Hannah, N., Franklin, C., Sun, Z., Vohralik, P., Watterson, I., Zhou, X., Fiedler, R., Collier, M., Ma, Y., Noonan, J., Stevens, L., Uhe, P., Zhu, H., Griffies, S., Hill, R., Harris, C., & Puri, K. (2013) The ACCESS coupled model: description, control climate and evaluation. Australian Meteorological and Oceanographic Journal, 63, 41-64. https://doi.org/10.1071/ES13004

Chylek, P., Li, J., Dubey, M. K., Wang, M., & Lesins, G. (2011). Observed and Model Simulated 20th Century Arctic Temperature Variability: Canadian Earth System Model CanESM2. Atmospheric Chemistry and Physics, 11, 22893–22907. https://doi.org/10.5194/acpd-11-22893-2011.

Commonwealth Scientific and Industrial Research Organisation & Bureau of Meteorology. Climate Change in Australia. http://www.climatechangeinaustralia.gov.au/.

Commonwealth Scientific and Industrial Research Organisation. (2024). Climate and communicable disease: Discussion paper. CSIRO, Canberra

Donohue, R., McVicar, T., Roderick, M., &Li, L. (2017). Australian 5km Potential Evaporation, Radiation and Related Products - Morton_wetarea. CSIRO. https://doi.org/10.4225/08/58c8f7ec94220.

Dunne, J. P., John, J. G., Shevliakova, E., Stouffer, R. J., Krasting, J. P., Malyshev, S. L., Milly, P. C. D., Adcroft, A. J., Cooke, W., Dunne, K. A., Griffies, S. M., Hallberg, R. W., Harrison, M. J., Levy, H., Wittenberg, A. T., & Zadeh, N. (2013). GFDL's ESM2 global coupled climate–carbon earth system models. Part II: carbon system formulation and baseline simulation characteristics. Journal of Climate, 26(7), 2247-2267. https://doi.org/10.1175/JCLI-D-12-00150.1.

Furlong, M., Adamu, A., Hickson, R. I., Horwood, P., Golchin, M., Hoskins, A., & Russell, T. (2022). Estimating the distribution of Japanese encephalitis vectors in Australia Using Ecological

Niche Modelling. Tropical Medicine and Infectious Disease, 7(12), 393. https://doi.org/10.3390/tropicalmed7120393.

Furlong, M., Adamu, A. M., Hoskins, A., Russell, T. L., Gummow, B., Golchin, M., Hickson, R. I., Horwood, P. F. (2023). Japanese Encephalitis enzootic and epidemic risks across Australia. Viruses, 15(2), 450. https://doi.org/10.3390/v15020450.

Golchin, M., Di Marco, M., Horwood, P. F., Paini, D. R., Hoskins, A. J., & Hickson, R. I. (2024). Prediction of viral spillover risk based on the mass action principle. One Health (Amsterdam, Netherlands), 18, 100737. https://doi.org/10.1016/j.onehlt.2024.100737.

Golchin, M., Sexton, Justin., & Hickson, R. (2025). Spillover Risk Change Estimates with Climate Variations. v1. CSIRO. Data Collection. https://doi.org/10.25919/yn9z-pj85

International Union for Conservation of Nature and Natural Resources. (2022). IUCN Red List of Threatened Species. https://www.iucnredlist.org.

Jones, D., Wang, W., & Fawcett, R. J. W. (2009). High-quality spatial climate data-sets for Australia. Australian Meteorological and Oceanographic Journal, 58, 233–48. https://doi.org/10.22499/2.5804.003.

Martin, G. M., Bellouin, N., Collins, W. J., Culverwell, I. D., Halloran, P. R., Hardiman, S. C., Hinton, T. J., Jones, C. D., McDonald, R. E., McLaren, A. J., O'Connor, F. M., Roberts, M. J., Rodriguez, J. M., Woodward, S., Best, M. J., Brooks, M. E., Brown, A. R., Butchart, N., Dearden, C... Wiltshire, A. (2011). The HadGEM2 family of met office unified model climate configurations. Geoscientific Model Development 4(3), 723–57. https://doi.org/10.5194/gmd-4-723-2011.

Mollentze, N. & Streicker, D. G. (2020). Viral Zoonotic Risk Is Homogenous among taxonomic orders of mammalian and avian reservoir hosts. Proceedings of the National Academy of Sciences, 117(17): 9423–30. https://doi.org/10.1073/pnas.1919176117.

Neale, R. B., Gettelman, A., Park, S., Chen, Lauritzen, P. H., Williamson, D. L., Conley, A. J., Kinnison, D. E., Marsh, D., Smith, A. K., Vitt, F. M., García, R. R., Lamarque, J. F., Mills, M. J., Tilmes, S., Morrison, H., Cameron-Smith, P., Collins, W., Iacono, M. J., … Taylor, M. A. (2012). Description of the NCAR Community Atmosphere Model (CAM 5.0). https://doi.org/10.5065/wgtk-4g06.

Phillips, S. J., Anderson, R. P., Dudík, M., Schapire, R. E., & Blair, M. E. (2017). Opening the black box: an open-source release of maxent. Ecography, 40(7), 887–93. https://doi.org/10.1111/ecog.03049.

Phillips, S. J., Anderson, R. P., & Schapire, R. E. (2006). Maximum entropy modeling of species geographic distributions. Ecological Modelling, 190(3), 231–59. https://doi.org/10.1016/j.ecolmodel.2005.03.026.

Sexton, J., Golchin, M., & Hickson, R. (2025). Species presence probability projections under climate change in Australia (2025,2050,2090) for Japanese Encephalitis Virus risk analysis. v1. CSIRO. Data Collection. https://doi.org/10.25919/feye-9073.

Voldoire, A., Sanchez-Gomez, E., Salas y Mélia, D., Decharme, B., Cassou, C., Sénési, S., Valcke, S., Beau, I., Alias, A., Chevallier, M., Déqué, M., Deshayes, J., Douville, H., Fernandez, E., Madec, G., Maisonnave, W., Moine, M. P., Planton, S., Saint-Martin, D... Chauvin, F. (2013). The

CNRM-CM5.1 Global climate model: description and basic evaluation. Climate Dynamics, 40(9), 2091–2121. https://doi.org/10.1007/s00382-011-1259-y.

Watanabe, M., Suzuki, T., O'ishi, R., Komuro, Y., Watanabe, S., Emori, S., Takemura, T., Chikira, M., Ogura, T., Sekiguchi, M., Takata, K., Yamazaki, D., Yokohata, T., Nozawa, T., Hasumi, H., Tatebe, H., Kimoto, M. (2010). Improved climate simulation by MIROC5: Mean states, variability, and climate sensitivity. Journal of Climate, 23, 6312-6335 https://doi.org/10.1175/2010JCLI3679.1.

3.3 Investigate climate change induced mutations in a pathogen's genome

Pathogens are constantly evolving through the accumulation of genetic mutations, allowing them to adapt to changing environmental conditions. Several studies have investigated the link between emerging mutations and climate, finding evidence of adaption amongst various species (Zhang et al, 2010; Akil et al., 2014; Dietrich et al., 2023). Investigating this potential link is critical to understanding the potential impact of changing climates.

To understand how climate change induced mutations in a pathogen's genome could have potential adverse impacts on survival, replication, and virulence, an analysis was undertaken to predict pathogen sensitivity to climate variables to understand how pathogens could change under different climate scenarios. The approach was to explore pathogen climate sensitivity by machine learning and statistical approaches using genome sequence alignments of pathogen species from different climates around the world, over time. JEV and influenza genomes from across the globe were explored and the correlations between pathogen mutations and climate changes established.

3.3.1 Method

Genomic dataset sources

Genomic sequences were collected from multiple sources. For JEV, we collected 238 genomes from the Bacterial and Viral Bioinformatics Resource Centre (BVBRC) (https://www.bv-brc.org). These genomes spanned the years from 2000 – 2022 and were from 6 host groups: Human, Sea Mammal, Nonhuman Mammal, Lab, Insect and Avian.

Influenza genomes spanning the years 2000 – 2020 were also collected from the BVBRC. Analysis was restricted to only the H1N1 strain of influenza, as it is a highly relevant pathogen that has shown evidence of adapting to climate change previously (Jiang et al., 2020). In total, only human sequences were considered, yielding 15,308 viral genomes in total for analysis.

Alignment and processing of genetic data

Genomic sequences were pre-processed to ensure only high-quality sequences were used and then aligned against each other using Multiple Alignment using Fast Fourier Transformation (MAFFT), a multiple-sequence alignment program (Katoh et al., 2002), producing a multi-sequence alignment. This alignment was then parsed with SNP-sites to identify all genetic variants before being converted to matrix form for processing by the machine learning algorithms.

Climate data source

Climate data was sourced from various sources across the globe for each pathogen. For influenza, which had high quality associated metadata providing more granular information about the sample location (in many cases down to the level of city), we sourced data from www.worldclim.org, which includes data from over 2 million weather stations with a spatial resolution of 5 minutes (~85km^2). Samples were associated with climate data from their nearest weather station.

For Salmonella and JEV, which did not have access to such fine grain metadata, average climate data for year of collection and country of collection was sourced from www.theglobaleconomy.com.

Random forest analysis

To investigate potential links of genetic variants and changes in the climate we utilised the random forest machine learning algorithm. Random forests are tree-based ensemble learning methods which provide interpretable information about the information contained within features with respect to a specific characteristic. In this case, we applied them to determine if there were specific genetic variants within our datasets that were linked to changes in climate conditions (e.g. changes in the minimum/maximum temperature or precipitation). Feature importance, as provided by the Random Forest algorithm, was used to determine the most informative/linked variants within each dataset which were then flagged for further analysis.

Classification based on associations

Classification Based on Associations (CBA) is a method of Association Rule Mining, which aims to determine the links between distinct features in a dataset and how they pertain to specific observations, e.g. the presence of a specific mutation or combination of mutations means the sample is more likely to be from a specific climate case. These methods allow for the identification of interactions between features, allowing for a better biological interpretation. This approach was applied to the JEV samples in order to extract more information from the otherwise limited dataset.

Protein structure

Protein structures were sourced from a database of x-ray crystallography determined structures (www.rcsb.org).

3.3.2 Results

Correlation of influenza mutations with changes in climate

We first analysed linkage between influenza mutations and changes in climate between the years 2000 – 2020. Due to the high granularity of the influenza dataset, we were able to associate influenza samples with specific locations and their associated minimum and maximum temperatures as well as precipitation.

Association between genetic variations and changes in the minimum and maximum temperatures were first explored using Random Forest. By stratifying the samples into High, Medium or Low based on their associated minimum and maximum temperatures, a number of correlated variants were identified. In total, 674 variants which were linked to maximum temperature were identified and 663 linked to minimum temperature. Using these informative features, a predictive model could classify a sample as originating from a high-temperature environment with an approximate 60% precision. The models were less accurate distinguishing between Medium and Low temperature samples (with precision scores of 49 and 46% respectively) suggesting the biggest difference was observed in the high temperature samples.

A similar analysis was conducted for association between genetic variants and precipitation. Of the variants, 711 were associated with precipitation levels but the overall power of the model was not as high as the temperature models (with an average precision for the different precipitation classes of 43%).

Comparison of the important variants for the three climate conditions (minimum temperature, maximum temperature and precipitation) showed a substantial overlap, with some variants being informative for multiple climate conditions. Overlap for the top 10 features for each condition is shown in Figure 29a. As expected, minimum and maximum temperature showed the greatest overlap but there still was overlap with precipitation. Interestingly, 4 of the top 10 variants were common to all 3 climate conditions.

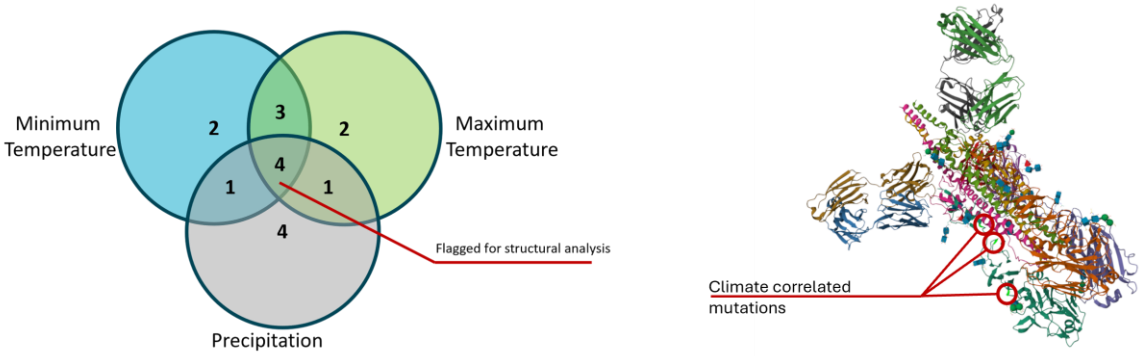

Figure 29 The top 10 variants associated with different climate characteristics showed significant overlap, with some variants common to all investigated characteristics (A). These were flagged for structural analysis. By visualising the variants in the context of the protein structure (B).

These variants were investigated further with three of them being present within the HA1 protein. The HA1 protein is a critical protein in influenza biology, forming a trimer on the surface of the virus and being heavily involved in infection and subsequent pathology (Aartse et al., 2021). In order to better understand the context in which these mutations existed; they were mapped to the structure of the HA1 trimer (Figure 29b). Visualisation of these variants revealed that all three are localised in the region of the protein that facilitate binding to human cells. Additionally, based on the structure all three mutations are facing and exposed to the surrounding environment suggesting they could interact and respond to changing environmental conditions.

Analysis of JEV mutations in the context of global climate events

Unlike influenza, the JEV dataset was significantly smaller with less than 300 high quality genomes available for analysis spanning 2000 - 2022. Due to the sparsity of the data, in-depth analysis of the relationships between genetic variations and granular climate variables such as temperature and precipitation was not feasible. Instead, the link to global El Niño and La Niña events were studied.

El Niño and La Niña are global recurring warming and cooling events respectively that affect the global climate patterns and there is emerging evidence that climate change is impacting this cycle, making it more intense (Wenju et al., 2023). Samples were classified as El Niño and La Niña based on their year of collection (see Table 12) and then analysed using the Random Forest algorithm.

This approach identified 612 linked features. By modelling the samples using this approach it was possible to predict whether the sample originated from an El Niño or La Niña year with an accuracy of 77% suggesting the selected variants were highly informative.

To investigate the link further, CBA was performed to identify interacting variants. This analysis was restricted to only the variants identified as informative. In total, 11 associations were identified linking multiple variants to El Niño (Table 12). These were all bi-variant associations, meaning a combination of two variants whose presence were highly suggestive of the sample originating during an El Niño year. These results could be indicative of the co-evolution of variants, but a more comprehensive dataset would be required to confirm. Additionally, 8 of the 11 association rules involved at least one variant within the 3' region of the JEV genome which is currently unannotated. If the link to this region can be confirmed with additional data than functional analysis could identify the method by which the virus is adapting to a changing climate.

Table 12 Association Rules between JEV variants and El Niño

VARIANT COMBINATION	SUPPORT
7013 and 12230	0.36
9889 and 12275	0.33
9217 and 19	0.33
12230 and 1002	0.33
9566 and 19	0.32
8013 and 19	0.32
12230 and 19	0.32
12656 and 7058	0.31
12230 and 1910	0.31
12230 and 5659	0.31
6231 and 10067	0.39

3.3.3 Discussion

The aim of this analysis was to investigate the link between genetic variations within pathogen genomes and changing climate conditions. Analysis of the influenza dataset identified several mutations that were linked to changes in temperature and precipitation, including several that were common across all climate categories. Additionally, structural analysis using high-quality X-ray crystallography structures showed that these common variants were present on the surface of the HA1 trimer, meaning they have the capacity to interact with the surrounding environment.

While this analysis identifies several variants that should be monitored closely to see if they continue to spread, functional implications need to be determined experimentally.

The JEV analysis revealed several variant combinations that were linked to the El Niño cycle. The preferential association of these variants in samples originating from El Niño years could be indicative of co-evolution, two variants emerging in tandem in response to the changing climate conditions. Climate change has been hypothesized to influence the El Niño/La Niña cycle, potentially intensifying the climate events. If these variants are associated with El Niño, then an intensifying of this climate cycle would lead to an increase in the frequency these variant combinations are observed.

While the analysis here has highlighted several variants across Influenza and JEV that show evidence of being linked to changing climate conditions, care must be taken when interpreting the results as correlation does not also equate to causation. Viral evolution is a complex process with many competing forces and while the variants here may be true examples of evolution, the driving force may be a hidden factor rather than climate, e.g. changed host behaviour or spread of medicines. By continuing to monitor and collect data on these variants across the globe, more evidence for their association with climate can be collected. Additionally, functional studies could provide insight into their mechanism of action and whether they are providing an advantage to the pathogen with regards to a changing climate.

The power of these association studies is also directly linked to the quality of data available. The Influenza dataset was comprised of high-quality genetic sequences from a diverse range of sources. Additionally, the associated metadata was highly granular providing an accurate location and time of sampling, in many cases down to the city and month. Many other pathogens lack this granularity of data. As an example, salmonella was also investigated. While there exist high quality genetic datasets for this bacteria, the associated metadata is poor with many samples lacking annotations or being limited to only the country and year of sampling. Such high-level annotations mean any analysis on climate variables such as temperature or precipitation must be done using averages from the whole country across the whole year. Such processing reduces much of the variation, making it challenging to determine any links or associations between genetic variations and climate. To address this, future work should focus on keeping accurate records of time and location of sampling. Collecting a proper representation across locations as well as over sufficiently long periods of time will add statistical power to the analysis methods, enabling a much more in-depth analysis of the correlation between specific mutations and changes in climate.

3.3.4 Next steps

The results presented here are suggestive of genetic adaptation but not definitive. Future work should focus on both methodical sampling of pathogen isolates ensuring high quality records of date and location of collection to enable better matching to climate conditions. A future avenue as well would be to extend the analysis to include not just the climate at the time of sampling but also during the preceding period. Adaptation events occur in response to external pressure and as such responses to a change in climate may not manifest immediately. Such a longitudinal analysis would require a more extensive dataset but would expand on the analysis here and also allow for modelling of how a pathogen could adapt in response to future climate scenarios.

3.3.5 References

Aartse, A., Eggink, D., Claireaux, M., van Leeuwen, S., Mooij, P., Bogers, W. M., Sanders, R. W., Koopman, G., & van Gils, M. J. (2021). Influenza A Virus Hemagglutinin Trimer, Head and Stem Proteins Identify and Quantify Different Hemagglutinin-Specific B Cell Subsets in Humans. Vaccines, 9(7), 717. https://doi.org/10.3390/vaccines9070717.

Akil, L., Ahmad, H. A., & Reddy, R. S. (2014). Effects of climate change on salmonella infections. Foodborne Pathogens And Disease, 11(12), 974–980. https://doi.org/10.1089/fpd.2014.1802.

Dietrich, J., Hammerl, J. A., Johne, A., Kappenstein, O., Loeffler, C., Nöckler, K., Rosner, B., Spielmeyer, A., Szabo, I., & Richter, M. H. (2023). Impact of climate change on foodborne infections and intoxications. Journal of Health Monitoring, 8(Suppl 3), 78–92. https://doi.org/10.25646/11403.

Jiang, D., Wang, Q., Bai, Z., Qi, H., Ma, J., Liu, W., Ding, F., & Li, J., (2020). Could Environment Affect the Mutation of H1N1 Influenza Virus? International Journal of Environmental Research and Public Health, 17(9):3092 – 3100. https://doi.org/10.3390/ijerph17093092.

Katoh, K., Misawa, K., Kuma, K., & Miyata, T. (2002). MAFFT: a novel method for rapid multiple sequence alignment based on fast Fourier transform. Nucleic Acids Research, 30(14), 3059–3066. https://doi.org/10.1093/nar/gkf436.

Cai, W., Ng, B., Geng, T., Jia, F., Wu, L., Wang, G., Liu, Y., Gan, B., Yang, K., Santoso, A., Lin, X., Li, Z., Liu, Y., Yang, Y., Jin, F.-F., Collins, M., & McPhaden, M. J. (2023). Anthropogenic impacts on twentieth-century ENSO variability changes. Nature Reviews Earth and Environment, 4, 407-418. https://doi.org/10.1038/s43017-023-00427-8.

Zhang, Y., Bi, P., & Hiller, J. E. (2010). Climate variations and Salmonella infection in Australian subtropical and tropical regions. Science of the Total Environment, 408(3), 524-530. https://doi.org/10.1016/j.scitotenv.2009.10.068.

Appendix A Extended results for statistical modelling of air quality and health service use: Section **Error! Reference source not found.**

This appendix contains extended results of the statistical modelling exploring the relationship between air quality and health service use using national data collections (refer to Section **Error! Reference source not found.**). Acronyms used in this appendix include 'Respiratory conditions' (RC), 'Heart, stroke and vascular conditions' (HSVC), ‘Burns’ (BC), and 'Mental and behavioural disorders' (MBD).

ED presentations

A.1.1 Respiratory conditions (RC) and heart, stroke and vascular conditions (HSVC)

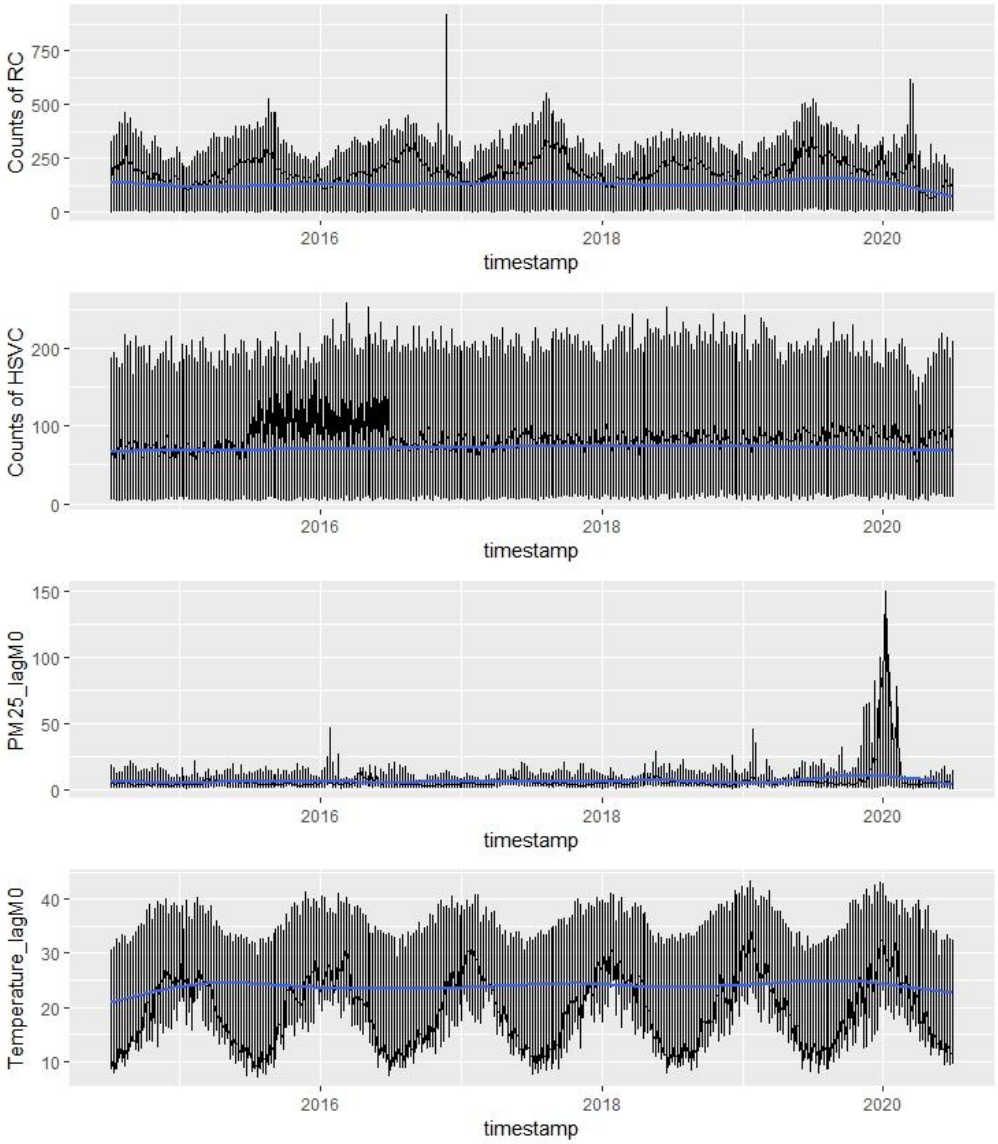

Figure A1 Time-series plots of counts of RC and HSVC, $PM_{2.5}$ and temperature

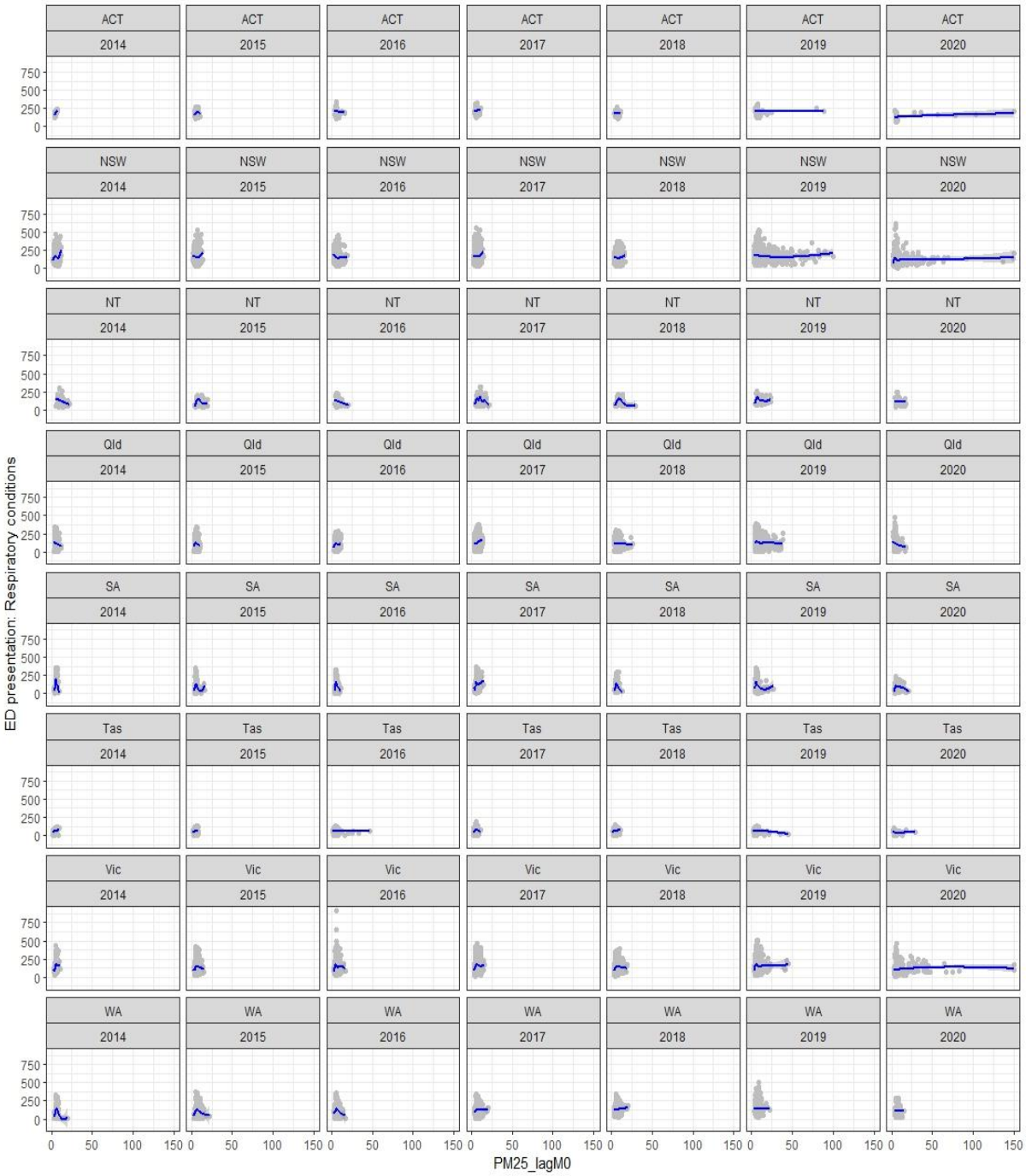

Figure A2 Scatter plots of counts of ED visits for respiratory conditions vs. $PM_{2.5}$

The scatter plot shows a weak relationship between the number of ED presentations and the level of the $PM_{2.5}$ concentration.

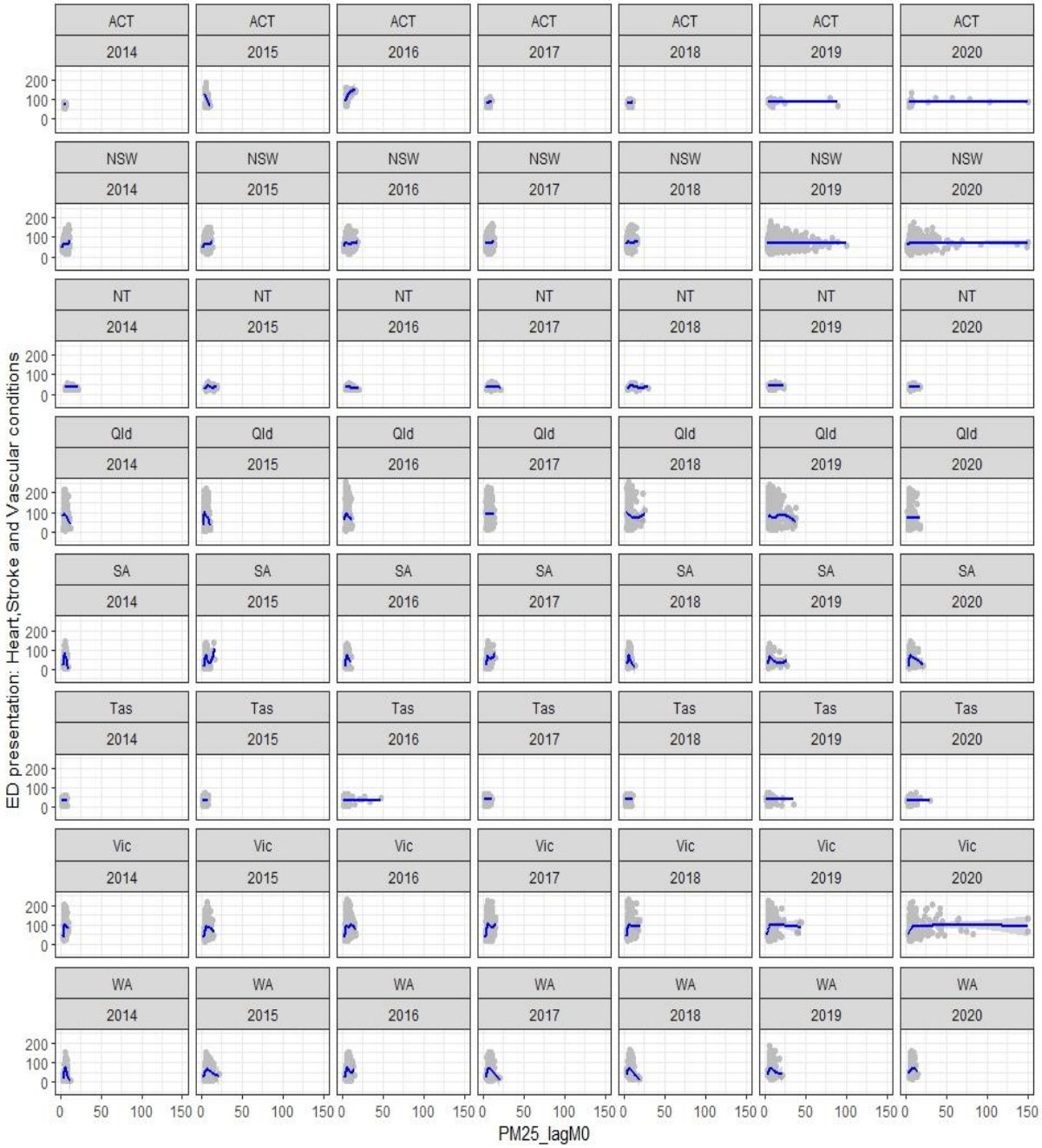

Figure A3 Scatter plots of Counts ED visits for HSV conditions vs. $PM_{2.5}$

Respiratory Conditions

The figure below shows the relative risks (RRs) for Respiratory conditions from Poisson GAM (left) and NB GAM (right) and diagnostic plots below these. As shown in the figure, the diagnostic plots for Poisson GAM shows the extent of overdispersion, and hence NB GAM was used to account for overdispersion.

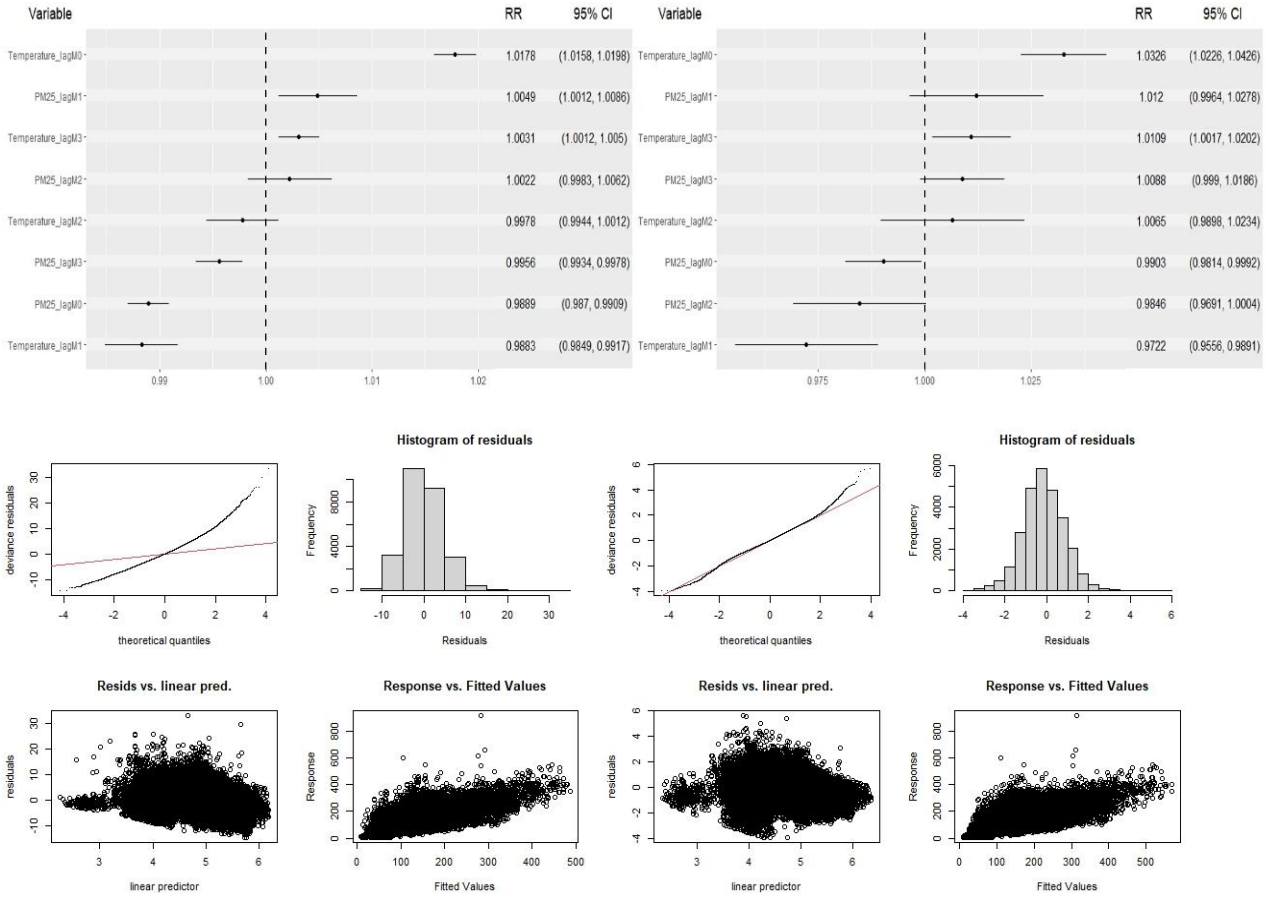

Figure A4 (Top) RR for Respiratory conditions and (Bottom) Diagnostic plots for Poisson GAM (left) and Negative binomial GAM (right)

Heart, stroke, and vascular conditions

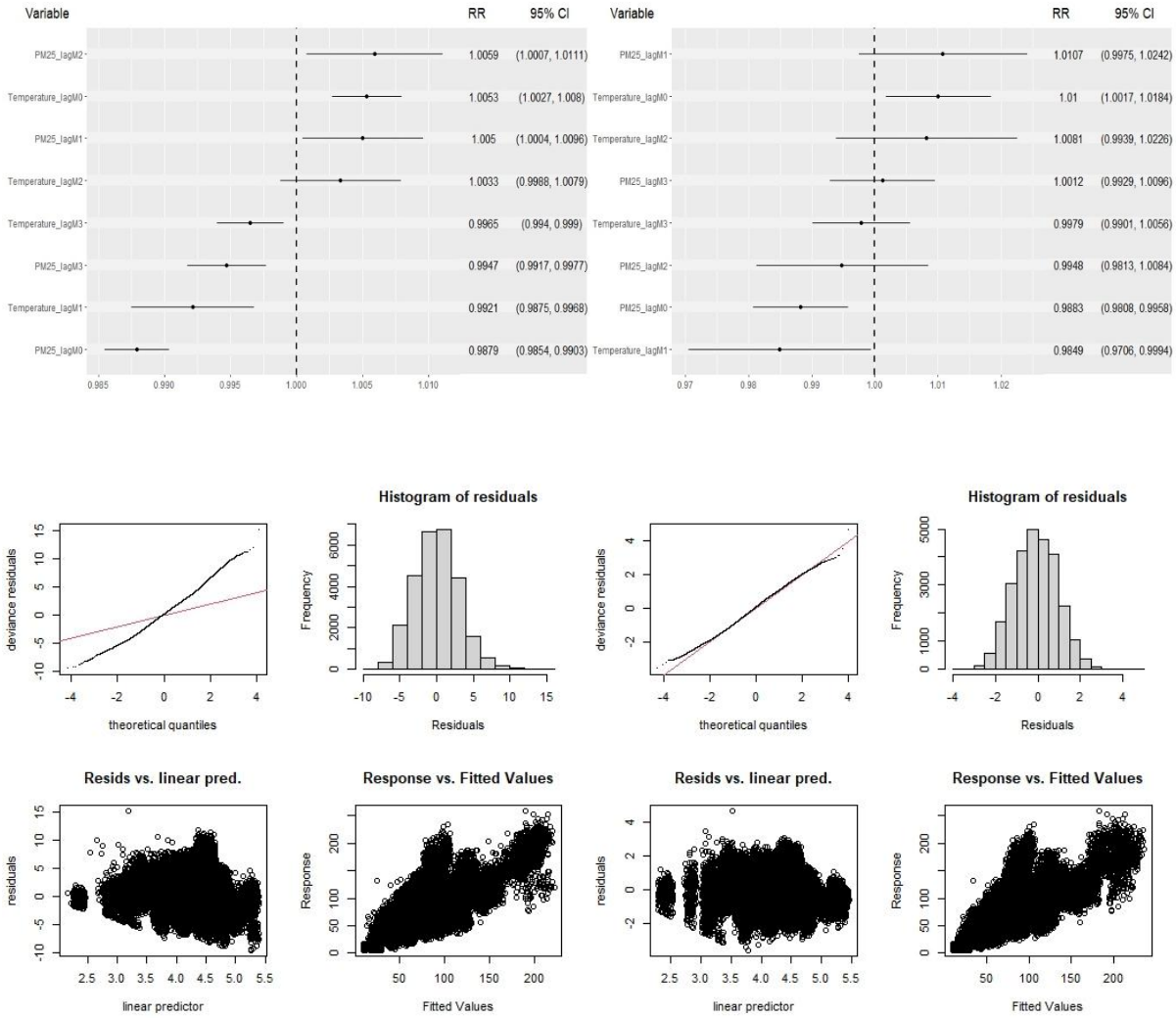

Figure A5 (Top) RR for Heart, Stroke and Vascular conditions and (Bottom) Diagnostic plots for Poisson GAM (left) and Negative binomial GAM (right)

A.1.2 Burns conditions and mental and behavioural disorders

Scatter plots showing temporal and spatial trends by conditions.

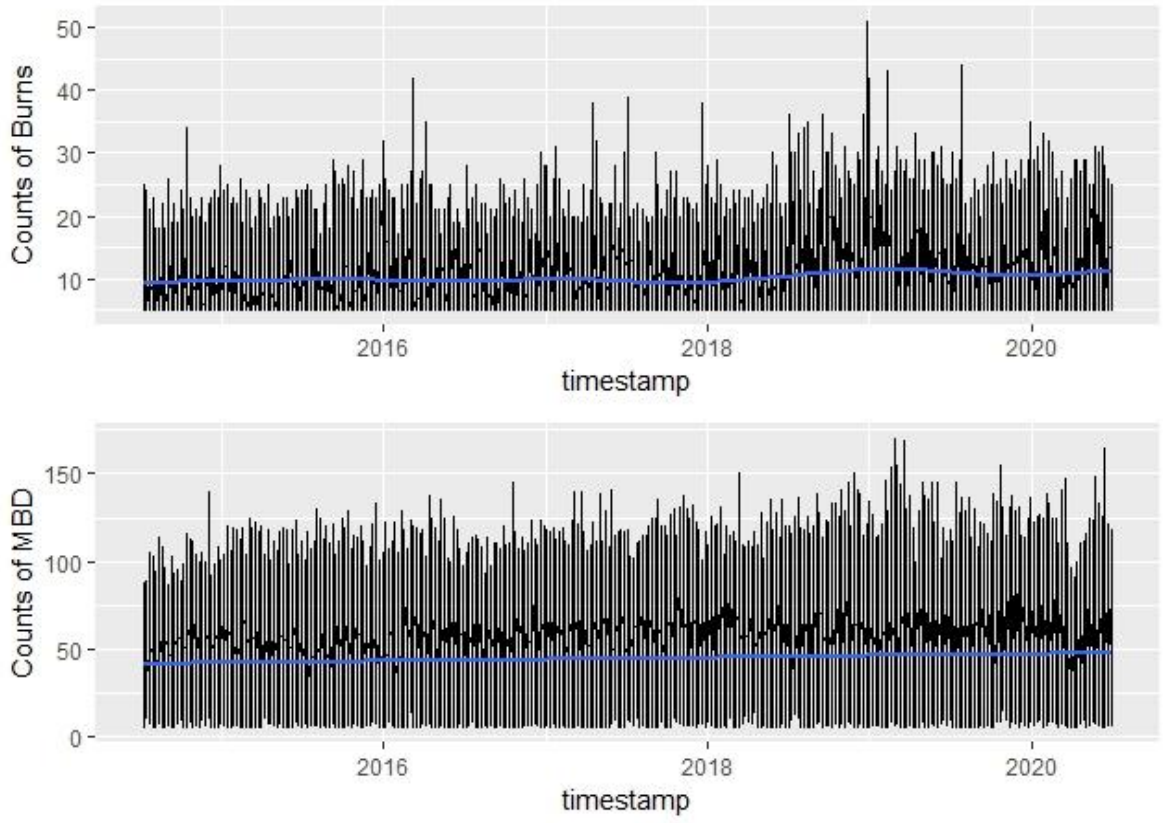

Figure A6 Time-series plots of counts of Burns and MBD

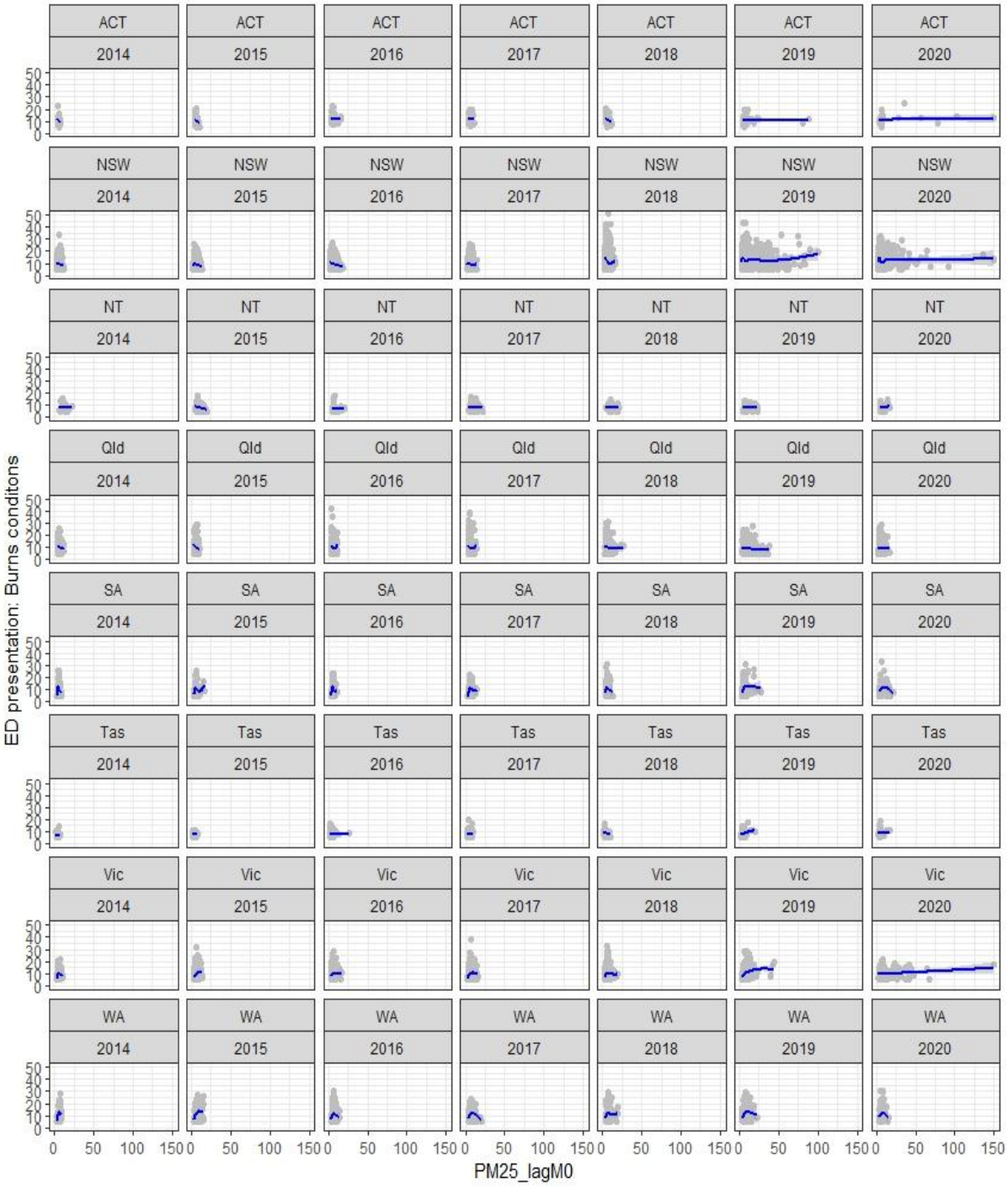

Figure A7 Scatter plots of counts of ED visits for burns conditions vs. $PM_{2.5}$

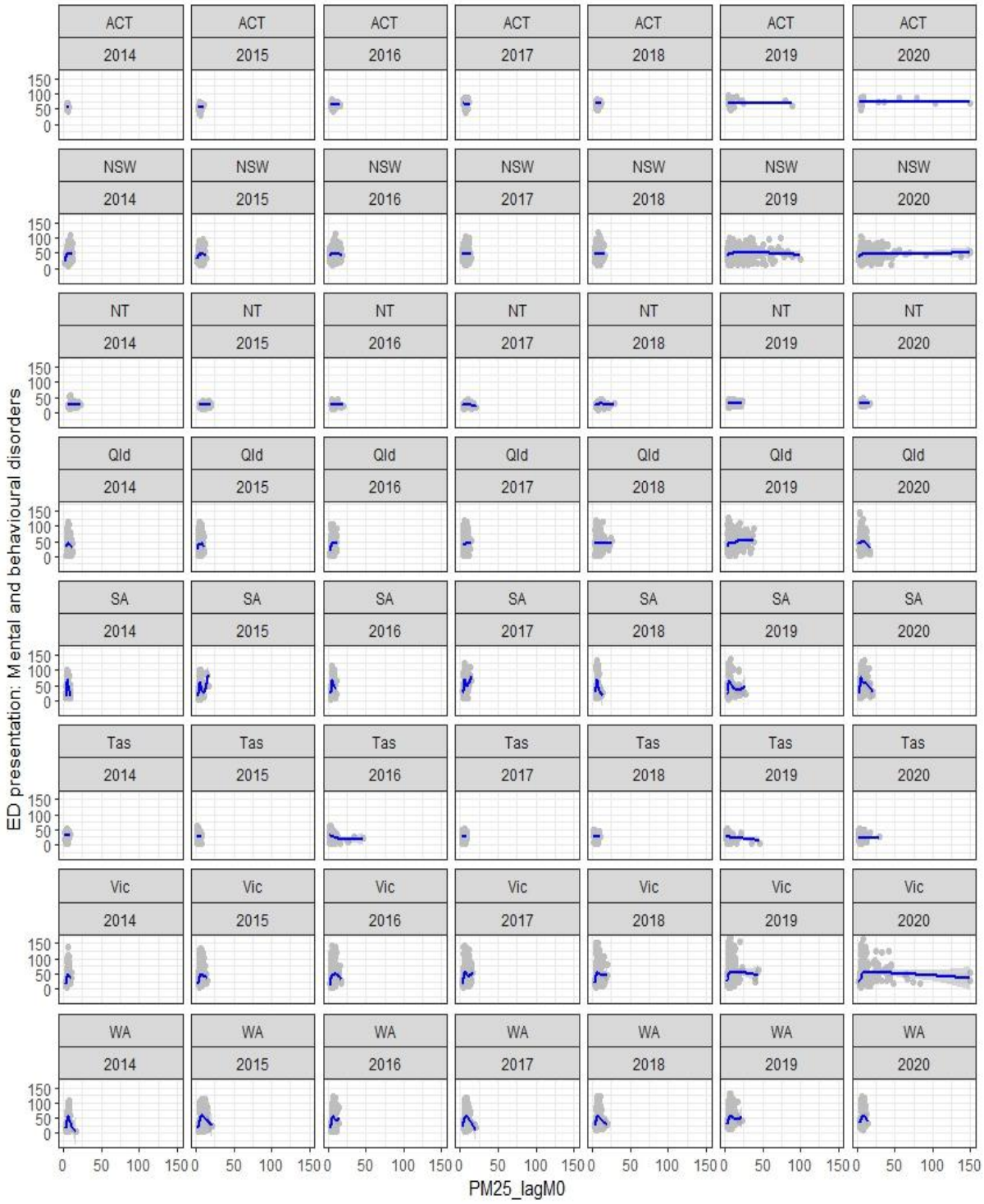

Figure A8 Scatter plots of counts of ED visits for mental health disorders vs. $PM_{2.5}$

Burns conditions

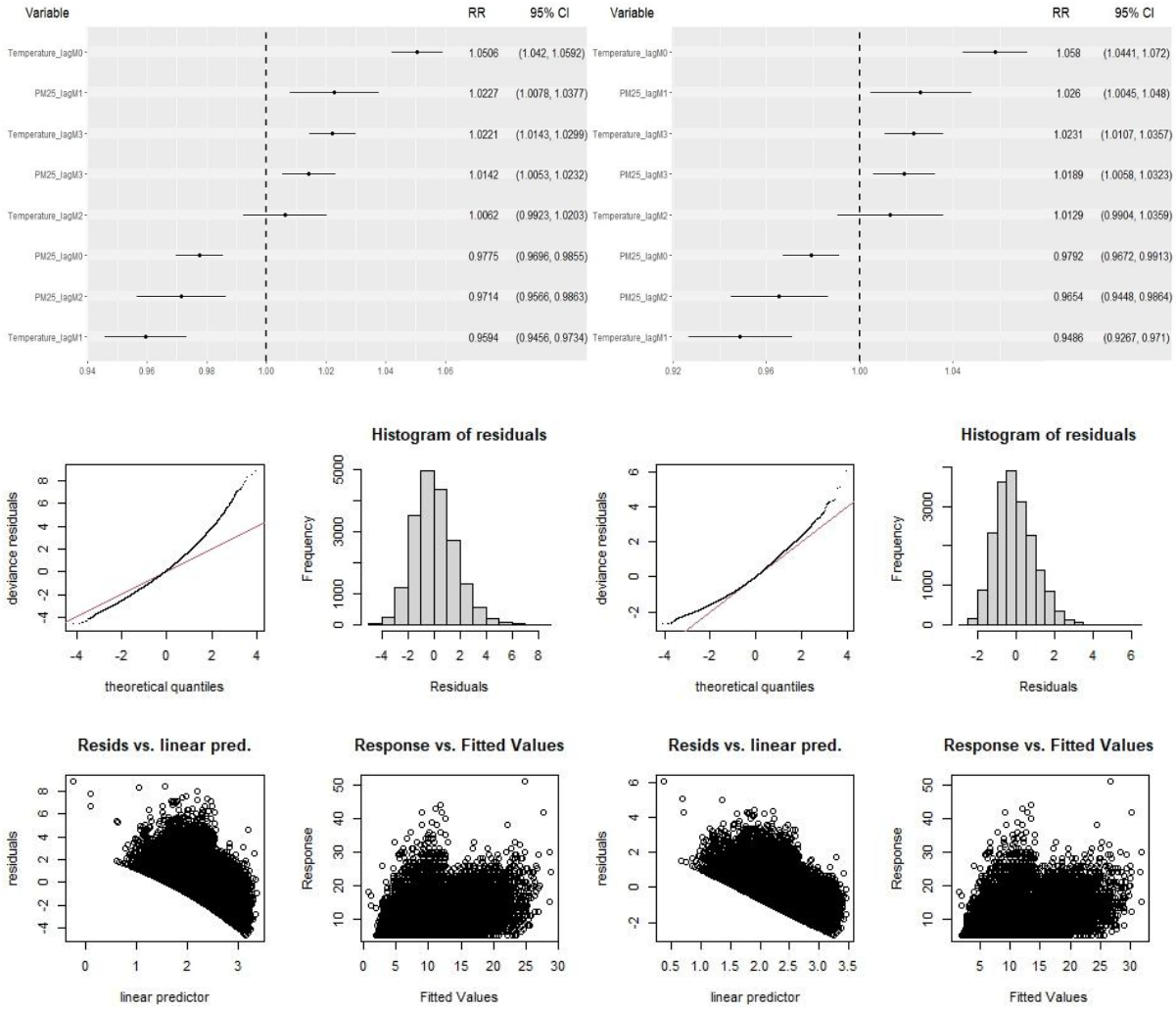

Figure A9 (Top) RR for Burns conditions and (Bottom) Diagnostic plots for Poisson GAM (left) and Negative binomial GAM (right)

Neither Poisson or negative binomial models fit well for Burns conditions due to very few non-zero counts or very small event counts.

A.1.3 Mental and behavioural disorders

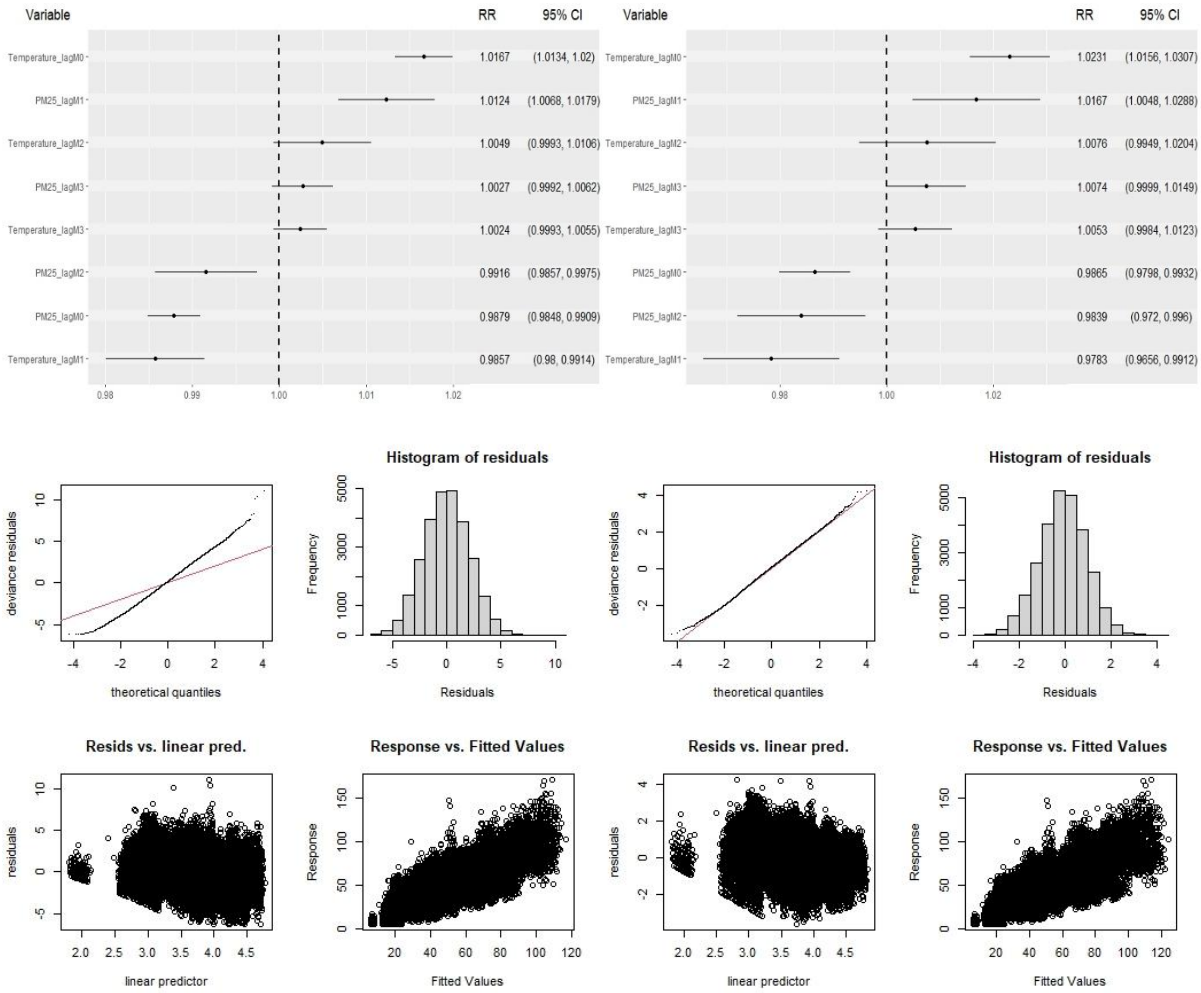

Figure A10 (Top) RR for Mental and behavioural disorders conditions and (Bottom) Diagnostic plots for Poisson GAM (left) and Negative binomial GAM (right)

Inpatient admissions

A.1.4 Time series plots

Time-series plots of air pollution ($PM_{2.5}$), maximum temperature, and outcomes of interest.

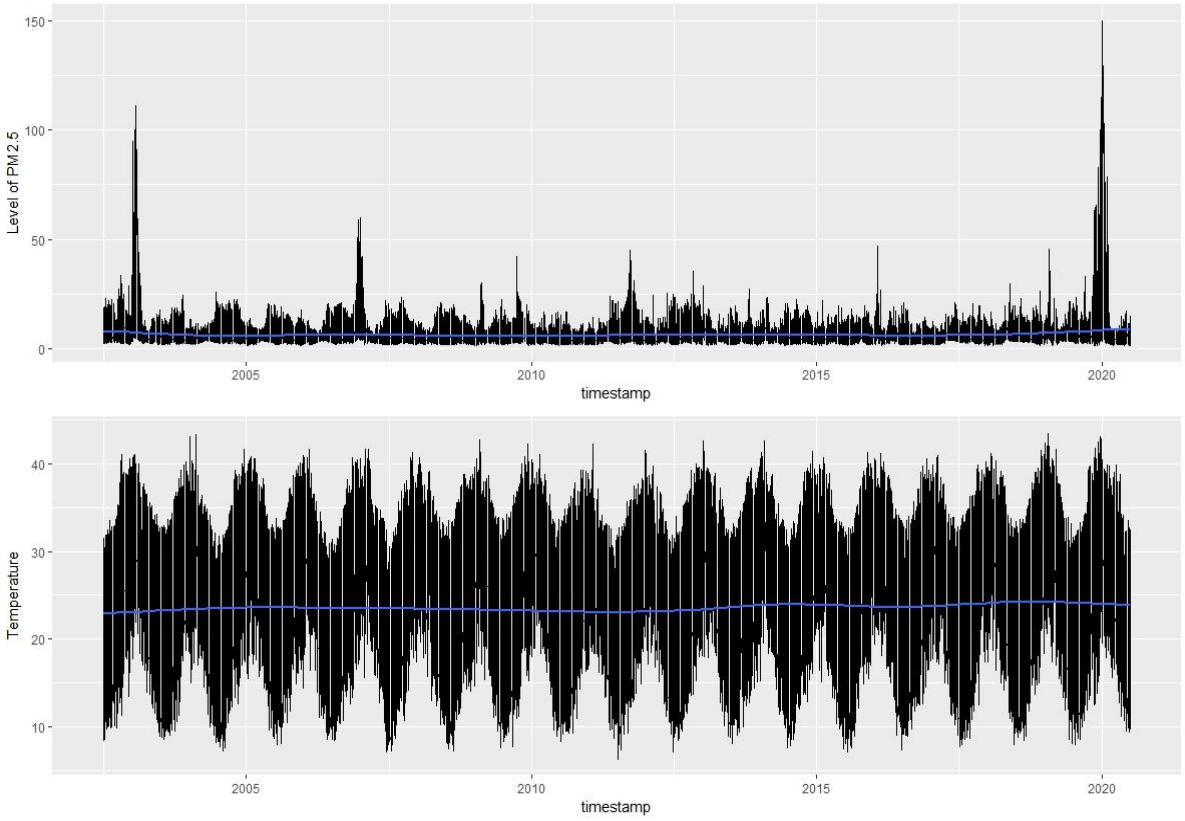

Figure A11 Time-series plots of air pollution variable ($PM_{2.5}$) and Temperature

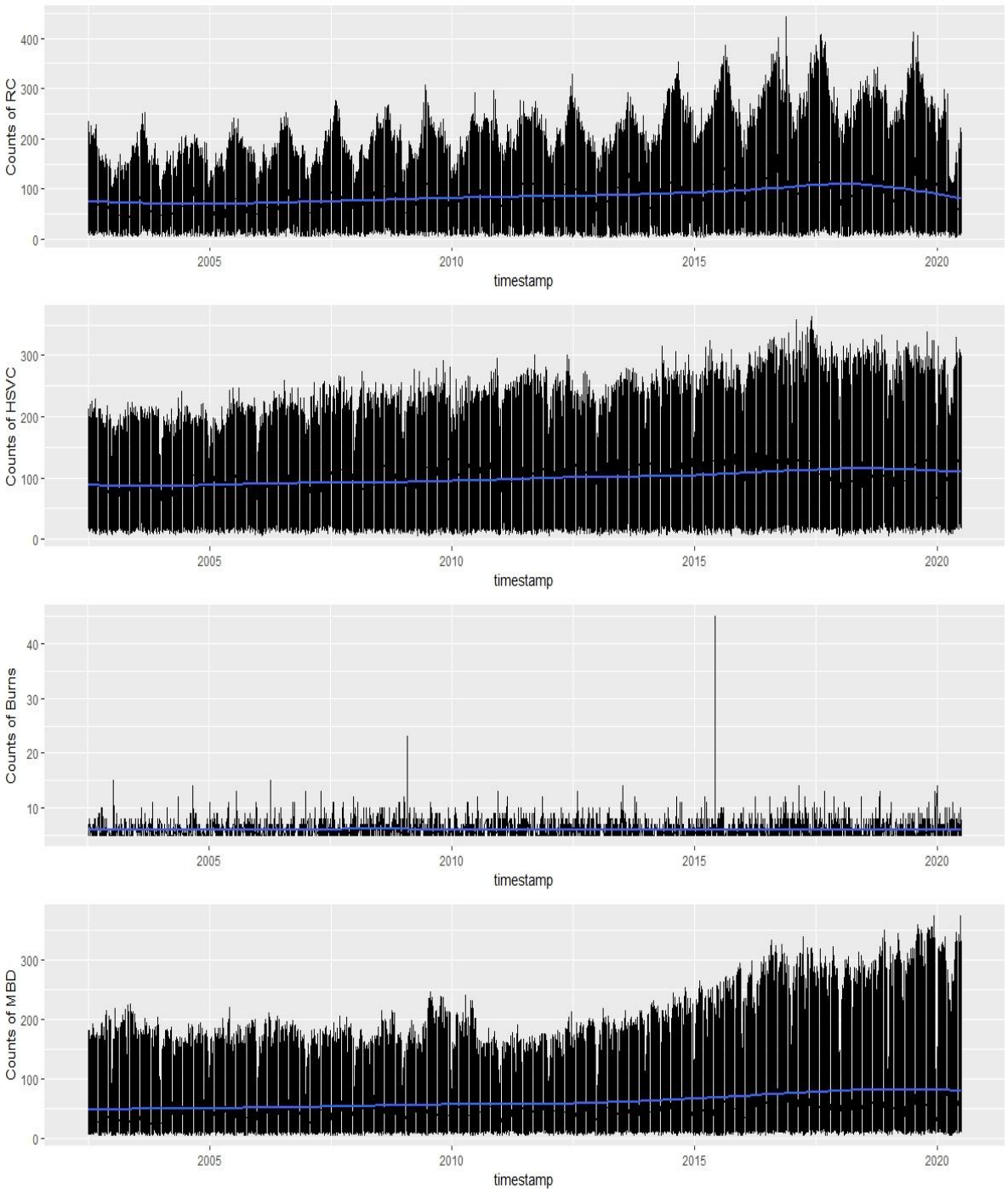

Figure A12 Time-series plots of inpatient admissions for the health conditions of interest

A.1.5 Respiratory conditions

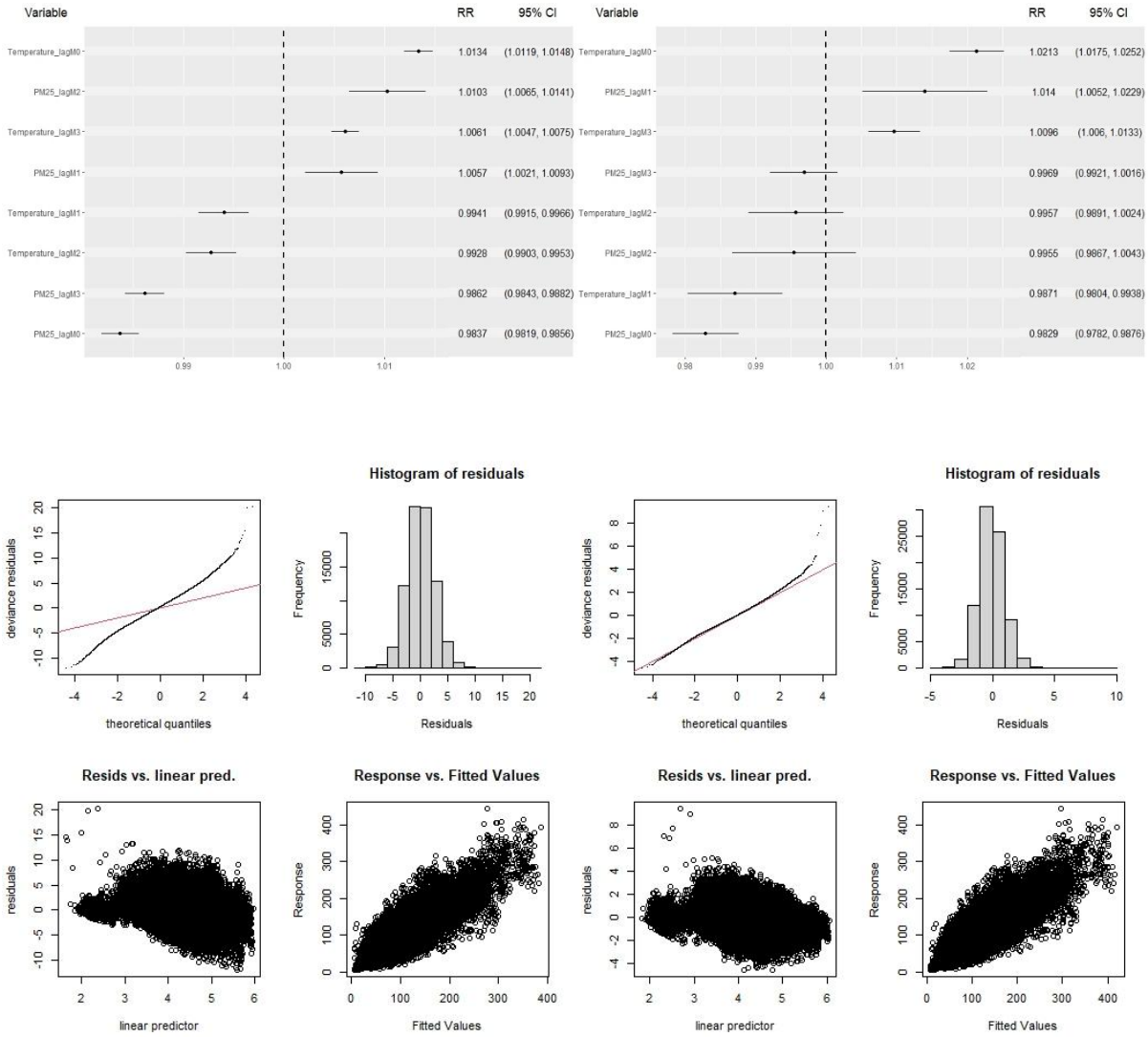

Figure A13 (Top) RR for inpatient admissions for Respiratory conditions and (Bottom) Diagnostic plots for Poisson GAM (left) and Negative binomial GAM (right)

A.1.6 Heart, stroke, and vascular conditions

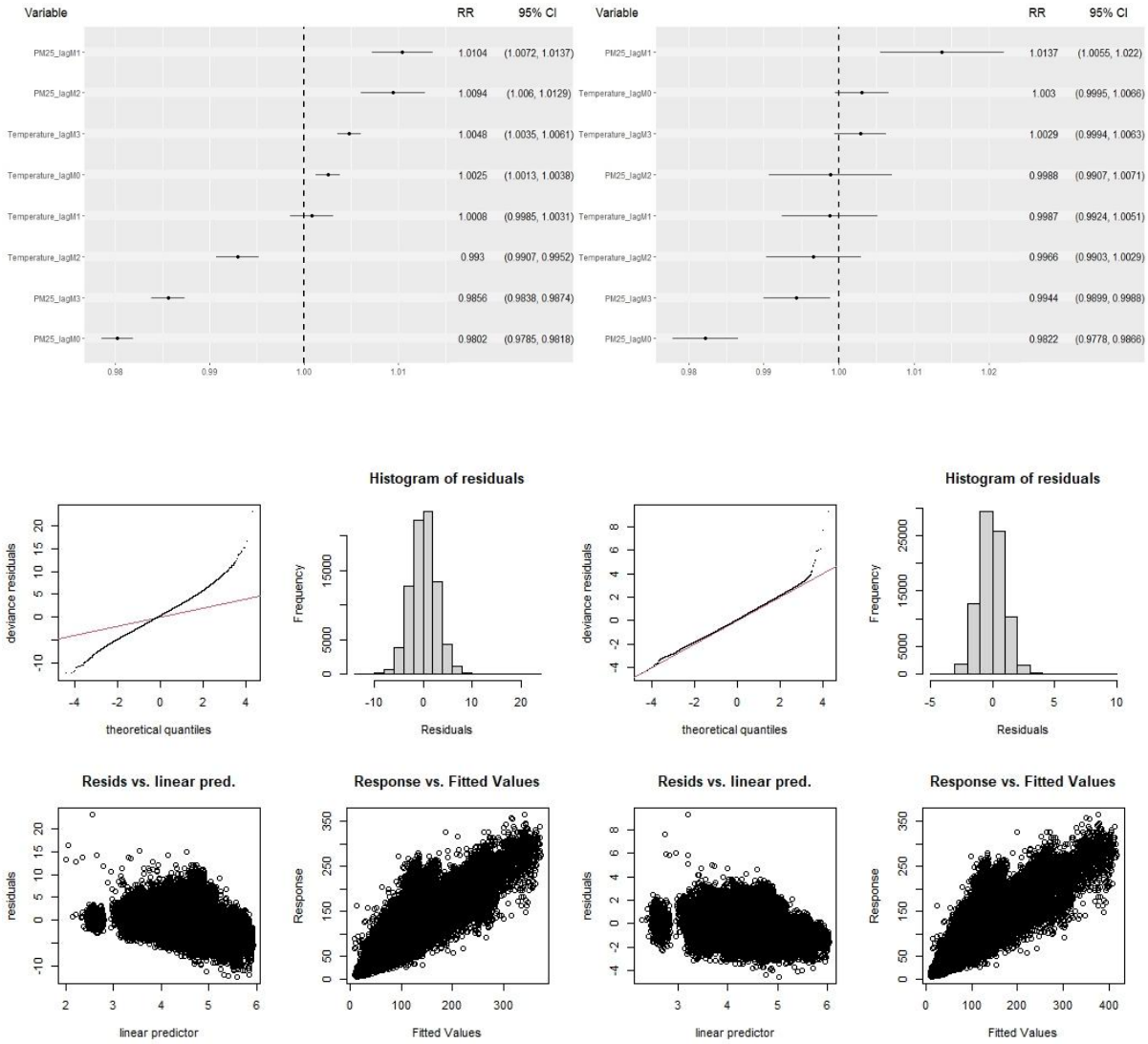

Figure A14 RR for inpatient admissions for Heart, Stroke, and Vascular conditions and (Bottom) Diagnostic plots for Poisson GAM (left) and Negative binomial GAM (right)

A.1.7 Mental and behavioural disorders

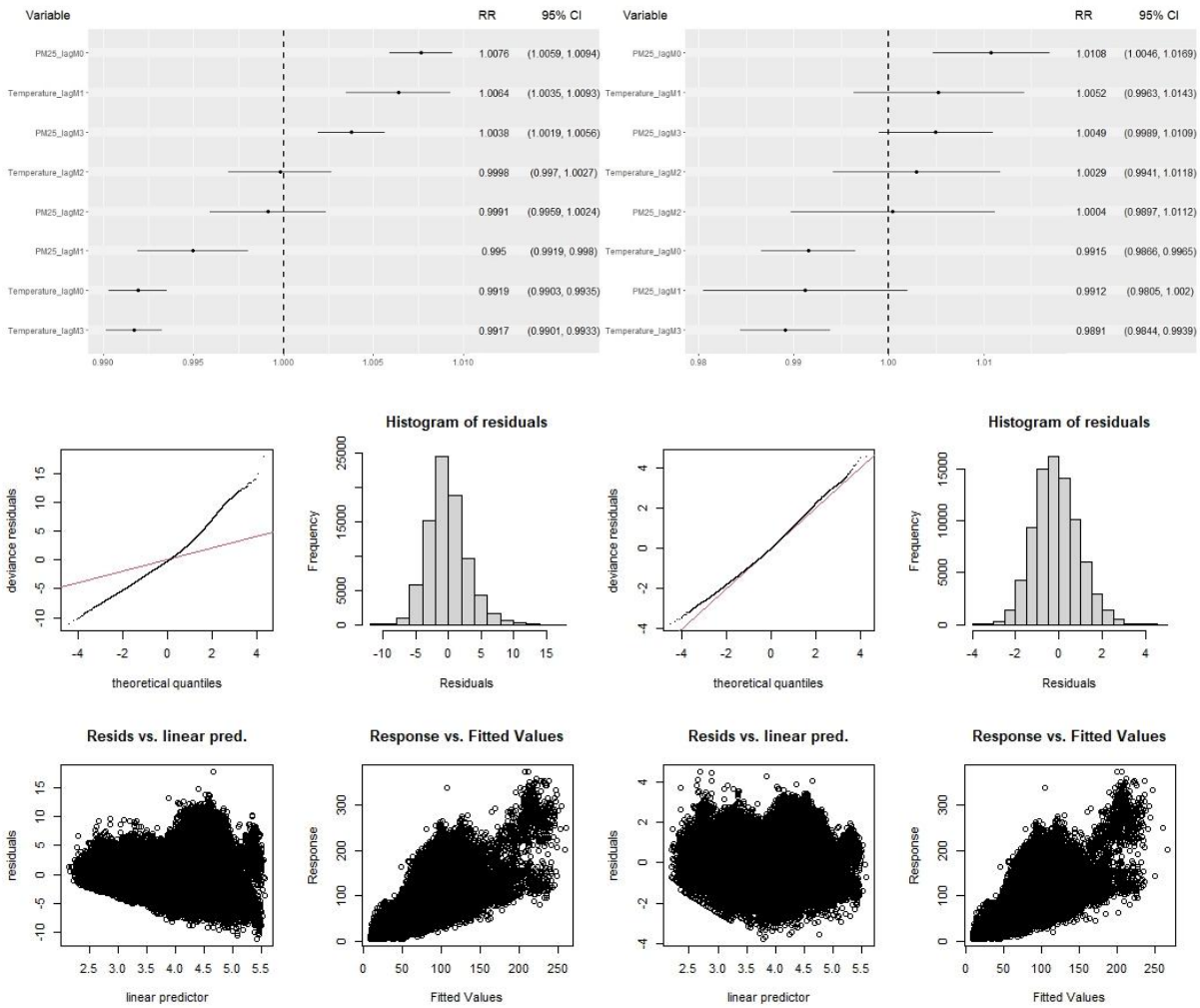

Figure A15 (Top) RR for inpatient admissions for Mental and behavioural disorders conditions and (Bottom) Diagnostic plots for Poisson GAM (left) and Negative binomial GAM (right)

A.1.8 Burns conditions

Note. Burn conditions were excluded from the analysis due to the limited sample size of 4624 cases over a 20-year period. The hospitalisation counts for burn cases varied between 5 to 45, and the proportions of burn cases across the SA4 regions were too small to allow for a reliable model fit. Hence, the inpatient admission data for burn conditions is not suitable for modelling the outcome of interest.

PBS

A.1.9 Time series plots of respiratory prescriptions, cardiovascular prescriptions, and mental health prescriptions

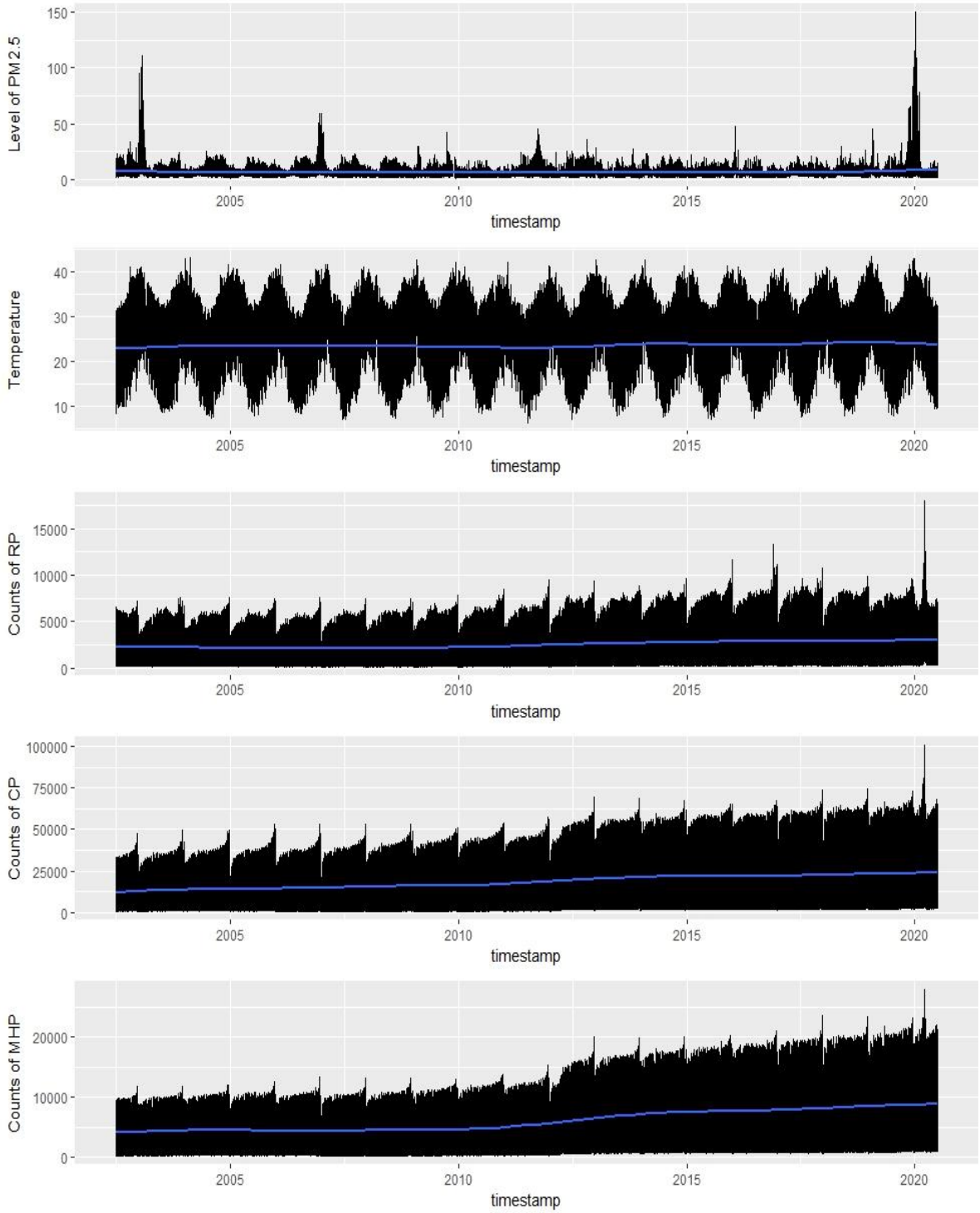

Figure A16 Time-series plots of outcomes of interest for PBS prescriptions

A.1.10 Respiratory prescriptions

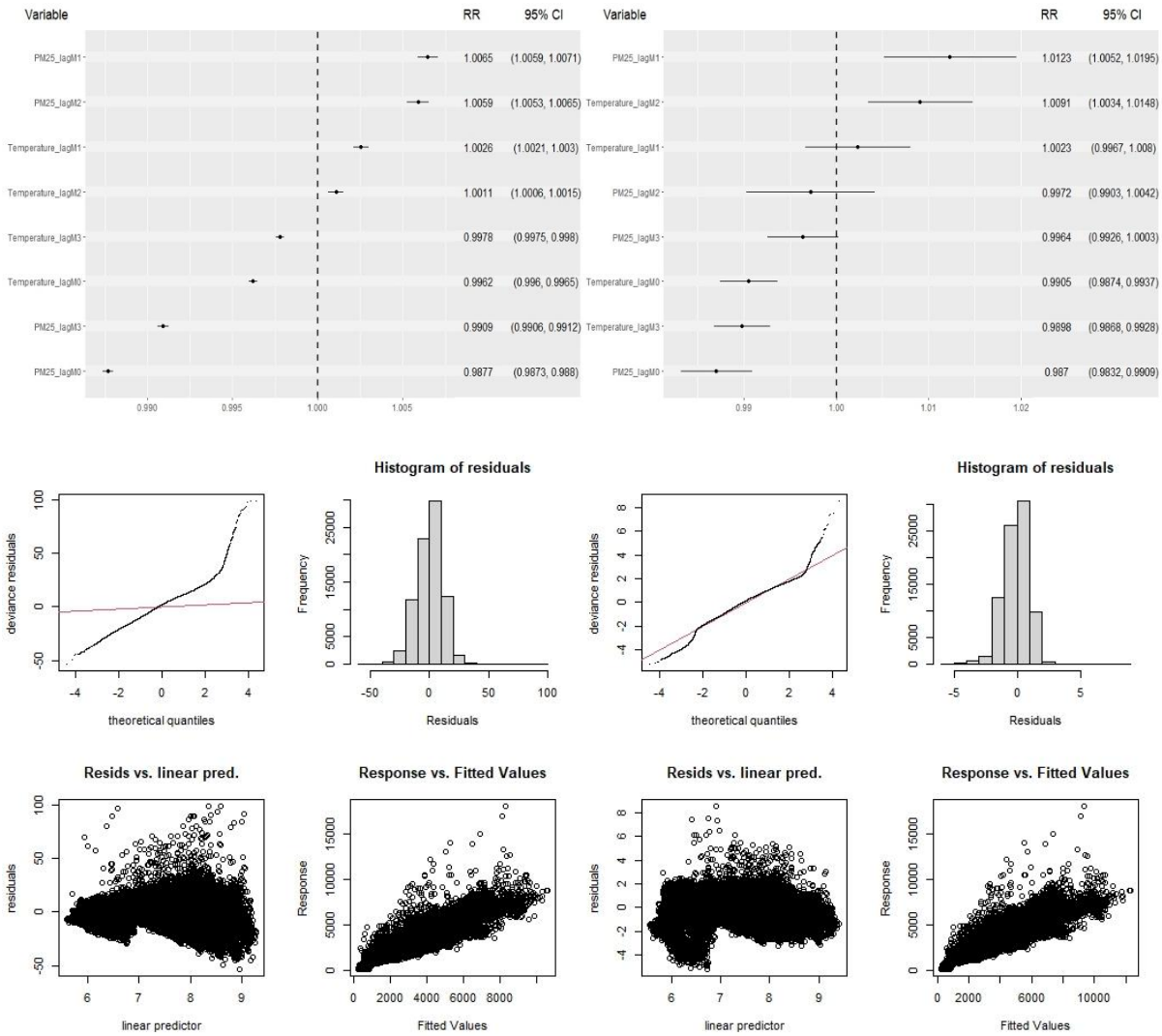

Figure A17 (Top) RR for Respiratory prescriptions and (Bottom) Diagnostic plots for Poisson GAM (left) and Negative binomial GAM (right)

A.1.11 Cardiovascular prescriptions

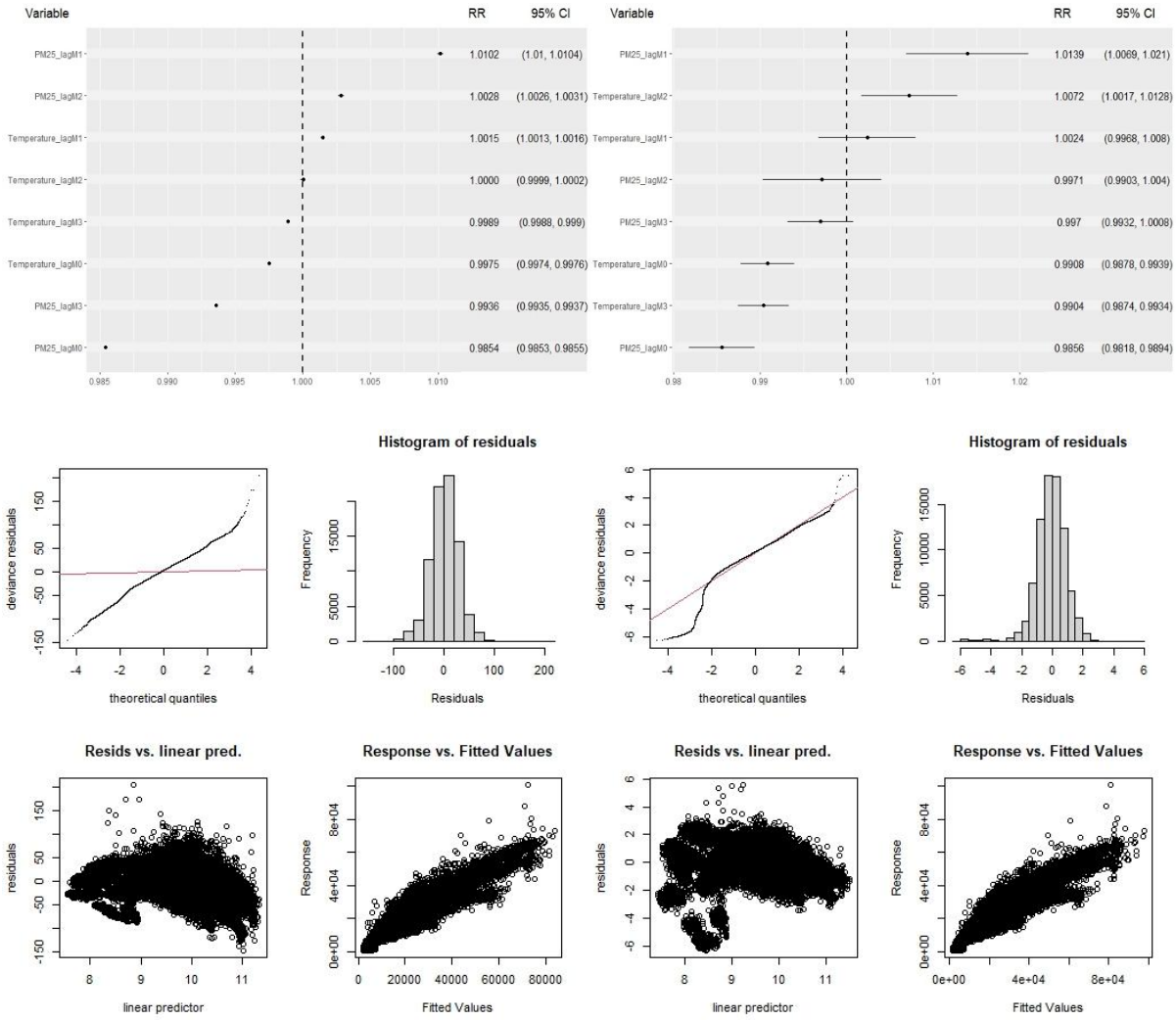

Figure A18 (Top) RR for Cardiovascular prescriptions and (Bottom) Diagnostic plots for Poisson GAM (left) and Negative binomial GAM (right)

A.1.12 Mental health prescriptions

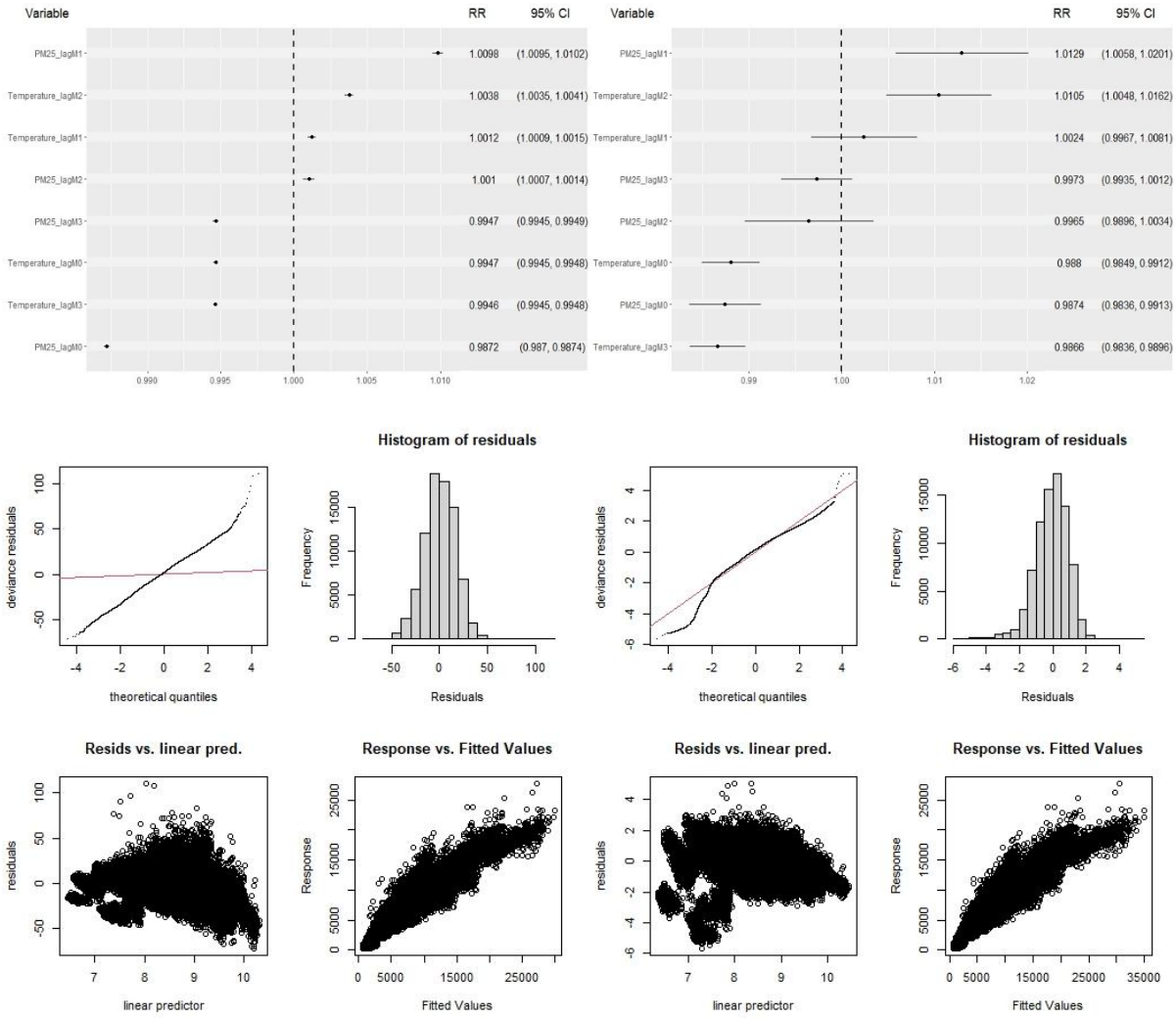

Figure A 19 (Top) RR for Mental health prescriptions and (Bottom) diagnostic plots for Poisson GAM (left) and Negative binomial GAM (right)

MBS

A.1.13 Time series plots of respiratory test items, cardiovascular diagnostic imaging services, cardiovascular diagnostic procedures and investigations, asthma cycle of care items, and Mental health services items.

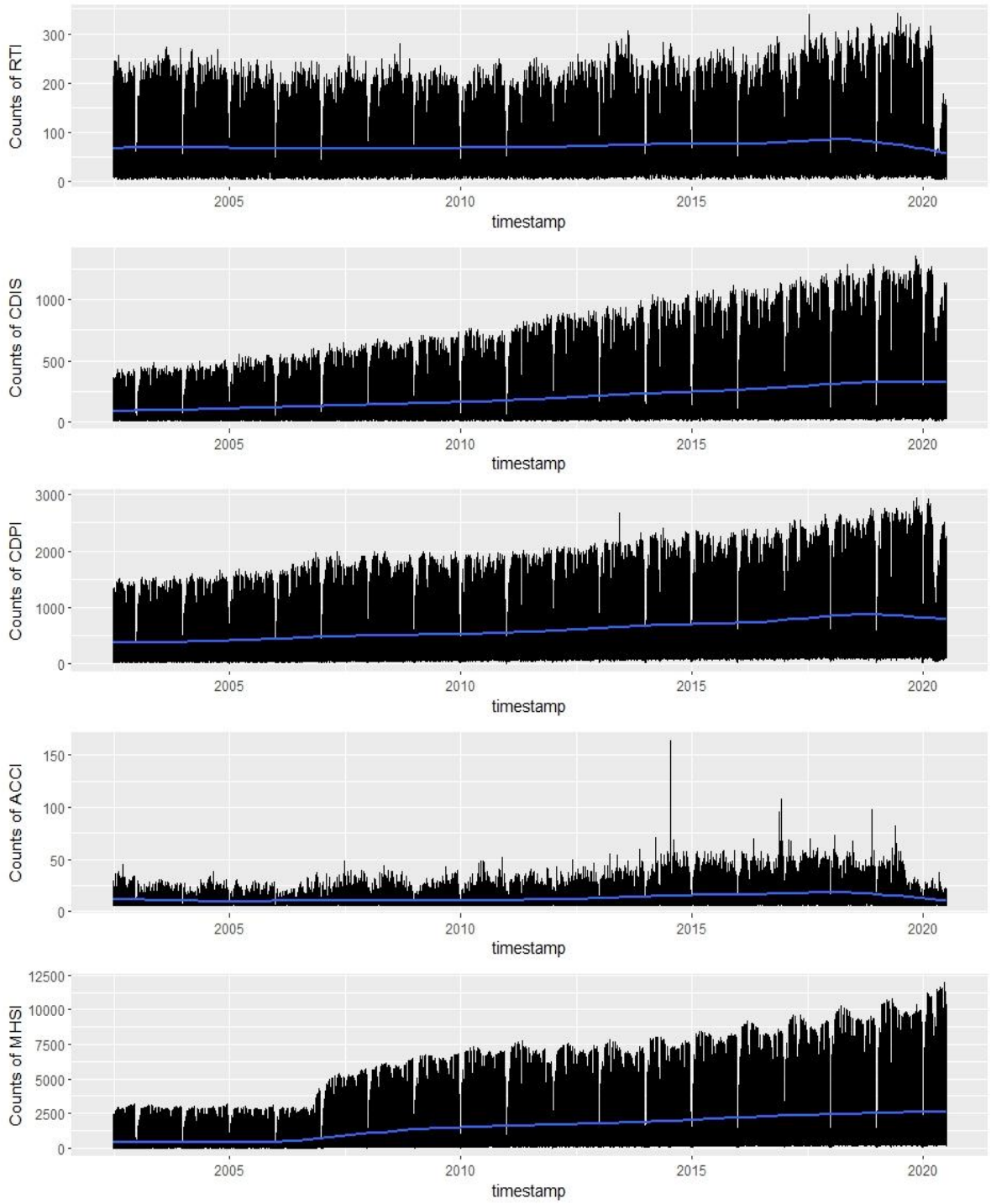

Figure A20 Time-series plots of outcomes of interest for MBS services

A.1.14 Respiratory test items

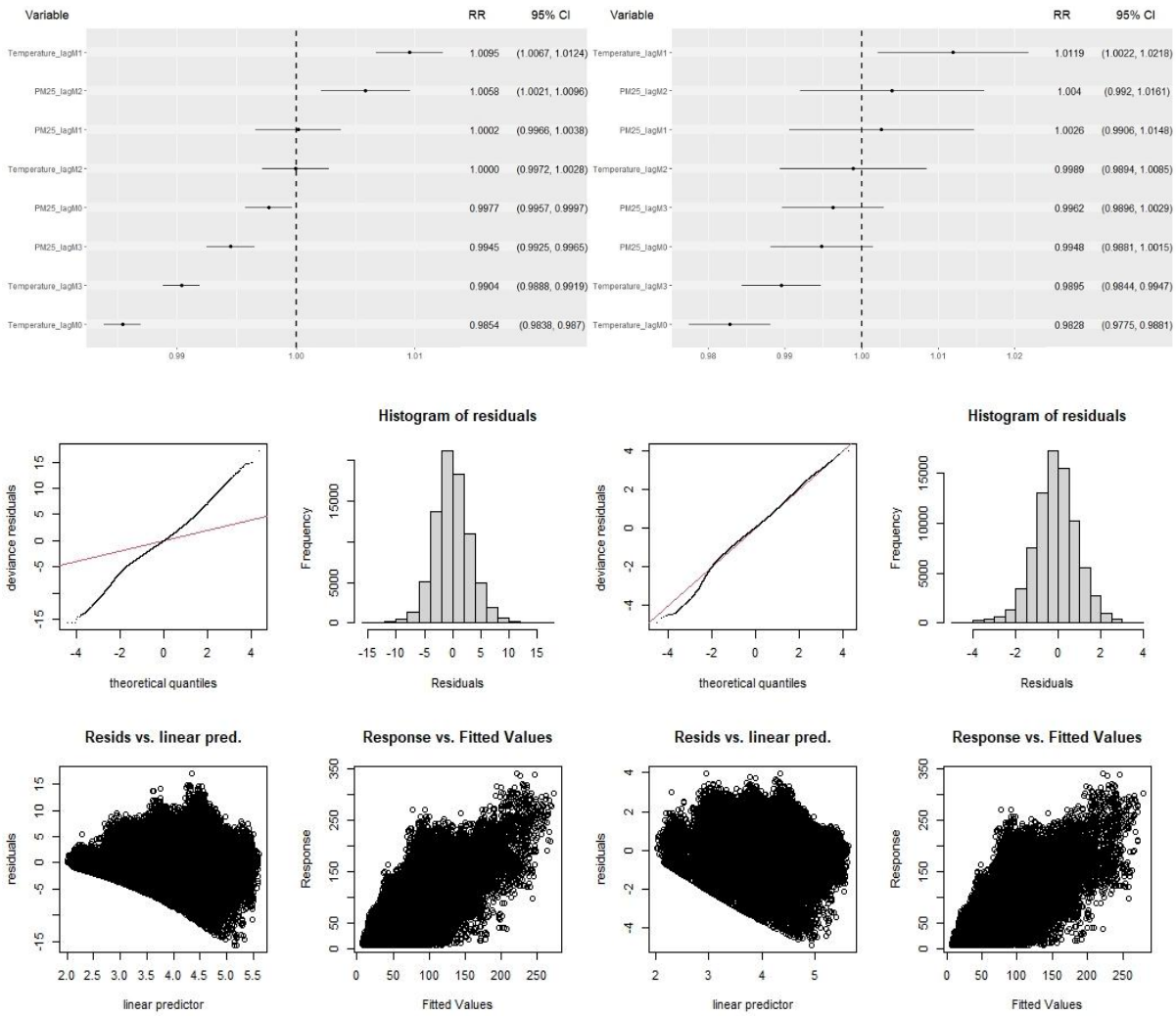

Figure A21 (Top) RR for MBS Respiratory test items and (Bottom) Diagnostic plots for Poisson GAM (left) and Negative binomial GAM (right)

A.1.15 Cardiovascular diagnostic imaging services

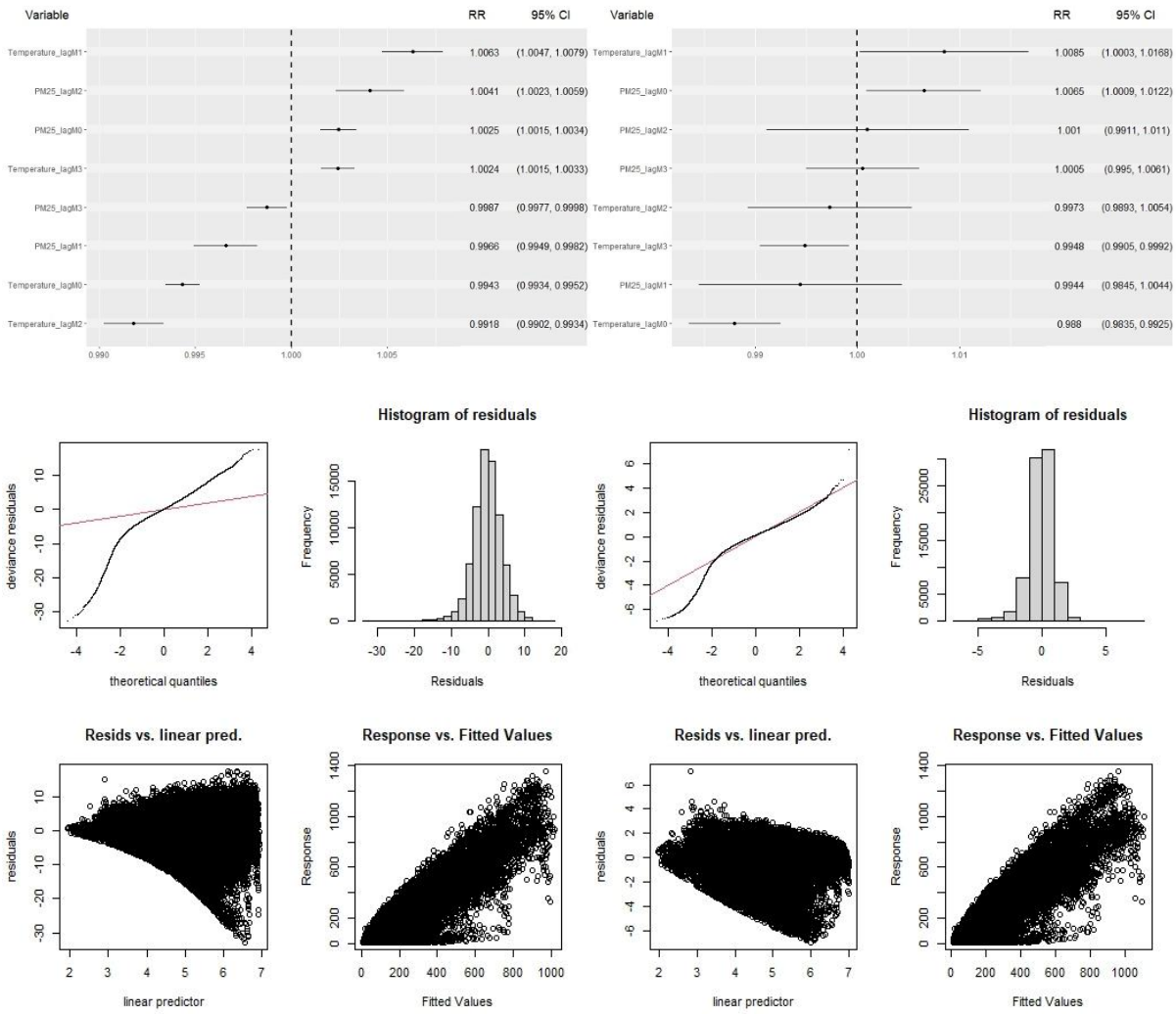

Figure A22 (Top) RR for MBS Cardiovascular diagnostic imaging services and (Bottom) Diagnostic plots for Poisson GAM (left) and Negative binomial GAM (right)

A.1.16 Cardiovascular diagnostic procedures and investigations

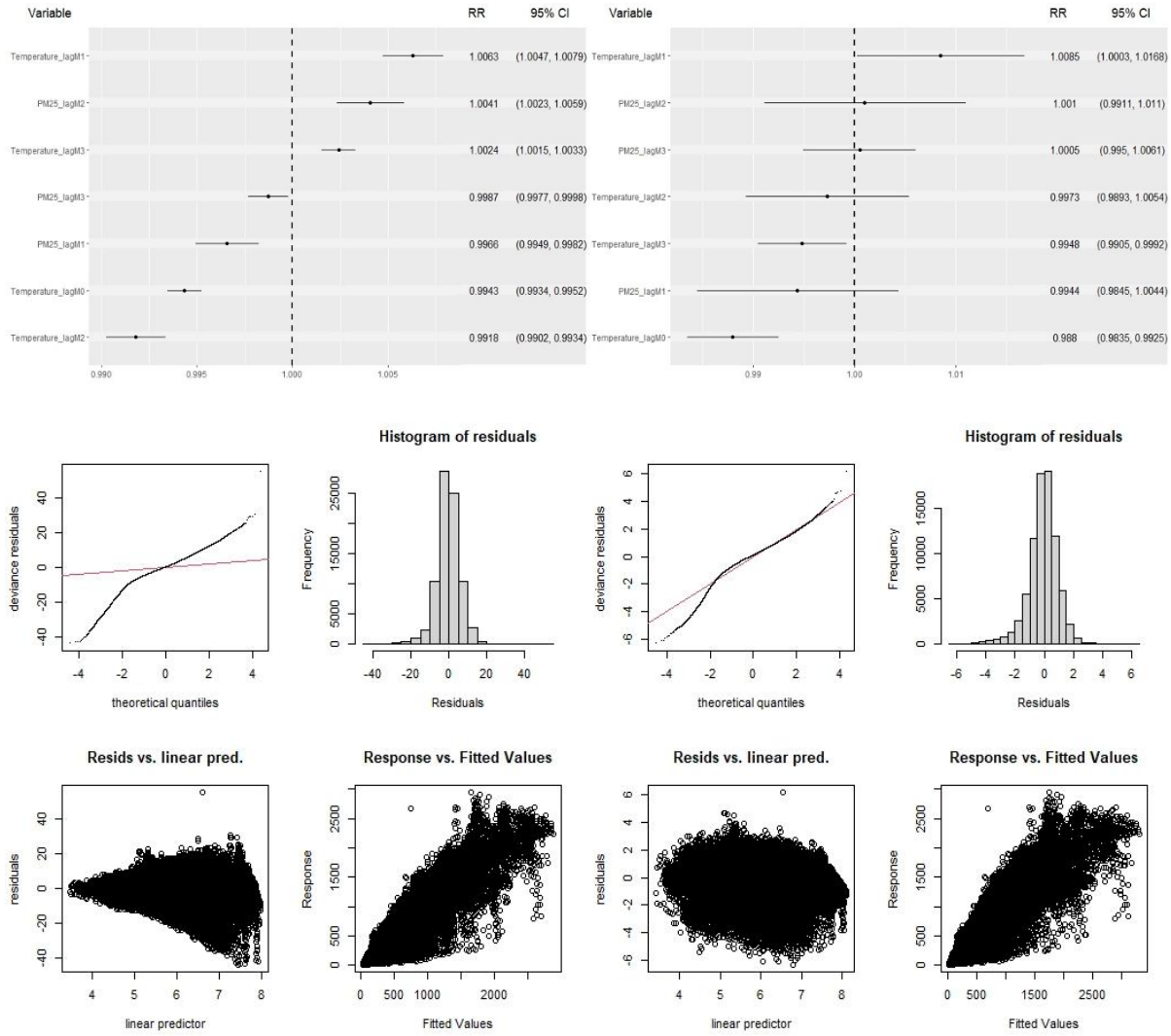

Figure A23 (Top) RR for MBS Cardiovascular diagnostic procedures and investigations and (Bottom) Diagnostic plots for Poisson GAM (left) and Negative binomial GAM (right)

A.1.17 Asthma cycle of care items

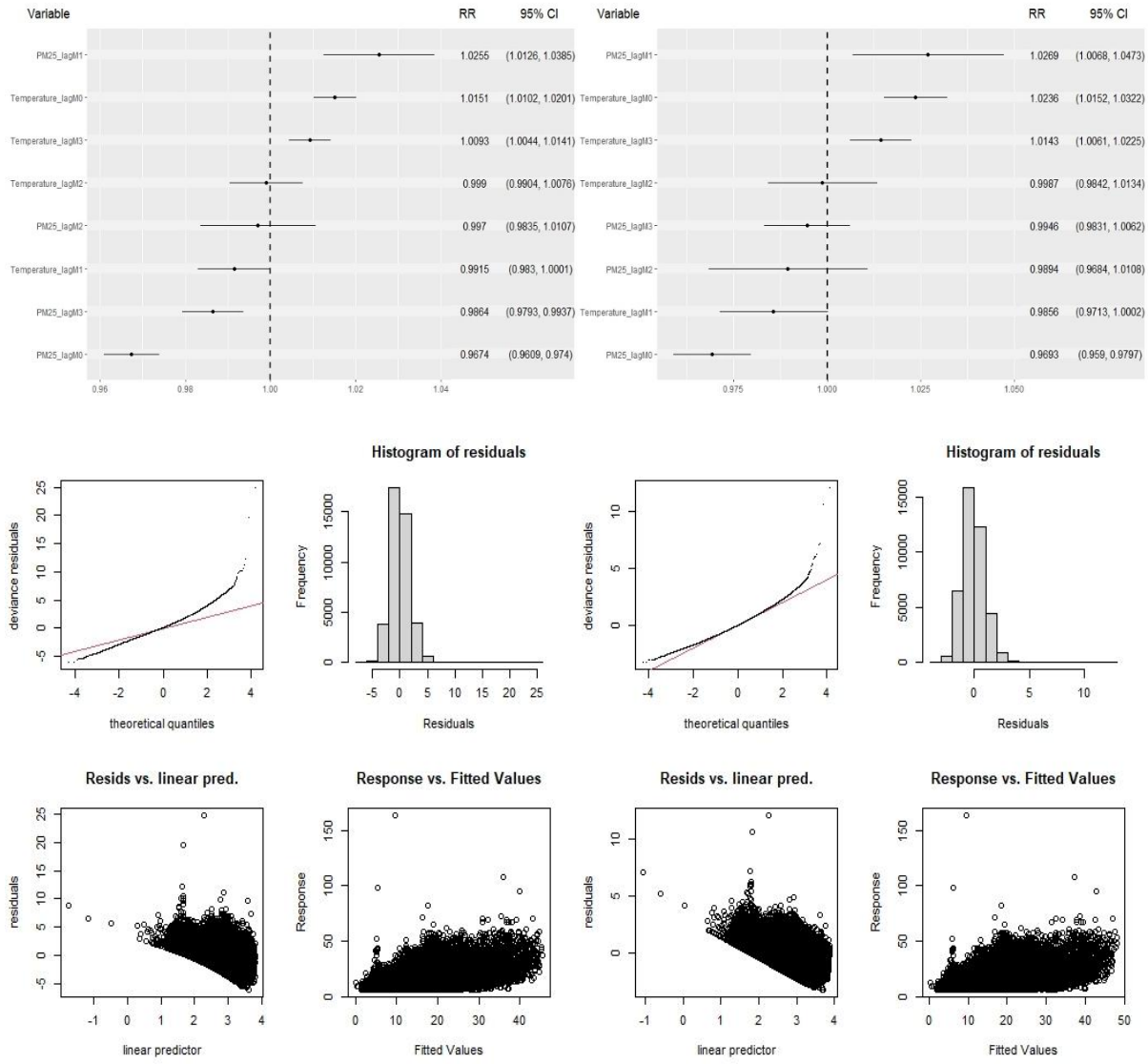

Figure A24 (Top) RR for MBS Asthma cycle of care items and (Bottom) Diagnostic plots for Poisson GAM (left) and Negative binomial GAM (right)

A.1.18 Mental health services items

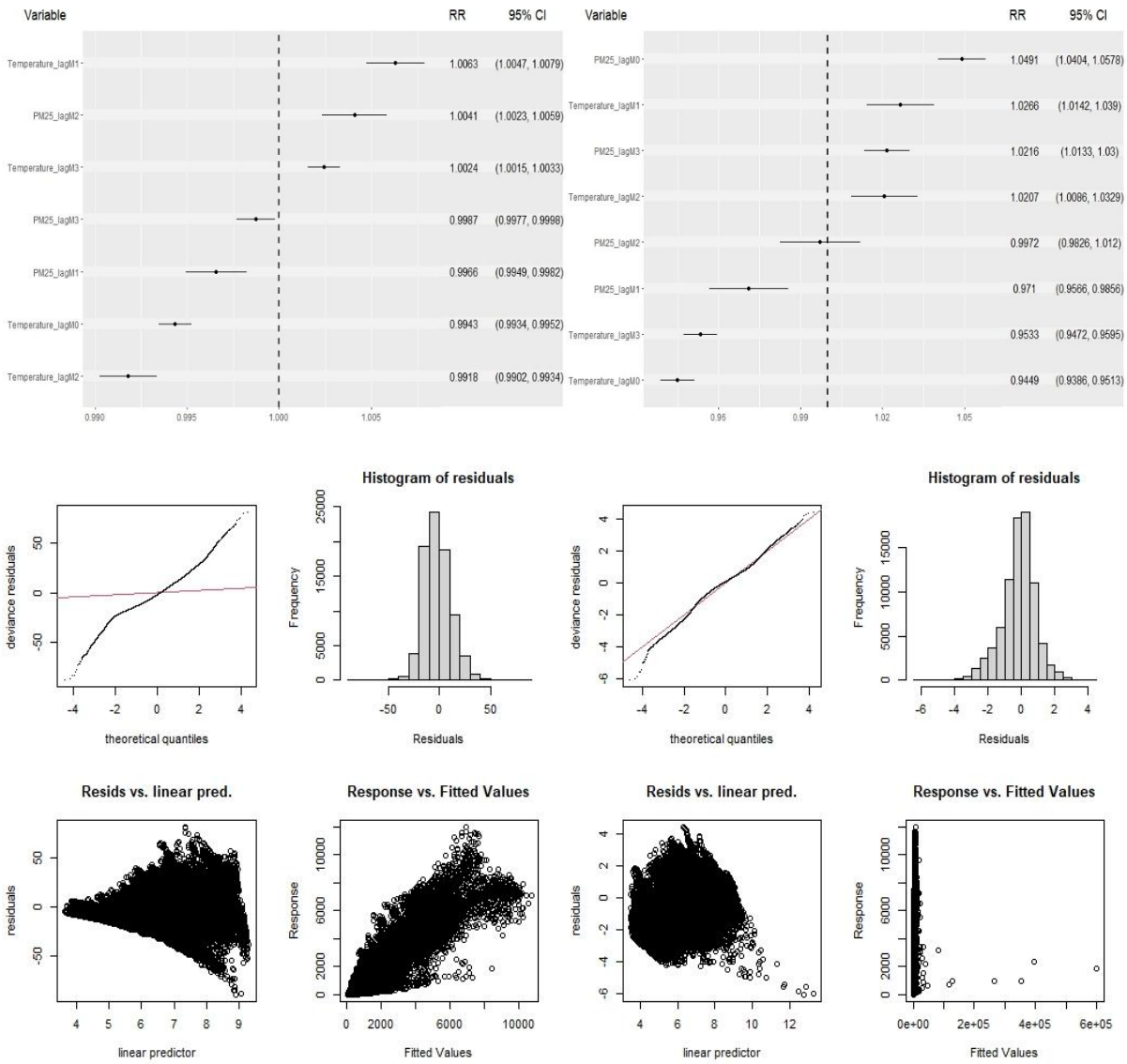

Figure A25 (Top) RR for MBS Mental health services items and (Bottom) Diagnostic plots for Poisson GAM (left) and Negative binomial GAM (right)

Appendix B Extended results for spillover risk proxies: Section 3.2

Spillover risk proxy: potential zoonotic virus density

Figure B1 Potential zoonotic virus density predictions under different climate models and scenarios

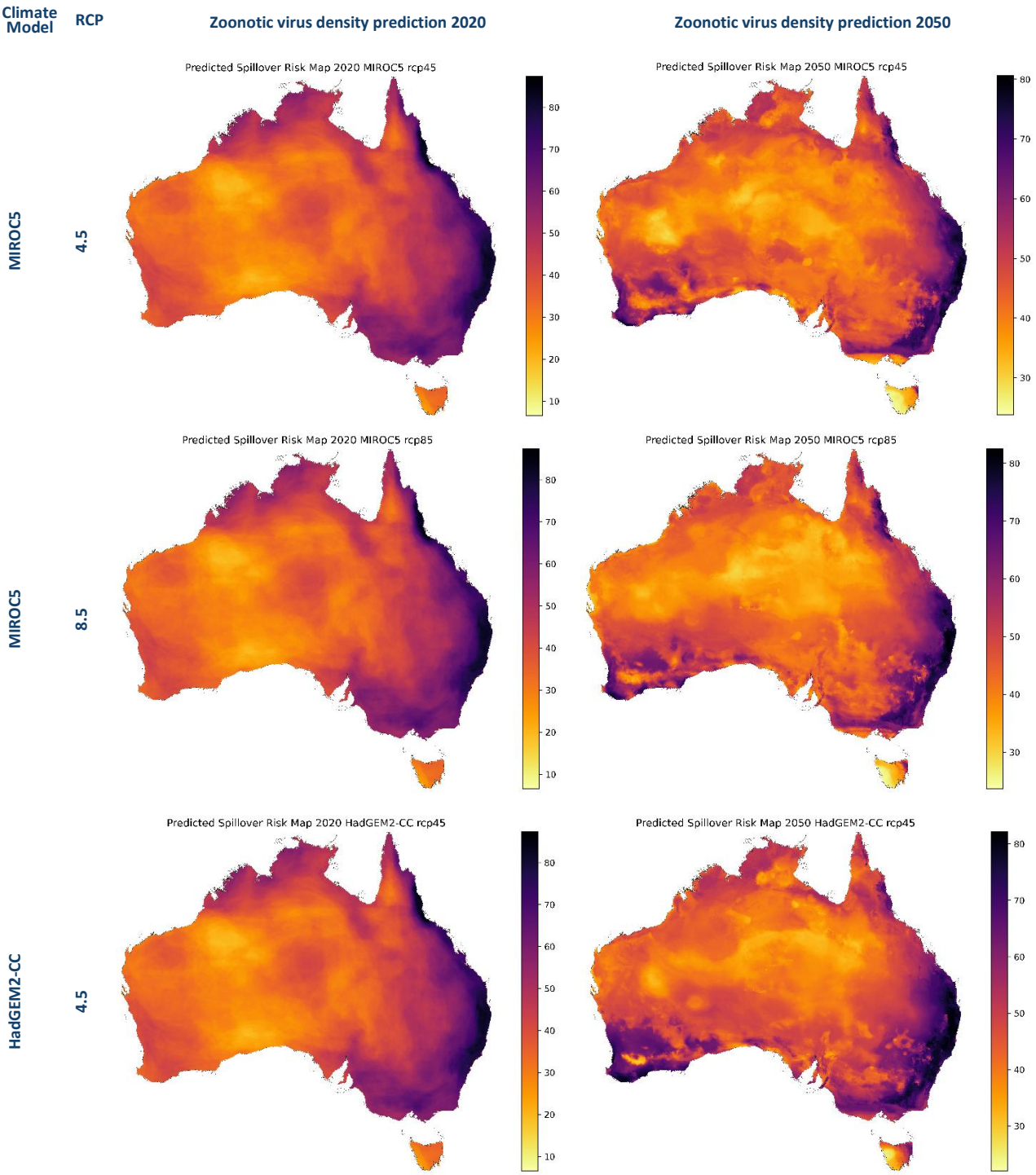

Climate Model	RCP	Zoonotic virus density prediction 2020	Zoonotic virus density prediction 2050
HadGEM2-CC	8.5	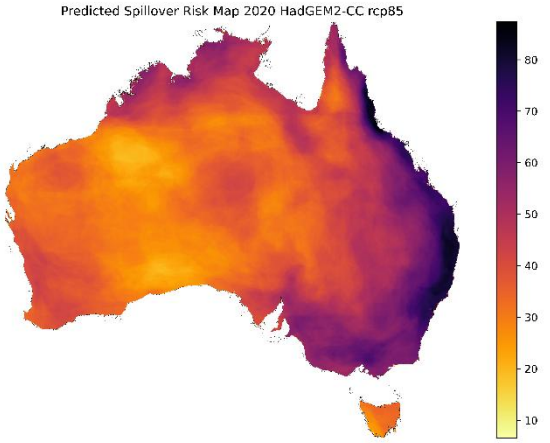	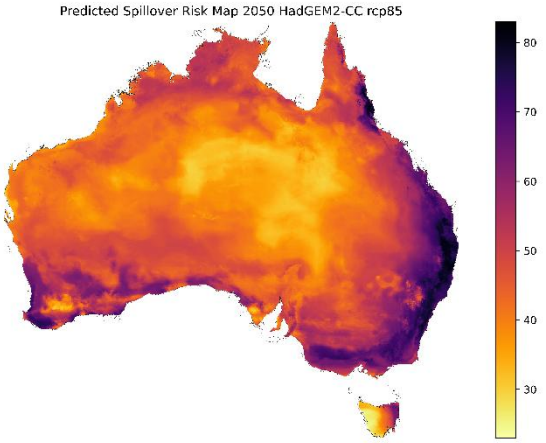
GFDL-ESM2M	4.5	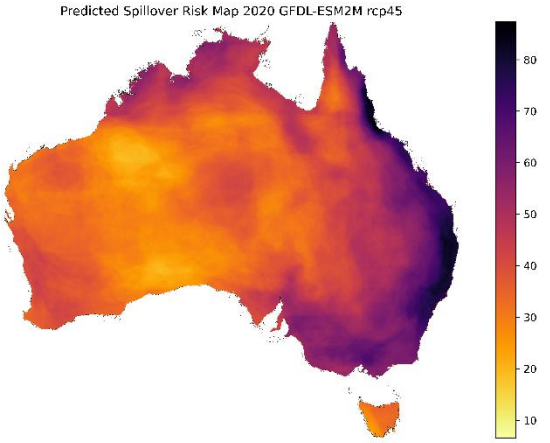	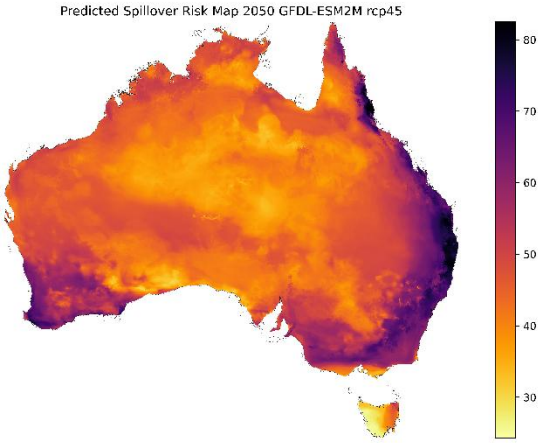
GFDL-ESM2M	8.5	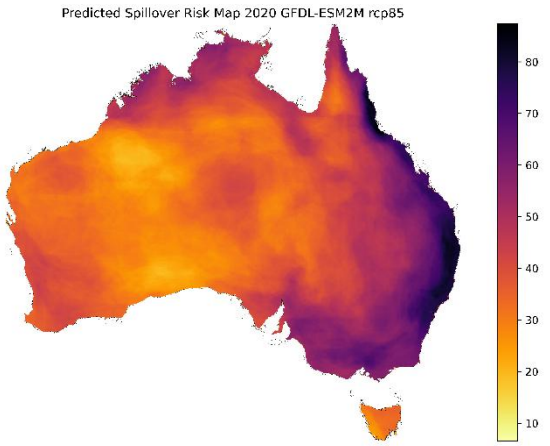	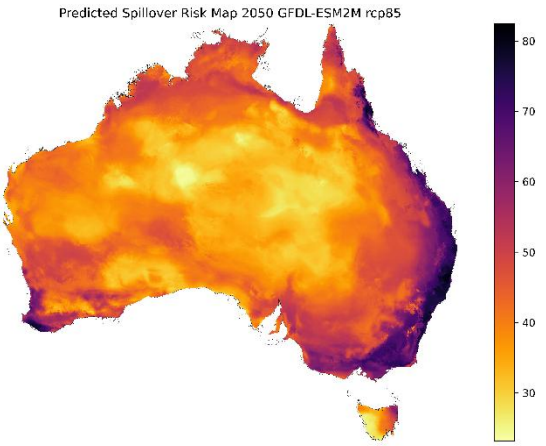
CanESM2	4.5	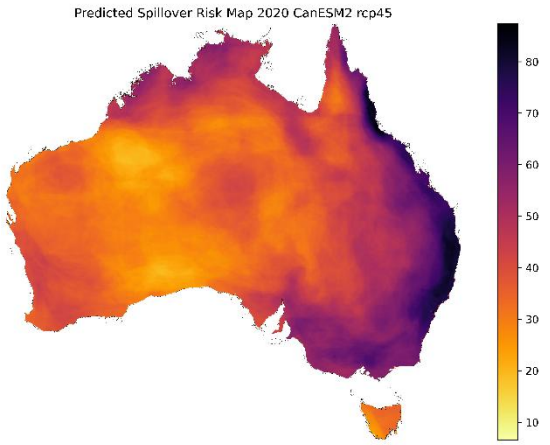	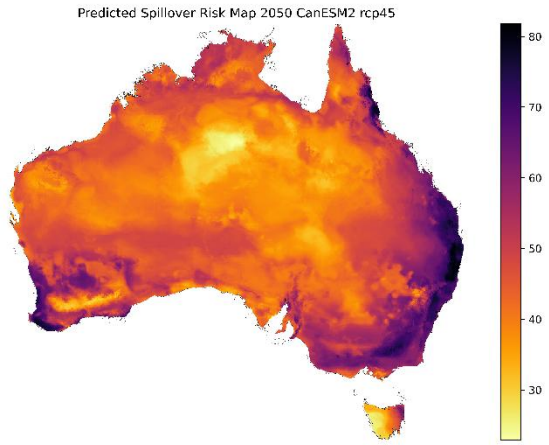

Climate Model	RCP	Zoonotic virus density prediction 2020	Zoonotic virus density prediction 2050
CanESM2	8.5	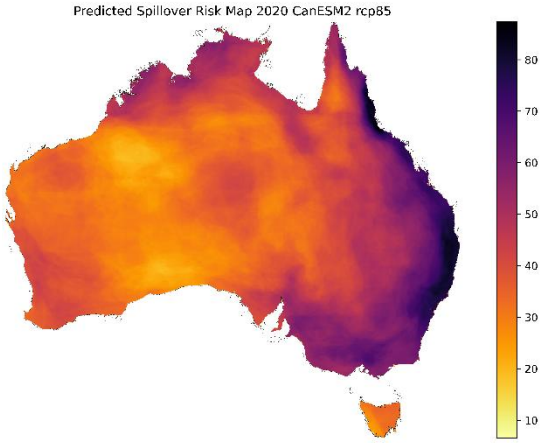	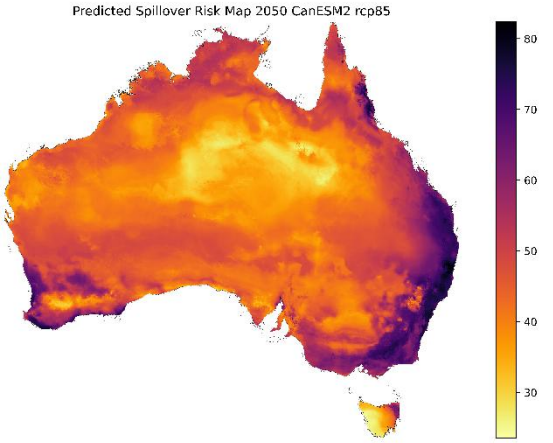
CNRM-CM5	4.5	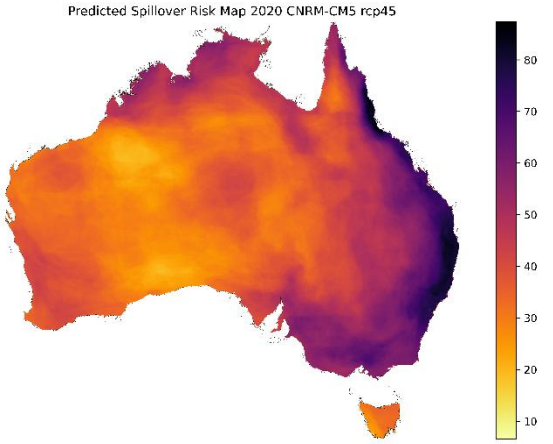	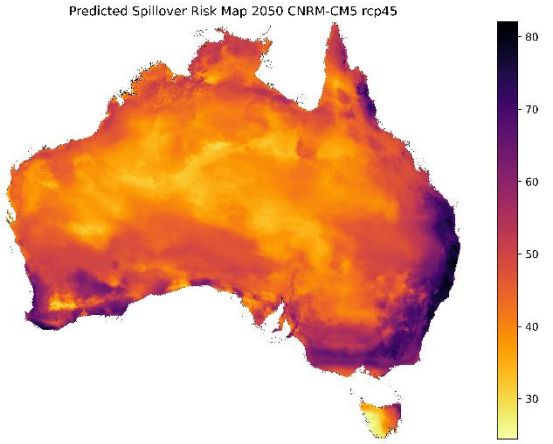
CNRM-CM5	8.5	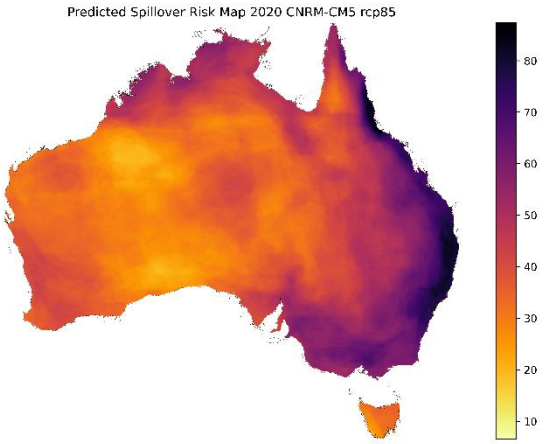	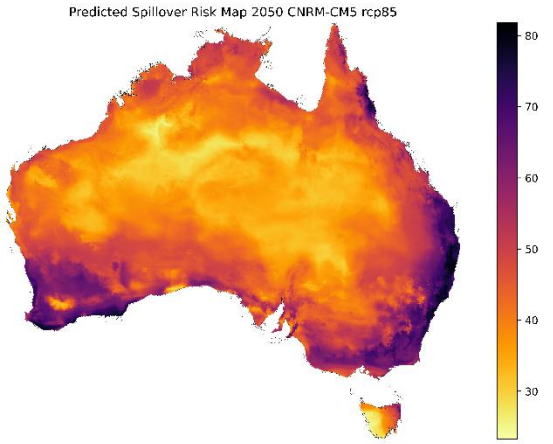
CESM1-CAM5	4.5	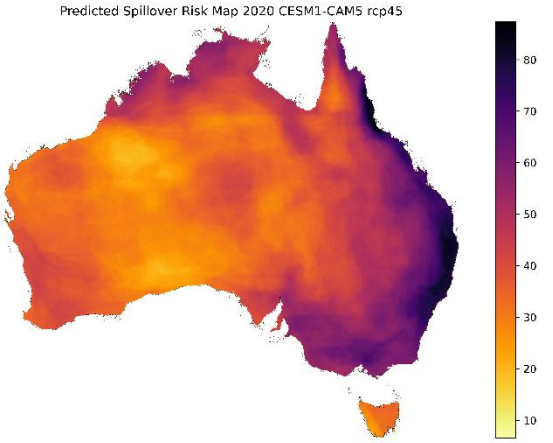	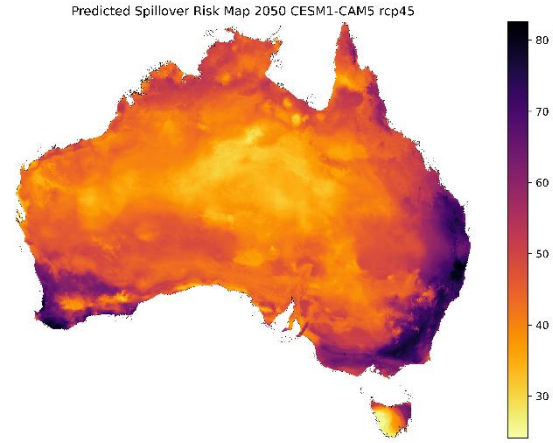

Climate Model	RCP	Zoonotic virus density prediction 2020	Zoonotic virus density prediction 2050
CESM1-CAM5	8.5	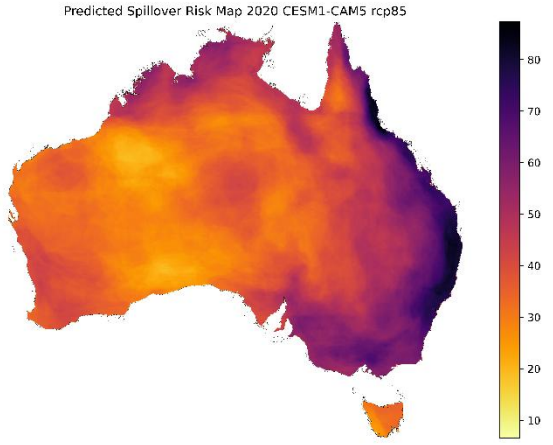	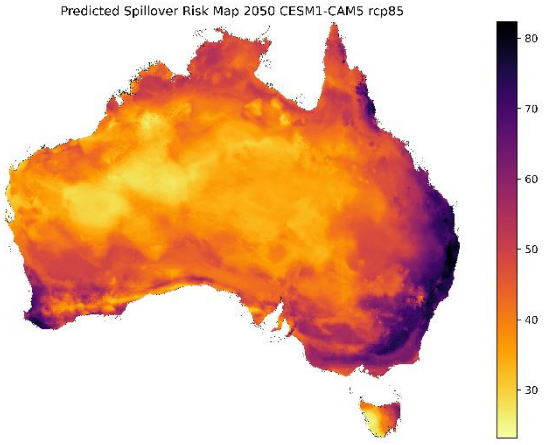
NorESM1-M	4.5	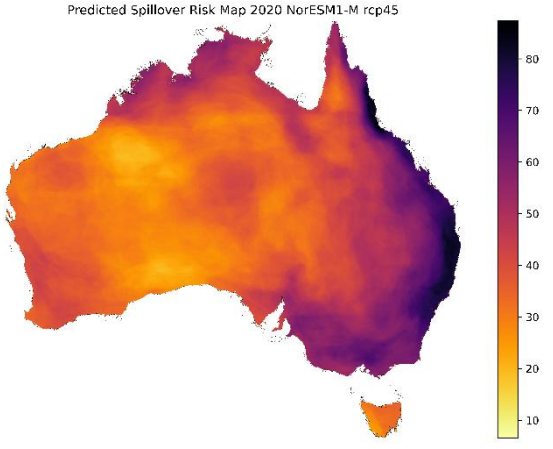	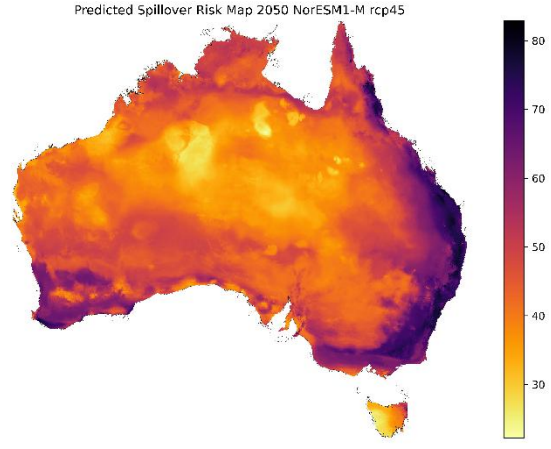
NorESM1-M	8.5	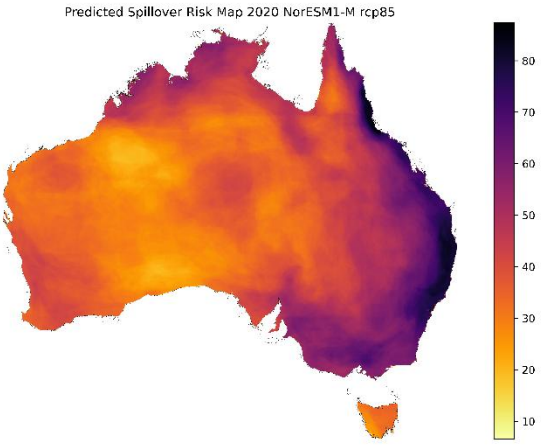	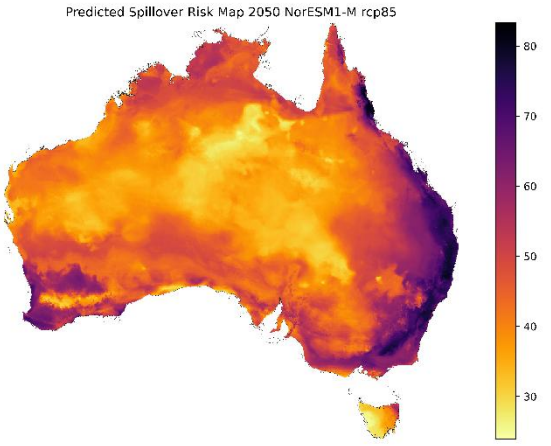
ACCESS1-0	4.5	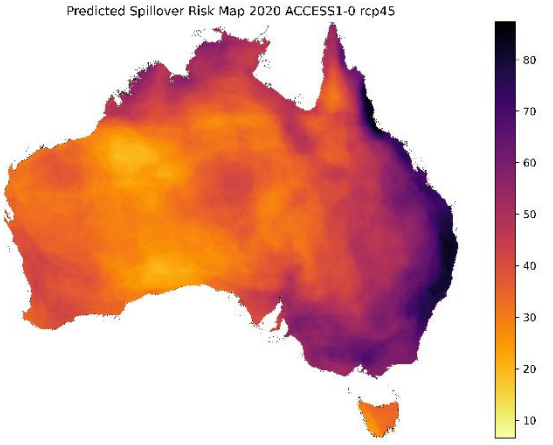	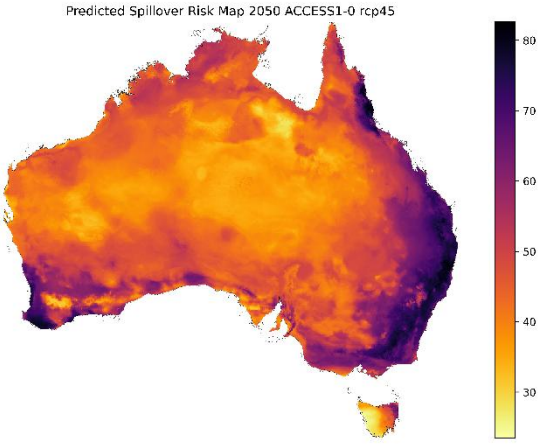

Climate Model	RCP	Zoonotic virus density prediction 2020	Zoonotic virus density prediction 2050
ACCESS1-0	8.5	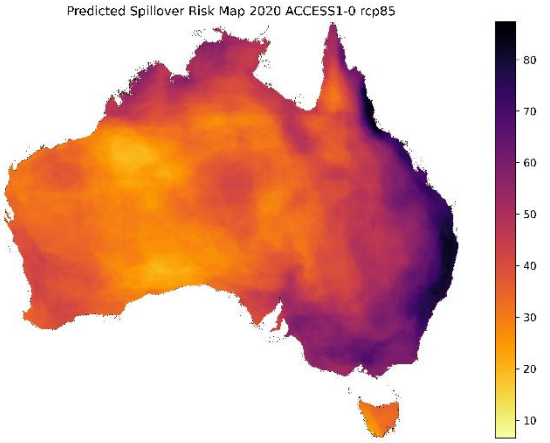	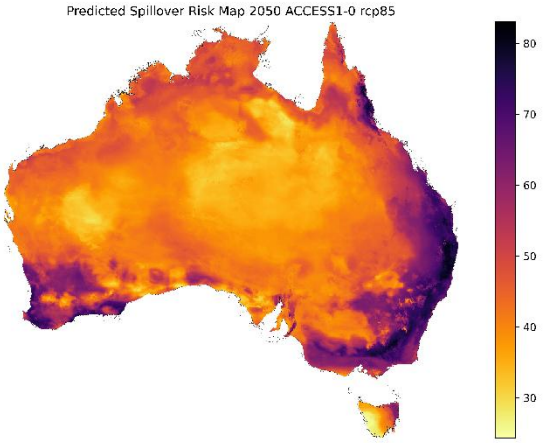

Figure B2 Climate models uncertainty analysis for the potential zoonotic virus density prediction

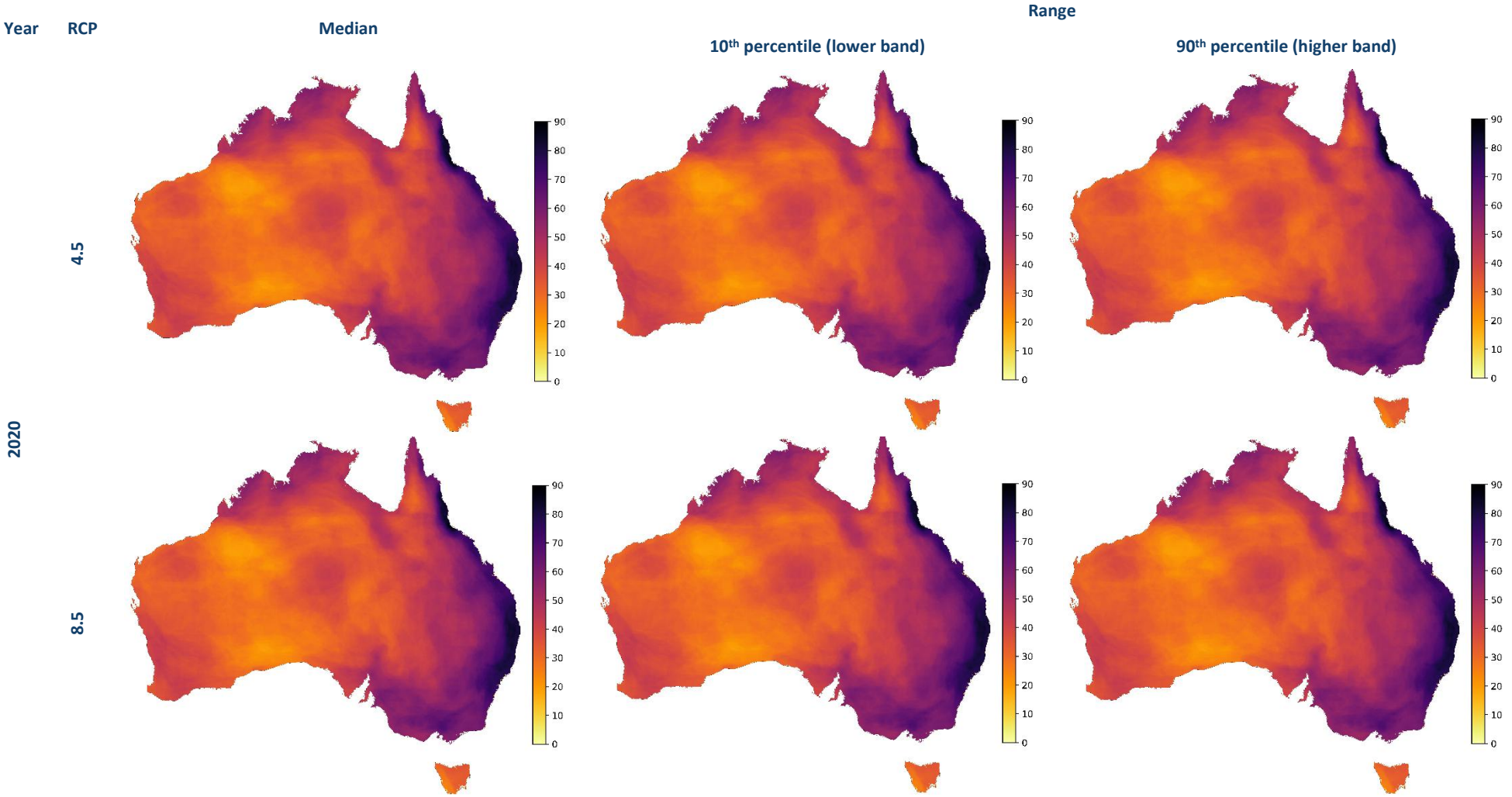

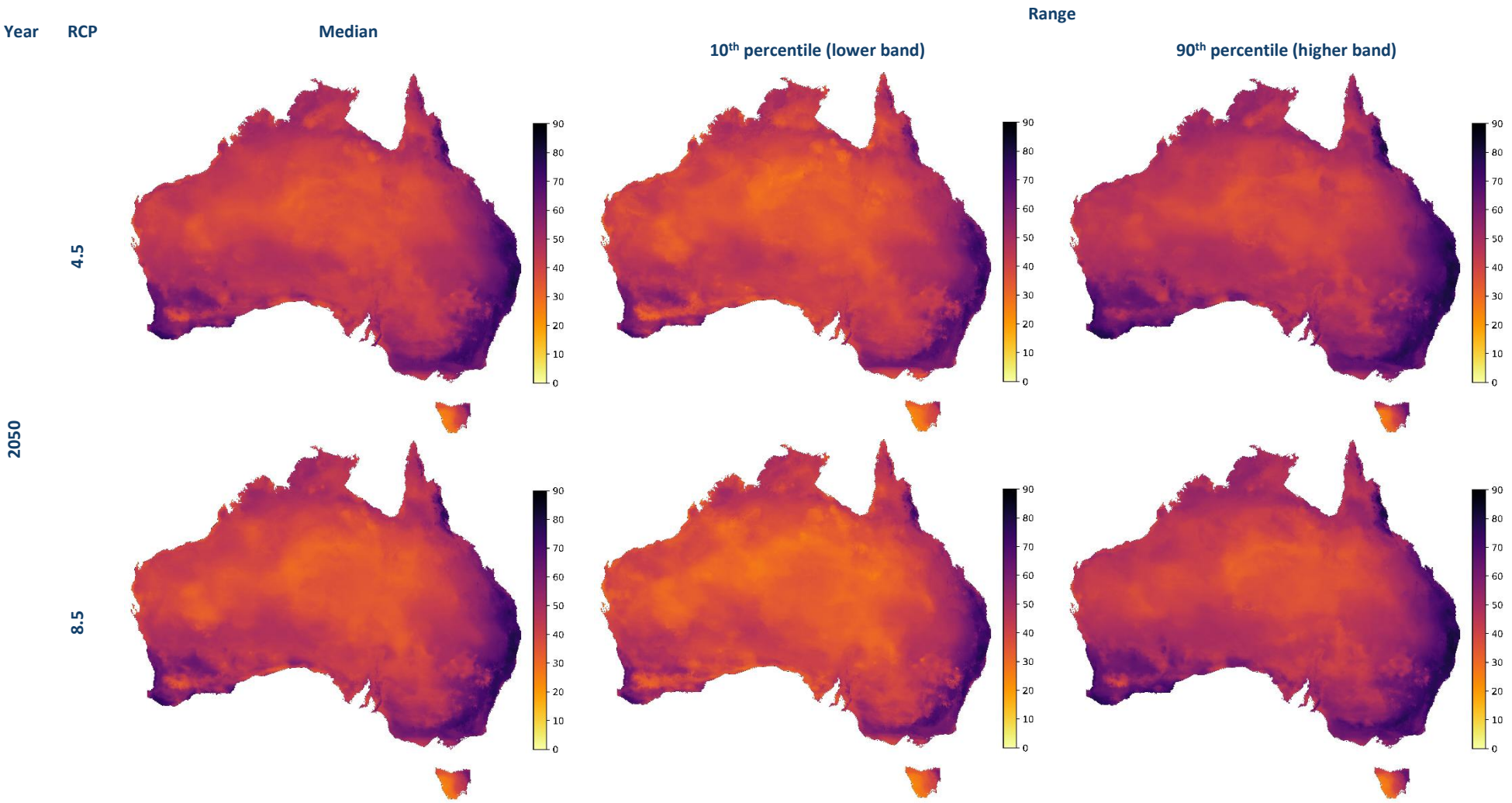
Year
RCP
Median
Range
10th percentile (lower band)
90th percentile (higher band)
2050
4.5
8.5
90
80
70
60
50
40
30
20
10
0

B.2 JEV risk proxy: (combined presence probabilities of species associated with the transmission of JEV)

Figure B3 Combined JEV species presence probability by scenario and period. Uncertainty in probabilities is captured by including the median (50th percentile) as well as the 10th and 90th percentile of model projections for every location.

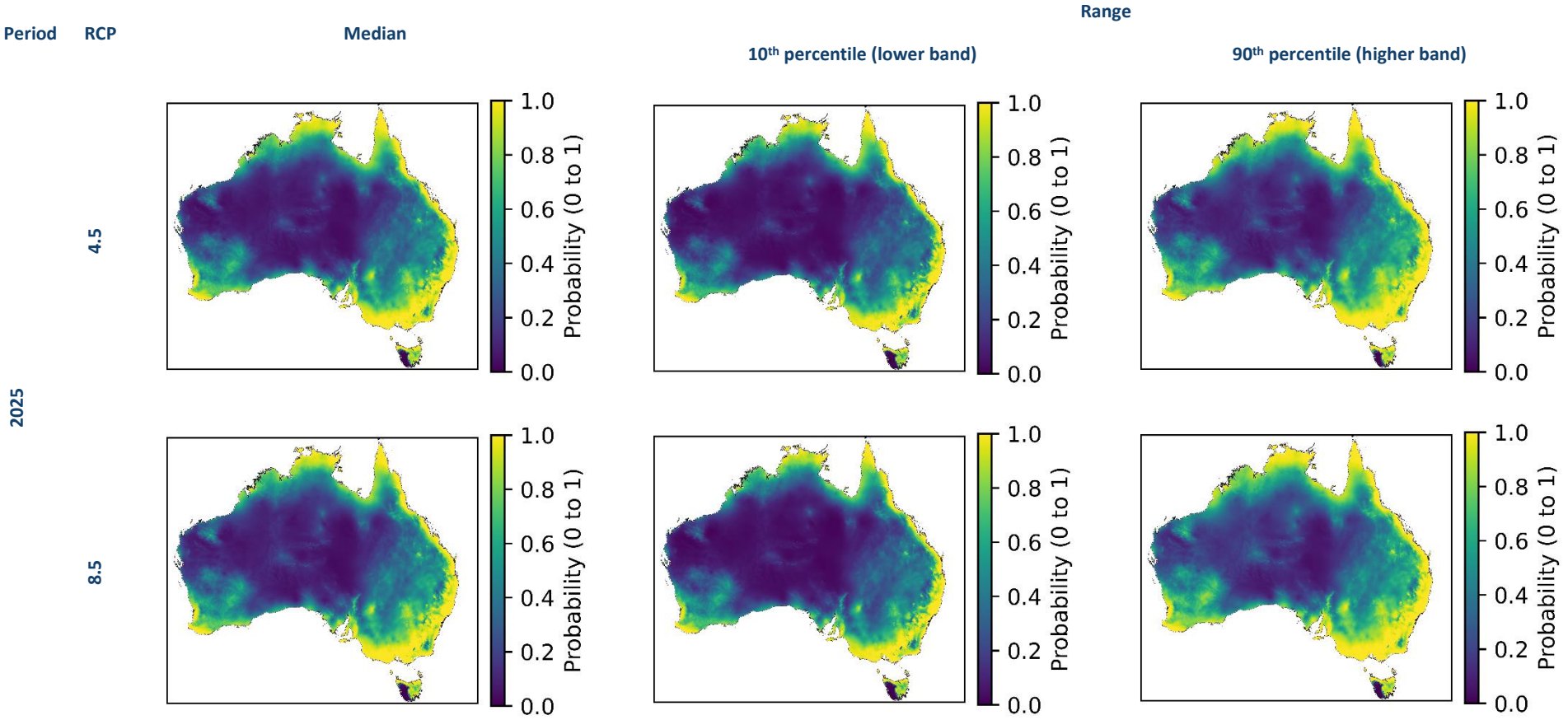

Period	RCP	Median	Range: 10th percentile (lower band)	Range: 90th percentile (higher band)
2050	4.5	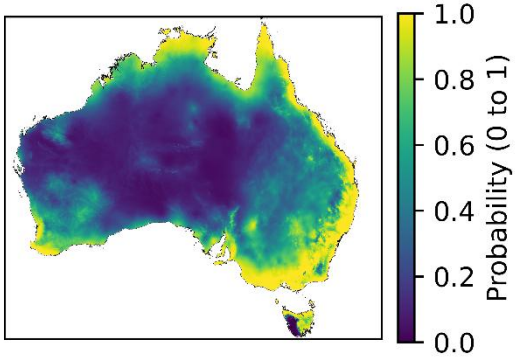	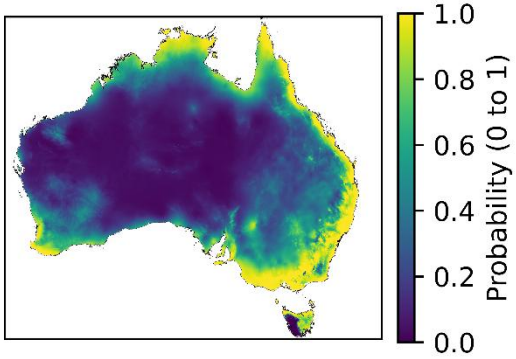	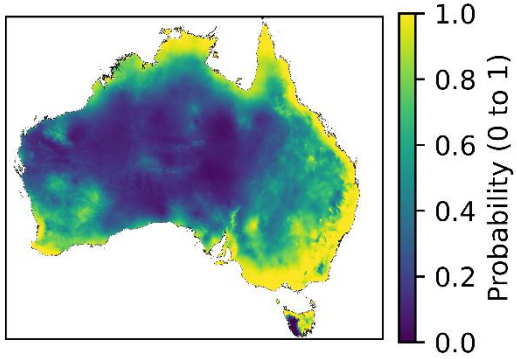
	8.5	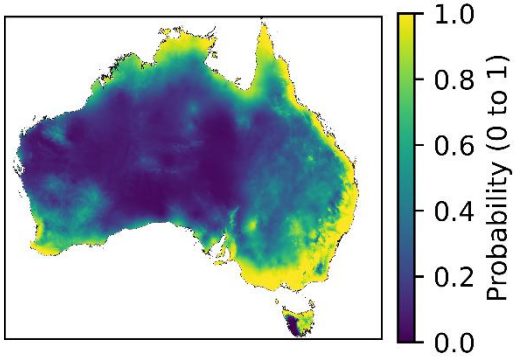	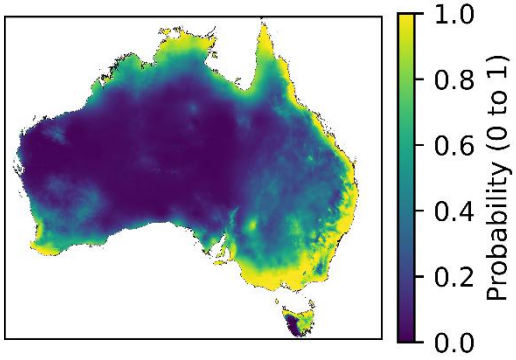	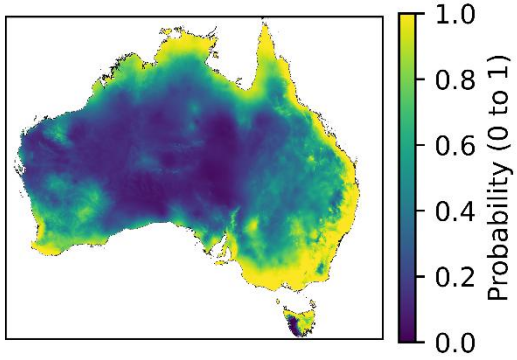

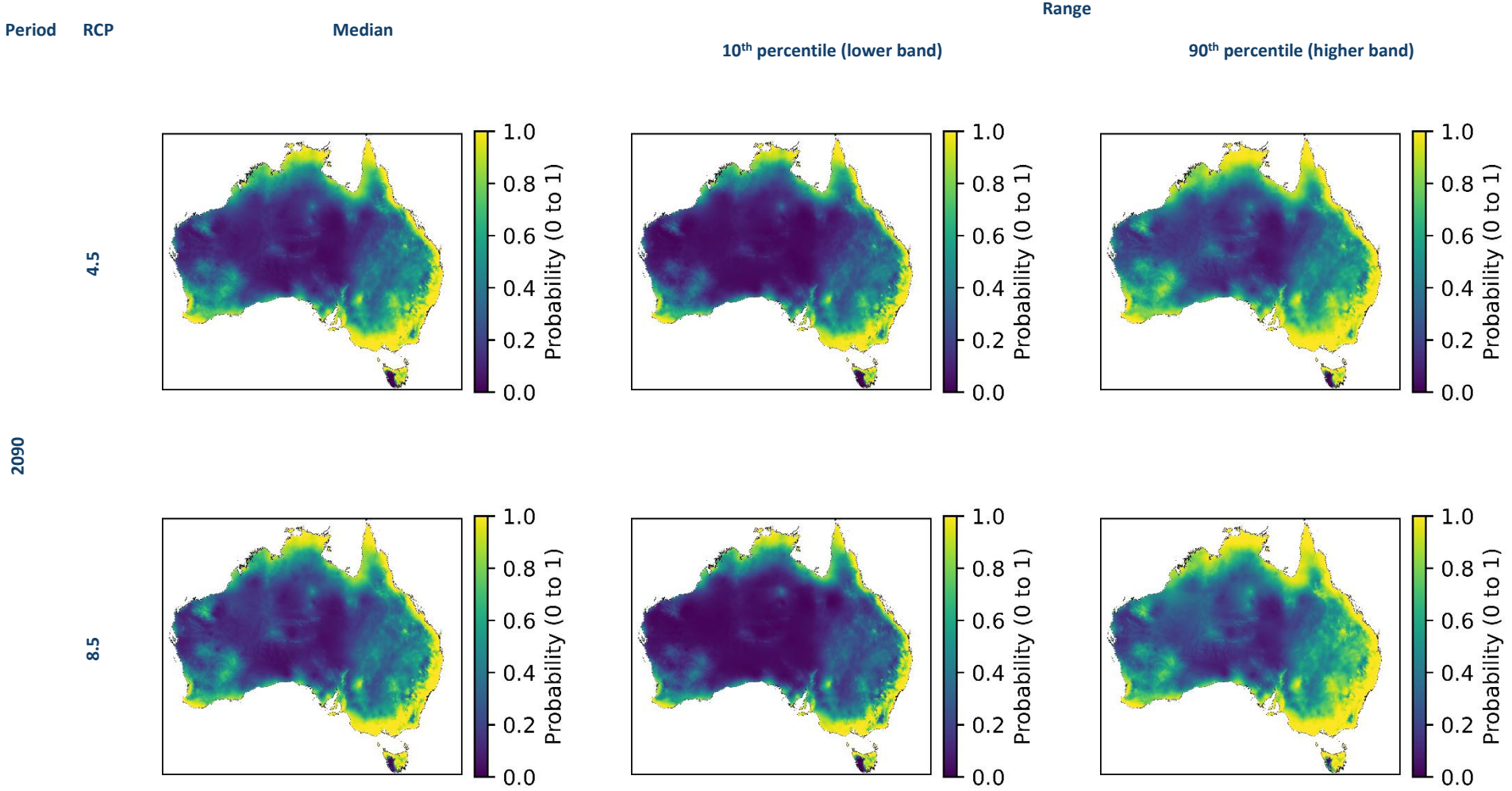
Period
RCP
Median
Range
10th percentile (lower band)
90th percentile (higher band)
2090
4.5
8.5
1.0
0.8
0.6
0.4
0.2
0.0
Probability (0 to 1)

Figure B4 Changes in combined JEV species presence probabilities from 2025 to 2050 and 2090 under RCP 4.5 and RCP 8.5. Uncertainty in probabilities is captured by including the median (50th percentile) as well as the 10th and 90th percentile of model projections for every location.

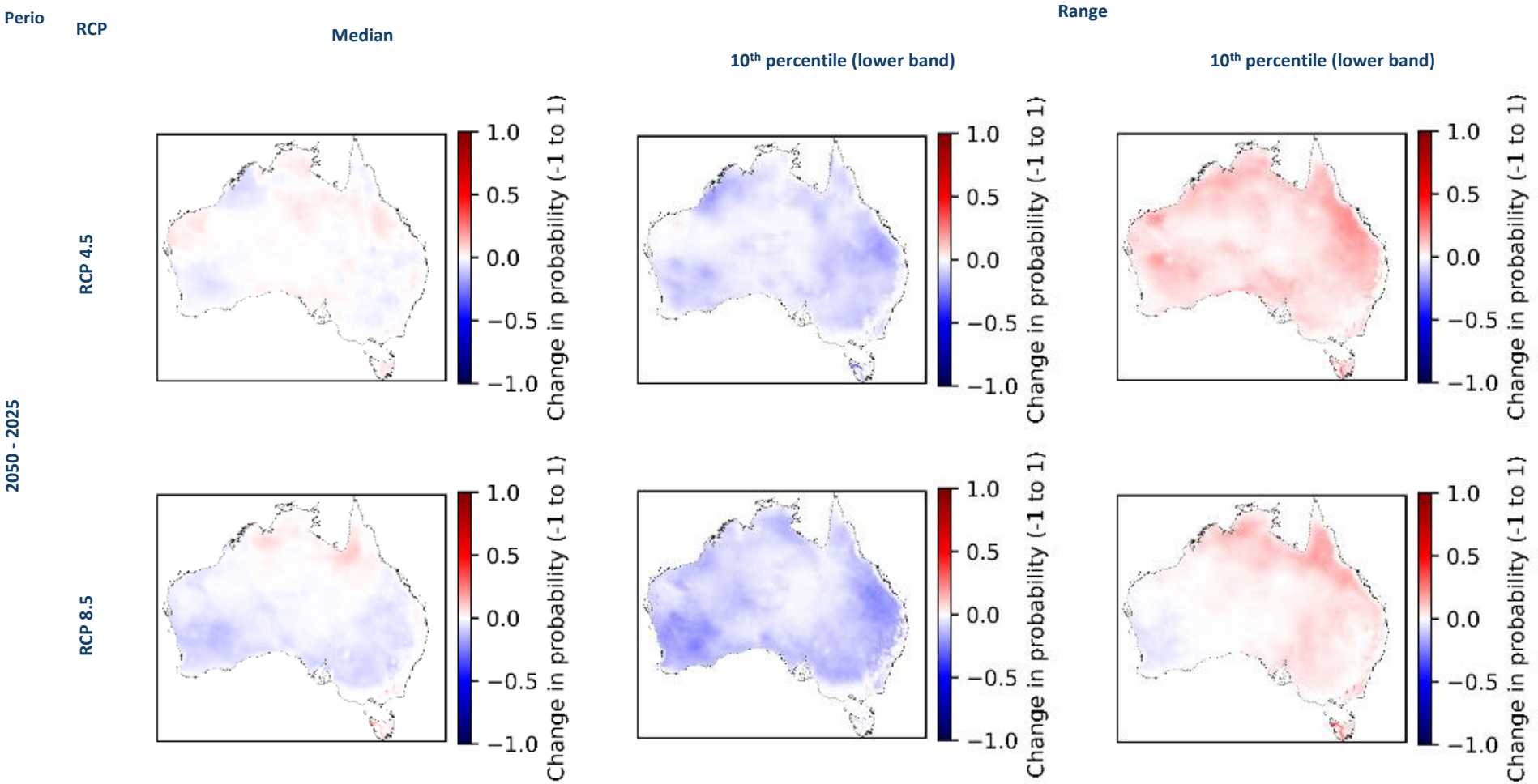

2090-2025

RCP 8.5

RCP 4.5

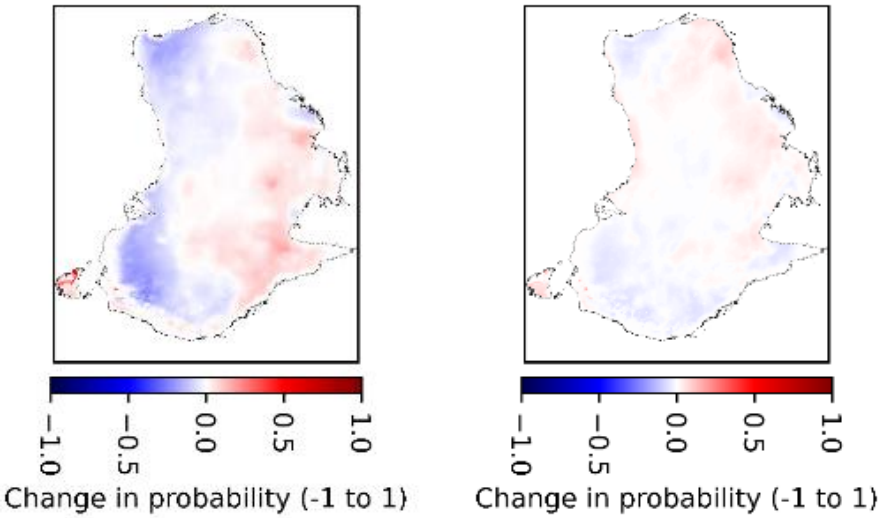

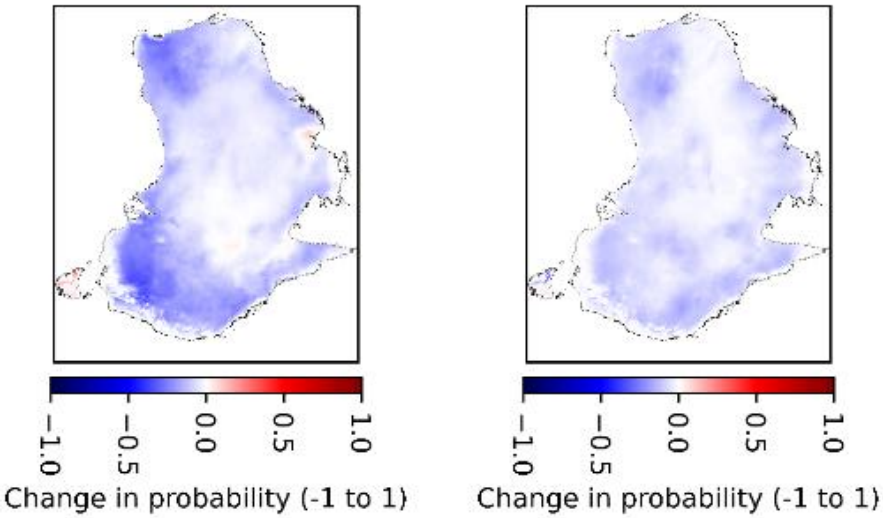

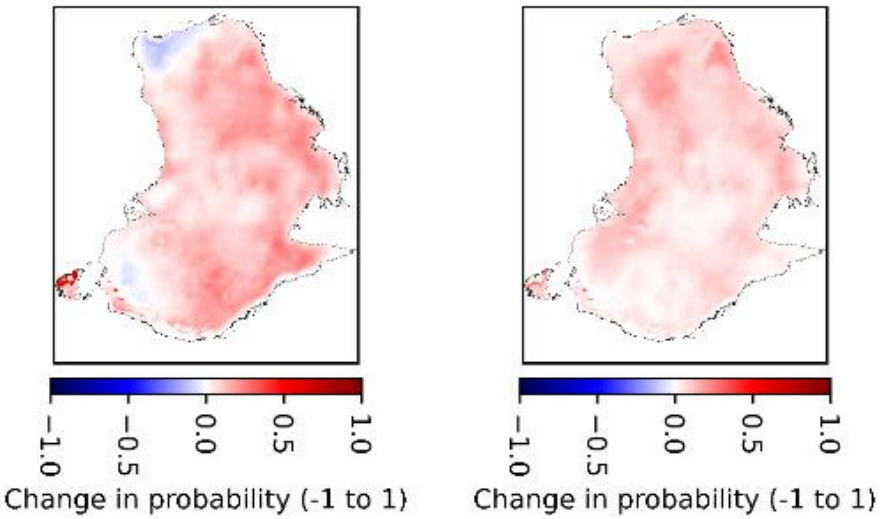

Appendix C Investigating the impact of climate on high prevalence bacterial and viral pathogens of concern using routinely collected surveillance data

We previously piloted this study using the historic Japanese Atmospheric Reanalysis (JRA55) (Kobayashi et al., 2015) and the fifth Coupled Model Inter-comparison Project (CMIP5) (Taylor et al., 2012) datasets. We used a collection of 25 climate models from the CMIP5 dataset and three specific Representative Concentration Pathways (RCP). Each RCP signifies a potential trajectory of future carbon emissions and its linked climate impacts. These pathways are labelled in order of escalating levels of warming as RCP2.6 (low carbon emission), RCP4.5 (intermediate carbon emission), and RCP8.5 (high carbon emission). It is important to note that while none of these scenarios may unfold precisely as projected, they do offer insights into how the Earth could react to a variety of potential future emission scenarios.

Our analysis determined that the annual average population density-weighted surface air temperature from JRA55 dataset as the most significant predictor for the annual influenza rate and the annual MRSA rate, having positive relationships with these rates. Using the annual average population density-weighted surface air temperature from CMIP5 and the established predictive models we determined future projections for influenza and MRSA rates (Figure A1) for the period 2030 to 2090.

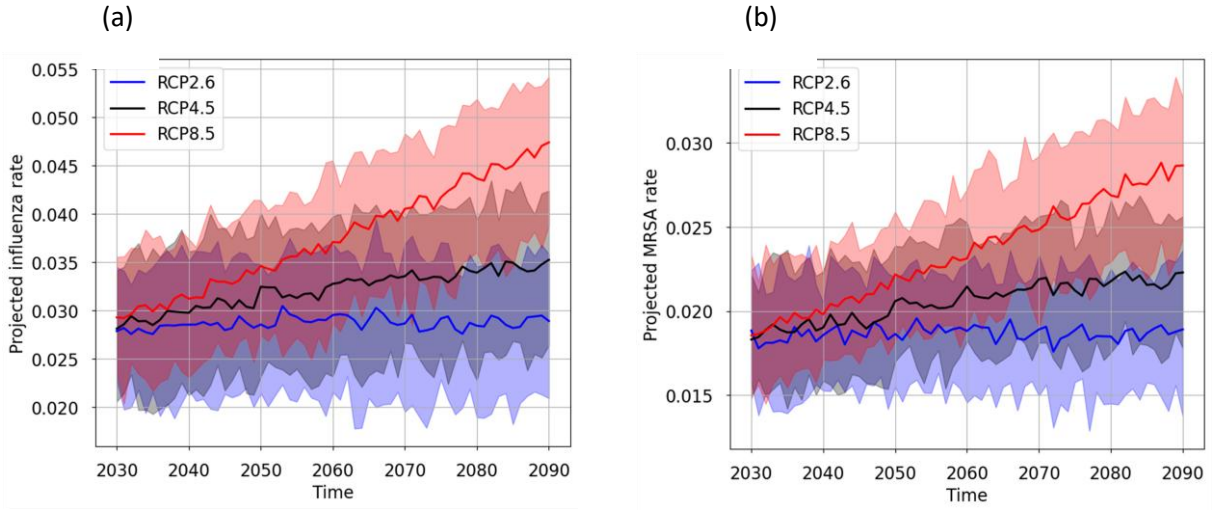

Figure C1 Time-series of projected influenza and MRSA rates from 2030 to 2090 from CMIP5 climate scenarios RCP2.6 (blue), RCP4.5 (grey), and RCP8.5 (red). The solid line in each plot corresponds the mean rate of 25 different climate models and the range is bounded by the 10% and 90% quantile across the climate model ensembles in that year.

As Australia's national science agency and innovation catalyst, CSIRO is solving the greatest challenges through innovative science and technology.

CSIRO. Unlocking a better future for everyone.

Contact us

1300 363 400
+61 3 9545 2176
csiro.au/contact
csiro.au

For further information

CSIRO Health and Biosecurity
Rajiv Jayasena
+61 3 9662 7383
rajiv.jayasena@csiro.au

CSIRO Health and Biosecurity
Shane Seabrook
+61 3 9662 7361
shane.seabrook@csiro.au